

**ROLE OF SONIC HEDGEHOG SIGNALING IN HUMAN
EMBRYONIC STEM CELLS AND ITS NEURAL DERIVATIVES**

WU MEIYUN SELENA

BSc (Hons) Clinical Science, King's College London, UK

A THESIS SUBMITTED

FOR THE DEGREE OF DOCTOR OF PHILOSOPHY

NUS Graduate School for Integrative Sciences and Engineering

NATIONAL UNIVERSITY OF SINGAPORE

2010

ACKNOWLEDGEMENTS

Looking back on the past 4 years of this PhD journey, I am extremely appreciative of the fact that the completion of this thesis would not have been possible without the support from many people. Hence, I would like to offer my humble and sincere thanks to:

Prof Miranda Yap, for taking me as your student. Thank you for always asking the hard questions to make me think and for always being supportive of my work. Your care and concern for all of us PhD students is heartfelt.

Dr Ken Chan, my supervisor and mentor, for patiently teaching and guiding me tirelessly throughout the past 4 years. I would not have come so far without you. Your brilliance inspires me and I hope that one day I can be as good a scientist as you are!

Prof Edward Manser, my thesis advisory committee member, for critically reviewing my work each time we meet.

Dr Andre Choo, the best PI that anyone can ask for. Thanks for always taking the time to meet with me and providing scientific and practical advice.

Dr Valerie Ng, my mentor and dearest friend in the lab. I'll always remember the crazy things we've done together. You have taught me so much and I'm grateful that you've always been a listening ear and an encouraging voice.

My collaborators, Stanley and Hock Chuan, for the pleasant partnership and patiently imparting your domain knowledge to this bioinformatics newbie.

Vanessa, my fellow classmate. Going through this journey together made the good times more fun and the bad times more bearable.

The Stem Cell group for being such great lab mates, especially Ker Sin, my lunch buddy, for being such a joy to work with and someone that I can always count on; Thian Thian and Julien for being such helpful team mates; Wenyu, for your friendship and being so ready to help me out each time; Louisa, my sweet cubby mate; Angela and Jayanthi for

running the lab so smoothly and my students Huizi, Huishan, Su Fung, Huiling, Jin Ju and Lydia for your helping hands.

The administrative staff in BTI who are so efficient and are responsible for making BTI such a special place to work in.

My AGS seniors: Linda, you're an angel for reading this manuscript; Sebastian, Dave, Pauline, Sandy, Andy and other seniors for sharing with me your experiences and giving me invaluable tips and advice on how to survive a PhD!

Grace, April, Eunice, TSG, cell group members from CEFC and friends who have been praying for me and cheering me on.

The most special people in my life, Mum, Dad and Sam, for your unfailing love and confidence in me. Mum and Dad, I am so blessed to have parents that pray for me daily

And finally, to my husband Stephen. Words cannot express my immense gratitude for your faithful love and support that gave me the strength to complete this journey. Thank you for walking each step of the way with me and taking such good care of me during the last three months. I love you.

This thesis is dedicated to my Lord and Saviour, Jesus Christ, who blessed me with this opportunity to do a PhD and provided me with all that I needed complete it. To whom all praise, honour and glory belong.

TABLE OF CONTENTS

ACKNOWLEDGEMENTS	i
TABLE OF CONTENTS	iii
SUMMARY	viii
LIST OF TABLES.....	ix
LIST OF FIGURES.....	xi
CHAPTER 1 INTRODUCTION.....	1
1.1 Background	1
1.2 Motivation.....	2
1.3 Objectives.....	3
1.4 Organization.....	3
CHAPTER 2 LITERATURE REVIEW.....	4
2.1 Overview of SHH signaling pathway	4
2.2 SHH processing, pathway components and signal transduction.....	4
2.2.1 SHH processing.....	4
2.2.2 SHH pathway components	5
2.2.3 SHH signal transduction.....	7
2.3 SHH in embryogenesis.....	9
2.4 SHH and neural development.....	10

2.5	SHH and proliferation	14
2.6	SHH in developmental disorders and cancer	15
2.7	Embryonic stem cells and induced pluripotent stem cells	16
2.8	Culture of hESC	18
2.9	Signaling pathways in hESC	19
2.10	Transcriptional networks in hESC	21
2.11	Applications of hESC research	22
2.12	Neural differentiation of hESC	24
2.12.1	Neural induction	25
2.12.2	Neural subtype specification	26
CHAPTER 3	MATERIALS AND METHODS	31
3.1	Molecular cloning	31
3.1.1	Cloning	31
3.1.2	Plasmids	32
3.2	Cell Culture	32
3.2.1	Immortalized mouse fibroblasts	32
3.2.2	Preparation of conditioned media from Δ E-MEFs	33
3.2.3	Human embryonic stem cells and induced pluripotent stem cells	33
3.2.4	Embryoid body formation	33
3.2.5	Generation of stable cell lines	34
3.2.6	Neurosphere formation	34
3.2.7	Neural differentiation	35
3.2.8	SHH conditioned media production	35
3.2.9	Transfection	36

3.2.10	Electrophysiology recording.....	36
3.3	Transcriptional profiling.....	37
3.3.1	RNA extraction.....	37
3.3.2	Reverse transcription, polymerase chain reaction (PCR) and quantitative real-time PCR analysis.....	38
3.3.3	DNA microarray.....	41
3.3.4	Microarray data analysis.....	42
3.3.5	In silico analysis of GLI binding sites.....	43
3.4	Protein and biochemical assays.....	43
3.4.1	Immunocytochemistry.....	43
3.4.2	Western blot.....	45
3.4.3	Flow cytometry analysis.....	46
3.4.4	Luciferase reporter assay.....	47
3.4.5	Cell proliferation assay.....	48
3.4.6	Apoptosis assay.....	48
3.4.7	Cell count.....	48
3.5	Statistics.....	49
 CHAPTER 4 ROLE OF SHH IN UNDIFFERENTIATED hESC.....		50
4.1	INTRODUCTION.....	50
4.2	Expression of SHH signaling pathway components.....	51
4.3	Activation of SHH signaling in undifferentiated hESC and role of GLI mediators.....	53
4.4	Effect of SHH on hESC pluripotency and proliferation.....	54
4.5	Activation of SHH signaling in hESC during differentiation.....	58

4.6	SHH signaling influences lineage determination during spontaneous differentiation.....	62
4.7	Summary.....	64
CHAPTER 5 ROLE OF SHH IN NEURAL DIFFERENTIATION		66
5.1	Introduction.....	66
5.2	Noggin treatment induces neural differentiation.....	66
5.3	Neuroprogenitors possess cilia.....	72
5.4	Overexpression of SHH in hESC.....	74
5.5	Overexpression of SHH enhances neural induction	76
5.6	Overexpression of SHH increases the proliferation of sorted neuroprogenitors... 	79
5.7	Overexpression of SHH leads to increase in DA neurons	81
5.8	Summary.....	84
CHAPTER 6 IDENTIFICATION OF SHH TARGET GENES IN NEUROPROGENITORS		86
6.1	Introduction.....	86
6.2	Microarray Analysis	87
6.3	Validation of differentially expressed genes (DEG).....	90
6.4	In silico analysis of potential GLI binding sites on DEG	93
6.5	Transcriptional activation of target gene promoters by SHH.....	95
6.6	SHH target genes discussion	98
6.6.1	Differentially expressed genes (DEG).....	100
6.6.2	Neural induction	100

6.6.3	Neuroprogenitor proliferation.....	101
6.6.4	Dorsal-ventral patterning.....	103
6.6.5	Dopaminergic neuron development and function	104
6.6.6	Axon guidance.....	105
6.6.7	Neural development.....	106
6.7	Summary.....	109
 CHAPTER 7 CONCLUSIONS AND RECOMMENDATIONS.....		110
7.1	Conclusions.....	110
7.2	Recommendations for future research.....	112
7.2.1	Loss of function study	112
7.2.2	Cross-talk between NOTCH and SHH signaling pathways	112
7.2.3	Exploration of novel target genes.....	113
7.2.4	MicroRNA and SHH signaling.....	114
 ABBREVIATIONS.....		115
 BIBLIOGRAPHY.....		117
 APPENDIX A MICROARRAY DATA.....		139
 APPENDIX B GLI BINDING SITES ANALYSIS		148
 APPENDIX C PUBLICATIONS		161

SUMMARY

Human embryonic stem cells (hESC) are pluripotent stem cells that have the unique ability to differentiate into cells of the three germ line lineages. Hence, they have wide potential to be used in cell replacement therapy and drug discovery. To realize the clinical potential of hESC, a deeper understanding of the molecular and cellular mechanism underlying their unique capacity for self-renewal and differentiation is required. This thesis is focused on the role of the Sonic Hedgehog (SHH) signaling pathway, a key pathway essential for the normal development of mammals. By testing the requirement of SHH in undifferentiated hESC cultures, it was revealed that exogenous SHH was not able to maintain the pluripotency or increase the proliferation of hESC. Instead, the SHH pathway was activated upon differentiation and exogenous SHH promoted differentiation to the neuroectoderm lineage. Using a defined neural differentiation protocol, it was found that overexpression of SHH in hESC resulted in a significant increase in neural stem cell marker expression as well as increased proliferation of neuroprogenitors. This demonstrated that SHH enhanced the neural induction and expansion of neuroprogenitors, which resulted in an increased yield of dopaminergic neurons derived from the neuroprogenitors. Transcriptional profiling of overexpressing SHH neuroprogenitors and *in silico* GLI DNA-binding site analysis identified putative direct and biologically relevant target genes of the SHH pathway. It also revealed an extensive network of genes involved in neural development, neuroprogenitor proliferation, neural specification and axon guidance. Therefore, this thesis contributes to the understanding of SHH signaling in hESC self-renewal and differentiation and provides a comprehensive view of the SHH transcriptional network in hESC-derived neuroprogenitors.

LIST OF TABLES

Table 2.1 Summary of DA differentiation from hESC.....	29
Table 3.1 List of primers used in RT-PCR	38
Table 3.2 List of primers used for real-time PCR.....	39
Table 3.3 List of antibodies used for immunocytochemistry	43
Table 3.4 List of antibodies used for Western blot analysis.....	45
Table 3.5 List of antibodies used for flow cytometry analysis	46
Table 6.1 List of top 20 significantly upregulated genes in SHH-NP. Genes are ranked according to their fold change values.....	88
Table 6.2 List of top 20 significantly downregulated genes in SHH-NP. Genes are ranked according to their fold change values.....	88
Table 6.3 List of SHH upregulated genes that have 6 or more putative GLI binding sites in the 5' promoter region. The number of binding sites were located 5 kb upstream of the transcription start site. The genomic coordinates and GLI binding start site(s) are on the NCBI36 (March 2006) Human Genome Assembly. Chr = chromosome, 1 = positive strand, -1 = negative strand of DNA.....	94
Table 6.4 List of SHH upregulated genes that have 6 or more putative GLI binding sites in the 3' downstream region. The number of binding sites were located 5 kb upstream of the transcription start site. The genomic coordinates and GLI binding start site(s) are on the NCBI36 (March 2006) Human Genome Assembly. Chr = chromosome, 1 = positive strand, -1 = negative strand of DNA.....	95
Table 6.5 Promoter-luciferase plasmids containing GLI binding sites on selected SHH target genes. Promoter coordinates refer to the genomic coordinates of the promoter sequences present in the Switchgear luciferase plasmids. The GLI binding site refers to starting genomic position of which GLI binding motif is found on. Coordinates are from the March 2006 Human Genome Assembly. Chr = chromosome	96
Table 6.6 Summary of target genes of SHH in hESC-derived neuroprogenitors	99

Table A 1 List of significantly upregulated genes (> 1.5-fold) in SHH-NP. Genes are ranked according to their fold change values..... 139

Table A 2 List of significantly downregulated genes (>1.5-fold) in SHH-NP. Genes are ranked according to their fold change values..... 144

Table B 1 List of SHH upregulated genes that have putative GLI binding sites within 5 kb of the 5' upstream region from the transcriptional start site. 148

Table B 2 List of SHH upregulated genes that have putative GLI binding sites within 5 kb of the 3' downstream region from the transcriptional start site. 152

Table B 3 List of SHH downregulated genes with putative GLI binding sites within 5 kb of the 5' upstream region from the transcriptional start site..... 155

Table B 4 List of SHH downregulated genes with putative GLI binding sites within 5 kb of the 3' downstream region from the transcriptional start site.tart 158

LIST OF FIGURES

Figure 2.1 Processing of the Shh full-length protein to form the Shh-N signaling peptide. 5

Figure 2.2 Shh signaling pathway. In the absence of the Shh ligand, Ptch1 inhibits Smo activity by preventing its accumulation at the cilia. In this state the Gli3 transcription factor is cleaved to a repressor form and translocates to the nucleus to repress transcription. In the presence of Shh, Ptch1 moves away from the cilia and Smo moves to the cilia, possibly with the help of intraflagellar transport (IFT) proteins. Gli2 and Gli3 are no longer cleaved and the full length Gli activator translocates to the nucleus to initiate transcription of target genes, e.g. *Ptch1* and *Gli1*. Hhip, Gas1 and Cdo are membrane proteins that bind to the Shh ligand to help regulate the Shh signal. This figure was modified from Simpson *et al.*, 2009. 8

Figure 2.3 Expression of Shh during development. Whole-mount *in-situ* hybridization of *Shh* in E9.5 days post coitum mouse embryo showing (A) the cross section of the spinal cord (dotted line ') showing *Shh* expression in the notochord (arrow head) and floor plate above. (B) The expression of *Shh* in the floor plate throughout the neural tube. Labeled are the subdivisions along the rostral-caudal axis of the forebrain, midbrain, hindbrain and the spinal cord. This figure was reproduced from Epstein *et al.*, 1999..... 10

Figure 2.4 Formation of the neural tube. (A) During neural induction, the neural plate is flanked by the non-neural ectoderm. The notochord (N) lies below the neural plate. (B) The neural plate folds up upon itself plate and fuses to form the neural tube. The underlying notochord secretes SHH which is necessary for the formation of the floor plate (F). The non-neural ectoderm eventually forms the epidermis. The arrows indicate the dorsal-ventral axis of the neural tube. This figure was modified from Briscoe *et al.*, 1999. 11

Figure 2.5 A model for how Shh patterns neurons of distinct cell fate in the spinal cord. Shh from the floor plate diffuses dorsally to establish a concentration gradient. The neural tube is divided into distinct progenitor domains (p0-3, pMN) that generate distinct neuronal subtypes: interneurons V0-V3 and motor neurons (MN). The progenitor domains are characterized by transcription factors that are broadly grouped into Class I and II genes. Shh induces the Class I genes *Nkx6-1*, *Nkx2-2* and *Olig2*, which are more ventrally expressed. The Class I genes *Dbx1*, *Dbx2*, *Irx3* and *Pax6* are dorsally expressed and repressed by SHH. 13

Figure 2.6 Human embryonic stem cells (hESC) derived from the blastocyst are able to differentiate into cells from each germ layer. This figure was modified from Hyslop *et al.*, 2005b..... 17

Figure 2.7 Signaling pathways maintaining hESC self-renewal. The WNT ligand binds to the Frizzled receptor which allows β -Catenin to translocate to the nucleus and activate transcription. FGF2 binds to the FGF receptors (FGFR) and activates the PI3K/Akt and MAP kinase pathways. IGF2 secreted from feeder cells binds to the IGF1 receptor (IGFR1) and activates the PI3K/Akt pathway as well. Activin/Nodal/TGF β

belong to the TGF superfamily of proteins and signal via the Type I (ALK 4/5/7) and Type II receptors that form heterodimers, which subsequently activates SMAD2/3. BMP signalling signals via the Type I (ALK 1/2/3/6) receptors and activates SMAD1/5/8 to promote differentiation. 21

Figure 3.1 Schematic illustration of constructs for generating stable hESC lines. Top: pCHEF-IRES-DsRed2 containing the Shh transgene with DsRed2 reporter gene driven by CHEF promoter. Bottom: Control vector with only DsRed2 reporter gene. CHEF = chinese hamster elongation factor-1 α , IRES = internal ribosome entry site. 31

Figure 3.2 Summary of neural differentiation protocol. 35

Figure 4.1 hESC express SHH pathway components. (A-D) Representative images showing immunofluorescent staining of (A) PTCH1, (B) SMO, (C) GLI1, (D) GLI3. Middle panel shows corresponding DAPI nuclear staining in blue and right panel shows corresponding merged images. Scale bars represent 100 μ m. 51

Figure 4.2 Embryoid bodies (EB) express SHH pathway components. RT-PCR analysis of SHH signaling pathway components in undifferentiated hESC and differentiating EB over 14 days. EB were grown in differentiation media in suspension and harvested at indicated time points. 52

Figure 4.3 GLI mediators are functional in undifferentiated hESC. (A) Schematic of 8xGli-BS reporter plasmid. (B-D) Luciferase activity of 8XGli-BS luciferase reporter plasmid. (B) hESC were transiently transfected with 8XGli-BS or 8XmutGli-BS luciferase reporter plasmid together with the indicated expression vectors encoding GLI1, GLI2 and GLI3. (C-D) The 8XGli-BS luciferase reporter plasmid and GLI1 expression vector were co-transfected with increasing concentrations of (C) GLI3 and (D) SUFU expression vectors as indicated. Luciferase activities were calculated as a ratio of *Firefly* luciferase activity over *Renilla* luciferase activity and expressed as fold induction relative to vector control. Values shown are mean \pm SD of a representative experiment carried out in triplicate and repeated at least three times. 54

Figure 4.4 Exogenous SHH does not affect pluripotency. (A) FACS analysis of TRA-1-60 positive cells and (B) Real-time PCR analysis of pluripotent markers *OCT4* and *NANOG* expression in hESC maintained in conditioned media (CM), CM supplemented with 1 μ g/ml SHH (CM+SHH), CM without FGF2 (CM – FGF2) or CM without FGF2 supplemented with 1 μ g/ml SHH (CM–FGF2+SHH) over two passages. The expression level of each gene is shown relative to undifferentiated hESC maintained in CM, which was arbitrarily defined as 1 unit. The values shown are mean \pm SD of a representative experiment performed in triplicate and repeated three times. * = $p < 0.05$, ns = non-significant. 55

Figure 4.5 Exogenous SHH does not affect proliferation of hESC. Flow cytometry analysis of EdU incorporation assay in undifferentiated hESC. Cells were synchronized with nocodazole for 16 hours and then treated with or without 1 μ g/ml SHH for 24 hours. Representative dot plots of biological triplicates showing EdU incorporation in hESC co-stained for OCT4. This experiment was repeated three times. 56

Figure 4.6 Exogenous SHH does not affect survival of hESC. Flow cytometry analysis of Annexin V apoptosis assay in undifferentiated hESC whereby cells were treated with or without 1 µg/ml SHH for 24 hours prior to assay. Representative dot plots showing apoptotic cells (Annexin V positive and PI negative) from biological triplicates and experiment repeated thrice..... 57

Figure 4.7 Activation of SHH signaling by endogenous SHH. (A) Quantitative Real-time PCR analysis of target gene *PTCH1* and *GLI1* and pluripotent markers *OCT4* and *NANOG* expression in hESC maintained in conditioned media (CM), or induced to differentiate with differentiation media (DM) or DM supplemented 5 µM RA (DM+5 µM RA) for 48 hours. Gene expression is expressed relative to hESC in CM condition. (B) Luciferase activity of the 8XGli-BS luciferase reporter plasmid, which was transfected into hESC and cultured similar conditions as above. Cells were treated with the vehicle control (DMSO/ Ethanol) or pathway inhibitors 10 µM cyclopamine and 50 µM forskolin. Cells were assayed for luciferase activity 48 hours post transfection. Luciferase activities were calculated as a ratio of *Firefly* luciferase activity over *Renilla* luciferase activity and expressed as fold induction relative to vehicle or vector control. Values shown are mean ± SD of a representative experiment carried out in triplicate and repeated at least three times. *, p<0.05..... 59

Figure 4.8 Activation of SHH signaling by exogenous SHH. The SHH expression vector was co-transfected with the 8XGli-BS luciferase reporter plasmid in the absence (vehicle-DMSO) or presence of 10 µM cyclopamine. *GLI1* was overexpressed as a positive control. Luciferase activities were calculated as a ratio of *Firefly* luciferase activity over *Renilla* luciferase activity and expressed as fold induction relative to vehicle or vector control. Values shown are mean ± SD of a representative experiment carried out in triplicate and repeated at least three times. * = p<0.05..... 61

Figure 4.9 Neuroectoderm markers expression are upregulated in EB after 14 days exposure to SHH. (A-C) EB were grown in SHH-CM or Control-CM suspension culture for 14 days and mRNA expression was analyzed by real time PCR to determine the expression of (A) SHH target genes, (B) neuroectoderm, (C) mesoderm and endoderm markers. Gene expression is expressed relative to undifferentiated hESC. Values shown are mean ± SD of a representative experiment carried out in triplicate and repeated at least three times. * = p<0.05 , compared to Control-CM treated EB. ns = non-significant. 63

Figure 4.10 Immunofluorescent staining of neural stem cell marker Nestin in SHH-CM and Control-CM treated EB. Middle panel shows corresponding DAPI nuclear staining in blue and right panel shows corresponding merged images. Scale bars represent 50 µm. 64

Figure 5.1 Noggin induced neural differentiation. Replated EB were treated for 10 days with noggin and compact clumps were formed that were (A) immunopositive for PAX6. The middle panel shows corresponding bright field image. (B) Bright field micrograph of typical neurospheres in culture. Scale bars represent 100 µm. 67

Figure 5.2 Neuroprogenitors express neuroectoderm markers. Neurospheres were harvested after 7 days in culture and mRNA expression was analyzed by real-time PCR

analysis for (A) neuroectoderm markers and *OCT4* in neuroprogenitors and (B) mesoderm and endoderm markers in undifferentiated hESC (HESC), 14-day-old embryoid bodies (14D EB) and neuroprogenitors (NP). The expression level of each gene is shown relative to undifferentiated hESC, which was arbitrarily defined as 1 unit. The values shown are mean \pm SD of a representative experiment carried out in triplicate and repeated twice. In (A), the line represents expression levels of each gene in undifferentiated hESC. 68

Figure 5.3 Neuroprogenitors express NSC markers. (A) Flow cytometry analysis of neuroprogenitors expressing A2B5, FORSE-1, p75, PSA-NCAM and CD133. The shaded histogram represents staining with the negative control and open histograms represent staining with the respective antibodies. (B-D) Representative images showing immunofluorescent staining of (B) PAX6, (C) NESTIN and (D) SOX1 on neuroprogenitors that were replated onto laminin-coated wells. Nuclei were stained with DAPI. Scale bars represent 50 μ m. 69

Figure 5.4 Neuroprogenitors are able to differentiate into astrocytes and functional mature neurons. (A-B) Immunocytochemistry was performed to detect (A) TH (red) and MAP2 (green) positive neurons and (B) β -III Tubulin (green) and GFAP (red) positive astrocytes. Scale bars represent 100 μ m. (C) Patch clamp recordings show spontaneous postsynaptic currents. 71

Figure 5.5 SHH is essential for the specification of DA neurons from neuroprogenitors. (A) Representative images showing immunofluorescent staining of TH (red) and β -Tubulin III (green) positive cells. Nuclei were stained with DAPI. Scale bars represent 50 μ m. (B) Quantification of the above images. TH+ nuclei were counted and expressed as a percentage of the total DAPI positive cells. Numbers presented represent the average percentage \pm SD from triplicate samples. * = $p < 0.05$ 72

Figure 5.6 The SMO receptor localizes to primary cilia of neuroprogenitors. (A-C) Representative confocal images showing immunocytochemistry of (A) undifferentiated hESC with acetylated tubulin (AcTb), pluripotent marker OCT4, and corresponding merged images. (B) Neuroprogenitors were similarly probed for AcTb and the neuroectoderm marker NESTIN (green, middle panel). (C) Neuroprogenitors were stimulated with 200 ng/ml SHH for 24 - 48 hours and stained for AcTb and the SMO receptor (green, middle panel). The arrow points to SMO which localizes to the base of the primary cilia. Scale bars represent 10 μ m. 73

Figure 5.7 SHH pathway is activated in neuroprogenitors. Real-time PCR analysis of genes *PTCH1* and *SMO* in neuroprogenitors (NP). Values are expressed relative to undifferentiated hESC and are mean \pm SD of a representative experiment performed in triplicate and repeated twice. * = $p < 0.05$ 74

Figure 5.8 Stable overexpressing-SHH hESC express SHH and DsRed. (A) Representative image of a typical overexpressing-SHH hESC colony maintained in pluripotent conditions showing immunocytochemistry for SHH. (B) Corresponding fluorescent image of DsRed2 and (C) merged images. Scale bar represents 100 μ m. 75

Figure 5.9 SHH-NP express the DsRed2 protein. Fluorescent image of SHH-NP and corresponding bright field image. Scale bars represent 50 μ m..... 76

Figure 5.10 Overexpression of SHH in hESC-derived neuroprogenitors. (A) Western blot analysis of SHH-NP, Vector-NP and H3-NP probed with the anti-SHH antibody which detected both the full length (45 kDa) and 19 kDa active fragment. Actin was used as a loading control. (B) Real-time PCR analysis of *SHH* and target genes *PTCH1* and *GLI1* in SHH-NP, Vector-NP and H3-NP. The expression value of each gene is shown relative to H3-NP, which was arbitrarily defined as 1. The values are mean \pm SD of a representative experiment performed in triplicate and repeated thrice. * = $p < 0.05$. 77

Figure 5.11 Overexpression of SHH in hESC-derived neuroprogenitors lead to increased expression of neuroectoderm markers. (A) Real-time PCR analysis of neuroprogenitors for neuroectoderm markers. The expression value of each gene is shown relative to H3-NP, which was arbitrarily defined as 1. The values are mean \pm SD of a representative experiment performed in triplicate and repeated thrice. * = $p < 0.05$ (B) Western blot of neuroprogenitors probed with SOX1 and NESTIN antibodies with ACTIN as a loading control. Values indicate quantification of protein based on the band intensities from the Western blot normalized to Actin using LI-COR Odyssey software. 78

Figure 5.12 Overexpression of SHH in hESC-derived neuroprogenitors lead to increased expression NSC surface markers. Histogram representation of FACS analysis of CD133, A2B5 and p75 showing percentage positive cells. * = $p < 0.05$. All values shown are mean \pm SD of a representative experiment performed in triplicate and repeated thrice. 79

Figure 5.13 Overexpression of SHH results in increase proliferation of multipotent p75+/PSA-CAM+ neuroprogenitors. (A) 1×10^5 sorted cells were seeded into 24-well ultra-low suspension plates and neurospheres formed after 3-5 days. Cells were harvested 7 and 14 days after and counted by trypan blue exclusion. * = $p < 0.05$. All values shown are mean \pm SD of a representative experiment performed in triplicate and repeated thrice. 80

Figure 5.14 Overexpression of SHH in hESC-derived neuroprognitors leads to an increase in TH+ neurons. (A) Immunofluorescent images of SHH-NN, Vector-NN and H3-NN differentiated neuroprogenitors stained for TH (purple) and β -Tubulin III (green). Nuclei are stained by DAPI. Scale bars represent 100 μ m. These are representative images of an experiment repeated four times with similar results. (B) Quantification of the above images. TH+ nuclei were counted and expressed as a percentage of the total β -Tubulin III positive cells. Numbers presented represent the average percentage \pm SD from triplicate samples. * = $p < 0.05$ 83

Figure 5.15 Neurons express dopaminergic neuron marker genes. Real-time PCR analysis of DA neurons. The expression value of each gene is shown relative to H3-NN, which was arbitrarily defined as 1. The values are mean \pm SD of a representative experiment performed in triplicate and repeated thrice. * = $p < 0.05$ 83

Figure 6.1 Analysis of SHH-NP expression profiling. (A) Microarray gene expression heat map comparing SHH-NP with H3-NP and Vector-NP showing top 20 upregulated and downregulated genes. Shades of red denotes upregulation while shades of green denote downregulation. (B) Upregulated genes were classified into categories by Gene ontology Biological Processes terms and ranked according to false discovery rates in ascending order. Frequencies of upregulated genes in each category are shown as percentages..... 90

Figure 6.2 Known SHH target genes identified by microarray profiling were validated by real-time PCR. RNA for the microarray study was re-probed by real-time PCR analysis. The expression value of each gene is shown relative to H3-NP, which was arbitrarily defined as 1. The values are mean \pm SD of biological triplicates. * = $p < 0.05$. .. 90

Figure 6.3 Differentially expressed genes identified from the transcriptional profiling were validated by real-time PCR and Western blot analysis. (A-B) Real-time PCR analysis of RNA used for the DNA microarray study probed for (A) upregulated genes and (B) downregulated genes. The expression value of each gene is shown relative to H3-NP, which was arbitrarily defined as 1. The values are mean \pm SD of biological triplicates. * = $p < 0.05$. (C) Cell lysates from SHH-NP, Vector-NP and H3-NP were probed with antibodies against upregulated targets EGFR, FOXA2 and downregulated targets, MSX1 and PAX3. Actin was used as a loading control..... 91

Figure 6.4 Target genes of SHH are upregulated in iPSC(IMR90)-derived neuroprogenitors treated with exogenous SHH. iPSC(IMR90) cells were differentiated into NP and were treated with (or without) 200 ng/ml recombinant SHH from the start of the differentiation process. Gene expression was analyzed after 1 week in culture by real-time PCR. The expression value of each gene is shown relative to untreated NP, which was arbitrarily defined as 1. The values are mean \pm SD of triplicates and the experiment was repeated twice. * = $p < 0.05$ 92

Figure 6.5 SHH is able to transactivate the promoters of target genes. Luciferase reporter genes containing fragments of promoters of target genes were co-transfected in to H3-NP along with Renilla vector and in indicated cases, with or without the SHH expression vector. Luciferase activities were calculated as a ratio of *Firefly* luciferase activity over *Renilla* luciferase activity and expressed as fold induction relative to pCDNA3.1 vector control. Values shown are mean \pm SD of a representative experiment carried out in triplicate and repeated at least three times. * = $p < 0.05$, ns = not significant. 97

Figure 6.6 The transcriptional network of SHH in hESC-derived neuroprogenitors. Target genes of the pathway are indicated by the solid lines while suggested consequences of pathway activation are indicated by dotted lines..... 108

CHAPTER 1 INTRODUCTION

1.1 Background

Human embryonic stem cells (hESC) are a widely envisioned source of cells for use in cell replacement therapy. In particular, medical conditions arising from the loss of neurons, like Parkinson's disease, Alzheimer's disease, stroke and spinal cord injuries, are potential beneficiaries of the cell replacement therapy. The inherent limited capacity of the central nervous system for self-repair means that transplantation of functional neurons into the sites of injury is one potential approach to restore physiological function. Unfortunately, the lack of transplantable neurons has rendered these conditions to be currently incurable. Therefore, the ability of hESC to differentiate to all cell types of the body has spurred intensive research towards understanding the biology of hESC self-renewal as well as to differentiate hESC towards cells of the neural lineage.

The process of neural differentiation is governed by both extrinsic signals from the microenvironment like growth factors, substrates and cell-to-cell contact, and intrinsic gene regulation. Therefore, to achieve efficient directed differentiation of neurons, it is essential that there is sufficient knowledge of the differentiation process and the underlying molecular mechanisms controlling cell fate choices.

Principles gleaned from developmental biology studies have been effective when applied to *in vitro* neural differentiation of hESC. The process requires the use of inductive signals applied in a timely and coordinated fashion, with the aid of stromal cells or genetic manipulation (Kawasaki *et al.*, 2000; Carpenter, 2001; Zhang *et al.*, 2001; Chung *et al.*, 2002; Perrier *et al.*, 2004; Gerrard *et al.*, 2005; Du *et al.*, 2006; Hedlund *et al.*, 2008). As a result, hESC have been successfully differentiated into a great variety of cells that make up the central nervous system including dopaminergic neurons, motor neurons, glial cells, astrocytes, oligodendrocytes, neural crest stem cell cells and retinal cells (Bjorklund *et al.*, 2002; Faulkner and Keirstead, 2005; Lamba *et al.*, 2006; Lee *et al.*, 2006; Lim *et al.*, 2006; Lee *et al.*, 2007a).

The Sonic Hedgehog (SHH) signaling pathway is one of the key pathways that control the development of the central nervous system in mammals. It is also important in the development of many other organs such as the limbs, bone, lung and the gut. As a morphogen, SHH is one of the crucial patterning factors used in conjunction with other molecules to efficiently generate several subtypes of neurons, including motor neurons and dopaminergic neurons from hESC (Perrier *et al.*, 2004; Lee *et al.*, 2007b).

1.2 Motivation

Given the importance of hESC, it is essential to understand the mechanisms that direct the balance between the states of self-renewal and differentiation. Several developmentally important signaling pathways like the fibroblast growth factor (FGF) and transforming growth factor beta (TGF β) pathways have been identified to be instrumental in governing hESC self-renewal (Vallier *et al.*, 2005, Xu *et al.*, 2005). However, the exact cellular and molecular mechanisms are still being elucidated. To date, there has not been any in-depth study investigating the potential function of the SHH signaling pathway in hESC.

Despite being able to obtain several neural cell types from hESC, there are gaps in the understanding of the molecular pathways controlling the differentiation of hESC along the neural lineage. This is reflected in current neural differentiation protocols that often result in a heterogeneous population of neural cells that are at different stages of differentiation (Pruszek *et al.*, 2007). Furthermore, the specific ways by which SHH is able to direct neural differentiation towards the motor neuron and dopaminergic neuron lineages is often obscured as SHH is studied together with its partner molecules (Lee *et al.*, 2000, Kim *et al.*, 2002, Yan *et al.*, 2005). Therefore, a systematic study into the role of SHH in neural differentiation and the gene networks it controls will provide insight into the hESC differentiation process. The knowledge gained can also potentially be used in the future to better control the developmental fate of cells and achieve more efficient differentiation of hESC to the desired neural cell type.

1.3 Objectives

Hence, the proposed research work revolves around two principle objectives which is to investigate the role of SHH signaling pathway in the:

1. Self-renewal and maintenance of pluripotency in undifferentiated hESC
2. Directed differentiation of hESC towards the neural lineage

Objective 1 was achieved by examining the capacity of the SHH pathway in maintaining pluripotent marker expression and cell proliferation of undifferentiated hESC. Objective 2 was achieved by studying the effect of overexpression of SHH in hESC-derived neuroprogenitors and identifying novel downstream target genes of the SHH pathway in neuroprogenitors.

1.4 Organization

This thesis has 7 chapters. Chapter 1 describes the background, motivation and objectives of this thesis. It follows with Chapter 2 which presents a literature review of the SHH pathway and its function during mammalian development. It also covers the current understanding of undifferentiated hESC and strategies for *in vitro* differentiation of hESC to the neural lineage. Chapter 3 provides details on the materials and methods used in this thesis. Chapter 4 evaluates the presence and activation of the SHH pathway in hESC. It also studies the effect of SHH during spontaneous differentiation. Chapter 5 presents the directed neural differentiation of hESC and the changes observed from overexpression of SHH in hESC-derived neuroprogenitors. Chapter 6 examines the regulated genes by SHH and proposes novel target genes of the SHH pathway in hESC-derived neuroprogenitors. Chapter 7 is a summary of the findings of this thesis and provides recommendations for future work.

CHAPTER 2 LITERATURE REVIEW

2.1 Overview of SHH signaling pathway

The Hedgehog gene was first discovered by Nusslein-Volhard and Wieschaus (Nusslein-Volhard and Wieschaus, 1980) during a *Drosophila* mutant screen for genes that were important for the “development of the fruit fly larval body plan”. The larvae of the mutated gene had spiky cuticles, which prompted the authors to name the gene *hedgehog* (*hh*). Since its discovery, the *hh* gene has been discovered in many species, including the puffer fish, zebrafish, chick, mouse and human (Ingham, 2001). Many key components of the SHH pathway are evolutionarily conserved from the *Drosophila* to the zebrafish, and to mammals, which signifies its importance. At the same time, there are important intraspecies divergences within the pathway that reflect its ability to control development in a species-specific manner (Huangfu, 2006). *Drosophila* carries a single *hh* gene while vertebrates have 3 *Hh* genes: Sonic hedgehog (*Shh*), Indian hedgehog (*Ihh*) and Desert hedgehog (*Dhh*). All 3 Hh proteins are able to bind to the Patched 1 (Ptch1) receptor (Pathi *et al.*, 2001) and can function redundantly (Zhang *et al.*, 2001). However, their differences in expression patterns enable them to play different roles in development (Ingham, 2001; Varjosalo and Taipale, 2008). Shh is the most broadly expressed Hh protein that mediates the most functions in development (Varjosalo and Taipale, 2008), and hence will be the focus of this thesis.

2.2 SHH processing, pathway components and signal transduction

2.2.1 SHH processing

The Shh protein is synthesized as an approximately 45 kDa precursor which is then processed to a 19 kDa active signaling peptide (Figure 2.1). The signal peptide is cleaved when the full-length precursor protein is transported into the endoplasmic reticulum. The precursor protein then undergoes proteolytic autoprocessing in a reaction catalyzed by its own C-terminal domain, to generate the smaller 19 kDa N-terminal signaling molecule (Shh-

N). Following that, a cholesterol moiety is added to the C-terminus of Shh-N. Then, a palmitic acid moiety is added to the N-terminus of Shh-N (Porter *et al.*, 1996; Chamoun *et al.*, 2001; Lee and Treisman, 2001). These modifications result in an active 19 kDa fragment that contains all its known signaling activity. The cholesterol modification of Shh enables the ligand to attach tightly to cell membranes and is proposed to be required for the distribution of Shh-N *in vivo* (Guerrero and Chiang, 2007).

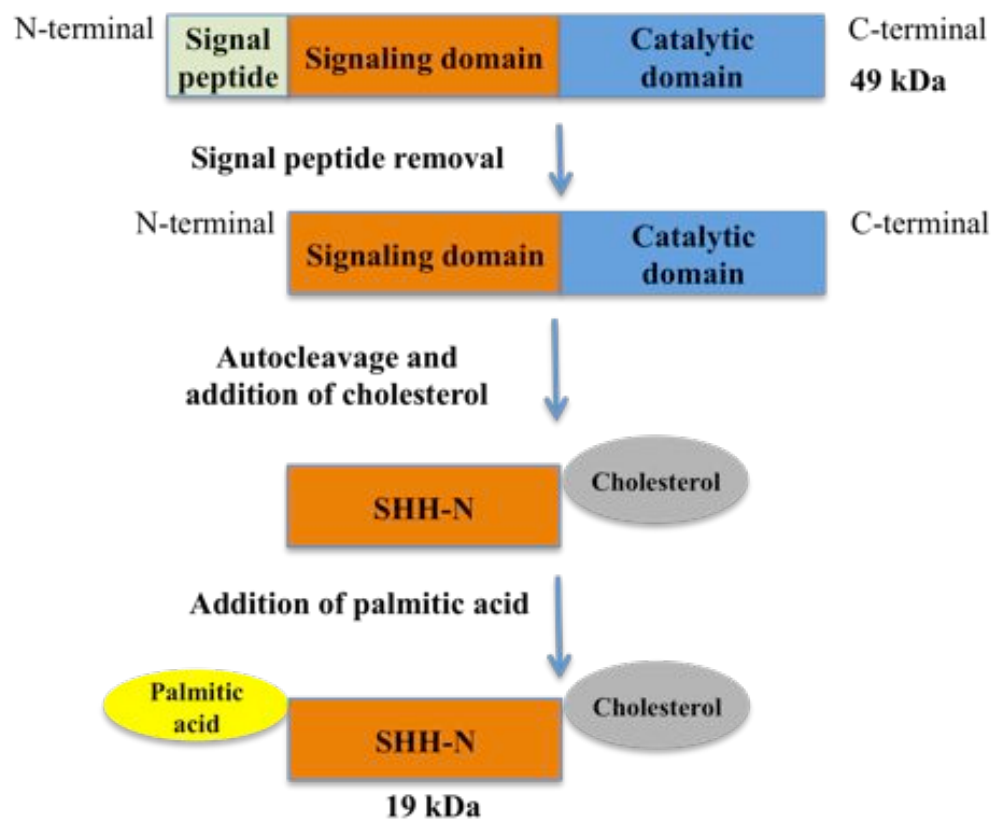


Figure 2.1 Processing of the Shh full-length protein to form the Shh-N signaling peptide.

2.2.2 *SHH* pathway components

The Shh pathway signals via two receptors, Smoothed (Smo) and its negative regulator Ptch1, which are predicted to have 7 and 12 transmembrane spans respectively. In mammals, there are two Ptch members, Ptch1 and Ptch2 that have similar amino acid

identities (Carpenter *et al.*, 1998). The secretion of Shh depends on Dispatched, a 12-span transmembrane protein homologous to Ptch (Burke *et al.*, 1999; Ma *et al.*, 2002).

In mammals, there exist three transcriptional effectors of the pathway: GLI-Kruppel family member 1 (Gli1), Gli2 and Gli3. The Gli3 protein exists in 2 forms, the full-length form which can activate transcription and the truncated form that represses transcription of Shh dependent genes (Wang *et al.*, 2000). Gli3 is normally phosphorylated and proteolytically processed to the repressor form and this cleavage is inhibited by Shh (Wang *et al.*, 2000; Wang and Li, 2006). Gli3 functions mainly as a repressor of Shh signaling by repressing target gene expression (Sasaki *et al.*, 1997; Wang *et al.*, 2000). While Gli2 is similarly processed like Gli3 by the proteasome, the processing appears to be inefficient due to differences in their C-terminus regions (Pan *et al.*, 2006; Pan and Wang, 2007). Gli1 lacks the N-terminal repression domain present in Gli2 and Gli3 and therefore functions only as an activator (Ruiz i Altaba, 1999; Sasaki *et al.*, 1999). Gli1 and Gli2 act primarily as transcriptional activators and have overlapping functions (Park *et al.*, 2000; Bai and Joyner, 2001). Since transcription of Gli1 is controlled by active Shh signaling (Dai *et al.*, 1999) and Gli1 knockout mutant mice are viable (Bai and Joyner, 2001), Gli1 is believed to be a secondary effector of the Shh signal transduction and serves to amplify the response to Shh (Bai *et al.*, 2002).

In mammalian Shh signaling, there are other additional molecules that regulate the activity of the Shh signaling by binding to Shh. Cdo and Boc are cell surface immunoglobulin superfamily members that bind to Shh to promote its activity (Tenzen *et al.*, 2006; Yao *et al.*, 2006; Zhang *et al.*, 2006). Another cell surface protein Gas1 is similarly a positive component of the signaling pathway (Allen *et al.*, 2007). Gas1 and Cdo promote Shh signaling by acting synergistically with Ptch1 to enhance Shh binding to Ptch1 (Allen *et al.*, 2007; Martinelli and Fan, 2007). On the other hand, the hedgehog inhibitory protein (Hhip) is a membrane-associated protein that binds and diminishes the effect of Shh ligand by sequestration. *Hhip* is a transcriptional target of Shh (Chuang and McMahon, 1999; Jeong and McMahon, 2005), and is part of the negative feedback loop to limit the range of Shh

signaling. Therefore, these molecules modulate the range and concentration of Shh, and are necessary for Shh to carry out its function as a long-range morphogen.

There are other negative regulators of the pathway. Suppressor of fused (Sufu) is one such protein, which inhibits Gli proteins from initiating transcription by sequestering Gli proteins to the cytoplasm (Kogerman *et al.*, 1999; Stone *et al.*, 1999; Dunaeva, 2003). Sufu also binds with Gli proteins while they are bound to DNA and inhibits their ability to initiate transcription (Cheng *et al.*, 2002). Rab23 is another cytoplasmic protein that was recently identified to be a negative regulator of Shh signaling (Eggenchwiler *et al.*, 2001). Rab23 works downstream of Smo and is suggested to be a link between Smo and Gli whereby it inhibits the formation of the Gli2 activator form (Eggenchwiler *et al.*, 2006). However, the exact mechanism of Rab23 has yet to be elucidated.

2.2.3 SHH signal transduction

The mammalian Shh signal transduction pathway requires the primary cilium, a small microtubule-based structure that extends out of the cell surface and acts as a microenvironment for signal transduction. Intact cilia and intraflagellar transport components necessary for cilia assembly are crucial for Shh signaling (Huangfu *et al.*, 2003). Essential components of the pathway Smo, Ptch1, Sufu, Gli2 and Gli3 have been detected on the cilium of cells in the mouse neural tube, limb bud and embryonic fibroblasts (Corbit *et al.*, 2005; Haycraft *et al.*, 2005; Rohatgi *et al.*, 2007). In the absence of Shh, Ptch1 inhibits Smo by preventing Smo from accumulating at the cilia (Rohatgi *et al.*, 2007) (Figure 2.2). Full length Gli2 and Gli3 are then phosphorylated by kinases and targeted for proteolysis to generate the repressor form. The Gli repressor proteins then move to the nucleus to repress transcription of target genes.

Upon stimulation with Shh, Ptch1 is internalized into the cell and Smo is able to move into the primary cilium (Corbit *et al.*, 2005; Rohatgi *et al.*, 2007). Live cell visualization of Smo tagged to a fluorescent protein revealed that intraflagellar transport proteins are required to move Smo from intracellular pools to the primary cilium (Wang *et*

al., 2009). The relief of inhibition of Ptch1 results in the phosphorylation of the cytosolic C-terminus of Smo, which then induces a conformational change in Smo and activates downstream signaling (Zhao *et al.*, 2007).

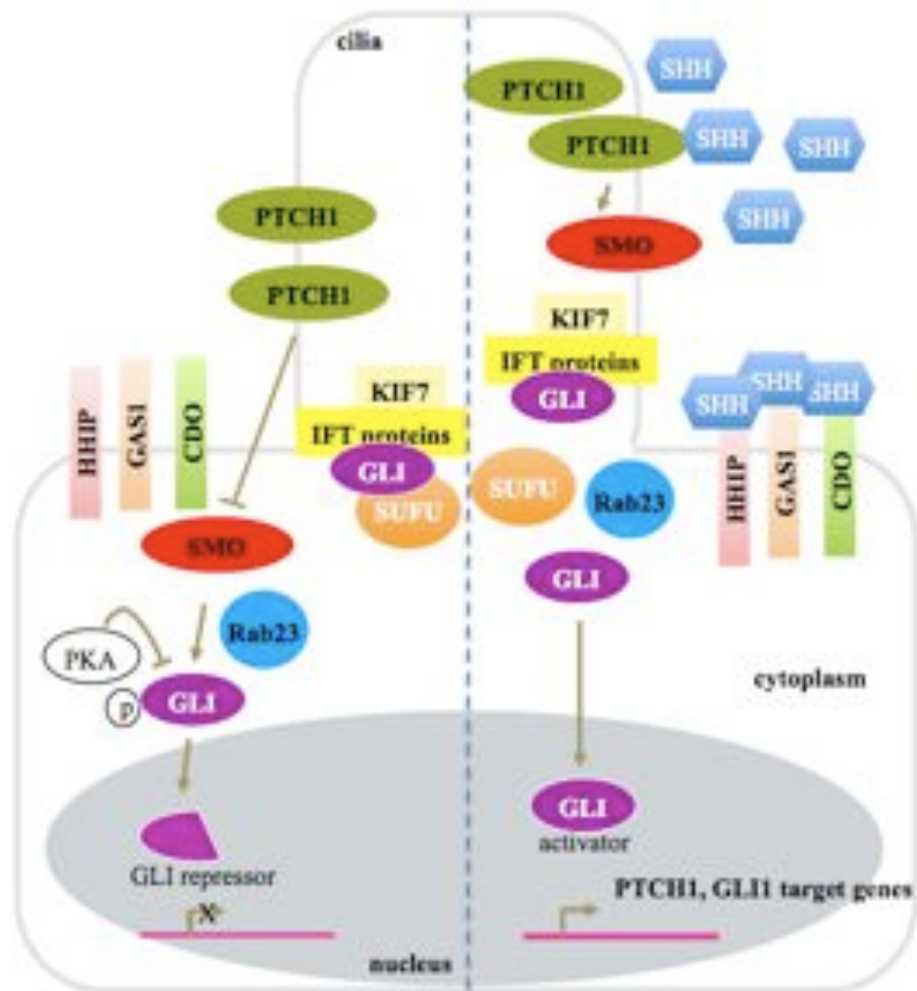


Figure 2.2 Shh signaling pathway. In the absence of the Shh ligand, Ptch1 inhibits Smo activity by preventing its accumulation at the cilia. In this state, the Gli3 transcription factor is cleaved to a repressor form and translocates to the nucleus to repress transcription. In the presence of Shh, Ptch1 moves away from the cilia and Smo moves to the cilia, possibly with the help of intraflagellar transport (IFT) proteins. Gli2 and Gli3 are no longer cleaved and the full length Gli activator translocates to the nucleus to initiate transcription of target genes, e.g. *Ptch1* and *Gli1*. Hhip, Gas1 and Cdo are membrane proteins that bind to the Shh ligand to help regulate the Shh signal. This figure was modified from Simpson *et al.*, 2009.

A novel pathway component, Kif7, has been recently identified to transduce the signal from Smo to the Gli proteins (Cheung *et al.*, 2009; Endoh-Yamagami *et al.*, 2009;

Liem *et al.*, 2009) (Figure 2.2). Kif7 is the mammalian ortholog of costal-2, which is an important component of the Hh pathway in *Drosophila*. Kif7 is located at the cilia and interacts with the Gli proteins and controls its processing (Cheung *et al.*, 2009; Liem *et al.*, 2009). Gli repressor forms are no longer produced and Gli activators are formed instead. This processing of the Gli proteins requires the help of intraflagellar transport proteins as well (Haycraft *et al.*, 2005; Huangfu and Anderson, 2005). At the same time, Sufu has also been shown to control Gli2 and Gli3 stability independently of the cilia (Chen *et al.*, 2009).

2.3 SHH in embryogenesis

The Shh signaling pathway plays a critical role in the growth of a myriad of tissues and organs of the mammal. This includes the nervous system, lungs, heart, left-right asymmetry of the body, limbs, gastrointestinal tract and teeth, among many others (Ingham, 2001; Hooper and Scott, 2005).

The Shh knockout mouse model demonstrated the widespread requirement for Shh in embryonic patterning (Chiang *et al.*, 1996). The Shh knockout mice died at birth and analysis of the embryos revealed severe defects like the absence of limbs and spinal column, smaller brains and cyclopia (Chiang *et al.*, 1996). Shh is first secreted from the notochord, which is a rod-like structure derived from the mesoderm (Roelink *et al.*, 1994). Shh diffuses from the notochord to the overlying neural tube and induces the formation of the floor plate cells which in turn secretes Shh (Roelink *et al.*, 1994; Marti *et al.*, 1995) (Figure 2.3). Together, the floor plate and notochord are the main signaling centers that confer ventral character to the neural tube. Elsewhere, in the embryo, Shh is expressed in the zone of polarizing activity (ZPA) in the limb bud that controls the polarity of limbs (Echelard *et al.*, 1993).

The expression of Shh is controlled by several enhancer-elements that are located near or within the Shh gene or distal to the transcription start site (Epstein *et al.*, 1999). They cooperatively regulate the expression of Shh along the rostral-caudal axis of the neural tube, including parts of the forebrain, midbrain and spinal cord (Epstein *et al.*, 1999) (Figure 2.3).

The expression of Shh is also regulated by Forkhead box A2 (FoxA2) transcription factor as FoxA2 binds to the Shh floor plate enhancer 2 to drive transcription of *Shh* in the floor plate (Jeong, 2003).

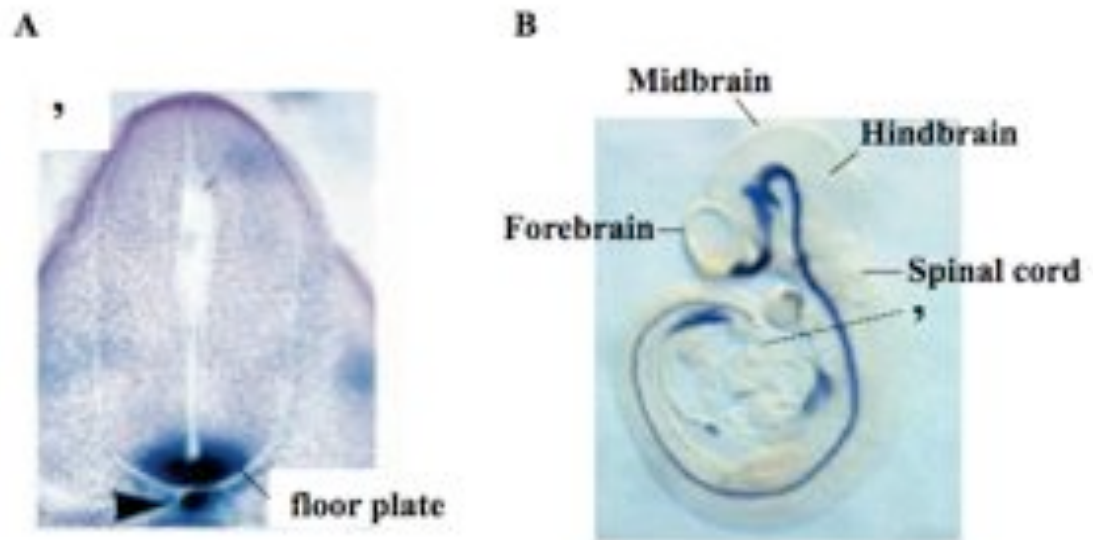


Figure 2.3 Expression of Shh during development. Whole-mount *in-situ* hybridization of *Shh* in E9.5 days post coitum mouse embryo showing (A) the cross section of the spinal cord (dotted line ' in B) showing *Shh* expression in the notochord (arrow head) and floor plate above. (B) The expression of *Shh* in the floor plate throughout the neural tube. Labeled are the subdivisions along the rostral-caudal axis of the forebrain, midbrain, hindbrain and the spinal cord. This figure was reproduced from Epstein *et al.*, 1999.

2.4 SHH and neural development

During the initial phase of neural induction, the ectoderm is induced by signals from the underlying mesoderm to divide into three regions, the neural plate, non-neural ectoderm and neural plate border, which will eventually give rise to the central nervous system (CNS), epidermis and the neural crest, respectively (Figure 2.4). Neurulation occurs when the epithelium on the neural plate thickens and the ends fold up and fuse together to form the neural tube along the rostral (head) and caudal (tail) axis (Colas and Schoenwolf, 2001). The folded edges form the dorsal part of the tube while the area closest to the underlying notochord is the ventral area.

After neurulation, the epithelial cells on the neural plate (or neuroepithelial cells) undergo an expansion phase where they proliferate rapidly. Their progeny, termed neural precursors, assume positional identities and eventually leave the cell cycle and give rise to a diverse array of post-mitotic neurons that make up the CNS.

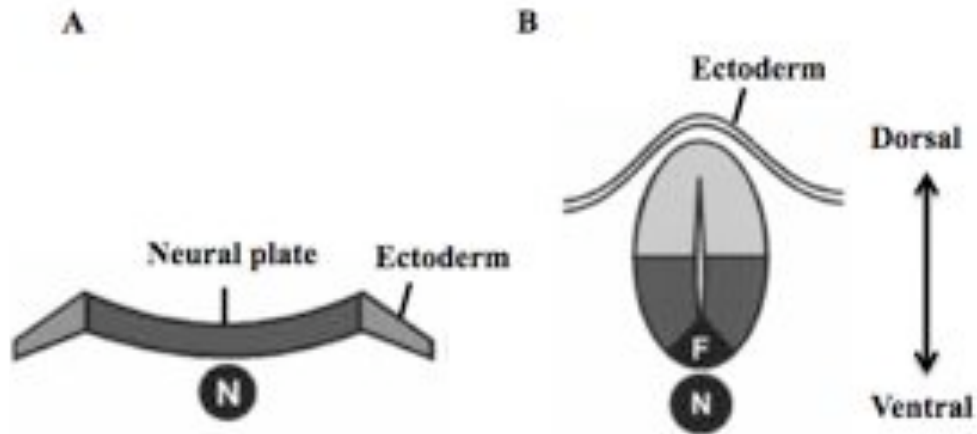


Figure 2.4 Formation of the neural tube. (A) During neural induction, the neural plate is flanked by the non-neural ectoderm. The notochord (N) lies below the neural plate. (B) The neural plate folds up upon itself and fuses to form the neural tube. The underlying notochord secretes SHH which is necessary for the formation of the floor plate (F). The non-neural ectoderm eventually forms the epidermis. The arrows indicate the dorsal-ventral axis of the neural tube. This figure was modified from Briscoe et al., 1999.

The position of the neuroepithelial cells along the rostral-caudal and dorsal-ventral axis determines the morphogens the cells get exposed to, that will restrict and specify the eventual identity of the progeny. The rostro-caudalizing signals come mainly from retinoic acid (RA), Wnt and fibroblast growth factors (FGF) that organize the neural tube into the forebrain, midbrain, hindbrain and spinal cord. The Shh and bone morphogenetic proteins (BMP) play important roles in patterning the dorsal-ventral aspect of the neural tube.

The BMP signal the ectoderm to become the epidermis while blocking specification of the neuroectoderm (Muñoz-Sanjuán and Brivanlou, 2002). Bmp are secreted from roof plate cells in the dorsal neural tube and induce formation of neural crest stem cells and dorsal interneurons (Barth *et al.*, 1999). Antagonists of Bmp signaling like chordin, noggin and follistatin are secreted from the notochord below and this antagonism of Bmp signaling

permits neuroectoderm differentiation. Bmps also intersect with the Shh pathway to limit the ventralizing activity of Shh (Liem *et al.*, 2000).

The function of Shh in specifying the diverse and distinct neuronal cell fates in the neural tube, in particular in the spinal cord, has been extensively studied. The neuroepithelium in the ventral half of the spinal cord can be divided into progenitor domains known as pMN, p3, p2, p1 and p0 (Figure 2.5). Eventually, 5 populations of neurons will arise from their respective progenitor domains. They are namely motor neurons (MN) and the interneurons V3, V2, V1 and V0 that help to coordinate motor output (Jessell *et al.*, 2000; Briscoe and Ericson, 2001). Loss-of-function studies have shown that without Shh, the neural tube lacked the floor plate and p3, pMN and p2 domains, while p1 and p0 domains were displaced dorsally (Litingtung and Chiang, 2000).

Shh which is initially secreted from the notochord and floor plate cells, diffuses along the dorsal-ventral axis to form a concentration gradient of Shh, which is responsible for specifying cell fates (Briscoe and Ericson, 1999). In chick neural tube explant cultures, different concentrations of Shh managed to induce different identities of cells. Higher concentrations of Shh were required to induce the most ventral neuronal subtypes while lower concentrations specified more dorsal neuronal subtypes (Ericson *et al.*, 1997) (Figure 2.5). The Ptch1 receptor for Shh is similarly expressed in a gradient in the neural tube with the highest levels at the floor plate (Goodrich *et al.*, 1996).

Shh is proposed to achieve patterning of the neural tube by regulating homeodomain transcription factors, which are expressed in distinct positions in the neural tube (Figure 2.5) (Briscoe *et al.*, 2000). The homeodomain transcription factors are divided into two classes: Class I and II. At the dorsal neural tube, the class I transcription factors like paired box 7 (Pax7), Pax6, developing brain homeobox 1 (Dbx1) and Dbx2 are repressed by Shh while the Class II proteins like NK2 homeobox 2 (Nkx2-2) and Nkx6-1 are induced by Shh (Mansouri and Gruss, 1998; Briscoe *et al.*, 1999, 2000; Sander *et al.*, 2000). The Class I and II proteins in adjacent domains also cross-repress one another. For instance, the targeted removal of Nkx6-1 resulted in the normally dorsal domains of Dbx2 expanding into the ventral region

and the disruption in formation of the pMN domain and corresponding motor neurons (Sander *et al.*, 2000). Therefore, different sensitivities to the repressive or activating effects of Shh and a cross repressive action of the class I and II proteins result in a code that leads to defined progenitor domains. This eventually translates to generation of specific post-mitotic neurons that have unique positional identity.

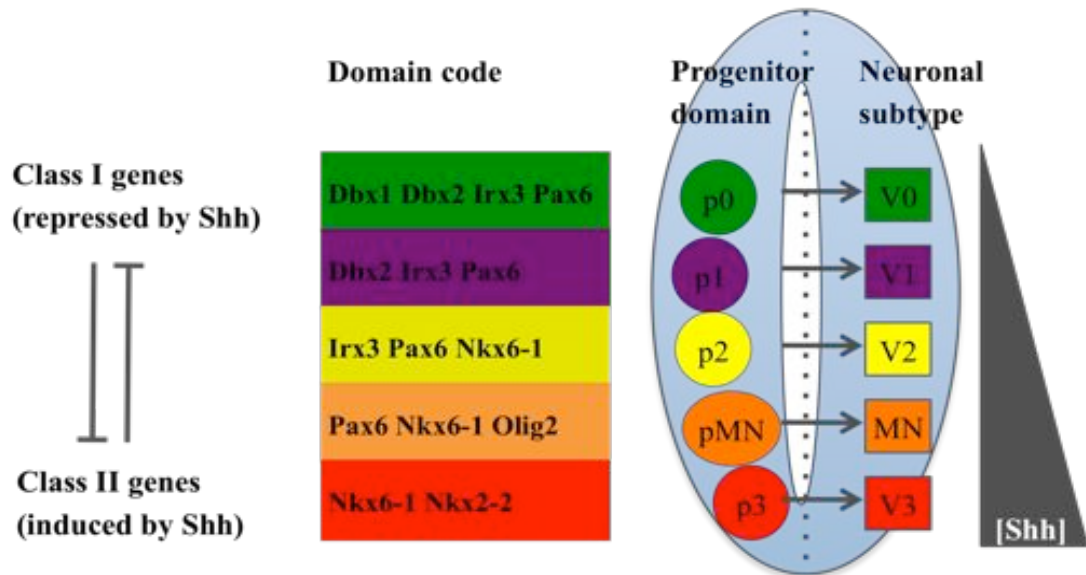


Figure 2.5 A model for how Shh patterns neurons of distinct cell fate in the spinal cord. Shh from the floor plate diffuses dorsally to establish a concentration gradient. The neural tube is divided into distinct progenitor domains (p0-3, pMN) that generate distinct neuronal subtypes: interneurons V0-V3 and motor neurons (MN). The progenitor domains are characterized by transcription factors that are broadly grouped into Class I and II genes. Shh induces the Class I genes Nkx6-1, Nkx2-2 and Olig2, which are more ventrally expressed. The Class I genes Dbx1, Dbx2, Irx3 and Pax6 are dorsally expressed and repressed by SHH.

The confirmation of Shh as a morphogen working through long distances was provided by studies whereby disruption of the Shh transduction pathway resulted in transformations of neuronal fates. The ectopic expression in the neural tube of the mutated form of Ptc1, which was insensitive to Shh binding, resulted in cells having a dorsal identity instead of the expected ventral identity (Briscoe *et al.*, 2001). Similarly, Smo knockout mutant mice that were unable to transduce the Shh signal did not form the floor plate nor the MN, V3, V2, or V1 interneurons (Wijgerde *et al.*, 2002). Conversely, ectopic expression of a

constitutively active form of Smo was able to mimic the effect of Shh to induce ventral cell types throughout the neural tube in a cell autonomous manner (Hynes *et al.*, 2000).

All the Gli proteins are required to mediate responses to Shh during patterning of the neural tube (Bai *et al.*, 2004). Gli2 knockout mice do not specify the ventral most cells in the neural tube (Ding *et al.*, 1998; Park *et al.*, 2000). Shh is also required to inhibit the repressive action of Gli3 that is normally expressed in the neural tube. In the absence of Shh, Gli3 acts primarily to dorsalize the neural tube (Litington and Chiang, 2000). Shh thus acts to prevent Gli3 repressor formation and induce the formation of Gli3 activator protein, which is required for ventral specification of the neural tube (Koebernick and Pieler, 2002; Bai *et al.*, 2004)

2.5 SHH and proliferation

The patterning of the neural tube must be accompanied by expansion of the neuroepithelial cells to generate sufficient numbers before they exit the cell cycle and begin terminal differentiation to diverse neuronal cell types (Lupo *et al.*, 2006; Wilson and Stice, 2006). Several studies have shown that another function of Shh is to promote the proliferation and survival of neuroepithelial cells. This was demonstrated when ectopic activation of the pathway via the constitutively active Smo induced overgrowth of the dorsal neural tube (Hynes *et al.*, 2000). Similarly, mouse embryos that lacked the inhibitory protein Hhip had noticeably larger neural tubes (Jeong and McMahon, 2005). At the same time, blockade of Shh signaling in neuroepithelial cells resulted in a decrease in cell survival and proliferation (Cayuso *et al.*, 2006a). Later on in development after the structures of the brain are formed, Shh also regulates the proliferation of neural precursors in the cerebellum (Dahmane and Ruiz i Altaba, 1999; Wechsler-Reya and Scott, 1999; Pons *et al.*, 2001).

In the adult brain, Shh maintains the neural stem cells (NSC) population that are found in two areas, the hippocampal gyrus and the subventricular zone of the lateral vesicles. NSC from these two areas of the brain express components of the Shh pathway (Palma *et al.*, 2005), and conditional removal of the Smo receptor reduces the ability of the NSC to

proliferate and reform neurospheres in culture (Machold *et al.*, 2003). On the other hand, exposure to Shh increases the proliferation of the NSC (Lai *et al.*, 2003; Palma *et al.*, 2005). Shh controls proliferation of cells via cell cycle proteins like Cyclin D1 and N-Myc (Kenney and Rowitch, 2000; Kenney *et al.*, 2003; Oliver *et al.*, 2003). The mode of action of Shh in cell survival is also attributed to the induction of the anti-apoptotic factor, Bcl2 (Bigelow *et al.*, 2004; Cayuso *et al.*, 2006b).

2.6 SHH in developmental disorders and cancer

Striking consequences arise from deregulation of the SHH pathway during human development. Mutations in the *SHH*, *PTCH1* and *GLI2* genes causes the developmental disorder holoprosencephaly (Roessler *et al.*, 1996; Ming *et al.*, 2002; Roessler *et al.*, 2003). Holoprosencephaly is characterized by forebrain malformation and associated with mental retardation and severe craniofacial anomalies like cyclopia or proboscis formation (Ming and Muenke, 1998). The most severe form is embryonic lethal. The mutations in *SHH* have been reported to result in impaired synthesis of SHH and dysregulation of target genes (Schell-Apacik *et al.*, 2003; Singh *et al.*, 2009). Mutations in *GLI3* have also been implicated in two other congenital syndromes, Greig cephalopolysyndactyly and the Pallister-Hall syndrome (Biesecker, 2006).

Dysregulation of the SHH pathway in adults can also lead to several cancers. One of the first known cancers linked to the SHH pathway is the nevoid basal cell carcinoma syndrome (Gorlin's syndrome), a disorder that predisposes the patient to developmental anomalies and different neoplasms, most often basal cell carcinoma. Constitutive activation of the SHH pathway following *PTCH1* mutation accounts for 30-40% of patients with Gorlin's syndrome (Mullor *et al.*, 2002). Medulloblastomas, a cancer of the brain, is also caused by mutations in SHH pathway components, resulting in the activation of the pathway (Dahmane *et al.*, 2001; Berman *et al.*, 2002). Therefore, therapeutic drugs targeting the SHH pathway are currently being developed, such as inhibition of the pathway with a small

molecule inhibitor of Smo, which eliminated medulloblastomas in the mouse model and promoted tumor-free survival of the mice (Romer *et al.*, 2004).

Given the importance of SHH in early mammalian development, there is significant value in studying its function in human embryonic stem cells (hESC), which are *in vitro* counterparts of the inner cell mass of the pre-implantation human embryo. hESC therefore serve as an effective *in vitro* system to study complex events underlying human nervous system development (Ben-Nun and Benvenisty, 2006; Dvash *et al.*, 2006).

2.7 Embryonic stem cells and induced pluripotent stem cells

Embryonic stem cells (ESC) have two characteristics that distinguish them from other stem cells, in that they are capable of long-term self-renewal and they can differentiate to all cell types present in the body. Nearly three decades ago, the first mouse ESC (mESC) were isolated from the inner cell mass of the blastocyst from the pre-implantation embryo. (Evans and Kaufman, 1981).

The blastocyst is formed after a fertilized egg undergoes multiple cellular divisions and is composed of 3 layers - the outer trophoblast that eventually becomes the placenta, a hollow cavity and finally the inner cell mass, which will eventually develop into the embryo. During gastrulation, the inner cell mass undergoes spatial reorganization to generate the three embryonic germ layers – ectoderm, mesoderm and endoderm. The ectoderm gives rise to the nervous system, skin and eyes; the mesoderm gives rise to the circulatory system including the heart, bone, muscles and kidneys; while the endoderm gives rise to the gastrointestinal tract, respiratory tract, liver and pancreas. As ESC are derived from the inner cell mass, they retain the ability to differentiate to cell types of all three germ layers *in vitro* (Figure 2.6).

It was not until 14 years later that similar cells were isolated from human embryos generated through *in vitro* fertilization (Bongso *et al.*, 1994) and subsequently propagated indefinitely in culture (Thomson *et al.*, 1998). Since then, there has been intense research on hESC worldwide. Like mESC, hESC are able to differentiate into all cell types of the body

too. However, there are crucial differences between mESC and hESC, one of which is the difference in signaling pathways required to maintain pluripotency. mESC self-renew via the leukaemia inhibitory factor (LIF) activated JAK/STAT pathway. However, this pathway has been found to be dispensable for maintenance of hESC (Humphrey *et al.*, 2004). mESC and hESC also have differing cell morphology and gene expression profiles (Ginis *et al.*, 2004; Wei *et al.*, 2005). Interestingly, a recently mESC-like cell line, known as epiblast stem cells (EpiSC) have been found to be a more similar to hESC than the traditional mESC (Brons *et al.*, 2007; Tesar *et al.*, 2007). EpiSC are derived at a later stage of embryonic development from the post-implantation embryo as compared to mESC, which could account for their resemblance with hESC. Therefore, the study of SHH signaling in hESC offers to augment the current understanding of the role of SHH in humans, that is based largely on the mouse model.

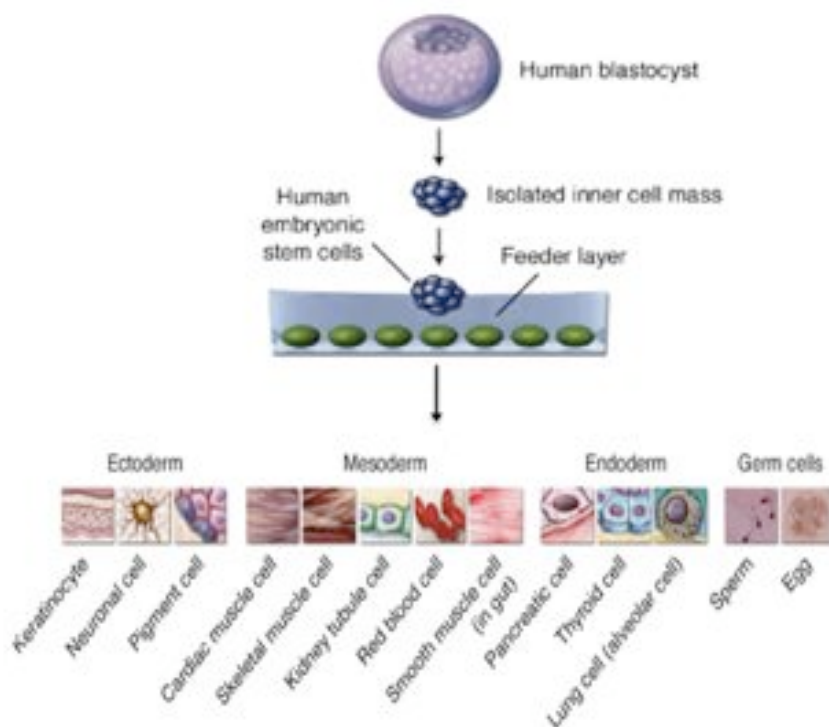


Figure 2.6 Human embryonic stem cells (hESC) derived from the blastocyst are able to differentiate into cells from each germ layer. This figure was modified from Hyslop *et al.*, 2005b.

A breakthrough in stem cell research occurred recently when researchers genetically reprogrammed adult somatic cells to a stem cell-like state (Takahashi and Yamanaka, 2006). These cells termed as induced pluripotent stem cells (iPSC) were established by introducing the four ‘Yamanaka’ factors – Oct4, Sox2, c-myc and Klf4 into mouse embryonic fibroblasts. The expression of these 4 factors were sufficient to reprogram the cells back into a pluripotent state. The iPSC were shown to be able to differentiate into cells from all three germ layers, form teratomas *in vivo* and contribute to chimeras (Takahashi and Yamanaka, 2006). Human iPSC were subsequently derived from human dermal fibroblasts using the same four factors (Takahashi *et al.*, 2007). Another human iPSC cell line, iPSC(IMR90) which was used in this thesis, was reprogrammed from lung fibroblasts using an alternative panel of factors OCT4, SOX2, NANOG and LIN28 (Yu *et al.*, 2007). Since then, there have been a great number of laboratories that have generated iPSC from an array of differentiated cells from both the mouse and human sources using different approaches (Maherali and Hochedlinger, 2008; Feng *et al.*, 2009). iPSC present the possibility of producing patient-specific stem cells. Cells from patients can first be reprogrammed into iPSC, which can then be differentiated into the required cell type for subsequent autologous transplantation. This has been explored in the mouse model of Parkinson’s disease and sickle cell anemia (Hanna *et al.*, 2007; Wernig *et al.*, 2008). While iPSC and hESC can be distinguished by their global epigenetic methylation patterns, genetic and microRNA expression patterns, they are believed to behave in a largely similar manner (Chin *et al.*, 2009b; Doi *et al.*, 2009). The iPSC(IMR90) cell line will be used in this research thesis as a second pluripotent stem cell line to confirm the results observed in hESC.

2.8 Culture of hESC

There are several methods for maintaining hESC in an undifferentiated state *in vitro*. Traditionally, hESC are grown in co-culture with a mouse embryonic fibroblast (MEF) feeder layer (Thomson *et al.*, 1998; Reubinoff *et al.*, 2000). They can also be cultured without

feeders on an extra-cellular matrix, like Matrigel, but still requiring media conditioned by MEF (Xu *et al.*, 2001; Choo *et al.*, 2006) or human-derived fibroblasts (Richards *et al.*, 2003; Inzunza *et al.*, 2005). In the drive to move away from undefined factors in serum and possible xenopathogens present in animal-derived feeders or extracellular matrices, defined animal and serum-free media have been developed to qualify hESC for future clinical use (Chin *et al.*, 2009a).

In the various kinds of culture conditions, exogenous FGF2, TGF β and activin A are crucial factors required for the maintenance of self-renewal (Vallier *et al.*, 2004; Beattie *et al.*, 2005; Dvorak *et al.*, 2005; Xu *et al.*, 2005; Levenstein *et al.*, 2006; Xiao *et al.*, 2006). It must be noted that for mESC, despite its similarities to hESC, self-renew via the leukaemia inhibitory factor (LIF) activated JAK/STAT pathway. However, this pathway that has been found to be dispensable in hESC culture (Humphrey *et al.*, 2004).

2.9 Signaling pathways in hESC

The FGF and TGF β /Activin pathways are the principal signaling pathways that sustain hESC pluripotency and active signaling through both pathways are required for the maintenance of hESC (Xu *et al.*, 2008) (Figure 2.7). Exogenous FGF2 is widely used in the culture of hESC with conditioned media and at higher concentrations, in defined media (Xu *et al.*, 2005; Levenstein *et al.*, 2006). FGF2 directly activates the mitogen-activated protein kinase (MAPK) pathway (Li *et al.*, 2007) and the downstream targets of FGF2 signaling include members of the TGF β pathway (Greber *et al.*, 2007). FGF2 also maintains hESC self-renewal by promoting cell adhesion and survival (Eiselleova *et al.*, 2009) and preventing differentiation by suppressing the differentiating activity of BMPs present in the widely used commercial serum for culture of hESC. In feeder cultures, FGF2 also promotes cell growth by indirectly stimulating the fibroblasts to release factors like TGF β 1 and insulin-like growth factor 1 (IGF1) that can support hESC growth (Greber *et al.*, 2007). FGF2 has also been shown to induce the production of TGF β and IGF2 from fibroblasts derived from

differentiating hESC during culture to create a niche supporting self-renewal (Bendall *et al.*, 2007).

The FGF signaling pathway acts synergistically with the TGF β /Activin pathway to maintain hESC pluripotency (Vallier, 2005). The secreted factors of the TGF β superfamily like Nodal, Activin A and TGF β 1 are expressed by hESC (Beattie *et al.*, 2005) and they activate the downstream SMAD2/3 proteins to regulate gene expression. Recently, the transcription factor NANOG that controls hESC pluripotency has been found to be a direct target gene of SMAD2/3 proteins (Xu *et al.*, 2008; Vallier *et al.*, 2009). The importance of the pathway was demonstrated when inhibition of the pathway induced rapid differentiation of hESC (James, 2005; Vallier, 2005). The TGF β 1/Activin A pathway has been suggested to maintain hESC pluripotency by antagonizing BMP activity (Beattie *et al.*, 2005; James, 2005; Vallier, 2005) and blocking differentiation towards the neuroectoderm (Vallier *et al.*, 2004). On its own, exogenous Activin A is able to maintain hESC self-renewal in the absence of feeder layers or conditioned media (Xiao *et al.*, 2006). Activin A also induces the expression of the transcription factors *OCT4* and *NANOG* that regulate hESC pluripotency and also the genes of the FGF pathway like *FGF2* and the receptors *FGFR1*, 2 and 3 (Xiao *et al.*, 2006).

There are other signaling pathways operating in hESC (Figure 2.7), such the WNT signaling pathway that stimulates proliferation of hESC (Sato *et al.*, 2004; Dravid *et al.*, 2005; Cai *et al.*, 2007). The importance of WNT was recently demonstrated to enhance formation of iPSC, possibly by increasing cell proliferation during genetic reprogramming (Marson *et al.*, 2008). Other factors and pathways have also been implicated in promoting hESC renewal like sphingosine-1-phosphate (S1P) combined with platelet-derived growth factor (PDGF) pathway (Pebay *et al.*, 2005) and neurotrophins that activate the PI3K/Akt pathway (Pyle *et al.*, 2006). The NOTCH signaling pathway is another developmentally important pathway but was found to play a negligible role in undifferentiated hESC (Noggle *et al.*, 2006).

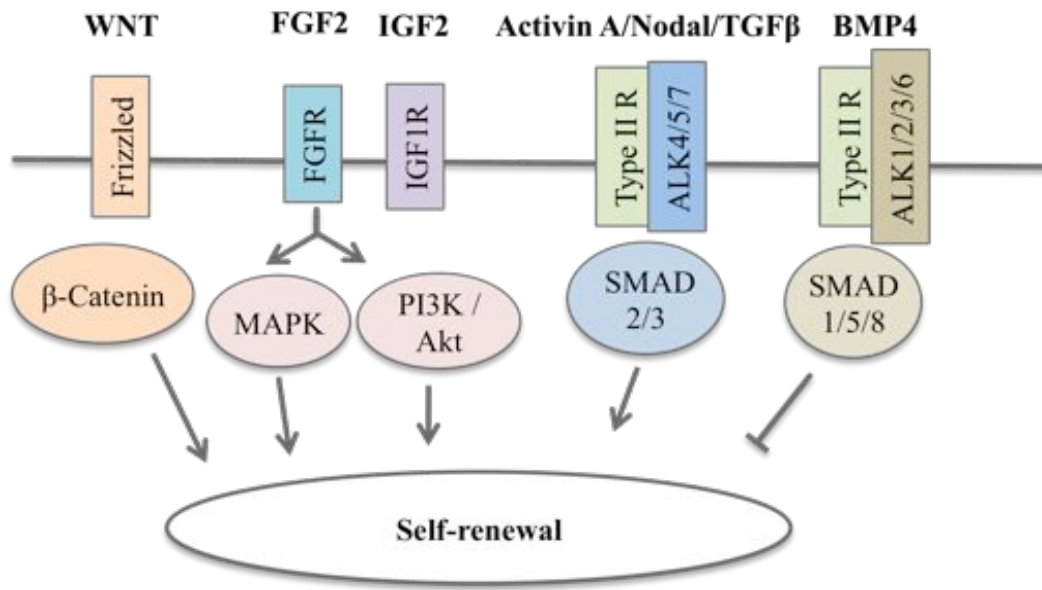


Figure 2.7 Signaling pathways maintaining hESC self-renewal. The WNT ligand binds to the Frizzled receptor which allows β -Catenin to translocate to the nucleus and activate transcription. FGF2 binds to the FGF receptors (FGFR) and activates the PI3K/Akt and MAP kinase pathways. IGF2 secreted from feeder cells binds to the IGF1 receptor (IGFIR) and activates the PI3K/Akt pathway as well. Activin/Nodal/TGF β belong to the TGF superfamily of proteins and signal via the Type I (ALK 4/5/7) and Type II receptors that form heterodimers, which subsequently activates SMAD2/3. BMP signals via the Type I (ALK 1/2/3/6) receptors and activates SMAD1/5/8 to promote differentiation.

The abovementioned studies present a complex picture in which hESC self-renewal is dependent on several signaling pathways. To date, there have not been studies to address the possible function of the SHH signaling pathway in undifferentiated hESC. As such, it warrants greater study so that a more complete understanding of how hESC self-renew may be attained.

2.10 Transcriptional networks in hESC

NANOG, OCT4 and SOX2 are transcription factors of a conserved core transcriptional regulatory network that is essential for specifying the undifferentiated state of ESC. These three factors bind to their own promoter to maintain their own expression and

they co-occupy their target genes to either repress or activate expression (Boyer *et al.*, 2005; Loh *et al.*, 2006). These 3 factors are hallmarks of the pluripotent undifferentiated state of ESC and the loss of their expression leads to ESC differentiation.

NANOG, named after the mythical Celtic land of Tir nan Og, is expressed in the inner cell mass of the early embryo and the developing germ cell (Nichols *et al.*, 1998; Chambers *et al.*, 2003; Mitsui *et al.*, 2003). Loss of Nanog results in embryonic lethality (Mitsui *et al.*, 2003). Inhibition of *NANOG* gene expression leads to hESC differentiation to the extraembryonic cell lineages (Hyslop *et al.*, 2005a; Zaehres *et al.*, 2005) while overexpression of NANOG allows hESC to proliferate independently of feeder cells (Darr *et al.*, 2006). The expression of NANOG is controlled by OCT4 and SOX2 as well as PBX1 and KLF4 (Kuroda *et al.*, 2005; Chan *et al.*, 2009).

OCT4 (also known as POU5F1) is a member of the POU family of homeobox transcriptional factors and like NANOG, has restricted expression in the inner cell mass and germ cells in the early embryo (Nichols *et al.*, 1998). Its expression levels govern different fates of ESC whereby an increase in Oct4 causes differentiation into the primitive endoderm while loss of Oct4 causes differentiation to the trophectoderm lineage (Hansis *et al.*, 2000; Niwa *et al.*, 2000).

SOX2 (SRY-related HMG box 2) is also expressed in the inner cell mass and epiblast of the blastocyst (Avilion *et al.*, 2003). Although Sox2 is also expressed in cells of the neuroectoderm lineage (Avilion *et al.*, 2003; Eminli *et al.*, 2008), the expression of SOX2 in ESC indicates pluripotency and a crucial factor in maintaining hESC pluripotency (Fong *et al.*, 2008). Besides transcriptional regulation of genes, the stem cell pluripotent state can be regulated by epigenetic modifications and microRNAs (Gan *et al.*, 2007; Xu *et al.*, 2009).

2.11 Applications of hESC research

There are many potential applications for hESC-derived specialized cells in human disease, for instance: hepatocytes for drug screening and toxicological studies,

cardiomyocytes to improve heart function after myocardial infarct, pancreatic beta-cells to replace insulin-producing cells destroyed in Type 1 diabetes and neurons to treat nervous system disorders (Hyslop *et al.*, 2005b). One nervous system disorder, Parkinson's disease, is a neurodegenerative movement disorder that affects individuals above the age of 60. It is characterized by tremor, rigidity and bradykinesia, arising from the death by apoptosis of dopaminergic (DA) neurons along the nigrostriatal pathway (de Lau and Breteler, 2006). DA neurons secrete dopamine that controls the activity of neural circuits. There is currently no cure for Parkinson's disease although medication can compensate for lack of dopamine. Parkinson's disease serves as a model for neuronal transplantation studies because the disease occurs due to death of a specific cell type (DA neurons) and in a particular area (substantia nigra in the midbrain).

The loss of function following neurodegeneration may potentially be restored by cell replacement therapy. Before hESC were available as a source for generating neurons, most of the effort to derive neurons *in vitro* was done using neural stem cells (NSC) isolated from embryonic or adult CNS tissues. They are also sometimes also referred to as neural progenitors. NSC are clonogenic and can be cultured for long periods and retain the ability to give rise to the three major cell lineages of the CNS, namely, neurons, astrocytes and oligodendrocytes (Gage, 2000). Animal studies have shown that transplantation of fetal NSC-derived neurons have been beneficial for the treatment of Parkinson's disease and stroke (Lindvall and Hagell, 2002; Olanow *et al.*, 2009, Jeong *et al.*, 2003). The transplanted NSC are also thought to enhance survival of endogenous cells at the injured site indirectly through paracrine effects and modulation of inflammatory response (Bacigaluppi *et al.*, 2008).

Fetal or adult NSC are however not ideal sources of neurons as they have limited expansion capability necessary for transplantation work, and tend to generate progeny that are more regionally restricted, depending on the region and developmental time frame that they were derived from. (Guillaume and Zhang, 2008). Consequently, the attention has now shifted towards deriving neurons from hESC. hESC present the ideal solution because they

have less lineage restriction and can proliferate to large numbers as the starting material for differentiation into the desired neuronal cell type.

The potential of hESC in cell replacement therapy has been demonstrated in animal models (Kim and De Vellis, 2009). hESC- and monkey ESC-derived neuron transplantation into animal models of Parkinson's disease have shown varying degrees of correction to the symptoms (Ben-Hur *et al.*, 2004; Takagi *et al.*, 2005; Cho *et al.*, 2008). Transplanted neuroprogenitors into the infarcted regions of the brains of rats after stroke was induced showed some improvement of sensorimotor function (Tabar *et al.*, 2005; Hicks *et al.*, 2009). On top of that, oligodendrocytes responsible for forming the myelin sheath around axons have been derived from hESC and were shown to improve spinal cord injuries in rats (Faulkner and Keirstead, 2005; Sharp *et al.*, 2009). This advancement has prompted the establishment of the first-ever human clinical trial using oligodendrocytes derived from hESC for treatment of acute spinal cord injury (Geron Corp., 2009).

However, there are several scientific hurdles that need to be overcome before hESC-based therapy can be a reality. These include preventing immune rejection of transplanted cells (Grinnemo *et al.*, 2008) and also ensuring the removal of residual undifferentiated cells that can proliferate to form tumours in the future (Bjorklund *et al.*, 2002). Finally, it requires that effective and efficient guidance of hESC down the differentiation pathway to achieve a pure population of the desired cell type in sufficient numbers. In order to overcome the last hurdle, there has been intense effort over the last few years to understand the mechanisms of neural differentiation.

2.12 Neural differentiation of hESC

To achieve directed differentiation of neurons, it is essential that there is sufficient knowledge of the differentiation process and the underlying molecular mechanisms controlling cell fate choices.

Within the numerous methods to derive neurons from hESC, the differentiation process generally follows a framework that first requires induction of differentiation to the neuroectoderm to obtain neuroprogenitors. This is then followed by the expansion and patterning of the neuroprogenitors such that they assume positional identity with a more committed cell fate. Lastly, the neuroprogenitors are further differentiated to more specific neuronal subtypes with unique characteristics.

2.12.1 Neural induction

Neural induction can be achieved by co-culture of hESC with stromal cells like PA6 (Mizuseki *et al.*, 2003; Park *et al.*, 2005) and MS5 (Perrier *et al.*, 2004; Lee *et al.*, 2007; Sonntag *et al.*, 2007). This co-culture method has been used to derive neural crest precursors (Pomp *et al.*, 2005), and more commonly, DA neurons (Perrier *et al.*, 2004; Park *et al.*, 2005; Takagi *et al.*, 2005; Chiba *et al.*, 2008). The ability of these stromal cells to promote differentiation is termed stromal-derived inducing activity (SDIA). This activity has been attributed to secreted factors from the stromal cells and also cell surface interactions that enhance neurogenesis (Kawasaki *et al.*, 2000; Vazin *et al.*, 2008, 2009). However, the molecular mechanism by which stromal cells induce differentiation remains to be elucidated.

Other groups have also employed the BMP inhibitor noggin to induce neural differentiation. To derive neuroprogenitors, noggin can be used with hESC grown either on a MEF layer (Ben-Hur *et al.*, 2004; Peh *et al.*, 2009), or in defined media in adherent cultures or in suspension as neurospheres (Gerrard *et al.*, 2005; Itsykson *et al.*, 2005). Noggin treatment upregulates the expression of neuroectoderm markers such as PAX6 and NESTIN (Pera *et al.*, 2004) and enriches the culture for neuroprogenitors expressing neuronal markers such as PSA-NCAM (Gerrard *et al.*, 2005; Itsykson *et al.*, 2005). It is proposed that by blocking BMP signaling which is instructive for extraembryonic endoderm specification (Pera *et al.*, 2004), noggin is able to promote neural differentiation and inhibit differentiation towards the endoderm lineage, thus increasing the proportion of neuroprogenitors obtained from hESC.

The other commonly adopted protocol begins with the formation of EB to induce differentiation. The EB are then plated on a defined substrate such as Matrigel or laminin and propagated in a defined media supplemented with FGF2 to form neuroprogenitors that express high levels of neuroectoderm markers (Zhang *et al.*, 2001; Cho *et al.*, 2008; Elkabetz *et al.*, 2008).

The methods described above produce neuroprogenitors that contain cells with a distinctive morphology known as rosettes that are considered a hallmark of neural differentiation. Rosettes are radially arranged small elongated cells resembling the early neural tube (Zhang *et al.*, 2001) and express neuroectoderm markers like PAX6, NESTIN, MUSASHI and SOX1 (Zhang *et al.*, 2001; Itsykson *et al.*, 2005; Elkabetz *et al.*, 2008). They are believed to have a default rostral forebrain character but at the same time, can be respecified to cells of the caudal fate like motor neurons (Pankratz *et al.*, 2007; Elkabetz *et al.*, 2008). Neuroprogenitors can be expanded as cellular aggregates termed neurospheres or as adherent cell cultures with mitogens such as epidermal growth factor (EGF) and FGF2 over an extended period of time (Shin *et al.*, 2006; Joannides *et al.*, 2007).

2.12.2 Neural subtype specification

Neuroprogenitors can be differentiated into several desired neural subtypes using inductive factors that activate multiple signaling cascades. The neural subtypes are evaluated by criteria like cellular morphology, expression (and non-expression) of lineage specific markers and the exhibition of functional activity e.g. the secretion of neurotransmitters or firing of action potentials. This section discusses the use of SHH to differentiate neuroprogenitors to motor neurons and DA neurons.

Given that SHH is crucial for the patterning of the neural tube, it is not surprising that SHH is one of the key factors used to limit the differentiation of hESC to neurons with specific regional identity. As with its *in vivo* function, SHH confers ventral identity to neuroprogenitors (Li *et al.*, 2005; Lazzari *et al.*, 2006), through the control of the Class I and II homeodomain factors (Okada *et al.*, 2004; Crawford and Roelink, 2007).

The derivation of motor neurons from ESC requires the combinatorial action of both SHH and RA, whereby the addition of SHH and RA increased the yield of Hb9 positive motor neurons that express the appropriate markers and display an electrophysiological response. (Wichterle *et al.*, 2002; Lim *et al.*, 2006; Li *et al.*, 2008). RA is a widely used chemical that promotes neural differentiation of ESC (Bain *et al.*, 1995; Carpenter, 2001; Reubinoff *et al.*, 2001; Park *et al.*, 2004; Baharvand *et al.*, 2007). It is also used as a patterning factor to promote differentiation of neurons towards a more caudal fate, e.g. motor neurons (Wichterle *et al.*, 2002; Li *et al.*, 2005). RA treatment induces neuroprogenitors to express genes commonly found in the hindbrain and spinal cord, like the Hox family genes, but not those found in the forebrain (Okada *et al.*, 2004). SHH is proposed to increase motor neuron differentiation via upregulation of its target gene, OLIG2, which is necessary for the development of motor neurons (Lu *et al.*, 2001; Zhou and Anderson, 2002). SHH also acts as a survival factor for OLIG2 positive motor neuron progenitors, thereby increasing the yield of post mitotic motor neurons (Li *et al.*, 2008).

The derivation of midbrain DA neurons from hESC-derived neuroprogenitors is also dependent on the timely application of SHH and FGF8. Midbrain DA neurons express a variety of other transcription factors such as engrailed homeobox 1/2 (En1, En2), LIM homeobox 1A/B (Lmx1A, Lmx1B), nuclear receptor related 1 (Nurr1), Pax2, Pax5, orthodenticle homeobox 2 (Otx2) and paired-like homeodomain 3 (Pitx3) that are important in the patterning, survival and maturation of DA neurons (Smidt and Burbach, 2007). As neurotransmitters, DA neurons release dopamine, whose production depends on the enzymes tyrosine hydroxylase (TH) and aromatic L-amino acid decarboxylase (AADC) for proper metabolism.

During development *in vivo*, DA neurons arise from Shh-positive midbrain floor plate cells (Kittappa *et al.*, 2007; Ono *et al.*, 2007; Bonilla *et al.*, 2008), and induction of DA neurons is dependent on both Shh and Fgf8 (Ye *et al.*, 1998). The downstream target of Shh, FoxA2 is an important determinant of DA differentiation as the loss of FoxA2 abolishes the ability of midbrain explants to form DA neurons *in vitro* (Kittappa *et al.*, 2007). FoxA2

induces the expression of *neurogenin2* (*Ngn2*), *Nurr1*, *Lmx1a* and *Lmx1b*, that are necessary for the development and maturation of DA neurons (Ferri *et al.*, 2007; Lin *et al.*, 2009).

FGF8 is expressed in the midbrain-hindbrain organizer and is important for the patterning of the midbrain (Crossley *et al.*, 1996). As such early treatment of neuroprogenitors with FGF8 helps to direct DA neuron differentiation towards the midbrain phenotype that expresses the midbrain marker *EN1* (Yan *et al.*, 2005). Another signaling molecule TGF β is also important for the induction of DA neurons (Farkas *et al.*, 2003), whereby it synergizes with SHH and FGF8 to increase the population of DA neurons derived from midbrain explants (Roussa *et al.*, 2004).

Based on the understanding from mouse developmental studies, many laboratories have been able to successfully derive mid-brain DA neurons from ESC (Table 2.1). The derivation of DA neurons can be accomplished by co-culturing hESC with stromal cells (Perrier *et al.*, 2004, Schulz *et al.*, 2004, Park *et al.*, 2005, Sonntag *et al.*, 2007), or feeder-free methods that uses FGF2 or noggin to induce differentiation. The patterning molecules SHH and FGF8 and other related factors like BDNF, GDNF, AA, cAMP and TGF β are also added during the extended culture to improve the yield of DA neurons. The gene and protein expression of DA-related markers like TH, EN1, PITX3, LMX1, PAX2, AADC and VMAT are often assayed to authenticate the identity of the cells as midbrain DA neurons. Currently the efficiency of DA neurons derivation is varies widely from 20%-85% (Table 2.1). This is probably due to use of different neural inducing factors, the duration of differentiation or inherent differences between the various hESC lines studied.

As presented in Table 2.1, several groups have extended their *in vitro* study to transplant the hESC-derived neuroprogenitors or neurons into mouse models (Schulz *et al.*, 2004, Park *et al.*, 2005, Roy *et al.*, 2006, Sonntag *et al.*, 2007, Cho *et al.*, 2008, Chiba *et al.*, 2008). Most groups have reported a low survival of transplanted cells. Using the parkinsonian rat model generated by unilateral injection of 6-hydroxydopamine into brain, Cho *et al.* reported that only around 2.7% of the transplanted neurons survived after 12 weeks. Nonetheless, there was behavioural recovery of the parkinsonian rats as displayed by the

Table 2.1 Summary of DA differentiation from hESC.

Reference	Neural induction	Factors	Markers	Efficiency	<i>In vivo</i> Transplantation
Perrier <i>et al.</i> , 2004	MS5	SHH, FGF8, BDNF, GDNF, cAMP, TGF β , AA	TH, EN1, AADC, LMX	60-70% TH of total neurons	No
Schulz <i>et al.</i> , 2004	MedII (HepG2-conditioned media)	FGF2, GDNF, BDNF	TH, VMAT2, AADC	70% TH of total neurons	Few TH+ neurons survived
Yan <i>et al.</i> , 2005	FGF2	SHH, FGF8, AA, BDNF, GDNF	TH, EN1, AADC, VMAT2	30% TH of total cells	No
Park <i>et al.</i> , 2005	PA6-SHH	FGF8, AA, ITS	TH, PAX2, EN1	40% TH of total neurons	No surviving TH neurons
Roy <i>et al.</i> , 2006	FGF2, then co-culture with astrocytes	SHH, FGF8, GDNF, BDNF, 0.5% FBS	EN1, PAX2, OTX2, TH	70% TH of total neurons	1% survival of transplanted cells, behavioural improvement, teratomas observed
Sonntag <i>et al.</i> , 2007	MS5, Noggin	SHH, FGF8, BDNF, AA, cAMP, TGF β	TH, OTX2, PAX2	25% TH of total cells	Variable behavioural improvement, teratomas observed
Cho <i>et al.</i> , 2008	FGF2	SHH, FGF8, AA	TH, AADC, EN1	86% TH of total neurons	2.7% survival of transplanted cells, behavioural improvement, no teratomas observed
Chiba <i>et al.</i> , 2008	PA6, Noggin	Noggin	TH, EN1	Not known	Behavioural improvement, teratomas observed

VMAT = vesicular monoamine transporter, ITS = insulin, transferrin, selenite, HepG2 = human hepatocellular liver carcinoma cell line GDNF = glial cell derived neurotrophic factor, BDNF = brain-derived neurotrophic factor, PA6, MS5 = stromal cell lines, FBS = fetal bovine serum, AA = ascorbic acid, cAMP = cyclic adenosine monophosphate

reduction in apomorphine-induced rotation and amphetamine-induced rotation in transplanted rats. However, the risk of teratoma formation following transplantation of hESC-derived neural cells remains (Roy *et al.*, 2006, Sonntag *et al.*, 2007, Chiba *et al.*, 2008).

Therefore, despite the encouraging initial successes, there needs to be 1) systematic studies to tease out the crucial steps and factors during neural differentiation so that a highly efficient and universal DA differentiation protocol can be obtained, 2) methods to maximise the functional effect of hESC-derived neural cells *in vivo* and 3) long-term transplantation studies to monitor the safety of transplanted cells, before hESC-derived neural cells can proceed onto clinical trials.

CHAPTER 3 MATERIALS AND METHODS

3.1 Molecular cloning

3.1.1 Cloning

The pCHEF-SHH-IRES-DsRed2 vector was constructed by subcloning the chinese hamster elongation factor-1 α (CHEF) promoter from the pCHEF1-EGFP plasmid (Chan *et al.*, 2008) into the pIRES2-DsRed2 plasmid (Clontech, CA, USA, www.clontech.com). The mouse *Shh* gene was amplified from the *Shh* cDNA clone (Open Biosystems, AL, USA <http://www.openbiosystems.com>) using the oligonucleotide primers containing *XhoI* and *Sall* at each end and cloned into the pCHEF-IRES-DsRed2 vector to construct the pCHEF-SHH-IRES-DsRed2 vector (Figure 3.1).

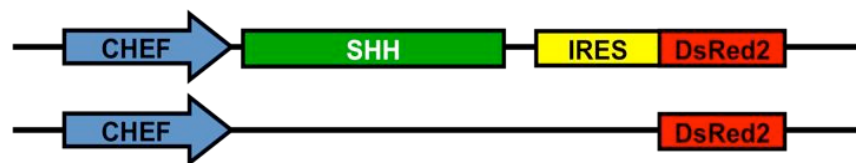


Figure 3.1 Schematic illustration of constructs for generating stable hESC lines. Top: pCHEF-IRES-DsRed2 containing the *Shh* transgene with *DsRed2* reporter gene driven by CHEF promoter. Bottom: Control vector with only *DsRed2* reporter gene. CHEF = chinese hamster elongation factor-1 α , IRES = internal ribosome entry site.

The pCHEF-DsRed2 vector was constructed by first amplifying *DsRed2* from pIRES2-DsRed2 using oligonucleotide primers containing *AgeI* and *XbaI* at each end. The EGFP sequence was excised from the pCHEF1-EGFP vector and the *DsRed2* was cloned in to construct the pCHEF-DsRed2 vector (Figure 3.1). IRES was not included in the pCHEF-DsRed2 vector control as stable cell lines could not be obtained from pCHEF-IRES-DsRed2 vectors.

The Suppressor of Fused (SUFU) expression vector was constructed by subcloning the entire open reading frame of the full length human *SUFU* cDNA clone (Open

Biosystems) into the expression vector pcDNA3.1(+) (Invitrogen, CA, USA, <http://www.invitrogen.com>). All final vectors were sequence-verified. Miss Tan Ker Sin from the Stem Cell Group, Bioprocessing Technology Institute, assisted in the cloning of all plasmids.

3.1.2 Plasmids

CMV expression vectors containing mouse Gli1, mouse Gli2 and human GLI3 were kind gifts from Chi-Chung Hui (Hospital for Sick Children, Toronto, Canada). The 8XGli-BS luciferase reporter plasmid containing 8 copies of Gli-binding sites and 8XmutGli-BS luciferase reporter plasmid containing 8 copies of the mutated binding site were obtained as a gift from Hiroshi Sasaki (Centre for Developmental Biology, RIKEN, Japan) (Sasaki *et al.*, 1997).

To measure the functional response of genes to GLI transcriptional activation, promoter luciferase reporters for selected genes were purchased from SwitchGear Genomics (Menlo Park, CA, USA, <http://www.switchgeargenomics.com>). The CMV expression vector containing mouse Shh was obtained from Open Biosystems.

3.2 Cell Culture

3.2.1 Immortalized mouse fibroblasts

The immortalized mouse fibroblast cell line Δ E-MEF was generated previously in our laboratory and conditioned media obtained from this feeder line has been shown to support the growth of hESC (Choo *et al.*, 2006). Δ E-MEFs were grown in high glucose DMEM (Invitrogen), 2mM L-Glutamine (Invitrogen), 50 units/ml penicillin and streptomycin (Invitrogen) and 10% FBS (HyClone Laboratories, UT, USA) and passaged every 3-4 days.

3.2.2 Preparation of conditioned media from ΔE -MEFs

ΔE -MEFs were treated with mitomycin-C (Sigma, MO, USA, <http://www.sigma.com>) for 2.5 hours and seeded onto gelatin (Invitrogen)-coated T75 flasks (Nunc, NY, USA, <http://www.nalgenunc.com>) in ΔE -MEF culture media to allow cells to stick onto the flask. After 24 hours, media was changed to hESC culture media KNOCKOUT (KO) media consisting of 85% KO-DMEM, 15% KO-Serum Replacer (KO-SR), 1 mM L-Glutamine, 1% non-essential amino acids (NEAA) and 50 units/ml penicillin and streptomycin (all from Invitrogen) and 0.1 mM 2-mercaptoethanol (Sigma). KO media was supplemented with 10 ng/ml FGF2 (Invitrogen) and allowed to equilibrate for 24 hours before collection and filtering through 0.22- μ m filter unit (Nalgene, NY, USA, <http://www.nalgenunc.com>) to obtain the conditioned media (CM) used for daily hESC culture feeding.

3.2.3 Human embryonic stem cells and induced pluripotent stem cells

Human embryonic stem cell line HES-3 (46, XX) was from ES Cell International (Singapore, <http://www.escellinternational.com>) while the induced pluripotent stem cell line iPSC(IMR90) was generously provided by JA Thomson from University of Wisconsin-Madison, USA (Yu *et al.*, 2007). Cells were cultured on Matrigel (BD Biosciences, CA, USA, <http://www.bdbiosciences.com>)-coated plates in CM supplemented with 10 ng/ml FGF2. For the iPSC(IMR90) cell line, CM was supplemented with 100 ng/ml FGF2. Cells were kept in a 5% CO₂ incubator at 37°C and media was changed daily. Cells were passaged every 7 days by mechanical dissociation of colonies following collagenase IV (Sigma) treatment.

3.2.4 Embryoid body formation

hESC were dissociated into small clumps by collagenase IV and cultured in suspension as embryoid bodies (EB) in ultra-low attachment plates (Corning Life Sciences, MA, USA, <http://www.corning.com/lifesciences>). Cells were grown in differentiation

medium (DM) (KO-DMEM supplemented with 20% fetal bovine serum, 1% NEAA, 1 mM L-glutamine, and 25 units/ml penicillin-streptomycin and 0.1 mM 2-mercaptoethanol) and fed every 3-4 days. For further differentiation, EB were then plated on gelatin-coated dishes and grown in DM for 1 week.

3.2.5 Generation of stable cell lines

The pCHEF-DsRed or pCHEF-SHH-DsRed plasmids were transfected into hESC using Lipofectamine 2000 (Invitrogen). After 24 hours, the media was changed and antibiotic selection with Geneticin (50 µg/ml, Invitrogen) was applied to the cells the next day for 2 weeks. The surviving colonies were individually hand-picked using the micropipette under fluorescence microscope to further expand the colonies. The cytokines, neurotrophin-3 and neurotrophin-4 (10 ng/ml, Peprotech EC, London, UK, <http://www.peprotech.com>), were added for 1-2 weeks to enhance the survival of selected cells. Geneticin (50 µg/ml, Invitrogen) was used continuously in culture to maintain positive selection.

3.2.6 Neurosphere formation

To initiate differentiation, undifferentiated hESC were broken into clumps and grown as EB for 4 days. EB were then transferred onto laminin-coated 6-well plates (Figure 3.2). Laminin-coated plates were prepared by coating them with 10 µg/ml laminin (Sigma) for 2 hours at 37°C or overnight at 4°C. Cells were grown in N2B27 media containing DMEM/F12, 1x N2, 1x B27 without Vitamin A, (all from Invitrogen), 1% NEAA, 1 mM L-glutamine, 25 units/ml penicillin-streptomycin and 0.1 mM 2-mercaptoethanol. N2B27 media was supplemented with 500 ng/ml Noggin and cells were fed every other day. After 10 days, compact clumps were formed and were cut up manually with a pipette and grown as neurospheres in suspension in N2B27 media supplemented with 20 ng/ml EGF (Peprotech) and 20 ng/ml FGF2. Media was changed every 3-4 days and the neurospheres were passaged every 6-7 days using TrypLE Express (Invitrogen), a gentle trypsin-like enzyme.

3.2.7 Neural differentiation

To induce dopaminergic differentiation, the neurospheres were first dissociated into small clumps using TrypLE Express (Invitrogen) and plated onto laminin-coated 24-well plates (Figure 3.2). The following growth factors were then added to pattern the cells: 200 ng/ml FGF8, 200 ng/ml SHH (both from R&D Systems, Minneapolis, MN, USA, www.rndsystems.com), and 200 μ M ascorbic acid (AA, Sigma). After 7-10 days, reformed rosettes were visible and were selectively excised using a 200 μ l pipette tip. The excised rosettes were then treated with TrypLE Express for 3-5 min and gently pipetted up and down to achieve an almost single-cell suspension. They were then replated onto laminin-coated coverslips at approximately 50,000-150,000 cells per cm^2 in N2B27 media. The following growth factors were added: 1 μ M cyclic adenosine monophosphate (cAMP, Sigma), 20 ng/ml brain-derived neurotrophic factor (BDNF, Peprotech) and 20 ng/ml glial cell line-derived neurotrophic factor (GDNF, Peprotech). The cells were fed every 3-4 days and allowed to differentiate for up to 14 days (Figure 3.2).

	hESC	Embryoid bodies	Noggin treatment	Neurospheres	Selection of rosettes	Differentiation of DA neurons
Days	7 days	4 days	10 days	7 days	7-10 days	7-10 days
Media	CM	KO	N2B27	N2B27	N2B27	N2B27
Growth factors	10 ng/ml FGF2		500 ng/ml Noggin	20 ng/ml EGF, 20 ng/ml FGF2	200 ng/ml SHH, 200 ng/ml FGF8, 200 μ M AA	SHH, FGF8, AA, 20 ng/ml BDNF, 20 ng/ml GDNF, 1 μ M cAMP
Substrate	Matrigel	Suspension	Laminin	Suspension	Laminin	Laminin / Coverslips

Figure 3.2 Summary of neural differentiation protocol.

3.2.8 SHH conditioned media production

To produce conditioned medium containing active SHH, 4×10^6 293-EcR Shh cells and HEK293 cells (both from American Type Culture Collection, VA, USA, www.atcc.org)

were plated on T175 flasks (Nalgene). Once the cells reached 50% confluence, growth media was changed to DM and 2.5 μ M Ponasterone A (Invitrogen) was added to 293-EcR Shh cells to induce expression of SHH. Culture medium was collected after 24 hours, filtered through a 0.22- μ m filter unit (Nalgene) and used as growth media for hESC-derived EB. Bulk quantities of CM were produced and pooled to ensure consistency.

3.2.9 Transfection

Transfection of plasmids into hESC was achieved using Lipofectamine 2000 (Invitrogen) according to manufacturer's instructions. Briefly, plasmids were diluted to the required concentrations in Opti-MEM Reduced Serum Medium (Invitrogen). Lipofectamine 2000 was diluted in Opti-MEM and allowed to stand for 5 min. The above mixture was then added to the diluted plasmids and incubated for 20 min at room temperature. The plasmid-lipofectamine complexes were then added to the cells in antibiotic-free media.

3.2.10 Electrophysiology recording

Electrophysiological properties of neurons were investigated in cultures using whole-cell patch-clamp recording techniques carried out by Dr Wei Shunhui from Singapore Bioimaging Consortium (SBIC), A*STAR. The cells were prepared by seeding neuroprogenitors as single cells on laminin-coated coverslips, in N2B27 containing media supplemented with 20 ng/ml BDNF, 20 ng/ml GDNF and 20 ng/ml NGF, for three weeks. Using the standard protocol, a neuron intended for postsynaptic recordings was patched with pipettes that were pulled from borosilicate glass capillary tubes using a pipette puller. The whole-cell pipette solution contained (in mM) 135 CsCl, 10 HEPES, 1 EGTA, 1 Na-GTP, 4 Mg-ATP and 10 QX-314 (pH 7.4, adjusted with CsOH). The resistance of pipettes filled with the intracellular solution varied between 4 and 5 M Ω . After formation of the whole-cell configuration and equilibration of the intracellular pipette solution, the series resistance was adjusted to 10 M Ω . Cells with initial resistance more than 15 M Ω were excluded from analysis. Synaptic currents were monitored using EPC-10 amplifier (HEKA, Germany). The

bath solution contained (in mM) 140 NaCl, 5 KCl, 2 CaCl₂ or 2 MgCl₂, 10 HEPES, and 10 glucose (pH 7.4, adjusted with NaOH). Spontaneous postsynaptic currents (PSCs) and membrane potential were monitored. The temperature in the recording chamber was controlled by TC344B dual temperature controller (Warner Instruments).

3.3 Transcriptional profiling

3.3.1 RNA extraction

RNA was extracted with RNeasy Kit (Qiagen, Hilden, Germany, <http://www1.qiagen.com>) and treated with DNase according to manufacturer's protocol. Briefly, cell pellets were lysed using buffer RLT and pipetting vigorously. 70% (v/v) ethanol was then added and the mixture was applied to the columns and centrifuged briefly for RNA to bind to the column membrane. The columns were washed with buffers RW1 and RPE. RNA was eluted with 30 µl of nuclease free water. In certain cases where there were limited cell numbers, RNA isolation was done using the RNeasy Mini Kit (Qiagen). The steps were largely the same as the RNeasy Micro Kit, except an additional washing step with 80% v/v ethanol to supplement the wash buffer RPE and a longer centrifugation step of 5 min for the columns to dry fully before elution of RNA. RNA was eluted with 14–20 µl of nuclease-free water. The concentration and purity of RNA samples were determined using the ND-1000 Spectrophotometer (NanoDrop Technologies, Rockland, DE, USA, <http://www.nanodrop.com>). RNA samples had consistent A₂₆₀/A₂₈₀ absorbance ratios above 1.8.

RNA extraction for microarray analysis was carried out using the TRIzol extraction method. Floating neurospheres were harvested and spent media was aspirated. 1 ml of TRIzol (Invitrogen) was added and the cells were lysed and homogenized using a syringe and needle. The lysis product was allowed to stand for 10 min at room temperature and 200 µl of chloroform was added. The mixture was vortexed vigorously for 15 secs and allowed to stand for another 10 min. The samples were then centrifuged at 4°C at 14 000g for 10 min, after which the colorless aqueous phase was carefully extracted without disturbing the organic

phase. An equal volume of isopropanol was then added to the aqueous phase containing RNA and kept at -20°C overnight to allow RNA precipitation. The following day, the samples were centrifuged at 4°C at 12 000 rpm for 10 min to obtain a white pellet containing RNA. The supernatant was removed and the pellet was washed in 1 ml of 70% (v/v) ethanol and centrifuged at 4°C at 12 000 rpm for 10 min. This washing step was repeated three times and then the pellet was air-dried for 15-20 min at room temperature until it became translucent. The pellet was then reconstituted in 50 µl nuclease-free water.

3.3.2 *Reverse transcription, polymerase chain reaction (PCR) and quantitative real-time PCR analysis*

Reverse transcription into cDNA was done using Superscript First Strand Synthesis System (Invitrogen) according to manufacturer's protocol. Briefly, a reaction mix containing 1 µg RNA, 50 µM oligo (dT) primer, 10 mM dNTP and water was heated for 5 min at 65°C and put on ice for at least 1 min. A second mix containing 5x First strand buffer, 0.1 M DTT, RNaseOUT and Superscript III reverse transcriptase was added to the first mix and reverse transcription reaction was carried out for 1 hour at 50°C and 15 min at 70°C.

PCR amplification of genes was performed using Platinum *Taq* (Invitrogen) with a program of 94°C for 5 min, 30 cycles of 94°C for 30 secs, 54-64°C for 1 min, and 72°C for 1 min and an extension step at 72°C for 10 min. The primers used for these analyses are listed in Table 3.1.

Table 3.1 List of primers used in RT-PCR

Gene	5' – 3' Primer sequence	Product size (bp)
SHH	F: CGGAGCGAGGAAGGGAAAG R: TTGGGGATAAACTGCTTGTAGGC	262
DHH	F: GTTGTAAGGAGCGGGTGAAC R: GCCAGCAACCCATACTTGTT	184
IHH	F: CTACGCCCCGCTCACAAAG R: GGCAGAGGAGATGGCAGGAG	375
HIP	F: TGACCCAGACTCACAATGGA R: CTCTGCGGATGTTTCTGTCC	315
PTCH1	F: CTTGCTCTGGAGCAGATTT R: CAGGACATTAGCACCTTCT	334

PTCH2	F: TGCCCTTGAGCACACATTTG R: GTACAAGGAAAGCCCAGAGA	229
SMO	F: ACGAGGACGTGGAGGGCTG R: CGCACGGTATCGGTAGTTCT	583
GLI1	F: AGTAGCTATGGCGAGCCCT R: TAGGAGCCTCCTGGAGATGT	331
GLI3	F: CAGCTCCACGACCACTGAA R: TCCATGGCAAACACCGTCC	317
OCT4	F: GAAGGATGTGGTCCGAGTGT R: GTGACAGAGACAGGGGGAAA	242
GAPDH	F: TGGTATCGTGGAAGGACTCA R: CCTGCTTCACCACCTTCTTG	250

For quantitative real-time PCR analysis, 0.5 µg of RNA was reversed transcribed. All samples were run in triplicates at a reaction volume of 25 µl containing Power SYBR Green PCR Master Mix (Applied Biosystems, Foster City, CA, USA, <http://www.appliedbiosystems.com>), and 200 nM primers. The reaction was run on the ABI Prism7000 Sequence Detection System (Applied Biosystems) using the following amplification parameters: 2 min at 50°C, 10 min at 95°C, and 40 cycles of 15 secs at 95°C and 1 min at 60°C. Data was analyzed using the $\Delta\Delta C_T$ method to obtain expression levels relative to endogenous GAPDH control in each sample as previously described (Chan *et al.*, 2008). The primers used for these analyses are listed in Table 3.2.

Table 3.2 List of primers used for real-time PCR

Gene	5' – 3' Primer sequence
AADC	F: AAGCACAGCCATCAGGATTCA R: ATCTGCCAATGCCGGTAGTCA
ACTC	F: ATTG GCAATGAGCGCTTCC R: TGCCAGCAGATTCCATACCA
AFP	F: TCCCTCCTGCATTCTCTGATG R: CCTGAGCTTGGCACAGATCC
BMP2	F: GCAACAGCCAACTCGAAATTC R: CACCAACCTGGTGTCCAAAAG
BOC	F: GGGCCTGGTCTAAGCAAAAAC R: TGGCACCATAGTATACGGGCA
COL2A	F: GCCATGAAGGTTTTCTGCAAC R: TTGGGAACGTTTGCTGGATT
EN1	F: TCGTTTTCCGGAGACTTGTTG R: GGCGGTTTCAGTCTCGCAGT

EGFR	F:	GCCGGATCGGTA	ACTGTATCAA
	R:	TCCGTTTCTTCT	TTTGCCCAG
FGF19	F:	CATGGTCCCAGAG	GAGCCT
	R:	GGGCGAAGAGAAC	ATGTCAGA
FOXA1	F:	GCTGGACTTCAAG	GCATACGA
	R:	GGGCAACGTAGAG	CCGTAAG
GATA4	F:	ACAGACCAGCTCC	AAGCAGG
	R:	CGTGACTGTCGGC	CAAGAC
GATA6	F:	GCGGCTTGGATTG	TCCTGT
	R:	TGCGCCATAAGGT	GGTAGTTG
GLI1	F:	CAGGCTGGACCAG	TACATCA
	R:	TGGTACCGGTGTG	GGGACAA
HES5	F:	CAGGAGCCCCATT	CTCAGAG
	R:	CCCTGATTGTCCT	AAAACGGC
HEY2	F:	TTCTTGTCACCCT	TTGGGAGA
	R:	AGTGCTCCCTCCT	TGCTTCAT
HHIP	F:	CATATTCAGGTTT	CCTTCAAACA
	R:	GCATAGTAAAAGC	AAAACATCCG
HNF4 α	F:	AGATTTAGCCGGC	AGTGCG
	R:	AGCGGCACTGGT	TCCTCTT
ID1	F:	TTCTCCAGCACGT	CATCGACT
	R:	TTCCGAGTTCAGC	TCCAACCTG
IGF2	F:	CATCTCCCTTCTC	ACGGGAAT
	R:	GTTGCTATTTTCG	GATGGCC
LMX1B	F:	TGCTATCCTGGGA	AACGCA
	R:	GGCACCTTGGTCT	GACTCTTG
MSI	F:	CAGACTACGCAGG	AAGGGCT
	R:	CCGCATCACCAGAC	ACTCC
MSX1	F:	GCCATGTCTCCTG	CATAGCTT
	R:	CGCTTTTCTTGC	CTGGTGTC
NANOG	F:	GAAAAACAACCTG	GCCGAAGAAT
	R:	GGTGCTGAGGCCT	TCTGC
NESTIN	F:	CGTCTTGGATCTT	TGCTCCC
	R:	AAAGGCTGGCACAG	GTGTCT
NGFR	F:	GGGCTGAGACTGG	ATACTGCC
	R:	ACCTCAATTCCCT	CCGATGC
NKX2-2	F:	ACGTTCTGACAAC	TGGTGGCA
	R:	TGGCAACAATCACC	ACCGA
OCT4	F:	AACGACCATCTGC	CGCTTT
	R:	GGCCGAGCTTAC	ACATGTT
OLIG1	F:	CCGAGCAAGGAA	AGCATTTT
	R:	CGACAGTCCCTT	CCTCTGGA
PAX3	F:	CACCGTTCACAGAC	CTCAACC
	R:	TCGTGCTTTGGTGT	ACAGTGC
PAX6	F:	CCAGCTTCACCAT	GGCAAAT
	R:	GGCAGCATGCAGG	AGTATGAG

PGF	F:	GGGAGCTTCCGCTTTGAAAG
	R:	CCTAGCTTGCCCCTCACGA
PITX2	F:	ACGCGAAGAAATCGCTGTGT
	R:	CTTGAACCAAACCCGGACTC
PITX3	F:	AACTCACCCCTGGCCCATC
	R:	TCCGCGCACGTTTATTTCA
PTCH1	F:	GTCAGTGTTCATCCGCGTGG
	R:	AGGCATAGGCGAGCATGAGTA
SHH	F:	AGTCATCAGTTCCATGGGCG
	R:	GCAGCGAGGAGACGAGGAC
SMO	F:	TTCAGTTTCAGCGGTGCCA
	R:	GGTGAGTGTGTGCAGCAGCT
SMTN3	F:	AAAGGGAAGCAGAACTGAGGG
	R:	GGCTTTCGCTATGAGCGCT
SNAI2	F:	ACTCCGAAGCCAAATGACAAA
	R:	GGTCAGCACAGGAGAAAATGC
SOX1	F:	CACAACTCGGAGATCAGCAA
	R:	GTCCTTCTTGAGCAGCGTCT
TH	F:	TACTGGTTCACGGTGGAGTTCG
	R:	CTTCACCTCCCCGTTCTGCTTA
TUJ1 (β-III Tubulin)	F:	GGACGAGATGGAGTTCACCG
	R:	GGACACCAGGTCGTTTCATGTT
ZIC2	F:	CAAGATCCACAAAAGGACCCA
	R:	CAAACCTCACACTGGAACGGCT

3.3.3 DNA microarray

Gene expression profiling was carried out for biological quadruplicates of H3-NP, Vector-NP and SHH-NP that were taken independently through the neural differentiation procedure. Total RNA was isolated as mentioned in 3.3.1. The RNA was then cleaned up using the Qiagen RNeasy Midi according to manufacturer's protocol. RNA was then concentrated using the salt/alcohol precipitation method. The QIAxcel System was used to check the integrity of RNA before proceeding to the next step of cDNA synthesis. Double stranded cDNA synthesis was prepared from 15 µg of RNA using the a T7-Oligo(dT) promoter primer kit (Affymetrix, CA, USA, <http://www.affymetrix.com>) and Superscript II reverse transcriptase. A Poly-A RNA control kit was included as a positive control for the subsequent labelling steps. The double-stranded cDNA was cleaned up using the GeneChip sample clean up module (Affymetrix) and subsequently labelled with biotin using the

Genechip IVT labelling kit to obtain biotin-labelled cRNA. The biotin-labelled cRNA was cleaned up with the GeneChip sample cleanup module and quantified using the spectrophotometer. An adjusted cRNA yield was calculated using an equation provided by Affymetrix to take into account any unlabeled RNA. 20 µg of purified cRNA was then fragmented and ran through the Qiaxcel system to ensure fragmentation was successful. A hybridization cocktail was then added to 15 µg of cRNA and 200 µl of this mixture was hybridized to the chips (HG-U133 Plus 2.0 Array) for 16 hours according to Affymetrix procedures. The next day, the hybridized probes were stained using the stain cocktail provided and washed using the Affymetrix Fluidics Station. The probes were then scanned with the GeneChip Scanner 3000 and the digitized image (.CEL) files were obtained.

3.3.4 Microarray data analysis

Microarray data analysis was done by Dr. Stanley Ng from the A*STAR Singapore Immunology Network. Normalized expression signals were computed from .CEL files using RMA (Irizarry *et al.*, 2003). Differential hybridized features were identified using Limma, an R software package that implements linear models for microarray data (Smyth *et al.*, 2005). In Limma, p-values were compiled from four sets of technical replicate data and obtained from moderated t statistics or F statistics using empirical Bayesian methods. p-values were then adjusted for multiple testing with Benjamini and Hochberg's method to control the false discovery rate (Benjamini and Hochberg, 1995). All differentially regulated genes were filtered using the statistic criteria of adjusted p-values <0.05 and a 1.5-fold change in expression ratio compared to both Vector-NP and H3-NP.

Statistically significant over- or under- representation of particular GO term pathways were identified with either a classical hypergeometric test or a conditional hypergeometric that uses the relationships among GO terms to decorrelate the results (Falcon and Gentleman, 2007). All computations were done using the statistical programming language R in combination with Bioconductor tools.

3.3.5 *In silico analysis of GLI binding sites*

The identification of GLI binding sites on the promoter region of SHH regulated genes was done by Mr Yeo Hock Chuan from the A*STAR Bioprocessing Technology Institute, Bioinformatics group. The regulatory sequences 5 kb upstream and downstream of the 1.5-fold differentially regulated genes were extracted from the Biomart database (<http://www.biomart.org/>) in May 2009. The human genome assembly used was dated March 2006. To scan the regulatory sequences for putative GLI binding sites, the MATCH executable from TRANSFAC database was used, using TRANSFAC's 'V\$GLI_Q2' position-weighted matrix to describe the binding specificity. The TRANSFAC profile 'minFN20083.prf' was used to minimize false negative sites.

3.4 Protein and biochemical assays

3.4.1 *Immunocytochemistry*

Cells were fixed with 4% paraformaldehyde for 30 min and permeabilized with 0.1% Triton X-100 in PBS for 30 min and washed in 1% BSA in PBS. Cells were incubated overnight at 4°C with various primary antibodies in dilutions of 10% goat serum with 0.1% Triton X-100 in PBS (Table 3.3).

Table 3.3 List of antibodies used for immunocytochemistry

Primary antibody	Company	Species	Dilution
OCT4	Santa Cruz Biotechnology, CA, USA	Mouse	1:400
SMO	Santa Cruz	Rabbit	1:100
SMO	Lifespan Biosciences, WA, UK	Rabbit	1:250
PTCH1	Abcam, Cambridge, U.K	Rabbit	1:100
GLI1	Abcam	Rabbit	1:100
GLI3	Santa Cruz	Rabbit	1:100
Acetylated Tubulin	Sigma	Mouse	1:10000
PAX6	Developmental Studies Hybridoma Bank (DSHB), IA, USA	Mouse	1:50
NESTIN	Abcam	Rabbit	1:200

NESTIN	Neuromics, MN, USA	Mouse	1:200
SOX1	Abcam	Rabbit	1:250
TH	Chemicon, Temecula, CA, USA	Rabbit	1:250
β -Tubulin III	Chemicon	Mouse	1:500
GFAP	Dako, Glostrup, Denmark	Rabbit	1:500
MAP2	Chemicon	Mouse	1:200
Secondary antibody	Company	Species	Dilution
Anti-Mouse Alexa Fluor 488	Invitrogen	Goat	1:250
Anti-Rabbit Alexa Fluor 488	Invitrogen	Goat	1:250
Anti-Mouse Alexa Fluor 594	Invitrogen	Goat	1:250
Anti-Rabbit Alexa Fluor 594	Invitrogen	Goat	1:250
Anti-Rabbit Alexa Fluor 647	Invitrogen	Goat	1:250

Cells were then rinsed 3 times with 1% BSA in PBS for 5 min each time. After which, cells were incubated with secondary antibody for 2 hours at room temperature in 1% BSA in PBS. They were then rinsed three times with 1% BSA in PBS for 5 min each time. For cells grown on coverslips, coverslips were removed from the culture dish and transferred onto microscopy slides. Mounting medium containing DAPI (Vector Laboratories, CA, USA, <http://www.vectorlabs.com/>) was used for nuclei counter staining. Images were acquired using a Zeiss Axiovert 200M inverted fluorescent microscope (Carl Zeiss, Germany, www.zeiss.com).

For confocal microscopy to visualize cilia, cells were prepared as follows: hESC were seeded on Matrigel-coated coverslips and fed with CM for 2 days to allow clumps to attach and expand before being starved in DMEM media for 4-6 days. Neurospheres were dissociated into small clumps, seeded on laminin-coated coverslips and starved in DMEM media for 7-10 days. For both hESC and neurospheres, cells were stimulated with 500 ng/ml SHH for the last 1-2 days. The cells were then prepared for immunocytochemistry as stated above. Images were acquired with the Zeiss LSM 510 Meta Confocal Microscope (Carl Zeiss).

Quantitative immunocytochemical analysis of dopaminergic neurons was determined by counting the number of TH, β -Tubulin III and DAPI positive nuclei per field at 200x magnification for each independent experiment. At least 5 visual fields were randomly selected and at least 1000 cell nuclei were counted per experiment.

3.4.2 Western blot

Cell pellets were lysed using 1% Igepal lysis buffer and resolved on 4-12% NuPAGE gels (Invitrogen) and transferred onto polyvinylidene fluoride (PVDF) membranes (BioRad). Membranes were blocked in PBS with 5% low-fat milk and probed overnight at 4°C with primary antibodies (Table 3.4). For the anti-SHH blots, they were probed with anti-rabbit horse radish peroxidase (HRP)-conjugated secondary antibody (Amersham Biosciences NJ, USA, <http://www.amersham.com>) for 1 hour at room temperature. Signals were visualized using the Immobilon Western Chemiluminescent HRP Substrate (Millipore, MA, USA, <http://www.millipore.com>) with x-ray film. For the rest of the blots, they were probed with IRDye secondary antibodies (LI-COR, NE, USA, <http://www.licor.com>) for 1 hour at room temperature in the dark (Table 3.4). Signals were detected by direct infrared fluorescence with the Odyssey imaging system (LI-COR).

Table 3.4 List of antibodies used for Western blot analysis

Primary Antibody	Company	Species	Dilution
SHH	R&D	Rabbit	1:500
NESTIN	Abcam	Mouse	1:1000
SOX1	Abcam	Rabbit	1:1000
EGFR	Abcam	Rabbit	1:50
FOXA2	Abnova	Mouse	1:1000
PAX3	DSHB	Mouse	1:50
MSX1	R&D Systems	Goat	1:1000
ACTIN	Abcam	Mouse	1:20,000
ACTIN	Abcam	Rabbit	1:20,000
Secondary Antibody	Company	Species	Dilution
Anti-Rabbit IRDye 800	LI-COR	Goat	1:20,000
Anti-Rabbit IRDye 680	LI-COR	Goat	1:20,000
Anti-Mouse IRDye 800	LI-COR	Goat	1:20,000
Anti-Mouse IRDye 680	LI-COR	Goat	1:20,000
Anti-Goat IRDye 680	LI-COR	Donkey	1:20,000

3.4.3 Flow cytometry analysis

For detection of pluripotent markers OCT4 and TRA-1-60, hESC were dissociated with trypsin and harvested as single cells before fixation and permeabilization using Fix and Perm Cell Permeabilization reagents (Invitrogen). Cells were incubated with primary antibodies (Table 3.5) for 15 min at room temperature and then washed with 1% BSA in PBS. The secondary antibody was added and incubated for 15 min at room temperature. Cells were washed and resuspended in 1% BSA in PBS for flow cytometry analysis. As a negative control, cells were stained with the appropriate isotype control. Cells were acquired using a FACS Calibur (Becton Dickinson) and results were analysed with the CellQuest Software (Becton Dickinson).

For detection of NSC markers, neurospheres were dissociated with TrypLE Express and harvested as single cells before incubation with the primary antibody (Table 3.5) in 1% BSA in PBS for 30 min on ice. The cells were washed with 1% BSA in PBS and incubated with the secondary antibody anti-mouse APC for 30 min on ice. The samples were then washed with 1% BSA in PBS before being acquired on the FACS Calibur. As a negative control, cells were stained with the appropriate isotype control. Cells were acquired using a FACS Calibur and results were analysed with the FlowJo software (Treestar, OR, USA, <http://www.treestar.com>).

Table 3.5 List of antibodies used for flow cytometry analysis

Primary antibody	Company	Species	Dilution
A2B5	Chemicon Miltenyi Biotec, CA, USA	Mouse	1:100
CD133-APC	DSHB	Mouse	1:11
FORSE	Santa Cruz	Mouse	1:100
OCT4	Santa Cruz	Mouse	1:20
p75	Miltenyi Biotec	Mouse	1:100
PSA-NCAM-APC	Chemicon	Mouse	1:11
TRA-1-60		Mouse	1:50
Secondary antibody	Company	Species	Dilution
Anti-Mouse Alexa Fluor IgG ₁ 488	Invitrogen	Goat	1:100
Anti-Mouse APC	BD Bioscience	Goat	1:100
Anti-Mouse FITC	Dako	Goat	1:500

For sorting of p75+/ PSA-NCAM+ double positive cells, neurospheres from each cell line were harvested with TrypLE Express, washed once in 5% FBS in PBS, followed by incubating with anti-p75 and APC-conjugated PSA-NCAM antibody in 1% BSA in PBS for 30 min on ice. The cells were washed in 1% BSA in PBS and incubated with anti-mouse IgG₁-488 antibody in 1% BSA in PBS for 30 min on ice. The samples were washed in 1% BSA in PBS, resuspended in 5% FBS in PBS, and filtered through a 40 µm nylon cell strainer (BD Biosciences) to obtain single cells. Double positive cells were sorted using the FACS Aria 4-color laser sorter (Becton Dickinson) which was operated by the A*STAR Biopolis Shared Facility. Sorted cells were then seeded onto ultra-low attachment plates in N2B27 media with 20 ng/ml EGF and FGF2.

3.4.4 *Luciferase reporter assay*

For the 8xGli-BS luciferase reporter assay, hESC were plated in 24-well plates 4 days before transfection. The 8XGli-BS or 8XmutGli-BS luciferase reporter plasmid was co-transfected with 20 ng TK-Renilla internal control plasmid (pRL-TK, Promega, WI, USA, www.promega.com) and DNA expression vectors as indicated. Wherever required, the total amount of plasmid DNA transfected was adjusted to 1 µg by adding the control plasmid pCDNA3.1(+) (Invitrogen). To induce differentiation, hESC growth medium was changed 16 hours after transfection to DM or DM supplemented with 5 µM retinoic acid (RA, Sigma). Cells were harvested after 48 hours and assayed for luciferase activity.

For the Switchgear promoter luciferase assay, neurospheres were plated in laminin-coated 24-well plates in N2B27 media with EGF and FGF2 4-5 days prior to transfection to allow cells to reach confluence. The luciferase reporter plasmids were co-transfected with 12 ng pRL-TK internal control plasmid and the SHH expression vector as indicated. The total amount of plasmid DNA transfected was adjusted to 1.2 µg by adding the control plasmid pCDNA3.1(+). Cells were harvested after 48 hours and assayed for luciferase activity.

Luciferase activities were measured using the Dual-Luciferase system (Promega) according to manufacturer's protocol. Briefly, cells were washed with PBS buffer and lysed

directly in culture wells with 1x Passive Lysis Buffer. 50 µl of cell lysate was transferred to a microplate and 100 µl of Luciferase Assay Reagent II was added. *Firefly* luciferase levels were then measured for luminescence by the Infinite M200 microplate reader (TECAN, Zurich, Switzerland, www.tecan.com). Subsequently 100 µl of Stop & Glo Reagent was added and *Renilla* luciferase levels were measured as above. Luciferase activities were calculated as a ratio of *Firefly* luciferase activity over *Renilla* luciferase activity and expressed relative to an empty vector control. All transfection experiments were performed at with at least three biological replicates using different batches of cells and similar results were obtained.

3.4.5 Cell proliferation assay

To detect DNA synthesis in proliferating cells, incorporation of a thymidine analog 5-ethynyl-2'-deoxyuridine (EdU) was used (Invitrogen). hESC were treated with 10 mM nocodazole for 16 hours for cell cycle synchronization. Toxicity due to nocodazole was not observed and successful synchronization was validated by flow cytometry. Cells were then treated with 1 µg/ml recombinant SHH for 24 hours and EdU was added in 2 hours prior to harvest for assay. EdU incorporation in cells was detected according to manufacturer's instructions by using a FACS Calibur and results were analysed with the CellQuest Software.

3.4.6 Apoptosis assay

hESC were treated with 1 µg/ml recombinant SHH for 24 hours and apoptosis assay was carried out using the Annexin V-FITC apoptosis detection kit (Bender MedSystems, Vienna, Austria) according to manufacturer's instructions. Cells were co-stained with Propidium Iodide (PI) to stain for dead cells. Flow cyometry was performed on the FACS Calibur and the results were analysed with the CellQuest Software.

3.4.7 Cell count

p75+/PSA-NCAM+ positive neurospheres were harvested 7 and 14 days after isolation and treated with TrypLE Express to obtain a single cell suspension. The viable cell

number for each sample was determined using Trypan Blue exclusion with a hemocytometer (Neubauer).

3.5 Statistics

Statistical significance of differences between values was evaluated by an unpaired Student's t-test in Microsoft Excel. Significance was set at a p value of <0.05 .

CHAPTER 4 ROLE OF SHH IN UNDIFFERENTIATED hESC

4.1 INTRODUCTION

Several developmentally important pathways like the FGF, TGF β and WNT pathways have been identified as fundamental pathways governing hESC self-renewal and pluripotency (Hyslop *et al.*, 2005). However, the function of the SHH pathway in hESC is less well known. There are indications that the pathway could be involved in hESC self-renewal. Earlier studies attempting to understand the transcriptional network of NANOG, SOX2 and OCT4 have shown using chromatin immunoprecipitation-microarray, that the above transcription factors bound to the promoter region of GLI3 to repress its expression (Boyer *et al.*, 2005). A similar result was obtained in mESC whereby Nanog and Oct4 binding sites were identified upstream of *Ptch1*, *Gli1* and *Gli3* (Loh *et al.*, 2006). Furthermore, the expression of *Ptch1* and *Gli1* was downregulated upon knockdown of Oct4 and Nanog respectively (Mathur *et al.*, 2008). In hESC, *PTCH1* was similarly found to be downregulated upon knockdown of NANOG (Babaie *et al.*, 2007). These lines of evidence led us to study in this chapter the role SHH plays in undifferentiated hESC.

The expression of SHH pathway components was first examined in hESC and their differentiated progeny, embryoid bodies (EB). The state of pathway activation in both undifferentiated and differentiated hESC was then determined by using a GLI responsive luciferase assay. To understand the requirement of SHH for the maintenance of pluripotency, hESC were cultured in either pluripotent or sub-optimal conditions and supplemented with exogenous SHH. The expression of pluripotent markers was monitored and the effect of SHH on hESC proliferation and survival was also studied. Finally, the significance of SHH in promoting differentiation was studied by exposing spontaneously differentiating EB to exogenous SHH.

4.2 Expression of SHH signaling pathway components

To determine whether SHH signaling is present in hESC, components of the SHH signaling pathway were analyzed by immunocytochemistry. PTCH1 and SMO receptors were localized to the plasma membrane while GLI1 and GLI3 co-localized with the nuclear dye, DAPI (Figure 4.1).

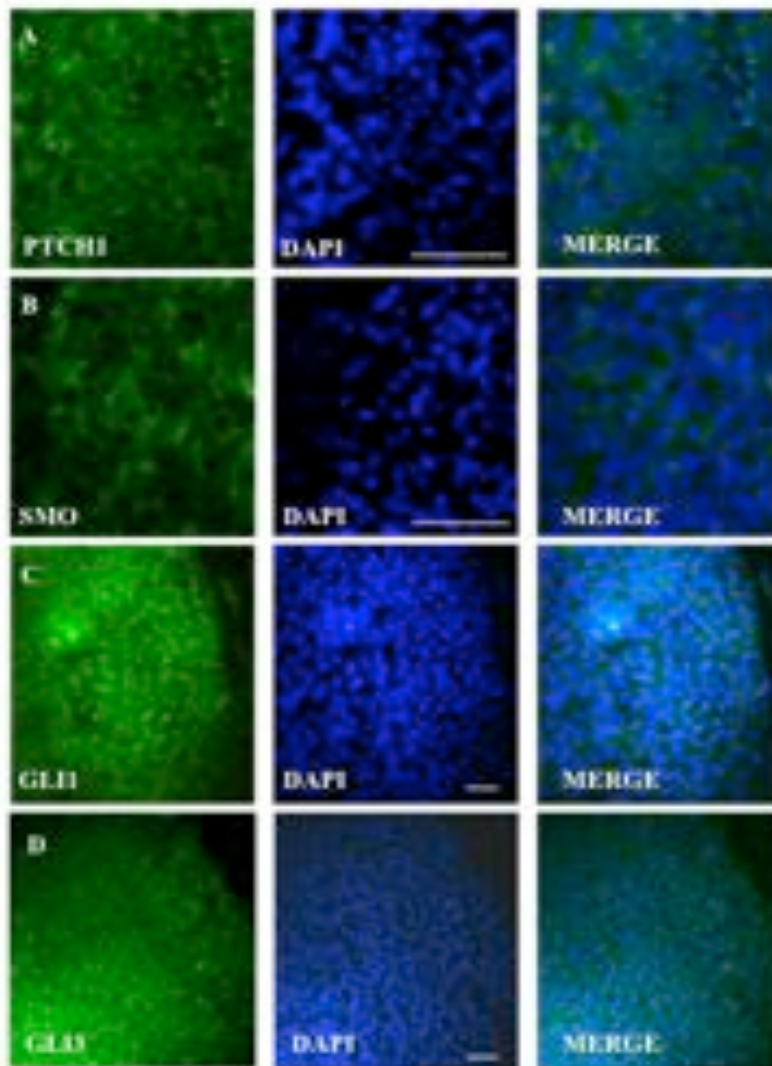


Figure 4.1 hESC express SHH pathway components. (A-D) Representative images showing immunofluorescent staining of (A) PTCH1, (B) SMO, (C) GLI1, (D) GLI3. Middle panel shows corresponding DAPI nuclear staining in blue and right panel shows corresponding merged images. Scale bars represent 100 μm .

The expression of pathway components was further confirmed by RT-PCR where low expression of *SHH* and *IHH* was detected whereas *DHH* was undetectable in

undifferentiated hESC. hESC also express the *PTCH1*, *SMO* but not *PTCH2* receptors and transcription factors *GLI1* and *GLI3*, along with the pluripotent marker *OCT4* (Figure 4.2). This confirms that hESC express SHH signaling components necessary for signal transduction.

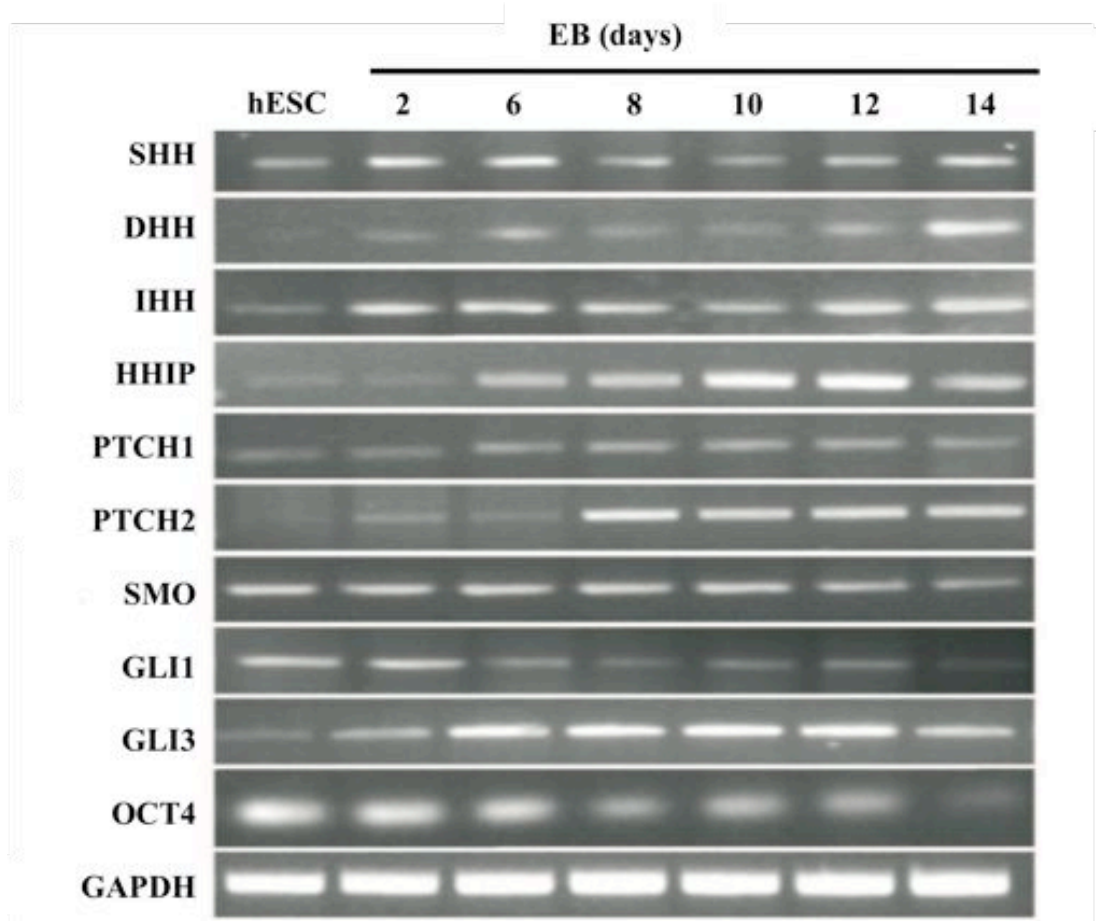


Figure 4.2 Embryoid bodies (EB) express SHH pathway components. RT-PCR analysis of SHH signaling pathway components in undifferentiated hESC and differentiating EB over 14 days. EB were grown in differentiation media in suspension and harvested at indicated time points.

During spontaneous differentiation, gene expression of *SHH*, *DHH* and *IHH* in EB was significantly higher compared to hESC over the entire 14-day differentiation period (Figure 4.2). Concomitantly, there were also an upregulation of *GLI3*, *HHIP*, *PTCH1* and *PTCH2* and a downregulation of *SMO* and *GLI1*. These results are consistent with previous data (Rho *et al.*, 2006), which reported similar mRNA expression of SHH pathway

components in hESC and EB. The presence of these SHH pathway components suggests that SHH signaling cascade may have functional importance in undifferentiated hESC and EB.

It was recently shown that the H1 and H9 hESC lines possess primary cilia containing the SMO and PTCH1 receptors and the authors also found low levels of SHH located at the base of the cilia (Kiprilov *et al.*, 2008). Results in Section 5.3 indicate that primary cilia are similarly present in the HES-3 cell line used in this study.

4.3 Activation of SHH signaling in undifferentiated hESC and role of GLI mediators

The presence of the SHH pathway components in hESC led us to investigate if SHH signaling is active in undifferentiated hESC. This was achieved using the GLI-mediated transcriptional activation assay with GLI-responsive luciferase reporter plasmid (Figure 4.3A) (Sasaki *et al.*, 1997a). Transfection of the 8XGli-BS luciferase reporter plasmid into hESC showed 7-fold induction of luciferase activity, as compared to the background luciferase levels of the 8XmutGli-BS luciferase reporter plasmid, indicating that there is endogenous activation of the SHH pathway in undifferentiated hESC (Figure 4.3B).

To identify the role of GLI mediators in undifferentiated hESC, three GLI mediators, GLI1, GLI2 and GLI3 expression vectors were also co-transfected with the wildtype 8XGli-BS or 8XmutGli-BS luciferase reporter plasmid into hESC. Expression of GLI1 and GLI2 in hESC induced a 4-fold and 3-fold increase in wildtype 8XGli-BS luciferase activity, respectively, while expression of GLI3 in hESC inhibited 8XGli-BS luciferase activity (Figure 4.3B). Co-expression of GLI3 and GLI1 in hESC showed that GLI3 suppressed luciferase reporter activation by GLI1 in a dose dependent manner (Figure 4.3C). Another component of the SHH pathway, SUFU, a negative regulator of GLI mediators, was also found to significantly downregulate luciferase activity when it was co-expressed with GLI1 in hESC (Figure 4.3D). These results are consistent with those previously reported (Stone *et al.*, 1999) and confirm the role of the GLI mediators in SHH signal transduction in hESC. Together, the results show that the SHH pathway is present in hESC and the signaling cascade downstream of SMO is functioning.

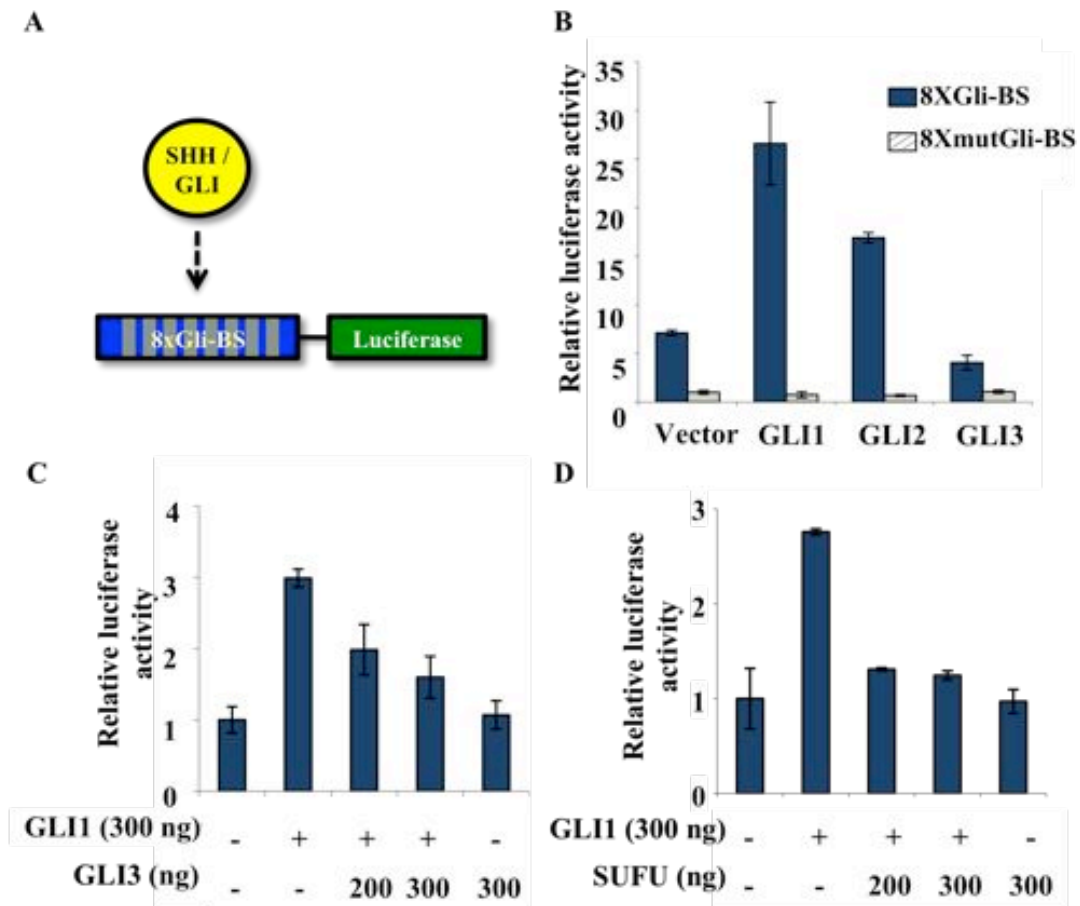


Figure 4.3 GLI mediators are functional in undifferentiated hESC. (A) Schematic of 8xGli-BS reporter plasmid. (B-D) Luciferase activity of 8XGli-BS luciferase reporter plasmid. (B) hESC were transiently transfected with 8XGli-BS or 8XmutGli-BS luciferase reporter plasmid together with the indicated expression vectors encoding GLI1, GLI2 and GLI3. (C-D) The 8XGli-BS luciferase reporter plasmid and GLI1 expression vector were co-transfected with increasing concentrations of (C) GLI3 and (D) SUFU expression vectors as indicated. Luciferase activities were calculated as a ratio of *Firefly* luciferase activity over *Renilla* luciferase activity and expressed as fold induction relative to vector control. Values shown are mean \pm SD of a representative experiment carried out in triplicate and repeated at least three times.

4.4 Effect of SHH on hESC pluripotency and proliferation

Since the SHH pathway was shown to be active in hESC, we examined whether addition of exogenous SHH affects hESC pluripotency. hESC were cultured in conditioned medium (CM) for two passages with or without 1 μ g/ml recombinant SHH and expression of pluripotent surface marker TRA-1-60 expression was evaluated by flow cytometry. Results showed that cells cultured over two passages in CM with exogenous SHH (CM+SHH)

maintained high levels of TRA-1-60 expression which are comparable to cells cultured in CM (Figure 4.4A). Similarly, real-time PCR analysis of pluripotent markers *OCT4* and *NANOG* showed that cells cultured in CM or CM+SHH had similar gene expression levels (Figure 4.4B,C). Addition of lower concentrations of SHH (10 ng/ml and 100 ng/ml) had similar results (data not shown). Therefore, hESC remained undifferentiated in the presence of high concentrations of SHH, suggesting that SHH does not induce differentiation.

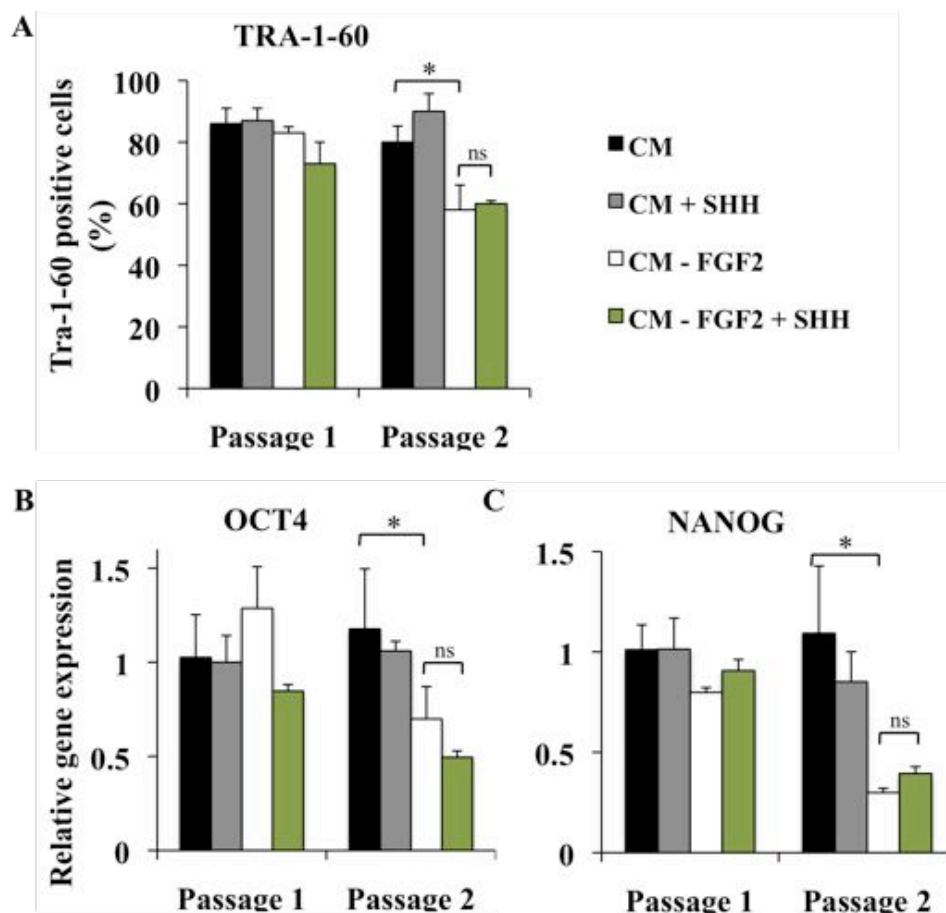


Figure 4.4 Exogenous SHH does not affect pluripotency. (A) FACS analysis of TRA-1-60 positive cells and (B) Real-time PCR analysis of pluripotent markers *OCT4* and *NANOG* expression in hESC maintained in conditioned media (CM), CM supplemented with 1 μ g/ml SHH (CM+SHH), CM without FGF2 (CM – FGF2) or CM without FGF2 supplemented with 1 μ g/ml SHH (CM–FGF2+SHH) over two passages. The expression level of each gene is shown relative to undifferentiated hESC maintained in CM, which was arbitrarily defined as 1 unit. The values shown are mean \pm SD of a representative experiment performed in triplicate and repeated three times. * = $p < 0.05$, ns = non-significant.

To determine if SHH maintains pluripotency when hESC are grown under spontaneous differentiation conditions, cells were cultured in CM without FGF2 (CM-FGF2), as FGF2 in CM has been shown to be necessary for the maintenance of pluripotency (Greber *et al.*, 2007). After the second passage, there was a drop in expression of TRA-1-60, *OCT4* and *NANOG* in CM-FGF2 cells compared to cells cultured in CM (Figure 4.4), indicating that cells were undergoing spontaneous differentiation. When 1 $\mu\text{g/ml}$ recombinant SHH was added daily to CM-FGF2 cells over two passages (CM-FGF2+SHH), there was a similar decrease in TRA-1-60, *OCT4* and *NANOG* expression levels when compared to CM-FGF2 cells (Figure 4.4). These results suggest that SHH treatment does not maintain pluripotency of hESC. It also showed that SHH did accelerate the differentiation of hESC, which are similar to that reported by Heo *et al.*, 2007, whereby mESC maintained their undifferentiated status with long term treatment of 0.5 $\mu\text{g/ml}$ SHH over 5 passages.

In order to study if SHH affects the proliferation of hESC, an EdU incorporation assay was used to investigate the cell proliferation of hESC after SHH treatment. hESC were treated with 1 $\mu\text{g/ml}$ SHH for 24 hours and cells were labeled with EdU during the last two hours. Cells were co-stained for OCT4 and analyzed by flow cytometry. Results showed that despite treatment with 1 $\mu\text{g/ml}$ SHH, the percentage of pluripotent OCT4 and EdU positive proliferating cells were similar to those of the control (without SHH) (Figure 4.5)

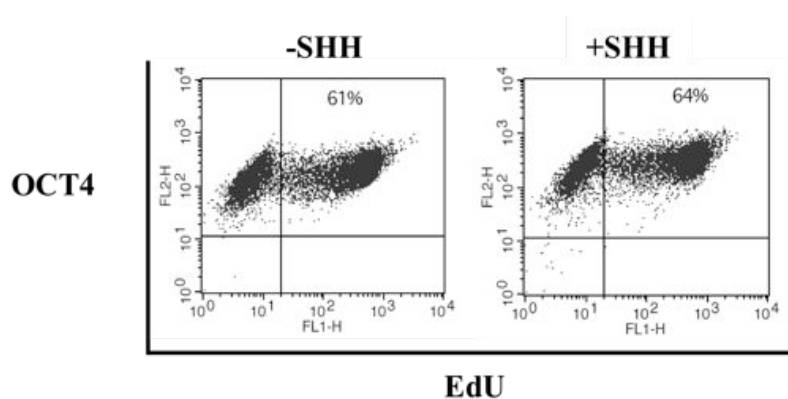


Figure 4.5 Exogenous SHH does not affect proliferation of hESC. Flow cytometry analysis of EdU incorporation assay in undifferentiated hESC. Cells were synchronized with nocodazole for 16 hours and then treated with or without 1 $\mu\text{g/ml}$ SHH for 24 hours. Representative dot plots of biological triplicates showing EdU incorporation in hESC co-stained for OCT4. This experiment was repeated three times.

The effect of SHH on apoptosis was also evaluated using the Annexin V assay and the apoptotic cell population (Annexin V positive PI negative) was similar in cells treated with or without SHH (Figure 4.6)

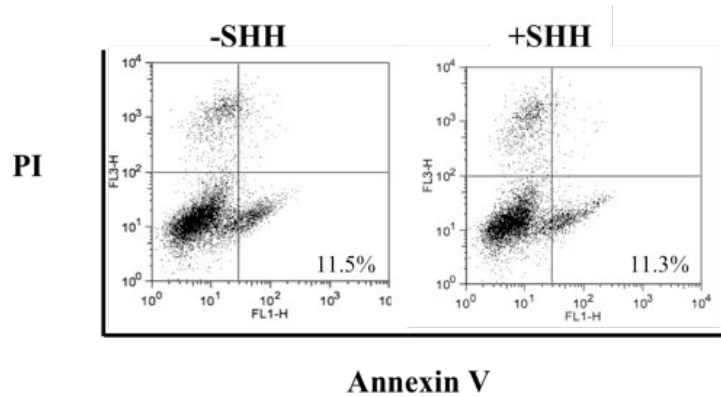


Figure 4.6 Exogenous SHH does not affect survival of hESC. Flow cytometry analysis of Annexin V apoptosis assay in undifferentiated hESC whereby cells were treated with or without 1 μ g/ml SHH for 24 hours prior to assay. Representative dot plots showing apoptotic cells (Annexin V positive and PI negative) from biological triplicates and experiment repeated thrice.

To further confirm the observations, an alternative method of introducing exogenous recombinant SHH was achieved by transient transfection of a CMV expression vector encoding the full length SHH into hESC. Western blot analysis confirmed the overexpression of SHH (data not shown). Despite the differential expression of cell cycle proteins upon overexpression of SHH, there was no change in the percentage of EdU positive proliferating cells (data not shown). These results suggest that SHH does not stimulate the proliferation of undifferentiated hESC, which is contrary to that reported in mESC whereby the authors observed an increase in mESC proliferation and expression of cell cycle components upon stimulation with as little as 50 ng/ml SHH (Heo *et al.*, 2007). SHH was also shown to stimulate undifferentiated mESC proliferation via the canonical Gli pathway and non-canonical Ca^{2+} /PKC and EGF receptor activation pathways (Heo *et al.*, 2007). This discrepancy could be due to the inherent difference in self-renewal properties between mESC and hESC or that the stimulatory effect of SHH on proliferation is tissue specific.

4.5 Activation of SHH signaling in hESC during differentiation

Having established the activation of the SHH pathway in undifferentiated hESC, pathway activation during early differentiation was studied by interrogating SHH target gene expression. hESC were maintained either in an undifferentiated state with CM, or induced to differentiate by culturing in differentiation medium (DM) or DM supplemented with 5 μ M retinoic acid (DM+RA) for 96 hours. Gene expression of *OCT4*, *NANOG* and the SHH target genes *PTCH1* and *GLI1* were then analyzed by real time-PCR. When cells were differentiated with DM, there was a 50% reduction in *OCT4* and *NANOG* gene expression compared to undifferentiated hESC (Figure 4.7A). Addition of RA (DM+RA) abolished *OCT4* and *NANOG* expression, showing loss of pluripotency (Figure 4.7A). The drop in pluripotency marker expression was accompanied by 1.5-fold upregulation of *PTCH1* expression in DM treated cells and a 4-fold upregulation in DM+RA treated cells. *GLI1* expression also increased by 2.5-fold in DM+RA treated cells (Figure 4.7A), implying that the SHH pathway is activated during differentiation.

In a different approach to study pathway activation, the 8XGli-BS luciferase reporter plasmid was transfected into hESC and treated in similar culture conditions as above. No increase in luciferase activity was observed for hESC cultured in DM. However, a significant induction of luciferase activity (2-fold) was observed in differentiating hESC treated with RA (Figure 4.7B). This induction in luciferase activity was inhibited by cyclopamine, an antagonist of the pathway that inhibits at the level of the SMO receptor (Taipale *et al.*, 2000). Addition of 10 μ M cyclopamine reduced the luciferase activity in CM and DM to a lower basal level as compared to the vehicle control in CM and DM (Figure 4.7B). There was also approximately 75% reduction in luciferase activity in DM+RA cells as compared to vehicle control in the same condition (Figure 4.7B). This indicates that endogenous SHH ligands activated the SHH pathway during differentiation as it is SMO-dependent. Similarly, the induction of luciferase activity was also inhibited by forskolin, an inhibitor of the pathway which activates protein kinase A (PKA) which in turn phosphorylates the GLI mediator

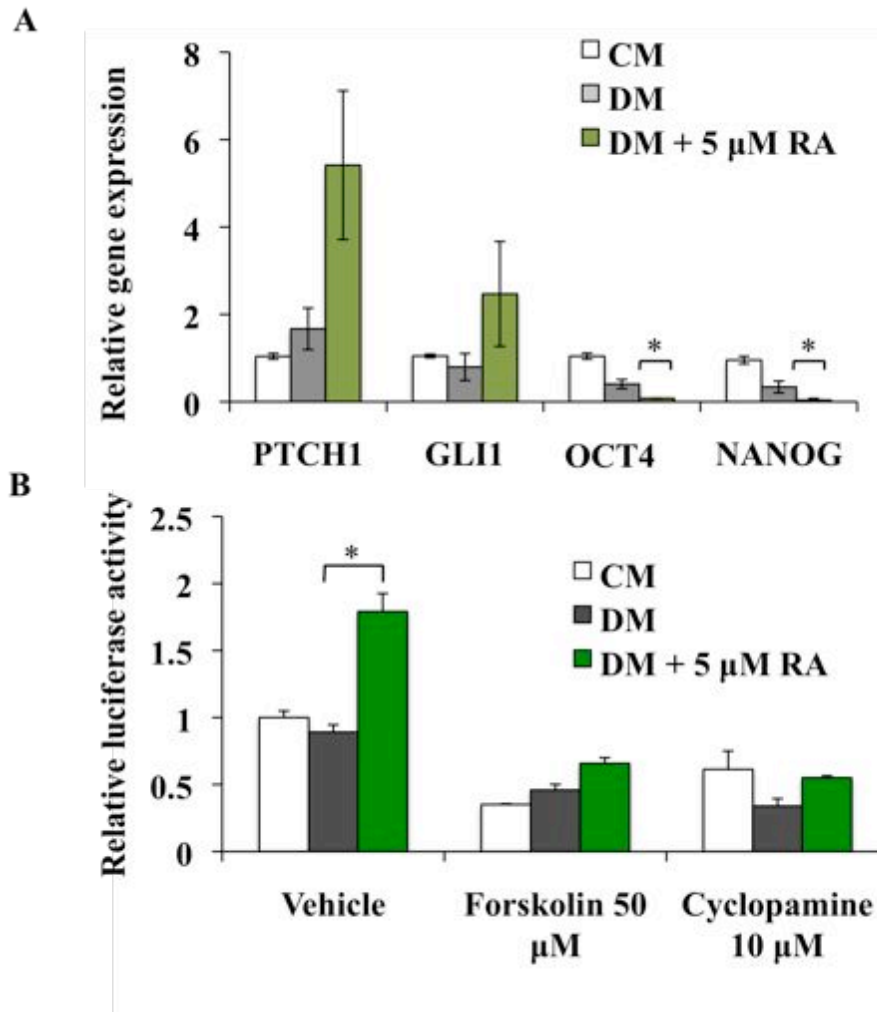


Figure 4.7 Activation of SHH signaling by endogenous SHH. (A) Quantitative Real-time PCR analysis of target gene *PTCH1* and *GLI1* and pluripotent markers *OCT4* and *NANOG* expression in hESC maintained in conditioned media (CM), or induced to differentiate with differentiation media (DM) or DM supplemented 5 μ M RA (DM+5 μ M RA) for 48 hours. Gene expression is expressed relative to hESC in CM condition. (B) Luciferase activity of the 8XGli-BS luciferase reporter plasmid, which was transfected into hESC and cultured similar conditions as above. Cells were treated with the vehicle control (DMSO/ Ethanol) or pathway inhibitors 10 μ M cyclopamine and 50 μ M forskolin. Cells were assayed for luciferase activity 48 hours post transfection. Luciferase activities were calculated as a ratio of *Firefly* luciferase activity over *Renilla* luciferase activity and expressed as fold induction relative to vehicle or vector control. Values shown are mean \pm SD of a representative experiment carried out in triplicate and repeated at least three times. *, $p < 0.05$.

proteins to the repressor form (Wang *et al.*, 2000; Sheng *et al.*, 2006). Here, the luciferase activity in all culture conditions were significantly reduced by more than 50% with the addition of 50 μ M forskolin as compared to vehicle control.

The GLI-mediated transcriptional activation assay corroborated with the target gene expression data, showing that the SHH pathway was activated in cells in DM with RA, and that the activation was SMO/GLI dependent (Figure 4.7B). The SHH pathway does not appear to be activated in DM treated cells possibly because they were partially undifferentiated as demonstrated by the presence of *OCT4* and *NANOG* transcripts (Figure 4.7A). And upon treatment with RA, a potent inducer of differentiation, there was rapid differentiation as *OCT4* and *NANOG* expression was abolished, and this was accompanied by high activation of the SHH pathway. RA treatment could also have induced the differentiating cells to express the SHH ligand (Okada *et al.*, 2004), thereby activating the pathway. Together with the gene expression studies, the results provide evidence that endogenous SHH signaling in hESC is present and can be further highly activated by the endogenous SHH during RA mediated differentiation.

To confirm that exogenous SHH activates the pathway during differentiation, SHH was overexpressed along with the 8xGli-BS luciferase reporter plasmid. Subsequently, there was a 2-fold increase in luciferase activity in hESC cultured in CM and in DM upon overexpression of SHH compared to the vector control (Figure 4.8). On top of that, overexpression of SHH elicited a greater increase in luciferase activity of around 3-fold in hESC cultured in DM+RA compared to the vector control. This result indicates that there is greater pathway activation by exogenous SHH during hESC differentiation with RA (Figure 4.8). Specificity of SHH induced luciferase activity was demonstrated by the addition of 10 μ M cyclopamine which resulted in a 50% reduction in luciferase activity in cells cultured in CM or DM+RA when compared to vehicle control. Overexpression of GLI1 in this assay served as a positive control for pathway activation (Figure 4.8).

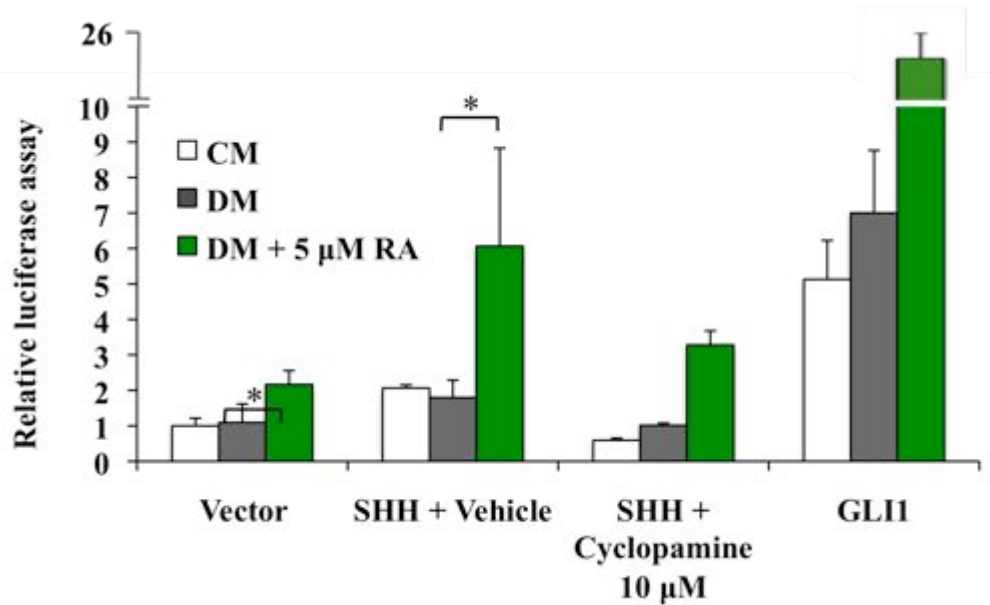


Figure 4.8 Activation of SHH signaling by exogenous SHH. The SHH expression vector was co-transfected with the 8XGli-BS luciferase reporter plasmid in the absence (vehicle-DMSO) or presence of 10 μ M cyclopamine. GLI1 was overexpressed as a positive control. Luciferase activities were calculated as a ratio of *Firefly* luciferase activity over *Renilla* luciferase activity and expressed as fold induction relative to vehicle or vector control. Values shown are mean \pm SD of a representative experiment carried out in triplicate and repeated at least three times. * = $p < 0.05$.

To confirm the pathway activation effect of overexpressing SHH plasmid, exogenous SHH was also introduced in the form of recombinant SHH (500 ng/ml) in the iPSC(IMR90) cell line and similar results were obtained (data not shown). Therefore, the results indicate that both endogenous and exogenous SHH can activate the pathway in hESC and higher activation occurs during RA differentiation. This implies that in the undifferentiated state, activation of the pathway by exogenous SHH is minimal but when the cells begin to differentiate, they become more responsive to SHH stimulation. RA is commonly used in several ES cell differentiation protocol as a caudalizing factor to generate cells of the neural lineage (Wichterle *et al.*, 2002; Bibel *et al.*, 2004), and its function could be partly attributed to its activation of the SHH signaling pathway. Coupled with the expression of SHH pathway components in EB (Figure 4.2) SHH could play a more important role during differentiation and led the study towards investigating the effect of SHH signaling on the lineage determination during early EB differentiation.

4.6 SHH signaling influences lineage determination during spontaneous differentiation

Expression of key components of the SHH pathway in EB and its activation during differentiation suggest that SHH may play a functional role during spontaneous differentiation. To examine the effect of SHH signaling in lineage determination during hESC differentiation, exogenous SHH secreted in the conditioned medium (SHH-CM) of an inducible SHH overexpressing cell line (293-EcR Shh) (Cooper *et al.*, 1998) with DM was used to culture differentiated hESC grown as EB for 14 days. The levels of secreted SHH in SHH-CM was confirmed using ELISA (data not shown). Conditioned media from the normal HEK293 cells (Control-CM) was used as control. Production of active N-terminal SHH from 293-EcR Shh cells was used as a more convenient and economical source of SHH than commercial recombinant SHH. Also, its usefulness in differentiation studies has been demonstrated whereby the SHH producing cells were co-cultured with mESC to promote motor neuron differentiation (Soundararajan *et al.*, 2007).

After 14 days in culture with SHH, expression of the pluripotent marker *OCT4*, SHH target genes *GLI1* and *PTCH1*, and differentiation markers were analyzed using quantitative real-time PCR. Long-term treatment of SHH-CM enabled sustained activation of the SHH pathway as shown by the upregulation of *GLI1* and *PTCH1* expression (Figure 4.9A).

OCT4 expression was downregulated in all conditions as compared to undifferentiated hESC indicating that the media used did not inhibit the ability of cells to differentiate (Figure 4.9A). An increased expression of neuroectoderm markers *SOX1*, *Musashi1 (MSI)*, *Msh homeobox 1 (MSX)* and *microtubule-associated protein 2 (MAP2)* was observed in SHH-CM treated EB compared to the control group (Figure 4.9B). The expression of endodermal markers *alpha-fetoprotein (AFP)* and *GATA binding protein 4 (GATA4)* were not significantly altered, although a 30% decrease in *GATA6* mRNA was observed. *IGF2*, a mesoderm marker, was downregulated, whereas there was no effect on *COL2A* expression level (Figure 4.9C).

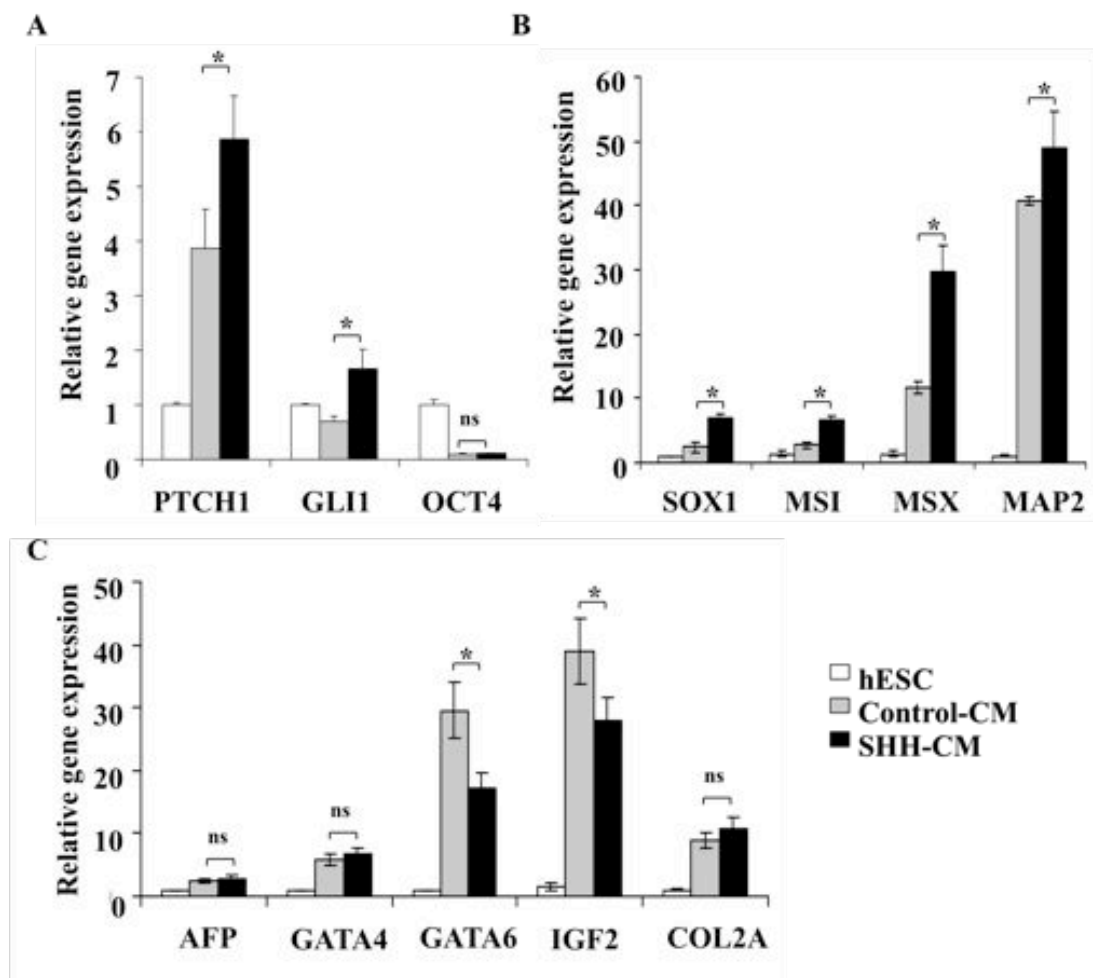


Figure 4.9 Neuroectoderm markers expression are upregulated in EB after 14 days exposure to SHH. (A-C) EB were grown in SHH-CM or Control-CM suspension culture for 14 days and mRNA expression was analyzed by real time PCR to determine the expression of (A) SHH target genes, (B) neuroectoderm, (C) mesoderm and endoderm markers. Gene expression is expressed relative to undifferentiated hESC. Values shown are mean \pm SD of a representative experiment carried out in triplicate and repeated at least three times. * = $p < 0.05$, compared to Control-CM treated EB. ns = non-significant.

Following the 14 day differentiation in suspension, EB were replated onto gelatin-coated dishes to further differentiate for an additional 7 days in SHH-CM or Control-CM. Immunocytochemistry results showed that in SHH-CM treated differentiated cells, the neural stem cell marker, NESTIN, is more highly expressed compared with Control-CM treated cells (Figure 4.10).

Therefore, the results indicate that long-term exposure of EB to exogenous SHH promotes differentiation towards the neuroectoderm lineage and increases NESTIN positive neural derivatives, but with no significant influences on mesodermal or endodermal lineages.

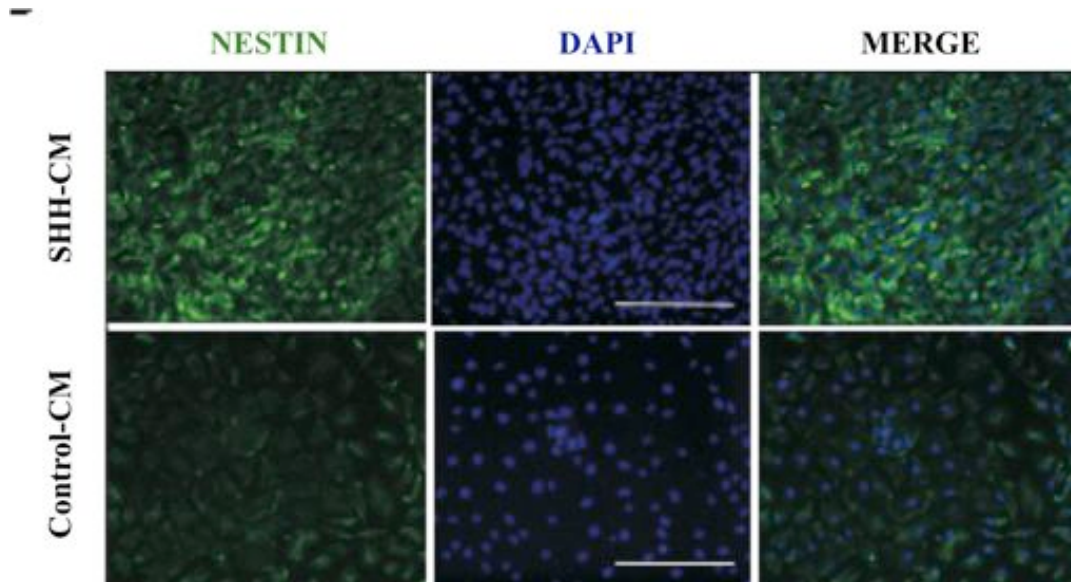


Figure 4.10 Immunofluorescent staining of neural stem cell marker Nestin in SHH-CM and Control-CM treated EB. Middle panel shows corresponding DAPI nuclear staining in blue and right panel shows corresponding merged images. Scale bars represent 50 μm .

These findings are consistent with the report by Maye *et al.*, 2004, showing the requirement of HH signaling in establishing the neuroectoderm in mESC EB, whereby EB derived from mutant mESC for the Smo receptor and Ihh were not able to generate neuroectoderm and their neural derivatives. The increase in NESTIN positive cells in the SHH treated population could be due to SHH supporting the proliferation of cells expressing NESTIN. This is supported by recent data that showed SHH promoted the survival of Sox1-positive mESC-derived neuroprogenitors (Cai *et al.*, 2008).

4.7 Summary

This chapter shows that the SHH pathway is functional and present in undifferentiated hESC. However, it is minimally active in undifferentiated hESC and

activation of SHH signaling does not maintain hESC pluripotency and proliferation. Instead, we propose that SHH signaling is poised for activation upon differentiation and influences the determination of early differentiated hESC towards the neuroectoderm lineage. The results presented here extend the understanding of extrinsic factors regulating hESC pluripotency and self-renewal.

CHAPTER 5 ROLE OF SHH IN NEURAL DIFFERENTIATION

5.1 Introduction

Most of the current neural differentiation protocols of hESC are based on co-cultures with stromal cells or treatment with FGF2 and noggin as inductive factors. SHH is then added after neural induction during the neural patterning phase to ventralize the cells so that neurons with ventral midbrain e.g. dopaminergic (DA) neurons or ventral hindbrain identity e.g. motor neurons can be obtained efficiently (Perrier *et al.*, 2004; Yan *et al.*, 2005; Sonntag *et al.*, 2007; Cho *et al.*, 2008; Li *et al.*, 2008). Apart from its role in ventralizing neuroprogenitors, there is evidence in mESC studies that suggest SHH signaling is required for neuroectoderm development and neuroprogenitor survival (Maye *et al.*, 2004; Cai *et al.*, 2008).

Therefore, this chapter sets out to systematically address the second aim of the thesis, which is to investigate the role of SHH in neural differentiation. Moving away from the spontaneous differentiation method employed in the previous chapter, a protocol that allows for a more controlled and reproducible neural differentiation was developed, so that the study could be focused on cells solely from the neural lineage. A stable overexpressing SHH hESC line was then generated and differentiated according to the developed protocol. Since evidence from Section 4.6 suggested that SHH promotes the spontaneous differentiation of hESC to the neuroectoderm lineage, it was postulated that overexpression of SHH would similarly increase the overall efficiency of neural differentiation. The effect of overexpression of SHH was investigated at two different stages of differentiation: 1) at the neuroprogenitor stage for expression of NSC markers and proliferation, and 2) at the terminally differentiated DA neuron stage.

5.2 Noggin treatment induces neural differentiation

To control the differentiation of hESC into the neural lineage, the BMP inhibitor noggin was used to induce neural differentiation, according to a protocol that was modified

from established methods as reported in Zhang *et al.*, 2001 and Pera *et al.*, 2004. Differentiation was initiated by culturing hESC as embryoid bodies (EB) for 4 days in KO media after which the EB were transferred onto laminin-coated plates and grown in serum free N2B27 media supplemented with 500 ng/ml noggin. After 10 days of noggin treatment, the clumps displayed a compact and tight morphology that occasionally contained at the edges small rosettes, which are radially organized columnar epithelial cells reminiscent of the neural tube *in vivo* (Zhang *et al.*, 2001). The tight clumps were stained positive for the neuroectoderm marker paired box gene 6 (PAX6) (Figure 5.1). The clumps were then dissected from surrounding fibroblastic cells and grown in suspension as cellular aggregates termed neurospheres (Figure 5.1).

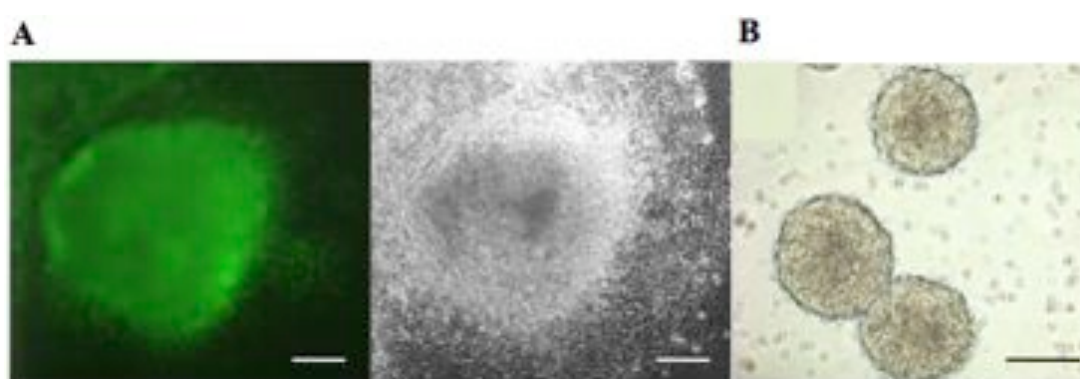


Figure 5.1 Noggin induced neural differentiation. Replated EB were treated for 10 days with noggin and compact clumps were formed that were (A) immunopositive for PAX6. The middle panel shows corresponding bright field image. (B) Bright field micrograph of typical neurospheres in culture. Scale bars represent 100 μm .

The culture media used for maintaining neurospheres was N2B27 supplemented with EGF and FGF2 and shall be simply referred to as N2B27. The neurospheres could be expanded by serial passaging for more than 5 passages but they were not passaged for any longer to avoid any changes in differentiation potential (Itsykson *et al.*, 2005).

The expression of neuroectoderm markers in the neurospheres were examined by real-time PCR and transcripts of *SOX1*, *MSI*, *NESTIN* and *PAX6* were observed to be upregulated by more than 2.5-fold when compared to hESC from the undifferentiated state (Figure 5.2A). Expression of the pluripotent marker *OCT4* was detected at very low levels in

the neurospheres (Figure 5.2A). When compared with spontaneously differentiated EB, neurospheres had very low expression levels of mesodermal and endodermal markers *alpha fetoprotein (AFP)*, *alpha-cardiac actin (ACTC)*, *GATA binding protein 6 (GATA6)* and *hepatic nuclear factor 4, alpha (HNF4a)* (Figure 5.2B). This confirmed that the neurospheres did not contain cells from other lineages.

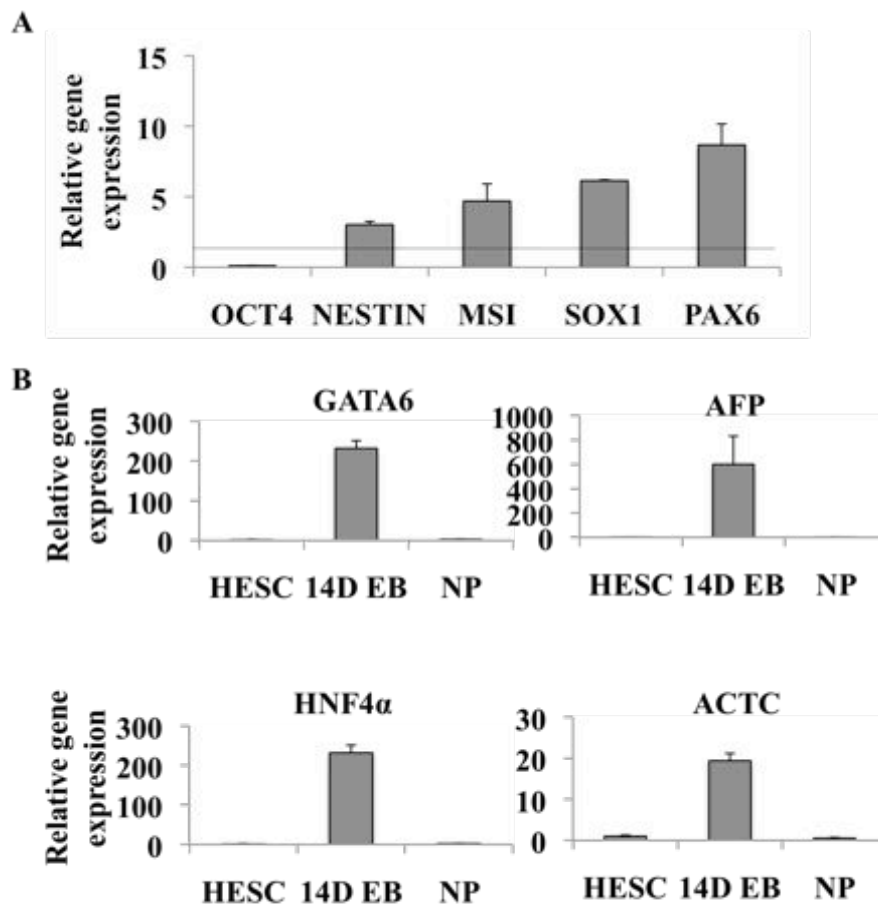


Figure 5.2 Neuroprogenitors express neuroectoderm markers. Neurospheres were harvested after 7 days in culture and mRNA expression was analyzed by real-time PCR analysis for (A) neuroectoderm markers and *OCT4* in neuroprogenitors and (B) mesoderm and endoderm markers in undifferentiated hESC (HESC), 14-day-old embryoid bodies (14D EB) and neuroprogenitors (NP). The expression level of each gene is shown relative to undifferentiated hESC, which was arbitrarily defined as 1 unit. The values shown are mean \pm SD of a representative experiment carried out in triplicate and repeated twice. In (A), the line represents expression levels of each gene in undifferentiated hESC.

Flow cytometry analysis showed that neurospheres expressed a comprehensive set of NSC surface markers (Pruszek *et al.*, 2007): A2B5 (34% ± 18%), FORSE-1 (51% ± 20%), p75 (83% ± 12%), PSA-NCAM (94% ± 3%) and CD133 (34% ± 11%) (Figure 5.3A). To further characterize the cells within the neurospheres, neurospheres were dissociated into smaller clumps and replated on laminin-coated plates and allowed to proliferate in N2B27 media. After 4-5 days in culture, rosettes were abundant in culture. Accordingly, immunofluorescent staining indicated that PAX6, NESTIN and SOX1 were detected in the rosettes (Figure 5.3B-D). These results demonstrate that neural induction was achieved using the protocol. From this point forth, the term neuroprogenitors refer to the cells within the neurospheres that express NSC markers.

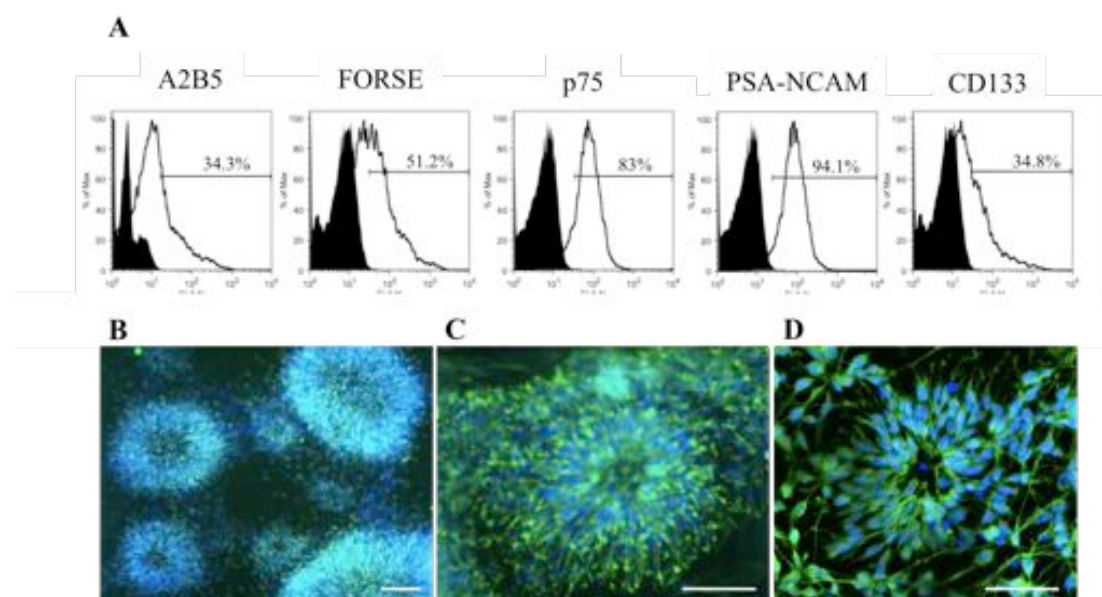


Figure 5.3 Neuroprogenitors express NSC markers. (A) Flow cytometry analysis of neuroprogenitors expressing A2B5, FORSE-1, p75, PSA-NCAM and CD133. The shaded histogram represents staining with the negative control and open histograms represent staining with the respective antibodies. (B-D) Representative images showing immunofluorescent staining of (B) PAX6, (C) NESTIN and (D) SOX1 on neuroprogenitors that were replated onto laminin-coated wells. Nuclei were stained with DAPI. Scale bars represent 50 μm.

The protocol established by Zhang *et al.* 2001 reported using FGF2 as the neural inducer, rosettes were present in replated EB after 7 days in a serum-free defined media. However, the formation of rosettes was not observed when FGF2 was applied in this study to replated EB,

even after extending FGF2 treatment to 14 days. Instead, noggin was the more efficient neural inducer, whereby rosettes were observed in cell clusters after 10 days treatment. In the study by Pera *et al.*, 2004, HES-3 colonies were grown on mouse feeder layers and treated with noggin for 10-14 days. In our protocol, extending noggin treatment to 14 days did not increase gene expression of *SOX1*, *NESTIN*, *PAX6* and *MSI* in neurospheres (data not shown), suggesting that 10 days of noggin treatment was a sufficient period of time to achieve neural differentiation.

This optimized differentiation scheme using noggin as neural inducer is an improvement on the currently published protocols. Firstly it eliminates the use of mouse feeder layer or stromal cells (Pera *et al.*, 2004; Perrier *et al.*, 2004) and secondly, it employs a serum-free, chemically defined media, both of which reduce biological variations. As cells are grown on an adherent layer, exclusion of fibroblastic or cystic cells is possible and only compact colonies containing rosettes continue to be propagated, which helps to ensure that a purer population of neuroprogenitors can be obtained. To confirm that the neuroprogenitors are multipotent, neuroprogenitors were further differentiated by replating them as monolayer cultures in N2B27 media without the mitogens EGF and FGF2. After 2 weeks, there was an abundance of cells with characteristic neuronal morphology. Immunofluorescence imaging showed that the neurons were positive for both the neuronal marker MAP2 and dopaminergic (DA) neuron marker tyrosine hydroxylase (TH) (Figure 5.4A). The presence of astrocytes was demonstrated by cells that stained positive for both the glial fibrillary acidic protein (GFAP) and neuronal marker β -Tubulin III (Figure 5.4B).

However, oligodendrocytes were rarely obtained. A similar observation has been reported (Peh *et al.*, 2009), suggesting that oligodendrocytic differentiation requires a more concerted effort which requires other growth factors and cell substrates (Gil *et al.*, 2009). Electrophysiological studies were carried out to verify whether the neurons differentiated from the neuroprogenitors were mature and functional. To allow maturation, differentiated neuroprogenitors were further cultured on laminin-coated coverslips for another 2 weeks with growth factors GDNF, BDNF and NGF (all 20 ng/ml). The whole-cell patch clamp technique

detected spontaneous postsynaptic currents in the neurons (Figure 5.4C). Therefore, the neural differentiation protocol used in this study efficiently generates neuroprogenitors from hESC, which can be further differentiated into functional neurons and astrocytes.

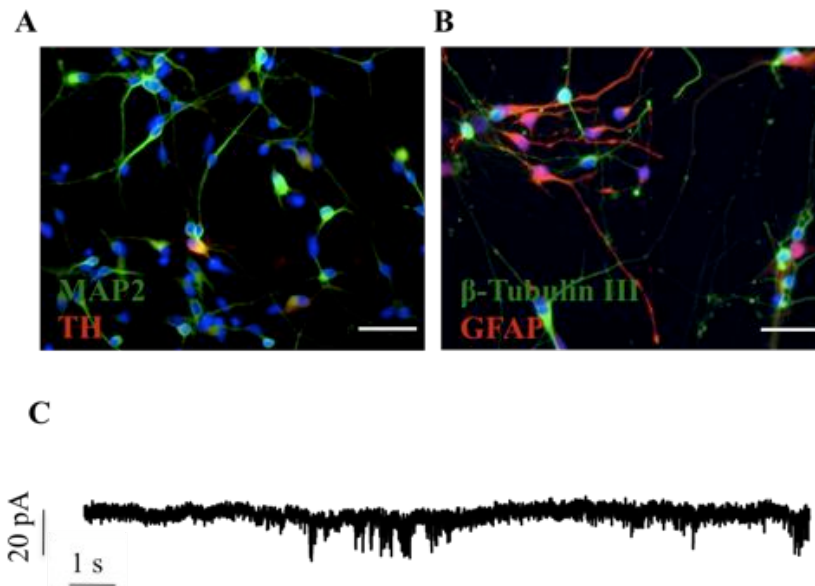


Figure 5.4 Neuroprogenitors are able to differentiate into astrocytes and functional mature neurons. (A-B) Immunocytochemistry was performed to detect (A) TH (red) and MAP2 (green) positive neurons and (B) β -III Tubulin (green) and GFAP (red) positive astrocytes. Scale bars represent 100 μ m. (C) Patch clamp recordings show spontaneous postsynaptic currents.

To confirm that the specification of DA neurons from neuroprogenitors was dependent on SHH, neuroprogenitors were first directed to differentiate to the DA lineage. To this end, neuroprogenitors were dissociated and plated onto laminin-coated wells for 7 days and treated with SHH, FGF8 and AA to pattern the cells (Perrier *et al.*, 2004; Sonntag *et al.*, 2007). After 7 days, rosettes that reformed in culture were harvested and seeded as single cells on laminin-coated coverslips and fed with recombinant SHH, FGF8, cAMP, AA, BDNF and GDNF for another 10-14 days to allow further differentiation. Neurons derived from this protocol co-expressed TH with β -Tubulin III, signifying that they were DA neurons (Figure

5.5A). The removal of SHH entirely from the protocol reduced the number of DA neurons significantly by around 3-fold (Figure 5.5A-B). This observation was comparable to that reported in a similar study done on mESC (Lee *et al.*, 2000) and established that application of SHH at the neural patterning stage was necessary for the efficient development of DA neurons from hESC.

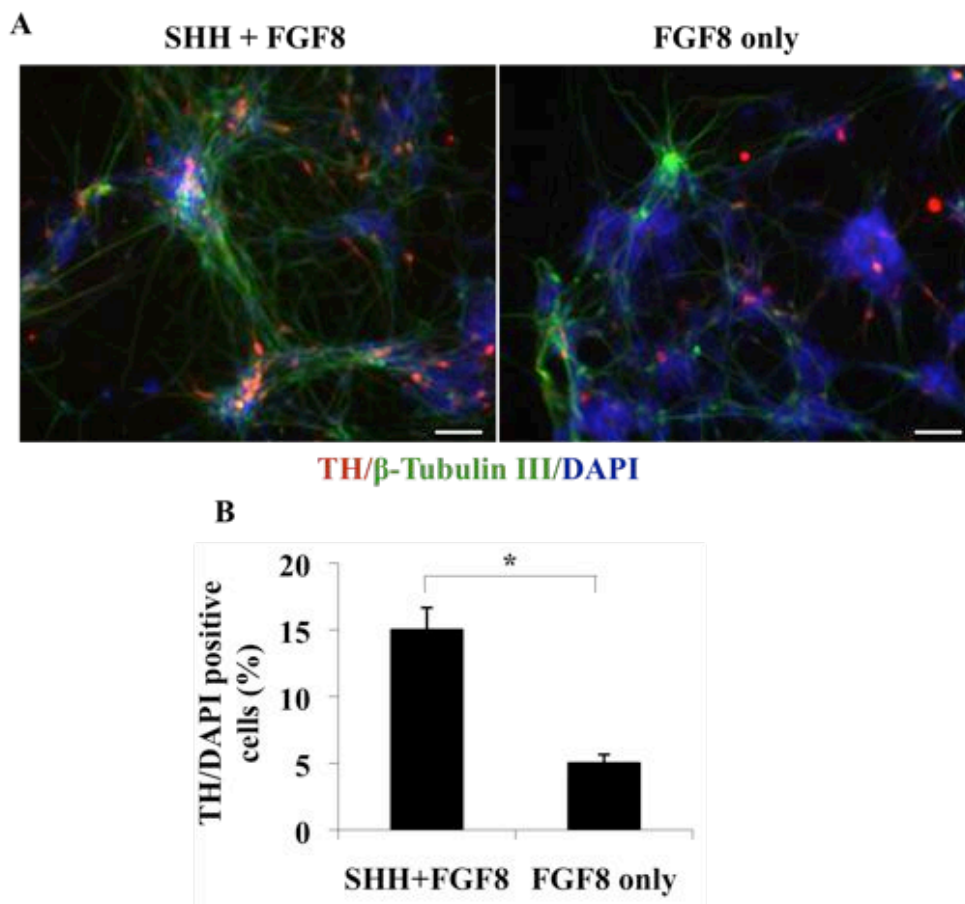


Figure 5.5 SHH is essential for the specification of DA neurons from neuroprogenitors. (A) Representative images showing immunofluorescent staining of TH (red) and β -Tubulin III (green) positive cells. Nuclei were stained with DAPI. Scale bars represent 50 μ m. (B) Quantification of the above images. TH+ nuclei were counted and expressed as a percentage of the total DAPI positive cells. Numbers presented represent the average percentage \pm SD from triplicate samples. * = $p < 0.05$.

5.3 Neuroprogenitors possess cilia

The neuroprogenitors were further characterized to determine if they possessed an intact primary cilium that is crucial for the SHH pathway to signal effectively (Huangfu *et*

al., 2003). Recent studies have shown that undifferentiated hESC line H1 and H9 possess primary cilia (Kiprilov *et al.*, 2008). Primary cilia are also present on most CNS neurons in the mouse brain (Whitfield, 2004) and are necessary for adult NSC formation (Han *et al.*, 2008). Therefore, it was important to establish if the neuroprogenitors and their parental HES3 cell line possessed cilia necessary for SHH signal transduction.

Undifferentiated hESC and neuroprogenitors were probed with the acetylated α -tubulin antibody that labels for microtubules within primary cilia. Small cilia projections were observed on OCT4 positive undifferentiated hESC (Figure 5.6A).

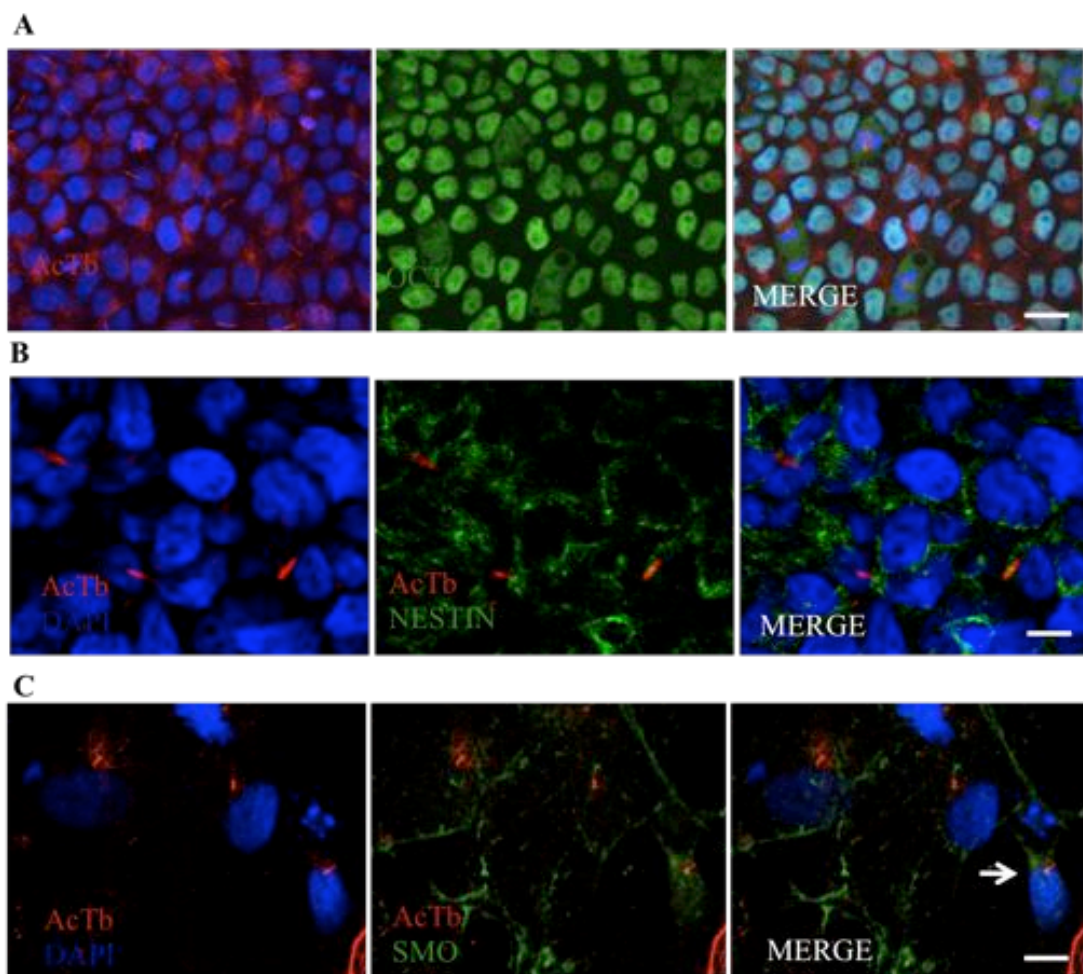


Figure 5.6 The SMO receptor localizes to primary cilia of neuroprogenitors. (A-C) Representative confocal images showing immunocytochemistry of (A) undifferentiated hESC with acetylated tubulin (AcTb), pluripotent marker OCT4, and corresponding merged images. (B) Neuroprogenitors were similarly probed for AcTb and the neuroectoderm marker NESTIN (green, middle panel). (C) Neuroprogenitors were stimulated with 200 ng/ml SHH for 24 - 48 hours and stained for AcTb and the SMO receptor (green, middle panel). The arrow points to SMO which localizes to the base of the primary cilia. Scale bars represent 10 μ m.

Preliminary results showed that similar cilia projections were also observed on NESTIN immunopositive neuroprogenitors (Figure 5.6B). The SHH receptor SMO was also found to localize with the primary cilia on neuroprogenitors (Figure 5.6C). The localization of SMO to the primary cilium is an indication of SHH pathway activation as demonstrated in the NIH3T3 fibroblasts (Rohatgi *et al.*, 2007; Wang *et al.*, 2009).

Real-time PCR showed there was approximately 2-fold upregulation of *PTCH1* and 1.7-fold of *SMO* transcripts in neuroprogenitors when compared to undifferentiated hESC (Figure 5.7). This indicates that SHH pathway is active in the neuroprogenitors. Taken together, the results support the finding in Section 4.5 that the SHH pathway is activated during neural differentiation and that hESC and neuroprogenitors possess the prerequisite components that can respond to SHH activation.

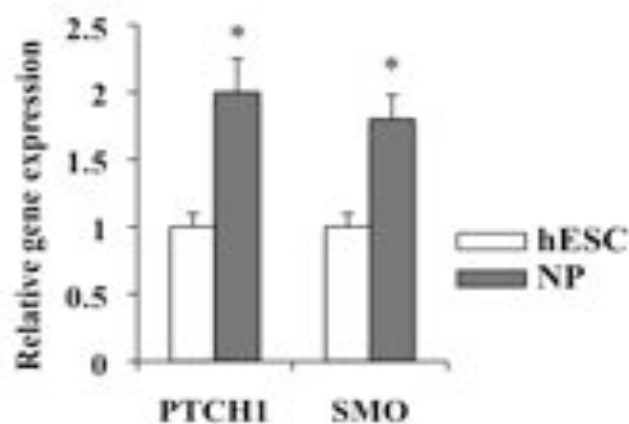


Figure 5.7 SHH pathway is activated in neuroprogenitors. Real-time PCR analysis of genes *PTCH1* and *SMO* in neuroprogenitors (NP). Values are expressed relative to undifferentiated hESC and are mean \pm SD of a representative experiment performed in triplicate and repeated twice. * = $p < 0.05$

5.4 Overexpression of SHH in hESC

To establish the role of SHH in hESC neural differentiation, a stable SHH overexpressing hESC line was generated. The overexpression of SHH was done in undifferentiated hESC so that exogenous SHH could be present throughout the differentiation

process. It would also overcome the limitation of diffusion of SHH into the inner layers of cells grown as clumps or spheres in suspension (Vallier *et al.*, 2004). Furthermore, overexpression of SHH was not predicted to affect the undifferentiated state as it was established in Section 4.4 that exogenous SHH did not induce differentiation when applied to hESC maintained in pluripotent conditions.

The cDNA encoding the mouse full-length *Shh* was cloned into an expression vector under the control of the Chinese hamster elongation factor 1 α (CHEF) promoter, which has been shown to enable high-level stable transgene expression in hESC (Chan *et al.*, 2008). The red fluorescent protein DsRed2 was linked through an IRES (internal ribosome entry site) to facilitate the monitoring of SHH expression. Undifferentiated hESC were transfected with the pCHEF-SHH-IRES-DsRed2 plasmid or the control empty vector pCHEF-DsRed2 plasmid and 2 SHH overexpressing stable cell lines were obtained after geneticin antibiotic selection. Only one of these lines was characterized more extensively in further experiments. Immunofluorescence staining of a typical colony of the overexpressing-SHH hESC line showed that the cells were SHH positive and co-expressed DsRed2 (Figure 5.8). The overexpressing SHH hESC line could be maintained in the undifferentiated state for over 10 passages and was karyotypically stable (data not shown).

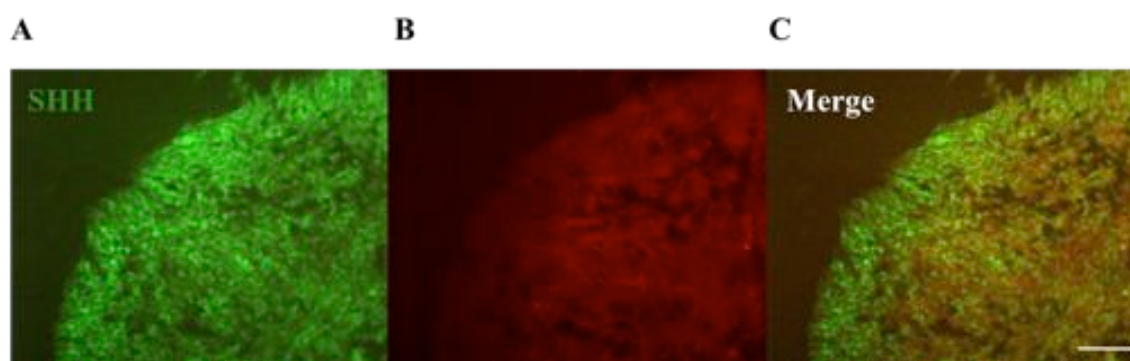


Figure 5.8 Stable overexpressing-SHH hESC express SHH and DsRed2. (A) Representative image of a typical overexpressing-SHH hESC colony maintained in pluripotent conditions showing immunocytochemistry for SHH. (B) Corresponding fluorescent image of DsRed2 and (C) merged images. Scale bar represents 100 μ m.

The wild-type HES3, vector-only and SHH overexpressing cell lines were subsequently differentiated into neuroprogenitors and referred to as H3-NP, Vector-NP and SHH-NP, respectively. The SHH-NP had sustained expression of the DsRed2 fluorescent protein (Figure 5.9).

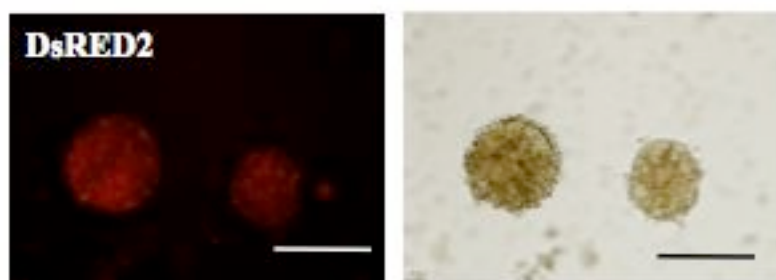


Figure 5.9 SHH-NP express the DsRed2 protein. Fluorescent image of SHH-NP and corresponding bright field image. Scale bars represent 50 μ m.

To confirm that overexpression of SHH was also consistently achieved in SHH-NP, SHH levels were assessed by Western blotting. Interestingly, the 45 kDa full length SHH protein was observed in all three cell lines. However, only the 19 kDa active N-terminal fragment of SHH was highly expressed in SHH-NP and was absent in both H3-NP and Vector-NP (Figure 5.10A). This could be due to impairment of the autoprocessing of full length SHH by hESC-derived neuroprogenitors and deserves further investigation. Quantification of SHH levels by ELISA demonstrated that the supernatant of SHH-NP cultures contained approximately 20-50 ng/ml of SHH (data not shown). Real-time PCR analysis showed that *SHH* was upregulated by 20-fold, while target genes *PTCH1* and *GLII* were upregulated by 7-fold and 4-fold respectively in SHH-NP when compared to H3-NP and Vector-NP (Figure 5.10B). These results confirmed that SHH is overexpressed in SHH-NP which results in the activation of the SHH pathway.

5.5 Overexpression of SHH enhances neural induction

To determine if overexpression of SHH would improve the efficiency of neural differentiation, SHH-NP were characterized with an array of NSC markers. SHH-NP were

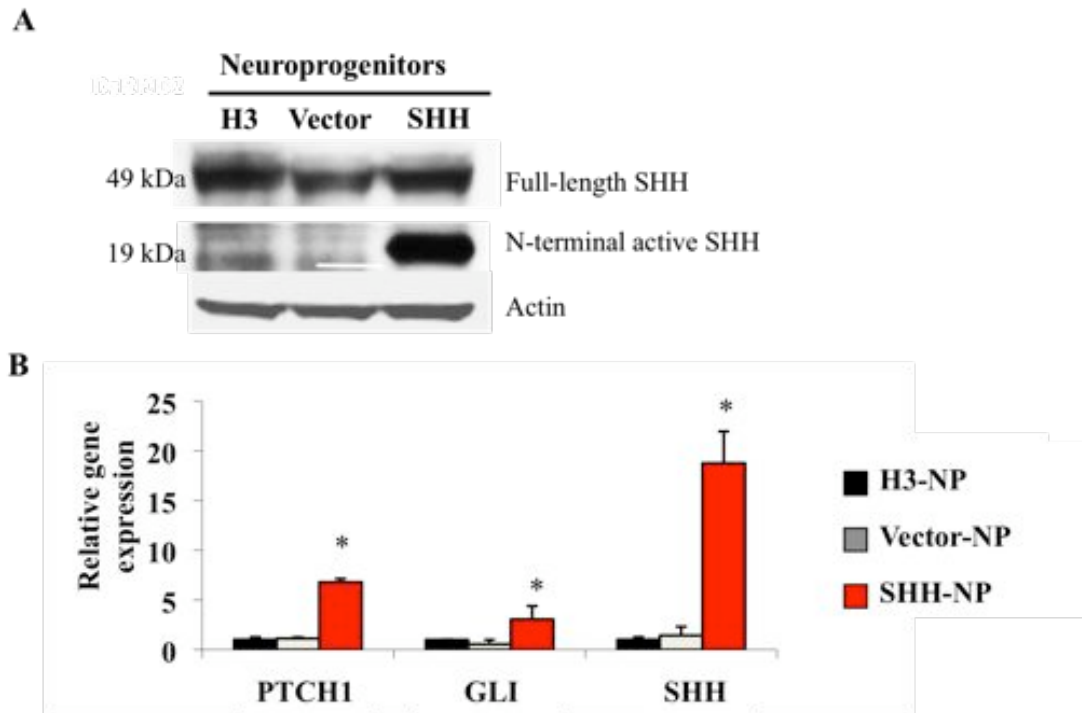


Figure 5.10 Overexpression of SHH in hESC-derived neuroprogenitors. (A) Western blot analysis of SHH-NP, Vector-NP and H3-NP probed with the anti-SHH antibody which detected both the full length (45 kDa) and 19 kDa active fragment. Actin was used as a loading control. (B) Real-time PCR analysis of *SHH* and target genes *PTCH1* and *GLI1* in SHH-NP, Vector-NP and H3-NP. The expression value of each gene is shown relative to H3-NP, which was arbitrarily defined as 1. The values are mean \pm SD of a representative experiment performed in triplicate and repeated thrice. * = $p < 0.05$.

analyzed by real-time PCR for neuroectoderm markers. SHH-NP had a 2-fold increase in *NESTIN* and 5-fold increase in *SOX1* expression in SHH-NP as compared to H3-NP and Vector-NP (Figure 5.11A). No significant difference in *MSI* and *PAX6* was observed. Western blot analysis corroborated with the gene expression studies as demonstrated by the increase in *NESTIN* and *SOX1* protein expression in SHH-NP (Figure 5.11B).

Flow cytometry analysis for NSC surface markers showed that SHH-NP had an average of 41% and 29% increase in CD133 expression compared to H3-NP and Vector-NP respectively (Figure 5.12). There was also an 80% and 30% increase in expression of A2B5 in SHH-NP and a 10% and 30% increase in p75 expression in SHH-NP, when compared to H3-NP and Vector-NP respectively (Figure 5.12).

A2B5 has been shown to be present on proliferative glial precursor cells in the fetal brain (Dietrich *et al.*, 2002), while p75 is expressed by NSC in the adult brain (Young *et al.*, 2007). CD133 has been used to isolate NSC from fetal brains (Uchida *et al.*, 2000), and shown that it was not expressed in more terminally differentiated neural cell types (Kania *et al.*, 2005). A2B7, p75 and CD133 have all been demonstrated to be cell surface markers to label for highly proliferative and multipotent neuroprogenitors derived from hESC (Carpenter, 2001; Jiang *et al.*, 2008; Peh *et al.*, 2009).

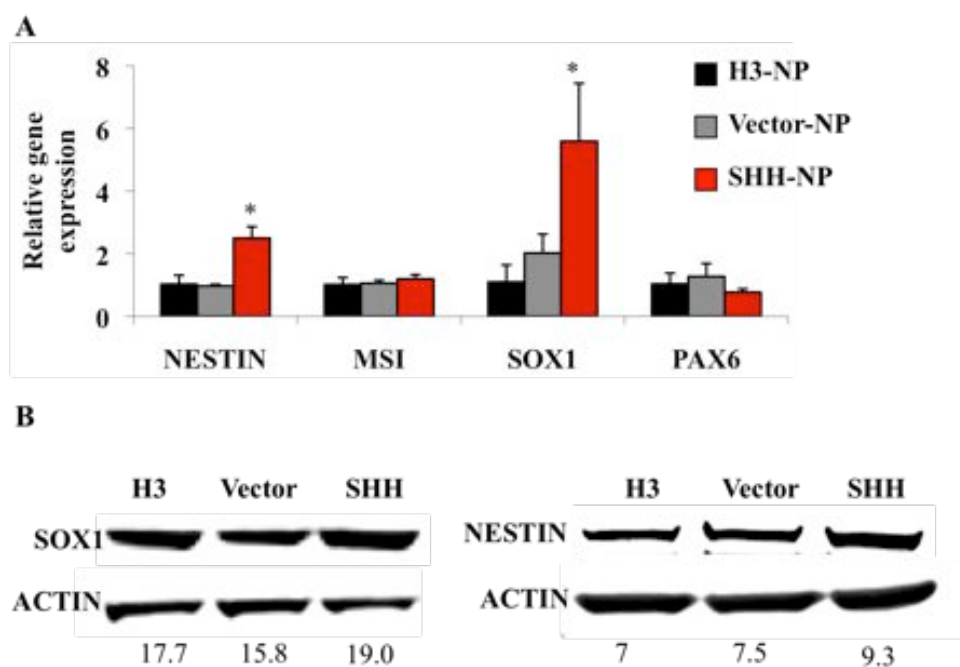


Figure 5.11 Overexpression of SHH in hESC-derived neuroprogenitors lead to increased expression of neuroectoderm markers. (A) Real-time PCR analysis of neuroprogenitors for neuroectoderm markers. The expression value of each gene is shown relative to H3-NP, which was arbitrarily defined as 1. The values are mean \pm SD of a representative experiment performed in triplicate and repeated thrice. * = $p < 0.05$ (B) Western blot of neuroprogenitors probed with SOX1 and NESTIN antibodies with ACTIN as a loading control. Values indicate quantification of protein based on the band intensities from the Western blot normalized to Actin using LI-COR Odyssey software.

Hence, the enrichment of cells expressing the 3 NSC surface markers plus NESTIN and SOX1 markers in SHH-NP demonstrate that overexpression of SHH promotes the derivation of neuroprogenitors from hESC. This corroborates with evidence Section 4.6, that long-term exposure of SHH promotes neuroectoderm differentiation.

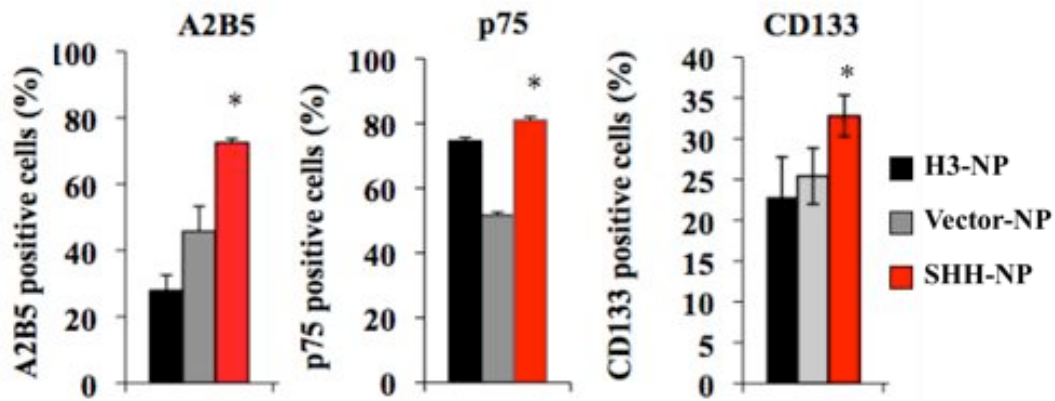


Figure 5.12 Overexpression of SHH in hESC-derived neuroprogenitors lead to increased expression NSC surface markers. Histogram representation of FACS analysis of CD133, A2B5 and p75 showing percentage positive cells. * = $p < 0.05$. All values shown are mean \pm SD of a representative experiment performed in triplicate and repeated thrice.

5.6 Overexpression of SHH increases the proliferation of sorted neuroprogenitors

As SHH is known to have proliferative effects on neuroepithelial cells and NSC in the adult brain (Kenney *et al.*, 2003; Cayuso *et al.*, 2006), there was interest to see if there was an increase in proliferation of neuroprogenitors with overexpression of SHH. The bulk populations of H3-NP, Vector-NP and SHH-NP did not show any increase in overall proliferation status as assessed by long-term observations and EdU assay (data not shown). This is possibly because the neuroprogenitors are a heterogeneous population (Figure 5.3) and changes in proliferation in a certain population may be obscured. Therefore, cell sorting based on the dual expression of p75 and PSA-NCAM was carried out.

After cell sorting, equal numbers of approximately 1×10^5 p75+/PSA-NCAM+ cells from each cell line were cultured in suspension as neurospheres. The neuroprogenitors had very low viability after sorting and there was a lag phase of around 3-5 days before visible neurospheres were formed. Once neurospheres were observed, they were allowed to expand further for another 7 and 14 days before being harvested for the trypan blue exclusion assay.

After 7 days, there was around a 2-fold increase of SHH-NP p75+/PSA-NCAM+ neuroprogenitors (Figure 5.13). This increase in cell proliferation continued after 14 days,

whereby there was almost a 2.5-fold increase in cell numbers of the p75+/PSA-NCAM+ population from SHH-NP compared to H3-NP and Vector-NP (Figure 5.13). Hence, the results suggested that the overexpression of SHH induced the proliferation of p75+/PSA-NCAM+ neuroprogenitors. Further studies will be required to understand if the increase in cell number was through an increase in survival, proliferation or both.

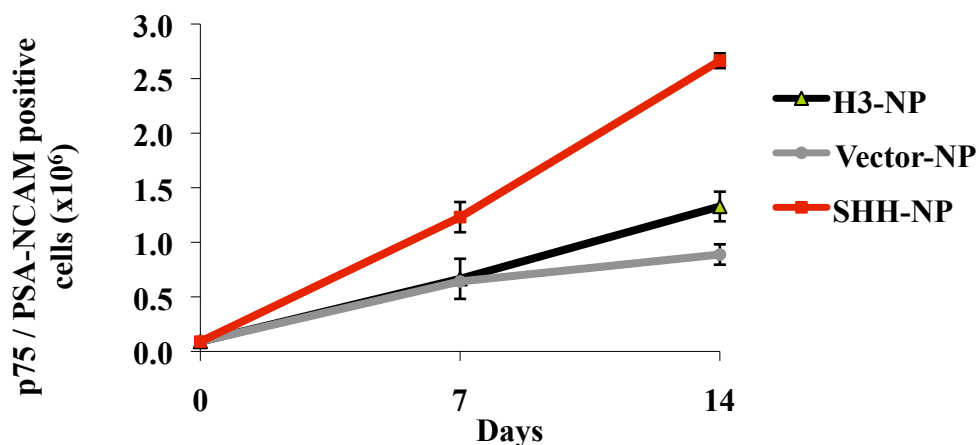


Figure 5.13 Overexpression of SHH results in increase proliferation of multipotent p75+/PSA-NCAM+ neuroprogenitors. (A) 1×10^5 sorted cells were seeded into 24-well ultra-low suspension plates and neurospheres formed after 3-5 days. Cells were harvested 7 and 14 days after and counted by trypan blue exclusion. * = $p < 0.05$. All values shown are mean \pm SD of a representative experiment performed in triplicate and repeated thrice.

A previous study by Cai *et al.*, 2008 suggested that Shh may not play an important role in neural determination, but rather, improves survival and proliferation of Sox1-positive cells during neurogenesis of mESC. The results here support the findings of that study, in that overexpression of SHH increases the expansion of hESC-derived neuroprogenitors. At the same time, data from Section 4.6 and Chapter 6 suggest that SHH may also play a role in neural induction or determination. More studies will have to be done to be able to ascertain the predominant mechanism, if any, by which SHH is able to promote derivation of neuroprogenitors from hESC.

5.7 Overexpression of SHH leads to increase in DA neurons

The enrichment of neuroprogenitors expressing NSC markers within SHH-NP offered the prospect that there may be downstream effects of an increase in differentiated progeny. In this case, the DA neuron lineage was chosen as a readout of neuroprogenitor differentiation efficiency because *noggin* has been shown to improve DA neuron differentiation from hESC differentiated on PA6 cells (Chiba *et al.*, 2008). In addition, it has been demonstrated that efficient derivation of DA neurons from neuroprogenitors required the presence of SHH. Therefore, the DA lineage would provide a reliable model to study the functional outcome of an increase in neuroprogenitor population.

The three cell lines, referred to as H3-NN (neuron), Vector-NN and SHH-NN in this section, were differentiated to DA neurons according to the protocol described in Section 5.2. Briefly, the neurospheres from each cell line were plated onto laminin-coated wells and both H3-NN and Vector-NN were treated with 200 ng/ml SHH, 200 ng/ml FGF8 and 200 μ M AA. SHH-NN cultures were treated with only AA and FGF8. Rosettes that reformed in culture from the 3 cell lines were then seeded as single cells on coverslips. The H3-NN and Vector-NN cultures were supplemented with similar concentrations of SHH, FGF8, cAMP, AA, BDNF and GDNF. SHH-NN was supplemented with the same growth factors with the exception of recombinant SHH. Although the concentration of SHH protein present in SHH-NN cultures was not determined, its level was expected to be high based on the western blot in Figure 5.9 and mRNA analysis in Figure 5.15. Therefore, this experiment sought to investigate the effect of overexpression of SHH from the undifferentiated stage through the entire process of neural differentiation as compared cells that were only exposed to SHH at the later stages of neural patterning and differentiation at concentrations commonly used (Perrier *et al.*, 2005, Yan *et al.*, 2005).

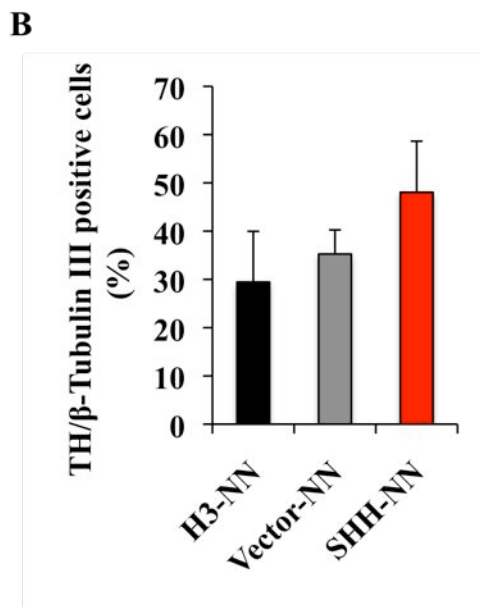
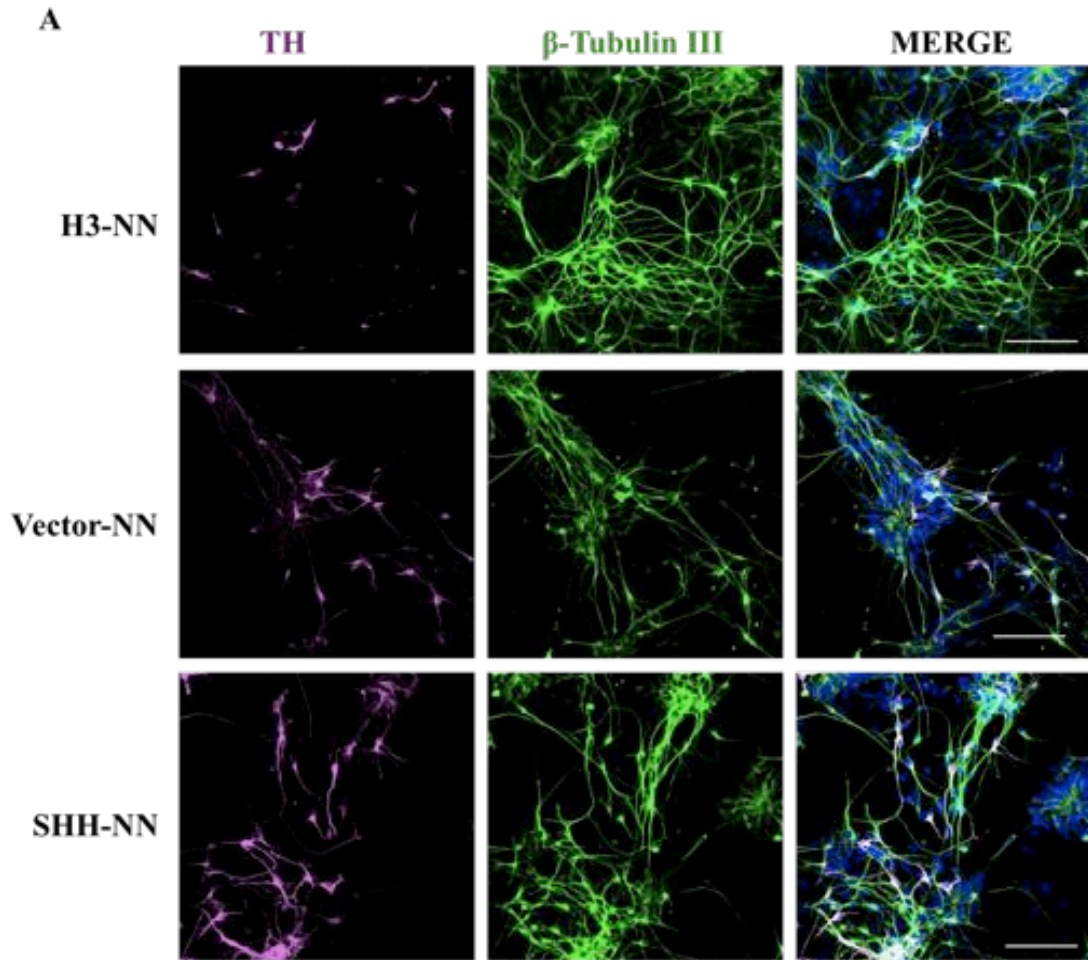


Figure 5.14 Overexpression of SHH in hESC-derived neuroprognitors leads to an increase in TH⁺ neurons. (A) Immunofluorescent images of SHH-NN, Vector-NN and H3-NN differentiated neuroprogenitors stained for TH (purple) and β -Tubulin III (green). Nuclei are stained by DAPI. Scale bars represent 100 μ m. These are representative images of an experiment repeated four times with similar results. (B) Quantification of the above images. TH⁺ nuclei were counted and expressed as a percentage of the total β -Tubulin III⁺ cells. Numbers presented represent the average percentage \pm SD from triplicate samples. * = $p < 0.05$.

In all three cultures, long neurite extensions were evident within 2-3 days and subsequently complex neurite networks were formed. After 14 days of differentiation, the neurons were probed with antibodies against β -Tubulin III and TH. Visualization by immunofluorescence showed that there were more TH+ β -Tubulin III neurons in SHH-NN cultures as compared to H3-NN and vector-NN (Figure 5.14A). Quantification of images was carried out and of the β -Tubulin III neurons in H3-NN and Vector-NN cultures, approximately 30% were TH+ neurons (Figure 5.14B). In contrast, approximately 50% of the β -Tubulin III neurons were TH+ neurons in SHH-NN cultures, representing a 20% increase in yield of TH+ neurons.

Markers for DA neurons were then examined by real-time PCR analysis in SHH-NN. *PTCH1* and *SHH* were upregulated in SHH-NN, affirming that the overexpression of SHH and activation of the pathway was sustained throughout the differentiation process (Figure 5.15). There was an approximately 1.5-fold increase in gene expression of the dopamine neuron enzymes *AADC* and *TH* in SHH-NN cultures compared to H3-NN and Vector-NN (Figure 5.15).

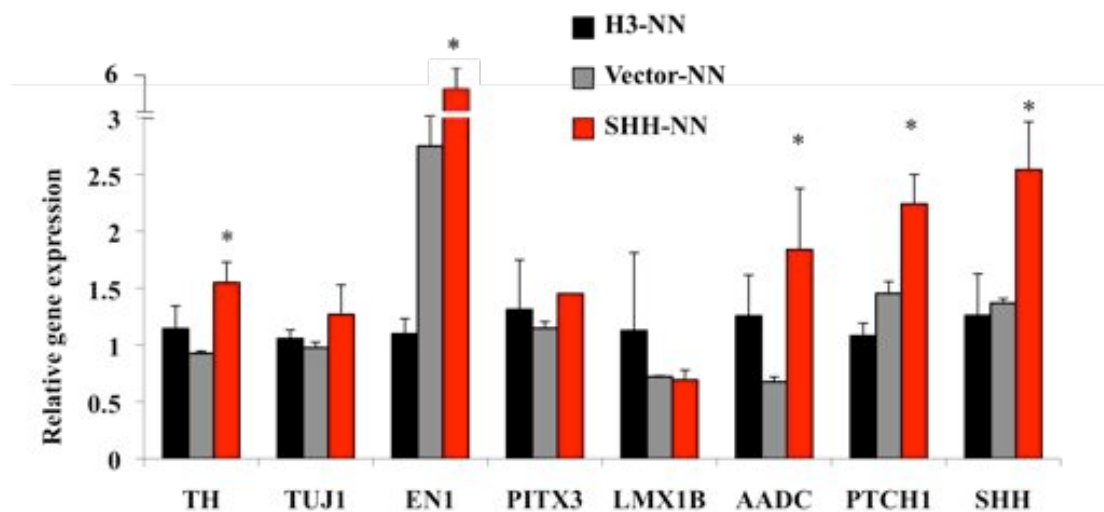


Figure 5.15 Neurons express dopaminergic neuron marker genes. Real-time PCR analysis of DA neurons. The expression value of each gene is shown relative to H3-NN, which was arbitrarily defined as 1. The values are mean \pm SD of a representative experiment performed in triplicate and repeated thrice. * = $p < 0.05$

There was also a 6-fold increase in the midbrain DA marker *EN1*. However, there were no significant changes in mRNA expression of the neuronal marker *TUJI* or other midbrain DA transcription factors *PITX3* and *LMX1B* in SHH-NN (Figure 5.15). Therefore, the results showed that overexpression of SHH led to the increased production of TH+ neurons that expressed appropriate gene markers of DA neurons. We postulate that the increase in TH+ DA neurons in SHH-NN cultures was due to the higher starting number of NSC in SHH-NP that were able to eventually differentiate successfully into DA neurons.

5.8 Summary

This chapter presents a series of experiments designed to understand the role of SHH in neural differentiation by studying the effect of its overexpression in differentiating hESC. An effective neural differentiation protocol was first developed based on established methods, requiring the use of noggin as the neural inducer. The neuroprogenitors derived expressed appropriate neural markers like NESTIN, SOX1, *PAX6* and *MSI* and surface markers FORSE-1, PSA-NCAM, A2B5 and CD133. The neuroprogenitors were able to differentiate into functional mature neurons and astrocytes. It was then confirmed that SHH was an important factor in the ability to obtain DA neurons from the neuroprogenitors. It was also established that the SHH pathway receptor SMO receptor localized with primary cilia present on neuroprogenitors upon SHH stimulation, validating the ability of the cells to respond to SHH. Next, a stable overexpressing SHH hESC line was established and subsequently led down the neural differentiation pathway. The overexpression of SHH resulted in the increase of neuroectoderm markers NESTIN and SOX1 in neuroprogenitors as compared to the control cell lines. There was a concomitant increase in cells expressing the NSC surface markers CD133, A2B5 and p75. Together, the results suggest that SHH can work with noggin to push hESC towards the neuroprogenitor fate. p75 and PSA-NCAM double positive neuroprogenitors had an increased cell number with the overexpression of SHH, suggesting that SHH has a role in promoting the expansion of neuroprogenitors.

Further differentiation of the neuroprogenitors showed that there was an increase in the yield of DA neurons from SHH-NP, when compared to H3-NP and Vector-NP that were only exposed to SHH in the later part of the differentiation protocol. This suggested that the enrichment of NSC within SHH-NP resulted in the increase in subsequent in DA neurons. Taken together, the results in this chapter elucidated the role of SHH in neural differentiation, which is to promote neural induction, neuroprogenitor expansion, as well as neuron specification towards the DA lineage.

CHAPTER 6 IDENTIFICATION OF SHH TARGET GENES IN NEUROPROGENITORS

6.1 Introduction

This chapter aims to identify genes regulated by SHH and uncover novel target genes of the pathway in hESC-derived neuroprogenitors. Even though it is known that SHH is required to direct the differentiation of hESC to several neural subtypes, the genes of the pathway that regulate the diversity of cellular responses arising from SHH activation have yet to be elucidated. Most of the current understanding of the SHH pathway in neural development was obtained from zebrafish or mouse studies. Therefore, hESC provide an excellent opportunity to discover novel target genes of SHH in humans.

There are some genes like *PTCH1*, *GLI1* and *HHIP* that are canonical target genes of the pathway in all cell types (Chuang and McMahon, 1999). There are also other genes that are cell type or tissue specific. For example, *FoxA2* (or *Hnf3 β*) in the neural floor plate (Roelink *et al.*, 1995; Sasaki *et al.*, 1997), *Nkx2-2* in neuralized mouse embryoid bodies (Vokes *et al.*, 2007), *Igfbp-6* in the prostate and epithelial cells (Yoon *et al.*, 2002; Lipinski *et al.*, 2005), *FoxF1* in the developing lung and foregut (Mahlapuu *et al.*, 2001), *sFRP-2* in the sclerotome and mesenchymal stem cells (Lee *et al.*, 2000; Ingram *et al.*, 2002), and *Sox14* in the spinal cord (Hargrave *et al.*, 2000). To add to the complexity, the same gene under similar SHH activation can be upregulated or downregulated, depending on the tissue that they are expressed in, e.g *Sfrp2* (Lee *et al.*, 2000; Ingram *et al.*, 2002).

Therefore, this chapter aims to identify genes that are regulated by SHH responsible for promoting neural differentiation in hESC. To achieve that aim, genome wide transcriptional profiling of neuroprogenitors overexpressing SHH (SHH-NP) was carried out to identify genes that were positively or negatively regulated compared to the wild type H3 neuroprogenitors (H3-NP) and vector-control neuroprogenitors (Vector-NP). The differentially expressed genes were then interrogated using bioinformatics to identify potential target genes that contain putative GLI binding site on their promoters. The outcome

of this analysis identified a list of putative direct and indirect SHH target genes that includes (a) genes that have been previously demonstrated to be induced by SHH in other tissues or organisms but not in hESC and (b) novel genes that have not been reported to be regulated by SHH in any cellular context.

6.2 Microarray Analysis

A comparative gene expression analysis of SHH-NP, Vector-NP and H3-NP was performed using the Affymetrix Human Genome U133 array, which analyzes the expression level of approximately 38,500 well characterized human genes. RNA from SHH-NP, Vector-NP and H3-NP were harvested after 1 week in culture and 12 microarray experiments were performed with quadruplicate RNA samples. For identification of relevant differentially expressed genes, only genes with more than 1.5-fold difference in expression were considered for further evaluation. On top of that, the genes had to be differentially expressed in both SHH-NP versus H3-NP and SHH-NP versus Vector-NP data sets. A total of 337 annotated genes were identified by the array: 182 were upregulated and 155 were downregulated in SHH-NP when compared to H3-NP and Vector-NP. The top 20 upregulated and downregulated genes are shown in Table 6.1 and Table 6.2 respectively. The remaining genes are listed in Appendix A. A heat map representation of the expression levels of the top 20 upregulated and downregulated genes is shown in Figure 6.1A.

The differentially expressed genes (DEG) were then categorized according to the Gene Ontology (GO) biological processes and the top 8 categories of genes enriched in SHH-NP were cellular developmental process, nervous system development, generation of neurons, neurite morphogenesis, neuron development, cellular morphogenesis during differentiation and cell adhesion (Figure 6.1B).

Table 6.1 List of top 20 significantly upregulated genes in SHH-NP. Genes are ranked according to their fold change values.

<i>Symbol</i>	Description	Fold change		p-value	
		SHH vs Vector	SHH vs H3	SHH vs Vector	SHH vs H3
<i>NKX2-2</i>	NK2 homeobox 2	17.496	15.376	3.89E-10	7.08E-07
<i>FOXD1</i>	forkhead box D1	8.568	7.644	1.05E-11	7.83E-08
<i>NTRK2</i>	neurotrophic tyrosine kinase, receptor, type 2	7.999	5.892	7.26E-10	9.23E-07
<i>FOXA1</i>	forkhead box A1	7.648	8.422	2.20E-12	3.68E-08
<i>HEY2</i>	hairy/enhancer-of-split related with YRPW motif 2	7.045	3.405	1.52E-09	1.63E-06
<i>DDC</i>	dopa decarboxylase (aromatic L-amino acid decarboxylase)	6.556	6.574	4.76E-10	7.88E-07
<i>SYT4</i>	synaptotagmin IV	6.507	2.800	2.16E-08	1.08E-05
<i>POSTN</i>	periostin, osteoblast specific factor	6.395	1.825	9.21E-05	4.18E-03
<i>CYP1B1</i>	cytochrome P450, family 1, subfamily B, polypeptide 1	6.131	5.502	1.33E-09	1.54E-06
<i>NTN1</i>	netrin 1	5.990	5.998	2.54E-10	4.95E-07
<i>PCDH8</i>	protocadherin 8	5.906	4.155	2.69E-05	1.68E-03
<i>C4orf18</i>	chromosome 4 open reading frame 18	4.671	2.875	2.74E-08	1.29E-05
<i>C8orf46</i>	chromosome 8 open reading frame 46	4.655	4.352	1.01E-08	6.08E-06
<i>SPARCL1</i>	SPARC-like 1 (hevin)	4.385	3.838	1.76E-11	8.75E-08
<i>STI8</i>	suppression of tumorigenicity 18 (breast carcinoma) (zinc finger protein)	4.335	4.123	4.90E-09	3.53E-06
<i>COL12A1</i>	collagen, type XII, alpha 1	4.178	1.989	3.06E-07	6.46E-05
<i>FSTL5</i>	follistatin-like 5	4.138	2.448	9.56E-06	7.78E-04
<i>PRMT8</i>	protein arginine methyltransferase 8	4.136	4.144	3.04E-08	1.31E-05

Table 6.2 List of top 20 significantly downregulated genes in SHH-NP. Genes are ranked according to their fold change values.

<i>Symbol</i>	Description	Fold change		p-value	
		SHH vs Vector	SHH vs H3	SHH vs Vector	SHH vs H3
<i>IDI</i>	inhibitor of DNA binding 1, dominant negative helix-loop-helix protein	0.167	0.193	3.22E-11	1.27E-07
<i>KBTBD10</i>	kelch repeat and BTB (POZ) domain containing 10	0.216	0.428	6.96E-04	1.90E-02
<i>GLT8D4</i>	glycosyltransferase 8 domain containing 4	0.236	0.247	1.42E-09	1.61E-06
<i>LPL</i>	lipoprotein lipase	0.238	0.150	1.29E-11	7.83E-08
<i>LGALS1</i>	lectin, galactoside-binding, soluble, 1	0.254	0.367	1.40E-07	3.92E-05
<i>COL1A2</i>	collagen, type I, alpha 2	0.268	0.410	1.54E-05	1.10E-03
<i>TFPI</i>	tissue factor pathway inhibitor (lipoprotein-associated coagulation inhibitor)	0.286	0.290	7.49E-08	2.53E-05
<i>PAX3</i>	paired box 3	0.292	0.267	1.19E-11	7.83E-08
<i>MSX2</i>	msh homeobox 2	0.301	0.222	7.38E-12	6.73E-08
<i>LGALS3</i>	lectin, galactoside-binding, soluble, 3	0.302	0.320	4.30E-09	3.25E-06
<i>CTTN</i>	cortactin	0.305	0.578	4.09E-04	1.28E-02
<i>SNAI2</i>	snail homolog 2 (Drosophila)	0.323	0.404	3.83E-09	3.03E-06
<i>ACTN3</i>	actinin, alpha 3	0.323	0.608	4.89E-04	1.47E-02
<i>CDH6</i>	cadherin 6, type 2, K-cadherin (fetal kidney)	0.329	0.390	4.04E-08	1.61E-05
<i>PDGFRA</i>	platelet-derived growth factor receptor,	0.339	0.527	6.58E-05	3.26E-03

	alpha polypeptide related RAS viral (r-ras) oncogene				
<i>RRAS</i>	homolog	0.342	0.506	3.39E-06	3.83E-04
<i>PLAU</i>	plasminogen activator, urokinase	0.355	0.422	6.27E-07	1.09E-04
<i>SMEK2</i>	SMEK homolog 2, suppressor of mek1 (Dictyostelium)	0.358	0.653	1.03E-03	2.54E-02
<i>MSX1</i>	msh homeobox 1	0.359	0.177	1.02E-10	2.93E-07
<i>APOE</i>	apolipoprotein E	0.364	0.429	1.99E-06	2.57E-04

The transcriptional profiling confirmed the upregulation of the canonical target genes of the SHH pathway in SHH-NP, namely *PTCH1*, *GLII* and *HHIP* as anticipated (Figure A.1). There was also a high fold change of neural tissue specific target genes *FOXA2* and *NKX2-2* (Table A.2). Meanwhile, there was downregulation of the known negatively regulated genes of the pathway including *BOC* and *CDON* (Tenzen *et al.*, 2006) (Table A.2). The expression patterns of *PTCH1*, *GLII*, *HHIP*, *FOXA2*, *NKX2-2* and *BOC* were validated by real-time PCR analysis (Figure 6.2). Together, this provided greater confidence that the other DEG found by the DNA microarray were valid targets of the pathway and could be expected to play a role in SHH dependent neural differentiation.

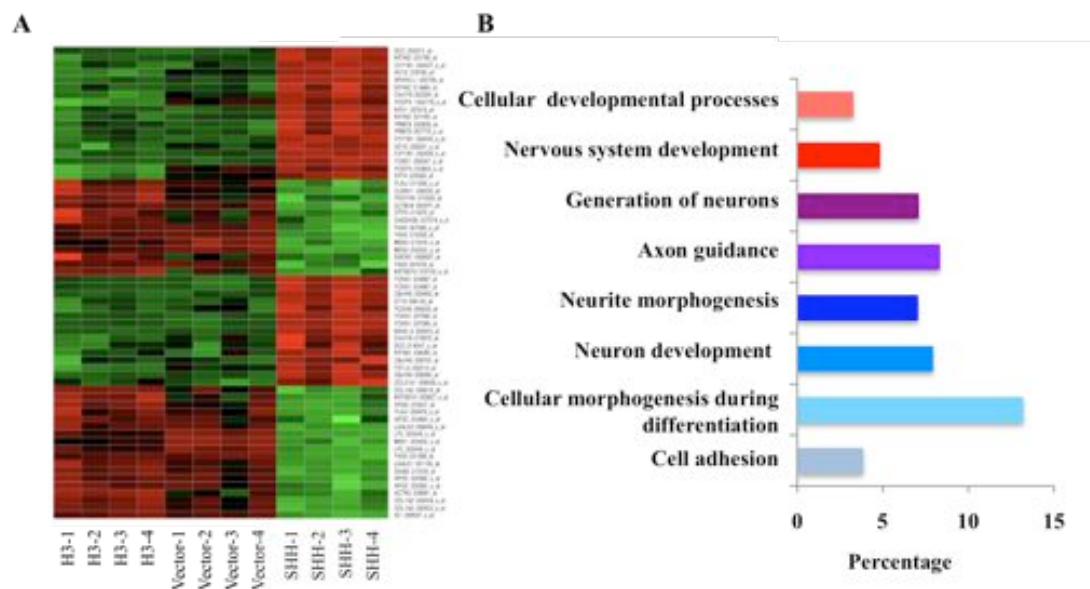


Figure 6.1 Analysis of SHH-NP expression profiling. (A) Microarray gene expression heat map comparing SHH-NP with H3-NP and Vector-NP showing top 20 upregulated and downregulated genes. Shades of red denotes upregulation while shades of green denote downregulation. (B) Upregulated genes were classified into categories by Gene ontology Biological Processes terms and ranked according to false discovery rates in ascending order. Frequencies of upregulated genes in each category are shown as percentages.

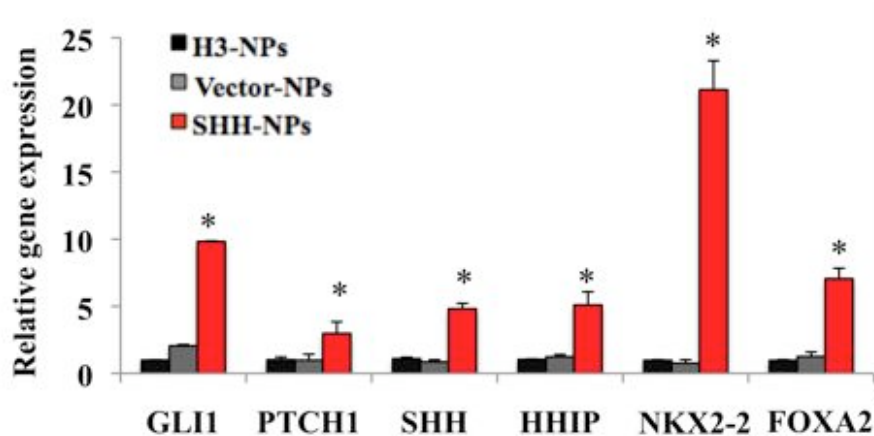


Figure 6.2 Known SHH target genes identified by microarray profiling were validated by real-time PCR. RNA for the microarray study was re-probed by real-time PCR analysis. The expression value of each gene is shown relative to H3-NP, which was arbitrarily defined as 1. The values are mean \pm SD of biological triplicates. * = $p < 0.05$.

6.3 Validation of differentially expressed genes (DEG)

Real-time PCR analysis was carried out to confirm the expression profile of 10 other selected upregulated genes, *AADC*, *EGFR*, *FGF19*, *FOXA1*, *HES5*, *HEY2*, *OLIG1*, *PGF*, *PITX2* and *STMN3* and 5 downregulated genes *BMP2*, *ZIC2*, *ID1*, *MSX1*, *PAX3* and *SNAI2* (Figure 6.3). The results paralleled the findings of the microarray analysis. The upregulation of *EGFR* and *FOXA2* and downregulation of *MSX1* and *PAX3* were also confirmed by Western blot (Figure 6.3)

To determine if the SHH regulated genes observed in the microarray experiment are broadly observed, the expression pattern of the validated genes from the above section were analyzed in another stem cell line. iPSC(IMR90) cells were differentiated into neuroprogenitors in the presence of 200 ng/ml recombinant SHH for the whole duration of the differentiation process. This concentration was chosen as it is the typical concentration that is used in most dopaminergic (DA) neuron differentiation protocols.

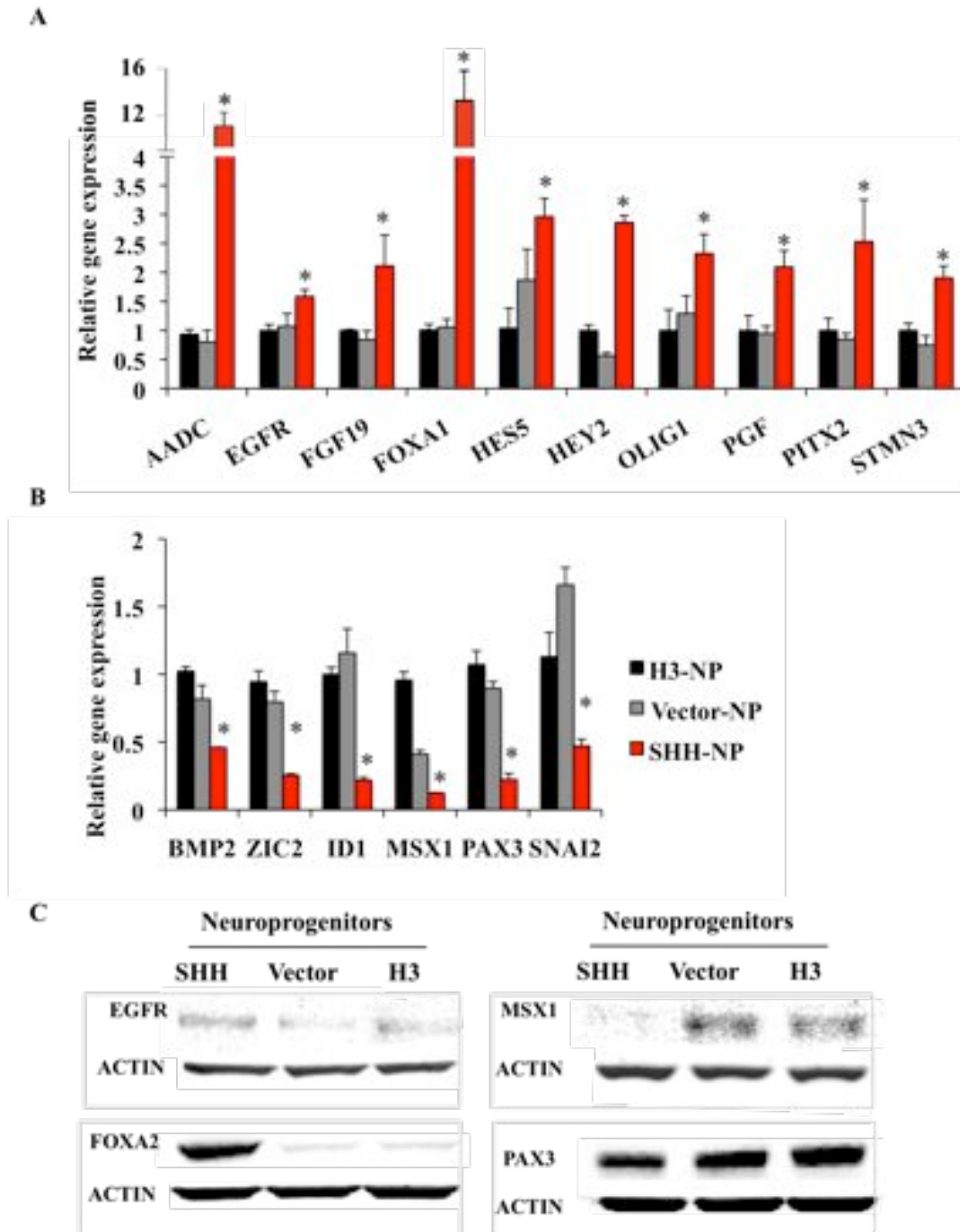


Figure 6.3 Differentially expressed genes identified from the transcriptional profiling were validated by real-time PCR and Western blot analysis. (A-B) Real-time PCR analysis of RNA used for the DNA microarray study probed for (A) upregulated genes and (B) downregulated genes. The expression value of each gene is shown relative to H3-NP, which was arbitrarily defined as 1. The values are mean \pm SD of biological triplicates. * = $p < 0.05$. (C) Cell lysates from SHH-NP, Vector-NP and H3-NP were probed with antibodies against upregulated targets EGFR, FOXA2 and downregulated targets, MSX1 and PAX3. Actin was used as a loading control.

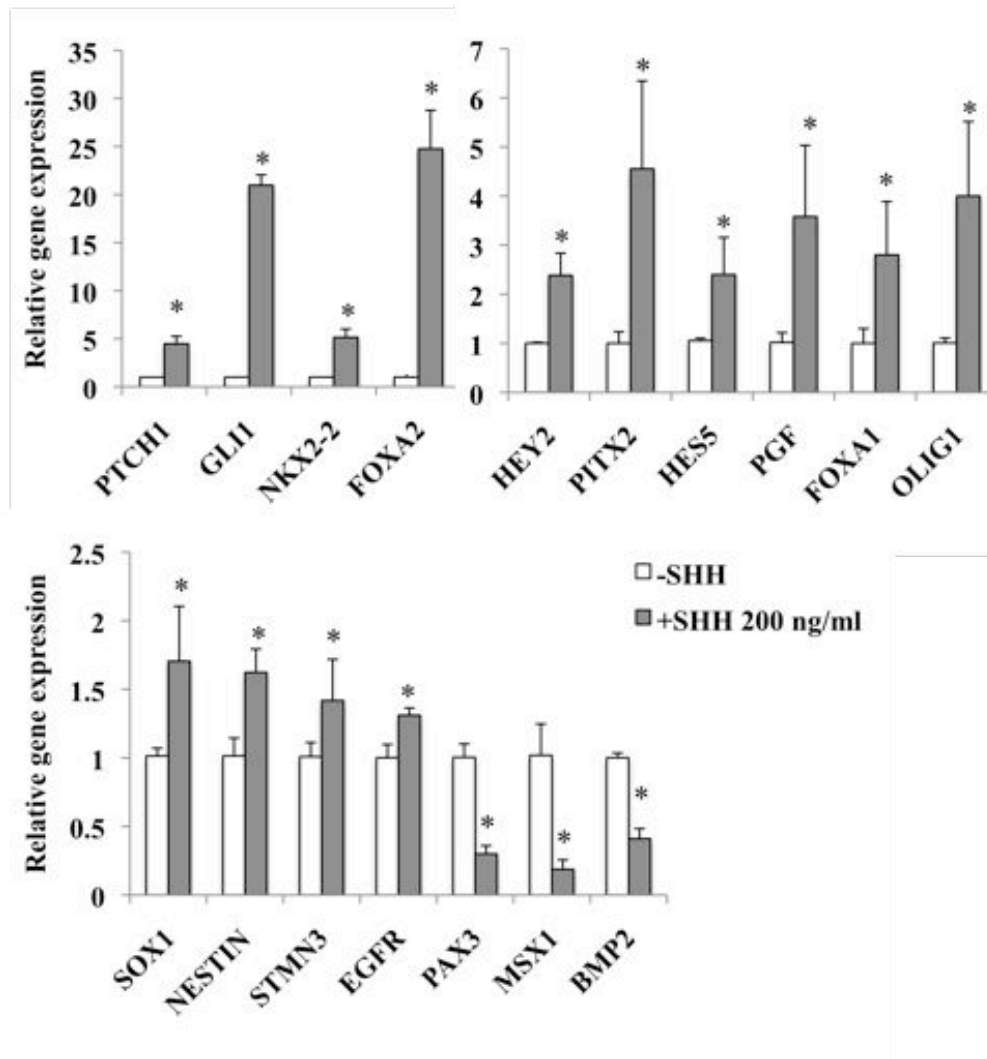


Figure 6.4 Target genes of SHH are upregulated in iPSC(IMR90)-derived neuroprogenitors treated with exogenous SHH. iPSC(IMR90) cells were differentiated into NP and were treated with (or without) 200 ng/ml recombinant SHH from the start of the differentiation process. Gene expression was analyzed after 1 week in culture by real-time PCR. The expression value of each gene is shown relative to untreated NP, which was arbitrarily defined as 1. The values are mean \pm SD of triplicates and the experiment was repeated twice. * = $p < 0.05$.

Real-time PCR analysis of iPSC(IMR90) neuroprogenitors showed that the expression of the target genes *PTCH1*, *GLI1*, *NKX2-2* and *FOXA2* were highly upregulated compared to untreated cells (Figure 6.4). The genes *HEY2*, *PITX2*, *HES5*, *PGF*, *FOXA1*, *FOXF1*, *NESTIN*, *SOX1*, *STMN3*, *EGFR* and *FOXF2* were also upregulated by more than 1.5-fold with recombinant SHH treatment (Figure 6.4). There was also an almost 80% decrease in *MSX1* expression and 50% decrease in *PAX3* and *BMP4* expression (Figure 6.4). The strong

correlation in the gene expression pattern between HES3- and iPSC(IMR90)-derived neuroprogenitors in response to SHH treatment confirmed further that the genes are genuine targets of SHH signaling.

6.4 In silico analysis of potential GLI binding sites on DEG

Some of the genes identified in the microarray study have been previously reported to be regulated by SHH signaling but there are also many others which are novel targets of the pathway. To better understand the molecular mechanisms by which SHH controls neural differentiation, it was necessary to investigate whether the DEG identified in the microarray were direct transcriptional targets or indirect downstream targets. To do so, *in silico* analysis was carried out by the Bioinformatics Group in Bioprocessing Technology Institute, to identify GLI binding sites on the promoters of differentially expressed genes. The TRANSFAC match program was used to search within 5 kb of the 5' upstream and 3' downstream region of differentially expressed genes for sites containing the GLI consensus binding sequence GACCACCCA (Kinzler and Vogelstein, 1990), which all 3 GLI proteins are able to bind (Agren *et al.*, 2004).

Of the 182 upregulated genes found in SHH-NP, 129 genes contained at least 1 putative GLI binding site within the 5kb region 5' upstream of their transcription start sites and 123 genes had at least 1 putative GLI binding site within the 5kb region 3' downstream of their transcription start sites. This suggests that they are direct targets of SHH signaling. Upregulated genes that have 6 or more GLI binding sites in their upstream and downstream regions are shown in Table 6.3 and Table 6.4 respectively. The remaining data can be found in Appendix B (Table B1 and Table B2)

Table 6.3 List of SHH upregulated genes that have 6 or more putative GLI binding sites in the 5' promoter region. The number of binding sites were located 5 kb upstream of the transcription start site. The genomic coordinates and GLI binding start site(s) are on the NCBI36 (March 2006) Human Genome Assembly. Chr = chromosome, 1 = positive strand, -1 = negative strand of DNA.

Gene Name	Chr	Strand	No. of NCBI36 (March 2006) genome coordinates binding sites
FZD9	7	1	8 ;72481606; 72481853; 72481875; 72482104; 72482320; 72483067;72484598;72485502
RAB33A	X	1	8 ;129129153; 129129588; 129130120; 129130516; 129130618;129131992;129132854; 129132880
VSX1	20	-1	8 ;25011505; 25012240; 25012526; 25012646; 25013160;25013277;25015330;25015527
LL22NC03-75B3.6	22	-1	7 ;43029839;43029989;43030996;43031831;43031863;43031997;43032026
NKX2-2	20	-1	7 ;21443440;21444126;21445002;21445631;21446000;21446079;21446266
STMN3	20	-1	7 ;61756113;61756586;61757610;61758173;61758187;61758959;61759752
ATBF1	16	-1	6 ;71551550;71552606;71553830;71554216;71555143;71555698
DSCR1	21	-1	6 ;34909918;34910454;34910621;34911242;34913941;34914009
FGF19	11	-1	6 ;69228284;69228297;69228830;69229223;69230020;69231791
FOXA2	20	-1	6 ;22512908;22513270;22513312;22513957;22514033;22517225
GLI1	12	1	6 ;56138973;56140064;56141787;56142041;56142299;56142451
HES5	1	-1	6 ;2451751;2453850;2453901;2454104;2454904;2455611
MFSD6	2	1	6 ;191004024;191004217;191004305;191004326;191005626;191007076
PGF	14	-1	6 ;74491925;74493288;74494277;74494969;74495100;74495713
PTCHD1	X	1	6 ;23259788;23259840;23260188;23260346;23261869;23262487

For the 130 genes downregulated by SHH, 121 genes had at least 1 putative GLI binding site in their 5' upstream while 116 genes had at least 1 putative GLI binding in their 3' region (Appendix B, Table B3 and Table B4).

GLI binding sites have been demonstrated in the known target genes of SHH: *Ptch1* (Agren *et al.*, 2004), *Gli1* (Dai *et al.*, 1999), *FoxA2* (Sasaki *et al.*, 1997), *Nkx2-9* (Santagati *et al.*, 2003), *Nkx2-2* (Vokes *et al.*, 2007) and *FoxF1* (Madison *et al.*, 2009). Based on our bioinformatics search, the same genes *PTCH1*, *GLI1*, *FOXA2*, *FOXF1*, *NKX2-2* and *SHH* had

4 or more putative GLI binding sites on their 5' promoter region, confirming the accuracy of the analysis.

Table 6.4 List of SHH upregulated genes that have 6 or more putative GLI binding sites in the 3' downstream region. The number of binding sites were located 5 kb upstream of the transcription start site. The genomic coordinates and GLI binding start site(s) are on the NCBI36 (March 2006) Human Genome Assembly. Chr = chromosome, 1 = positive strand, -1 = negative strand of DNA.

Gene Name	Chr	Strand	No. of binding sites	of NCBI36 (March 2006) genome coordinates
STMN3	20	-1	10	;61738659;61739139;61739997;61740022;61740381;61741203;61742099;61742424;61742438;61743022
NKX2-2	20	-1	8	;21435749;21435912;21436720;21436951;21436955;21437332;21437362;21440495
PGF	14	-1	7	;74475458;74475984;74476709;74477157;74477183;74477619;74477671
RASD1	17	-1	7	;17334611;17335648;17335794;17336270;17336351;17336501;17339086
NTN1	17	1	7	;9084482;9084698;9084856;9084914;9085197;9087102;9088076
HES6	2	-1	7	;238807423;238807492;238808274;238809654;238810489;238810734;238811159
FGD3	9	1	7	;94837741;94838378;94840147;94840156;94841107;94841942;94842654
DDC	7	-1	7	;50493623;50496104;50496411;50496677;50496987;50497308;50497329
C20orf100	20	1	7	;42130891;42131962;42132720;42132967;42133493;42133670;42134593
LMCD1	3	1	6	;8584290;8584452;8586437;8587144;8587365;8588169
FGF19	11	-1	6	;69218951;69218960;69219624;69221328;69223029;69223042
PLEKHH2	2	1	6	;43847492;43849284;43849516;43849649;43850535;43851004
FAM181A	14	1	6	;93465733;93465904;93467123;93467518;93468439;93469682
MLC1	22	-1	6	;48838431;48839817;48839886;48840090;48841198;48841581

6.5 Transcriptional activation of target gene promoters by SHH

To confirm that target genes with putative GLI binding sites on their 5' promoter region are responsive to SHH, plasmids containing the 5' promoter sequences tagged to a luciferase reporter were purchased for 8 target genes. *HEY2*, *FGF19*, *PGF*, *PITX2* and *STMN3* were chosen for further study as they have been implicated in neural development but have not been explored in ESC neural differentiation. The other genes *FOXA1*, *OLIG1* and *HES5* have important functions in neural development and have been associated with

SHH signaling (Lu *et al.*, 2000; Wall *et al.*, 2009; Yoon *et al.*, 2009). However, it has not been ascertained if they are direct targets of SHH. Plasmids for the promoters of *NKX2-2* and *FOXF1* were also purchased as positive controls. For each promoter-luciferase plasmid, the promoter sequence contained at least 1 putative GLI binding site (Table 6.5).

Table 6.5 Promoter-luciferase plasmids containing GLI binding sites on selected SHH target genes. Promoter coordinates refer to the genomic coordinates of the promoter sequences present in the Switchgear luciferase plasmids. The GLI binding site refers to starting genomic position of which GLI binding motif is found on. Coordinates are from the March 2006 Human Genome Assembly. Chr = chromosome

Gene	Chr	Promoter Coordinates	GLI site(s)	binding GLI binding motif
FOXA1	14	37133913-37135669	37135473	ccaCCACCcagg
FOXF1	16	85100854-85101796	85101068	cgCCACCaacg
			85101355	tgtGGAGGgcg
FGF19	11	69227793 - 69228889	69228860	ggcCCGCCcacc
HES5	1	2451406-2452421	2452316	cctGGAGGaca
HEY2	6	126111659 - 126112694	126111963	ggaCCACCgagt
NKX2-2	20	21442607 - 21443576	21443349	caaCCACCaacg
			21443536	gctGGTGGtg
OLIG1	21	33363427-33364526	33363804	aatGGTGGgagc
PITX2	4	111763490- 111764408	111764366	gaaCCACCaaac
PGF	14	74491865 - 74492941	74492684	tgtGGAGGccc
STMN3	20	61755116-61756117	61755533	ggtGGGGGgtct

hESC-derived neuroprogenitors were co-transfected with the promoter-luciferase plasmids and the pCMV-Shh expression vector. Transfection efficiency was normalized by co-transfection with pRL-TK as an internal reference and measured 48 hours post-transfection. The luciferase activities of positive controls *NKX2-2* and *FOXF1* reporter plasmids increased by approximately 1.7-fold and 1.6-fold upon co-transfection with the

SHH expression plasmid. Similarly, overexpression of SHH consistently resulted in a 1.5–2 fold increase in luciferase activity for the HES5, HEY2, FOXA1, OLIG1, PITX2, PGF and STMN3 reporters (Figure 6.5). No increase in luciferase activity was observed for FGF19 plasmid. This could be because one GLI binding site is not sufficient for the transactivation of the FGF19 promoter in response to SHH. These results provide additional evidence that SHH signaling regulates the expression of these genes through GLI transcriptional activation and that DEG containing putative GLI binding sites are potential direct targets of SHH signaling.

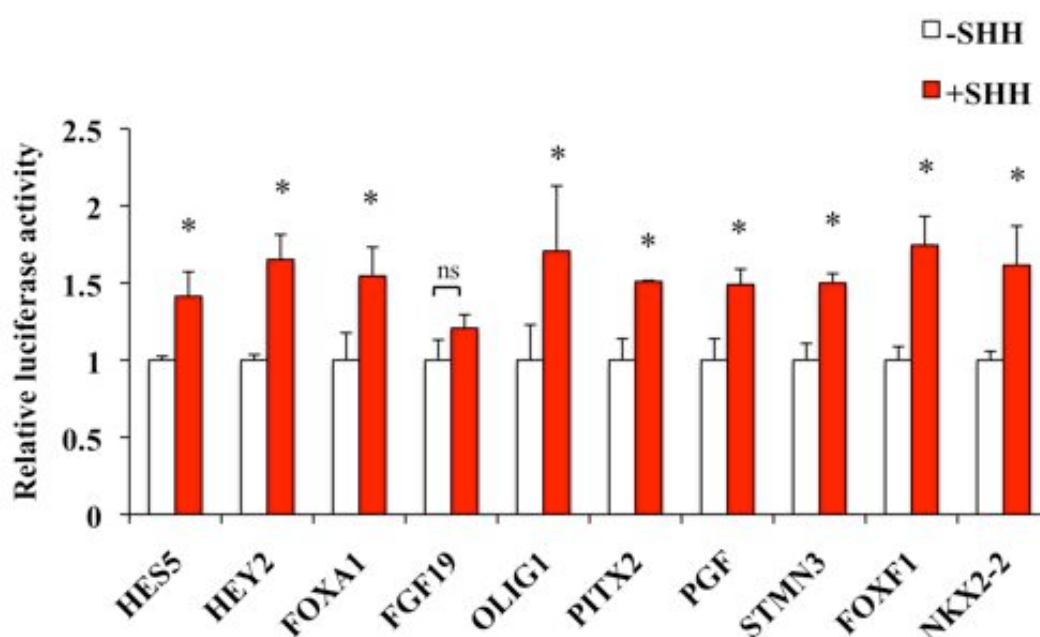


Figure 6.5 SHH is able to transactivate the promoters of target genes. Luciferase reporter genes containing fragments of promoters of target genes were co-transfected in to H3-NP along with Renilla vector and in indicated cases, with or without the SHH expression vector. Luciferase activities were calculated as a ratio of *Firefly* luciferase activity over *Renilla* luciferase activity and expressed as fold induction relative to pCDNA3.1 vector control. Values shown are mean \pm SD of a representative experiment carried out in triplicate and repeated at least three times. * = $p < 0.05$, ns = not significant.

However, as the increase in luciferase activation observed was only modest at around 1.5-2 fold, more studies are currently being carried out. They include the addition of the SHH pathway inhibitor cyclopamine as well site mutagenesis of the putative binding sites to

abolish the increase in luciferase values that may confirm the specificity of activation of the promoters by SHH.

It must be noted that the DEG identified by transcriptional profiling without any predicted GLI binding site on their promoter regions could still be direct targets of SHH signaling. In the study by Vokes *et al.*, 2007, a subset of Gli responsive genes identified by mouse Gli chromatin immunoprecipitation lacked a Gli consensus binding site. This suggested that certain direct target genes of Gli may not necessarily possess a Gli consensus binding site or that other transcriptional regulators could be involved in the co-binding of Gli to the promoters of target genes.

To complement the findings of this chapter, future studies can include chromatin immunoprecipitation of GLI-DNA complexes from SHH-NP. Subsequent PCR analysis can be carried out to see if DEG identified by transcriptional profiling are among the DNA sequences that are bound to GLI. This can provide additional confirmation of direct regulation of the DEG by SHH, including those genes that may not have GLI binding sites on their promoter regions.

6.6 SHH target genes discussion

In the following sections, the DEG identified by transcriptional profiling will first be discussed according to their broad functional categories. Genes from each functional category that have been validated by real-time PCR analysis or the promoter-luciferase assay (summarized in Table 6.6), will then be discussed in greater detail about their functions and possible roles in SHH-mediated neural differentiation.

Table 6.6 Summary of target genes of SHH in hESC-derived neuroprogenitors

Function	Gene	Name	Fold Change	Validation	No. of GLI BS on 5' upstream region	No. of GLI BS on 3' downstream region
SHH signaling pathway components	PTCH1	patched homolog 1 (Drosophila)	3.0	✓^	4	0
	GLI1	glioma-associated oncogene homolog 1 (zinc finger protein)	1.7	✓^	6	2
	HHIP	hedgehog interacting protein	2.2	✓	1	1
	BOC	Boc homolog (mouse)	0.6	✓	1	3
	CDON	Cdon homolog (mouse)	0.5	✓	1	0
Neural Induction / NSC proliferation	EBF3	early B-cell factor 3	2.2		3	0
	EGFR	epidermal growth factor receptor	1.8	✓^#	1	1
	NR2E1	nuclear receptor subfamily 2, group E, member 1	3.1		4	1
	NTRK2	neurotrophic tyrosine kinase, receptor, type 2	5.9		2	2
	CRB1	crumbs homolog 1 (Drosophila)	1.7		0	1
	HES5	hairy and enhancer of split 5 (Drosophila)	2.1	✓^	6	4
	HEY2	hairy/enhancer-of-split related with YRPW motif 2	5.2	✓^	3	0
	NES	nestin	1.6	✓^#	2	4
SOX1	SRY (sex determining region Y)-box 1	1.9	✓^#	0	3	
Dorsal-ventral patterning	BMP2	bone morphogenetic protein 2	0.6	✓^	1	1
	MSX1	msh homeobox 1	0.3	✓^#	0	4
	MSX2	msh homeobox 2	0.3		1	2
	PAX3	paired box 3	0.4	✓^#	?	?
	SNAI2	snail homolog 2 (Drosophila)	0.4	✓	1	1
	NKX2-2	NK2 homeobox 2	16.4	✓^	7	8
NKX6-1	NK6 homeobox 1	3.5	✓	2	1	
Dopaminergic	DDC	dopa decarboxylase (aromatic L-amino acid decarboxylase)	6.6	✓	0	7
	FOXA1	forkhead box A1	5.8	✓^	4	0
	FOXA2	forkhead box A2	3.4	✓^#	6	1
	PCDH8	protocadherin 8	5.0		1	5
Axon guidance	CXCL12	chemokine (C-X-C motif) ligand 12 (stromal cell-derived factor 1)	2.0		?	?
	NLGN1	neuroligin 1	1.8		2	1
	NRP1	neuropilin 1	1.9		4	3
	NRXN1	neurexin 1	1.8		?	?
	NTN1	netrin 1	6.0		3	7
	NTNG1	netrin G1	1.8		?	?
	PGF	placental growth factor	2.0	✓^	6	7
	PLXNC1	plexin C1	1.7		3	0
	SLIT1	slit homolog 1 (Drosophila)	2.4		1	4
	SLIT2	slit homolog 2 (Drosophila)	1.8		0	1
Generation of neurons / Neuron development	CSPG5	chondroitin sulfate proteoglycan 5 (neuroglycan C)	1.9		5	5
	FABP7	fatty acid binding protein 7, brain	1.7		0	4
	FGF19	fibroblast growth factor 19	1.9	✓^	6	6
	FZD9	frizzled homolog 9 (Drosophila)	2.0		8	4
	HES6	hairy and enhancer of split 6 (Drosophila)	1.9		3	7
	ID1	inhibitor of DNA binding 1	0.2	✓	5	5
	ID2	inhibitor of DNA binding 2	0.5		6	4
	ID3	inhibitor of DNA binding 3,	0.5		2	7
	NEUROD1	neurogenic differentiation 1	2.9		0	0
	OLIG1	oligodendrocyte transcription factor 1	3.5	✓^	3	5
	OTP	orthopedia homeobox	1.8		4	4
	PITX2	paired-like homeodomain 2	2.6	✓^	1	1
	POU3F2	POU class 3 homeobox 2	2.1		3	0
	RGMA	RGM domain family, member A	2.4		?	?
	SPOCK1	sparc/osteonectin, cwcv and kazal-like domains proteoglycan (testican) 1	1.6		3	2
	STMN3	stathmin-like 3	2.0	✓^	7	10

Fold change = average of the fold-change from SHH vs H3 and SHH vs Vector. neuroprogenitors. Genes in BOLD = Confirmed by promoter-luciferase reporter assay. ✓ = Validated by real-time PCR analysis. # = Validated by Western blot or FACS analysis. ^ = Validated by real-time PCR analysis in iPSC(IMR90) SHH-treated neuroprogenitors. ? = undetermined. BS = Binding sites.

6.6.1 Differentially expressed genes (DEG)

Gene Ontology (GO) biological processes was used to assign the DEG into functional categories. Based on the analysis, many of the DEG in SHH-NP corresponded to categories that are involved with neural differentiation (Figure 6.1). However, as the GO categories are hierarchical in nature, the same gene could be classified in multiple GO categories. Hence for better resolution of their potential function, the target genes from the overrepresented GO categories were clustered into more precise functional groups (Table 6.6). The analysis showed that the SHH target genes were those involved in neural induction, NSC proliferation, dorsal-ventral patterning, DA neuron development and function, axon guidance and neural development.

In a comparison with a recent study that conducted transcriptional profiling of Shh responsive genes in neuralized mouse embryoid bodies (EB) (Vokes *et al.*, 2007), several genes identified in that study to be upregulated by Shh overlapped with those described here, including *DDC*, *EBF3*, *FABP7*, *NKX6-1*, *NR2E1*, *NTN1*, *OLIG1*, *SLIT2* and *STMN3*. Vokes *et al.* also described data from another independent study (Tenzen *et al.*, 2006) that listed several genes that were downregulated by Shh in the mouse neural tube. Downregulated genes observed in both the SHH-NP and that listed in the Vokes *et al.*, study include *CNTNAP2*, *FAP*, *GLI3*, *MSX1*, *MSX2*, *PRRX1*, *SNAI2*, *TWIST1*, *ZIC2* and *ZIC5*. These conserved genes observed between species could prove to be important in SHH regulated neural differentiation and warrant more in-depth studies in the future.

6.6.2 Neural induction

The process of obtaining neurons from hESC precedes with the induction of hESC to differentiate towards the neural fate. Consistent with the evidence from Chapter 5 that SHH promotes neural induction of hESC (Figure 5.10, Figure 5.11), *NESTIN* and *SOX1* were

identified for the first time to possess putative GLI binding sites on their 5' and 3' promoter regions respectively (Table 6.6).

Nestin is an intermediate filament that is first expressed by neuroepithelial cells in the early neural tube (Lendahl *et al.*, 1990). Nestin is also expressed in proliferating neural precursors and adult NSC (Lothian and Lendahl, 1997; Fukuda *et al.*, 2003). Its widespread expression in the CNS signifies its importance and is a widely used marker for NSC, however the exact function of Nestin is not well understood. It is suggested to play a role in the distribution of cytoskeletal proteins during cell division (Chou *et al.*, 2003). While the expression of Nestin has been demonstrated to be regulated by POU transcription factors (Josephson *et al.*, 1998; Tanaka *et al.*, 2004), the presence of putative GLI binding sites on its 5' promoter region suggest that NESTIN is also a direct target of SHH signaling.

The bioinformatics analysis identified 3 putative GLI binding sites on the 3' downstream region of *SOX1*, suggesting it may be a downstream target gene of SHH. Sox1 is expressed early on in neuroectoderm development in the neural plate and later on, in neuroepithelial cells (Pevny *et al.*, 1998; Wood and Episkopou, 1999). It has an important function in neural induction as indicated by overexpression studies of Sox1, which drove pluripotent embryonal carcinoma cells and mESC towards the neuroectoderm lineage (Pevny *et al.*, 1998; Suter *et al.*, 2009). The continuous forced expression of Sox1 in neuroprogenitors also maintained cells at stage and prevented their differentiation (Suter *et al.*, 2009).

Therefore, these results suggest that SHH is able to promote neural induction of hESC through its target genes NESTIN and SOX1.

6.6.3 Neuroprogenitor proliferation

As SHH was demonstrated to induce the proliferation of sorted neuroprogenitors in the previous chapter, the DEG were examined for genes related to cell cycle or cell proliferation. Surprisingly, transcriptional profiling revealed that there was no significant induction of *Cyclin D1* or *N-MYC* in SHH-NP. *Cyclin D1* and *N-myc* have been reported to

be targets genes of Shh in neuronal precursors, and were shown to be responsible for SHH-induced proliferation (Oliver *et al.*, 2003). This indicates that *Cyclin D1* and *N-myc* are tissue-specific targets of SHH signaling and there are other means by which SHH induces proliferation in SHH-NP. Genes that are involved in proliferation like *HES5*, *HEY2* and *EGFR* which were identified in our study to be targets of SHH signaling could potentially mediate SHH-induced proliferation of neuroprogenitors (Table 6.6).

HES5 is a transcription factor belonging to the NOTCH signaling pathway. An active NOTCH pathway is important in neural development as it maintains the proliferation of neuroprogenitors and keeps them in the undifferentiated state (Gaiano *et al.*, 2000; Ohtsuka *et al.*, 2001; Iso *et al.*, 2003). The role of the NOTCH pathway in proliferation has been demonstrated in hESC-derived rosettes as inhibition of NOTCH signaling decreased the rosette like structures in culture (Woo *et al.*, 2009). HES5 has also been used as a marker to trace neural induction in hESC as it is expressed during the rosette/neuroprogenitor stage but is downregulated upon terminal differentiation (Placantonakis *et al.*, 2009). Transcriptional profiling of HES5 positive neuroprogenitors showed enrichment for SHH pathway genes *SMO*, *GLI2* and *GLI3* (Placantonakis *et al.*, 2009), providing evidence of cross-talk between the pathways. Hes5 has been previously shown to be induced by Shh in retinal explants (Wall *et al.*, 2009) but the results shown here for the first time proposes that HES5 is a direct target of SHH signaling (Figure 6.5).

This study also uncovered another NOTCH target gene HEY2 to be a direct target of SHH (Figure 6.5). Hey2 has been demonstrated to inhibit neurogenesis by repressing pro-neural bHLH genes like *Ngn2* and *Mash1* and maintaining the population of Nestin positive neural precursors (Sakamoto *et al.*, 2003). Therefore, the results suggest that SHH activates the NOTCH effector gene HES5 and HEY2 independently of a NOTCH ligand, which may in turn mediate the proliferation of neuroprogenitors.

The EGFR tyrosine kinase receptor is also suggested to be a mediator of SHH-induced proliferation as its expression is upregulated by SHH (Figure 6.3). The binding of the mitogen EGF to its receptor EGFR activates tyrosine kinase activity and leads to stimulation

of downstream pathways like the Ras/ERK and PI3K pathways that regulate cell proliferation and death. A study on the role of SHH in mESC revealed that both Gli activation and EGFR activation were required for the stimulation of proliferation of mESC by SHH (Heo *et al.*, 2007). Furthermore, SHH was able to induce EGFR signal transactivation in the absence of exogenous EGF (Heo *et al.*, 2007). Therefore, the upregulation of EGFR by SHH may induce proliferation of neuroprogenitors by activating EGFR signaling and also amplifying the response of neuroprogenitors to EGF present in culture.

6.6.4 Dorsal-ventral patterning

In harmony with the role of SHH as a ventralizing factor necessary for the development of several neural subtypes (Briscoe, 2009), transcriptional profiling showed the upregulation of NKX2-2 and NKX6-1 in SHH-NP as anticipated (Figure 6.2 and 6.3). These homeobox genes are induced by Shh in the neural tube and are necessary for the specification of ventral neuronal identity (Briscoe and Ericson, 2001). While NKX2-2 has been recently established to be a direct target gene (Vokes *et al.*, 2007), the data demonstrates for the first time that NKX6-1 may be a direct target of SHH as it contains 3 putative GLI binding sites upstream and downstream of its transcription start site (Table 6.6).

The overexpression of SHH also resulted in the downregulation of several genes that are important in dorsal specification like *PAX3*, *MSX1* and *SNAIL*, (Figure 6.3). These genes are normally expressed in the dorsal neural tube (Goulding *et al.*, 1991; Watanabe *et al.*, 1998; Liu *et al.*, 2004). Pax3 shares sequence similarity with another Class I protein Pax7, where it helps to restrict the ventral identity of neuroepithelial cells (Ericson *et al.*, 1996; Mansouri and Gruss, 1998). Msx1 and Msx2 are homeodomain factors induced by BMP signals that mediate the role of BMP signaling in dorsal neuronal specification (Hollnagel *et al.*, 1999; Ramos and Robert, 2005). SHH also negatively regulates the expression of *BMP2* (Figure 6.3), which encodes for secreted BMP2 protein of the BMP signaling pathway that is essential in the patterning of the dorsal neural tube (Liem *et al.*, 1997). The downregulation

of *MSX1* and *MSX2* by SHH could be due to direct inhibition the genes or by antagonizing the BMP pathway.

Therefore, the results show that SHH ventralizes neuroprogenitors via the target genes *NKX2-2* and *NKX6-1* and also through the inhibition of genes important in dorsal patterning. This implies that derivation of neural cells from the dorsal region from hESC, e.g. neural crest stem cells, might require inhibition of the SHH pathway to release the inhibition of key genes in dorsal specification.

As *BMP2* is also responsible for driving extraembryonic endodermal differentiation of hESC (Pera *et al.*, 2004), the downregulation of *BMP2* by SHH suggests that SHH can cooperate with *noggin* to further inhibit BMP signaling to enhance the differentiation of hESC to the neuroectoderm lineage.

6.6.5 Dopaminergic neuron development and function

SHH is an important factor for the genesis of DA neurons from hESC (Perrier *et al.*, 2004; Yan *et al.*, 2005). Transcriptional profiling showed that the closely related *FOXA1* and *FOXA2* genes were upregulated by SHH. The promoter-luciferase assay indicates that *FOXA1* is a direct target of SHH (Figure 6.5, Table 6.6).

FoxA1 and FoxA2 have overlapping functions in regulating the differentiation of DA progenitors by regulating the expression of other genes like *Ngn2*, *Lmx1A/B*, *Nkx2-2* and *Th* that are important for the specification and differentiation of DA neurons (Ferri *et al.*, 2007; Lin *et al.*, 2009). Midbrain DA progenitors from double FoxA1/FoxA2 knock out mutants failed to express key markers of mature DA neurons like *Nurr1*, *Th* or *Aadc*, displaying the requirement of FoxA1 and FoxA2 for the maturation of DA progenitors (Ferri *et al.*, 2007). In addition, overexpression of FoxA1 promoted neural induction of pluripotent embryonal carcinoma cells (Tan *et al.*, 2009), while overexpression of FoxA2 was able to induce DA neuron differentiation of mESC *in vitro*, even in the absence of active *Shh* signaling (Kittappa *et al.*, 2007). Therefore, SHH is likely to promote DA neuron differentiation from hESC through the actions of its target genes *FOXA1* and *FOXA2*.

The DA neuron marker *AADC* (or *DDC*) was also highly upregulated by SHH in neuroprogenitors (Figure 6.3). *AADC* is one of the enzymes necessary for the production of dopamine (Gjedde *et al.*, 1991). Although *AADC* does not contain any GLI binding site in its 5' promoter region, there are 7 GLI binding sites in the 3' promoter region, making it a possible direct target gene (Table 6.6). Alternatively, the upregulation of *AADC* could have been due to the upregulation of *FOXA1* and *FOXA2* as the *AADC* promoter contains a *FOXA2* binding site (Raynal *et al.*, 1998). Nevertheless, it suggests that SHH plays a role in mature DA neurons by promoting the expression of a key enzyme required for proper DA neuron function.

6.6.6 Axon guidance

During the development of the neuronal network in the CNS, the growth and extension of neurons with long axonal extensions require axon guidance to find their correct targets (Tessier-Lavigne and Goodman, 1996). Several genes relating to axon guidance were found to be upregulated by SHH (Table 6.6). They include the Slit and Netrin proteins that are instructive molecules that guide the growth of neuronal axons through chemoattraction or repulsion (Killeen and Sybingco, 2008). As *Shh* itself is also a chemoattractant for neurons (Charron *et al.*, 2003; Hammond *et al.*, 2009), the upregulation of many genes involved in axonal guidance suggest that SHH can enhance axonal outgrowth of neurons during hESC neural differentiation.

Transcriptional profiling and the promoter-luciferase assay identified *PGF* as a novel target gene of SHH (Figure 6.3, Figure 6.5). To the best of our knowledge, regulation of *PGF* expression by SHH has not been previously described. *PGF* is a ligand within the vascular endothelial growth factor (VEGF) family of proteins, which have a variety of functions in the nervous system (Ruiz De Almodovar *et al.*, 2009). VEGF can stimulate axonal outgrowth (Sondell *et al.*, 1999, 2000), enhance the survival of neurons during ischemia and also promote neurogenesis *in vivo* (Jin *et al.*, 2000, 2002). The specific role of *PGF* is less well understood. *PGF* has been shown to reduce the death of ischemic astrocytes (Freitas-Andrade

et al., 2008) and PGF treatment aided chemoattraction and growth cone formation of neurons from the dorsal root ganglion (Cheng *et al.*, 2004). VEGF and isoform 2 of PGF act via the neuropilin-1 (NRP-1) receptor (Migdal *et al.*, 1998). Interestingly, the expression of *NRP-1* is also induced by SHH (Table 6.6). Therefore, this study presents *PGF* to be a novel target of the SHH pathway in hESC-derived neuroprogenitors. Although the function of PGF in neuronal differentiation of hESC is not known, we propose that it may play a role in SHH-mediated axon guidance.

6.6.7 Neural development

Many of the target genes of SHH identified by transcriptional profiling were annotated by Gene Ontology biological processes classification to be important for the development of the nervous system.

One particular gene in that category, *STMN3*, was upregulated by around 2-fold in SHH-NP (Figure 6.3) The promoter-luciferase assay confirmed that *STMN3* was direct target gene of SHH (Figure 6.5, Table 6.6). *STMN3* (synonyms SCLIP or SCG10-like) belongs to the stathmin family of phosphoproteins that regulate microtubule assembly (Charbaut *et al.*, 2001). In a survey of stathmin family gene expression in human tissues, *STMN3* had wide expression in most human tissues with the highest mRNA concentrations in neural tissue like the fetal brain, spinal cord and cerebellum (Bieche *et al.*, 2003). Gain- and loss-of-function studies showed that *Stmn3* is essential for the growth of purkinje cells from the developing rat cerebellum (Poulain *et al.*, 2008). *STMN3* is also believed to be a regulator of neuronal morphogenesis (Baldassa *et al.*, 2007; Poulain *et al.*, 2008). Interestingly, *Stmn3* was also identified to be upregulated by *Shh* in neuralized mouse EB (Vokes *et al.*, 2007). This suggests that *SMTN3* may be an important target gene of SHH that could have a functional role in SHH-mediated neural differentiation.

Although the *FGF19* promoter-luciferase reporter did not show any increase in transactivation by SHH, the presence of 6 putative GLI binding sites in its 5' promoter region point towards the possibility that *FGF19* is a potential direct target gene of SHH in

neuroprogenitors. More studies will need to be done to confirm if it is indeed so. Nonetheless, the mouse ortholog of human *FGF19*, *Fgf15* has been demonstrated by luciferase assays to be a direct target of Shh (Saito *et al.*, 2005). The precise function of *Fgf19* in mammals is not well understood. Analysis of *Fgf19* expression in the chick neural tube found that *Fgf19* localized with *Nkx2-2* and *Nkx6-1* positive neuroepithelial cells (Gimeno and Martinez, 2007). In the same study, Shh and *Fgf8* were able to induce ectopic expression of *Fgf19* (Gimeno and Martinez, 2007). Along with our results, it suggests that *FGF19* may play a role in neural differentiation.

Pitx2 has been shown to be induced by Shh where it mediates Shh-dependent left-right asymmetry of the vertebrate body (Ryan *et al.*, 1998). The promoter-luciferase assay confirms that *PITX2* is a direct target gene of SHH (Figure 6.5). Its function in neural development however is not understood. *PITX2* has been described to be present in PSA-NCAM positive hESC-derived neuronal precursors (Freed *et al.*, 2008). *Pitx2* mutant mice revealed that *Pitx2* regulates the terminal neuronal differentiation in the midbrain by acting primarily as a regulator of neuronal migration (Martin *et al.*, 2004; Skidmore *et al.*, 2008). More studies have to be done to understand the role of *PITX2* in the SHH signaling network.

Olig1 is another gene that has been shown to be induced by Shh to promote oligodendrocyte formation (Lu *et al.*, 2000, 2001). *Olig1*, with *Olig2* is also necessary for motor neuron specification (Zhou and Anderson, 2002). While *Olig1* was found to be upregulated by Shh in mouse EB (Vokes *et al.*, 2007), chromatin immunoprecipitation analysis did not reveal any binding of Gli on *Olig1*. In our studies however, the promoter-luciferase assay confirm that *OLIG1* is a direct target gene of SHH in hESC-derived neuroprogenitors (Figure 6.5), indicating that SHH is potentially able to promote motor neuron and oligodendrocyte differentiation from hESC through induction of *OLIG1*.

ID1 was highly downregulated in SHH-NP (Figure 6.3) and the presence of 5 putative GLI binding sites on both the 5' upstream and 3' downstream regions, suggested that *ID1* is a direct negatively regulated target gene of SHH (Table 6.6). *ID1* belongs to a family of transcriptional regulators that inhibit neuronal differentiation by negatively regulating pro-

neural transcription factors, like *NEUROD1* and *MASH1* (Peddada *et al.*, 2006; Obayashi *et al.*, 2009). *ID1* is also target gene of BMP signaling and is repressed by noggin treatment during neural induction (Hollnagel *et al.*, 1999; Gerrard *et al.*, 2005). Thus, SHH may be able to promote neuronal differentiation indirectly by inhibiting *ID1*.

As depicted in Figure 6.6, the transcriptional profiling and GLI binding site analysis revealed the underlying gene network downstream of SHH signaling that could confer the multiple functions of SHH during hESC neural differentiation. As each of these functions are highly specific, involving a large number of interacting factors, SHH may have different roles in each of these contexts and require future study.

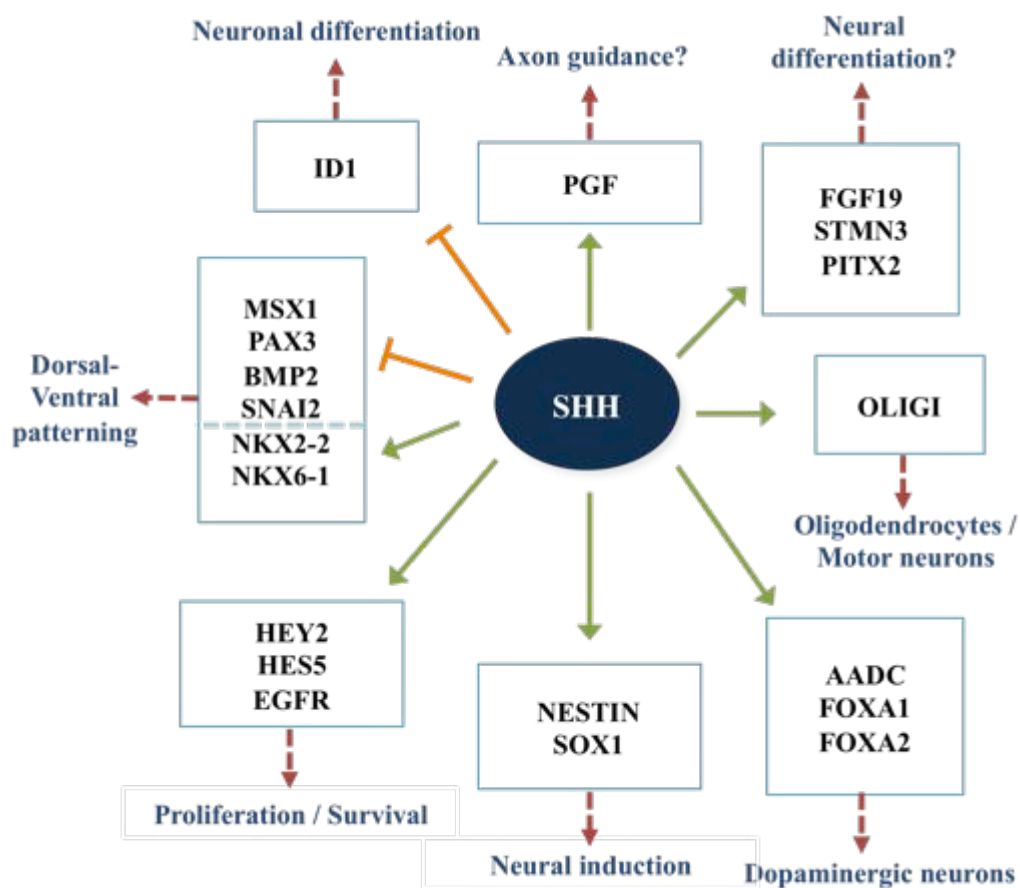


Figure 6.6 The transcriptional network of SHH in hESC-derived neuroprogenitors. Target genes of the pathway are indicated by the solid lines while suggested consequences of pathway activation are indicated by dotted lines.

6.7 Summary

Multiple genes are involved in the process of neural differentiation from hESC to terminal differentiation. As SHH is commonly used in combination with several growth factors at a time, the aim of this chapter was to dissect at the molecular level the specific target genes of the pathway that could potentially mediate SHH-driven neural differentiation of hESC. Gene expression changes resulting from the overexpression of SHH in neuroprogenitors were examined by transcriptional profiling. 182 genes were identified to be upregulated in SHH-NP and another 155 were downregulated. Analysis of the differentially expressed genes showed that they are involved in numerous cellular processes including neural induction, NSC proliferation, dorsal-ventral patterning DA neuron development and function, axon guidance and neural development. *In silico* analysis of the differentially expressed genes also revealed that many of them contained 1 or more putative GLI binding sites in the promoter region 5' upstream and 3' downstream of their transcriptional start site, suggesting that they are direct target genes of the pathway. Selected genes were further examined by using a promoter-luciferase assay that confirmed the transactivation of the promoters of *HES5*, *HEY2*, *FOXA1*, *OLIG1*, *PITX2*, *PGF* and *STMN3* by SHH. This provided evidence for the first time that the above genes are directly regulated by SHH. Therefore, this study has uncovered putative novel target genes of the pathway and we propose these downstream genes contribute to the overall effect of SHH in hESC neural induction, expansion and patterning.

CHAPTER 7 CONCLUSIONS AND RECOMMENDATIONS

7.1 Conclusions

This thesis set out with two major objectives, which were to elucidate the role of SHH signaling in (1) the self-renewal of undifferentiated human embryonic stem cells (hESC) and (2) the directed differentiation of hESC towards the neural lineage.

In the studies that aimed to address the first objective, several observations and conclusions were derived. hESC were found to express the major components of the SHH pathway, as evidenced by transcriptional and immunocytochemical analysis. A SHH/GLI responsive luciferase reporter assay showed that the pathway was active in hESC and there was a functional signaling cascade downstream of the SMO receptor. However, supplementation with exogenous SHH failed to maintain the pluripotency of SHH nor did it stimulate the proliferation of hESC. Further analysis with the GLI responsive luciferase reporter revealed that the pathway was minimally active in hESC but highly activated upon RA-induced differentiation. Furthermore, exogenous SHH was able to activate the pathway only when the cells were differentiated. Finally, long-term exposure of embryoid bodies to exogenous SHH increased the expression of neural markers. Therefore, these evidence point to a model whereby SHH is minimally active in hESC but is primed for activation upon differentiation, and consequently promotes differentiation toward the neuroectoderm lineage.

To meet the second objective, a directed neural differentiation protocol was first developed to efficiently differentiate hESC to neuroprogenitors using noggin as a neural inducer. SHH was then confirmed to be required for efficient specification of neuroprogenitors towards the dopaminergic (DA) neuron lineage as removal of SHH from the differentiation protocol resulted in a significant decrease in the population of DA neurons produced. A stable SHH overexpressing hESC line was then generated and differentiated according to the developed protocol to investigate the effect of SHH at the different stages of

neural differentiation. Investigation at the neuroprogenitor stage showed that overexpression of SHH increased the expression of neural stem cell markers in the neuroprogenitors. After obtaining a more homogenous population of neuroprogenitors by cell sorting, it was found that overexpression of SHH concomitantly increased the proliferation of these cells. These findings suggest that overexpression of SHH in hESC result in an enriched neuroprogenitor population with appropriate neural stem cell identity. Further differentiation of the neuroprogenitors showed that overexpression of SHH led to an increased production of DA neurons, which we postulate, was due to the higher starting neural stem cell population in overexpressing SHH neuroprogenitors.

These findings led to the hypothesis that apart from its known function in neural subtype specification, SHH has other functions in neural differentiation, which are to promote neural induction and neuroprogenitor proliferation.

Given the role of SHH in promoting neural differentiation, transcriptional profiling of overexpressing SHH neuroprogenitors was carried out to identify the molecular targets of the SHH pathway. 182 genes were found to be upregulated while another 155 genes were downregulated by more than 1.5-fold in overexpressing SHH neuroprogenitors when compared to the wild-type and vector control neuroprogenitors. Functional classification of the differentially expressed genes found that the largest significantly enriched class of genes were involved in neural development. Specifically, these genes have a range of functions in neural induction, neuroprogenitor proliferation, dorsal-ventral patterning, DA neuron development and axonal guidance. These findings show an extensive transcriptional network downstream of SHH activation in neuroprogenitors, which could potentially mediate the multiple functions of SHH during neural differentiation.

In order to identify potential novel direct targets of SHH, *in silico* analysis was carried out by searching for potential GLI consensus binding sites on the 5' upstream and 3' downstream promoter regions of the differentially expressed genes. This identified 129 upregulated genes that had 1 or more putative GLI binding sites within 5 kb of the 5' upstream promoter region, suggesting that these gene are direct targets of SHH signaling.

Promoter-luciferase assays showed the increase in transactivation of the promoters of *PGF*, *PITX2*, *OLIG1*, *STMN3*, *HES5* and *HEY2* by SHH. This results provides confirmation that these genes are putative direct target genes of SHH and provide new insight into the SHH signal transduction cascade in neuroprogenitors. Furthermore, as *HES5* and *HEY2* are target genes of the NOTCH signaling pathway, this study demonstrates potential functional cross-talk between the SHH and NOTCH signaling pathway in neuroprogenitors.

Taken together, the studies presented in this thesis have led to the understanding that the SHH pathway plays a minimal role in regulating hESC self-renewal but upon differentiation, SHH is able to promote neural induction, neuroprogenitor expansion and neuronal subtype specification. It also led to the elucidation of a gene network downstream of SHH activation that builds a more comprehensive understanding of how SHH carries out its roles in neural differentiation.

7.2 Recommendations for future research

7.2.1 Loss of function study

To complement the findings of this thesis, a loss of SHH function can be carried out using pharmacological reagents like the SMO receptor inhibitor cyclopamine (Taipale *et al.*, 2000). Alternatively, knockdown of SMO or GLI to abolish the ability of hESC to carry out SHH signal transduction can be performed. We can then investigate if it would lead to any impairment of the capacity of hESC to differentiate to neuroprogenitors or DA neurons. The results from the loss of function study would supplement the overexpression studies carried out and provide confirmation of the function of SHH in neural differentiation.

7.2.2 Cross-talk between NOTCH and SHH signaling pathways

The NOTCH signaling pathway is important for maintaining the proliferation of hESC-derived neuroprogenitors (Woo *et al.*, 2009). During NOTCH signaling, the members of the Jagged and Delta family bind to the NOTCH receptor, which is subsequently cleaved.

The intracellular portion of the receptor is then shuttled into the nucleus to activate transcription of target genes, like the HES and HEY family of transcription factors (Iso *et al.*, 2003). *HES5* and *HEY2* were shown in this thesis to be target genes of SHH in neuroprogenitors, thus these genes appear to be at the intersection of the SHH and NOTCH signaling pathways. Crosstalk between SHH and other NOTCH effectors have also been reported in other tissues and cell types as well (Hallahan *et al.*, 2004; Ingram *et al.*, 2008; Wall *et al.*, 2009), suggesting that there may be functional importance of the crosstalk in hESC-derived neuroprogenitors.

More studies can be carried out to investigate if SHH is able to activate *HES5* and *HEY2* independently of a NOTCH ligand. It would also be of interest to understand whether the effect of SHH on neuroprogenitor proliferation requires the activity of HES5 and HEY2. A recent study showed that hESC-derived rosettes treated with the NOTCH ligands, JAG1 and DLL4, plus SHH had the most robust growth compared to those treated with other signaling molecules like RA, noggin and WNT3a (Elkabetz *et al.*, 2008). Further studies can be done to examine the synergism, if any, between NOTCH and SHH signaling in maintaining proliferation of neuroprogenitors.

7.2.3 Exploration of novel target genes

The transcriptional profiling study has revealed several novel direct target genes of SHH signaling e.g. *PGF*, *FGF19*, and *STMN3* which have implicated in neural development but whose significance is uncertain. Two other SHH putative target genes identified in this study, namely *FABP7* and *PCDH8* were also picked up in other transcriptional profiling studies to be specifically upregulated in hESC-derived neuroprogenitors (Pankratz *et al.*, 2007) and dopaminergic neurons (Lee *et al.*, 2007), respectively. This suggests that these genes have possible functions in neural differentiation.

The relevance of the above genes can be clarified by studying their co-expression with Shh *in vivo*. Gain- or loss-of-function studies by overexpression or knockdown of the target genes in hESC will also shed light on their function in neural differentiation. In

addition, as the transcriptional profiling was performed on samples from a single time point, future work can include more time points, e.g. at the dopaminergic neuronal stage to capture dynamic gene expression changes that may offer more insights into their function.

7.2.4 *MicroRNA and SHH signaling*

MicroRNAs (miRNA) are post-transcriptional negative regulators of gene expression that bind to the 3' region of specific mRNA and represses their translation (Bartel, 2004). miRNA been linked to SHH signaling, where they are able to regulate the pathway that affects the development of the hindlimb (Hornstein *et al.*, 2005). Similarly in neuronal precursor cells, microRNAs were demonstrated to target Smo and Gli1, leading to inhibition of cell growth (Ferretti *et al.*, 2008). miRNA have also been implicated in medulloblastomas with aberrant constitutive SHH signaling, whereby the upregulated expression of a cluster of microRNAs synergized with SHH to induce proliferation of the cells (Northcott *et al.*, 2009; Uziel *et al.*, 2009).

Many miRNA are widely expressed in the mammalian brain and they are regarded to be involved in the regulation of neural development (Krichevsky *et al.*, 2003; Kim *et al.*, 2004; Kosik and Krichevsky, 2005) Recently, there has been evidence showing that miRNA are important in neural differentiation of mESC (Krichevsky *et al.*, 2006; Kim *et al.*, 2007). The profiling of different hESC lines with a bias to different neuronal cell types also suggested that the distinct expression of miRNA was instrumental in specifying cell fate (Wu *et al.*, 2007). Therefore, it would be interesting to investigate if there exists any collaboration between SHH and miRNA to promote neural differentiation of hESC.

ABBREVIATIONS

AA	Ascorbic acid
AcTb	Acetylated tubulin
AFP	Alpha feto protein
APC	Allophycocyanin
Bcl-2	B-cell leukemia/lymphoma 2
BDNF	Brain-derived neurotrophic factor
bHLH	Basic helix-loop-helix
BMP	Bone morphogenetic proteins
Boc	Biregional cell adhesion molecule-related/down-regulated by oncogenes (Cdon) binding protein
bp	Base pairs
BSA	Bovine Serum Albumin
c-myc	v-myc myelocytomatosis viral oncogene homolog (avian)
cAMP	Cyclic adenosine monophosphate
CD	Cluster of differentiation
cDNA	Complementary DNA
Cdo	Cell adhesion molecule-related/down-regulated by oncogenes
CM	Conditioned media
CMV	Cytomegalovirus
CNS	Central nervous system
COL2A	Collagen, type II, alpha 1
DAPI	4,6-diamino-2-phenylindole
DMSO	Dimethyl sulfoxide
DNA	Deoxyribonucleic acid
dNTP	Deoxy nucleotide triphosphate
DsRed2	Discosoma sp. red fluorescent protein 2
EB	Embryoid bodies
Edu	5-ethynyl-2'-deoxyuridine
EGF	Epidermal growth factor
ELISA	Enzyme-linked immunosorbent assay
EN1/2	Engrailed 1/2
FACS	Fluorescence Activated Cell Sorting
FBS	Fetal bovine serum
FGF (FGFR)	Fibroblast growth factor (receptor)
FITC	Fluorescein-5-isothiocyanate
FOXA	Forkhead factor A
Gas1	Growth arrest specific 1
GATA	GATA binding protein
GDNF	Glial cell-derived neurotrophic factor
GFAP	Glial fibrillary acidic protein
GLI	GLI-Kruppel family member GLI1
hESC	Human embryonic stem cells
HEK	Human embryonic kidney cells
HRP	Horse radish peroxidase
Ig	Immunoglobulin
iPSC	Induced pluripotent stem cells
kb	Kilo bases
kDa	Kilo dalton
Kif7	Kinesin family member 7
KLF4	Kruppel-like factor 4 (gut)
LIF	Leukemia inhibitory factor
LIN28	Lin-28 homolog (C. elegans)

LMX1A/B	LIM homeobox 1A/B
M	Mol/litre
MAP2	Microtubule-associated protein
MAPK	Mitogen-activated protein kinase
mESC	Mouse embryonic stem cells
mRNA	Messenger RNA
MSI	Musashi
N-myc	v-myc myelocytomatosis viral related oncogene, neuroblastoma derived (avian)
NANOG	Nanog homeobox
NEAA	Non-essential amino acids
NP	Neuroprogenitors
NSC	Neural stem cells
NURR1	Nuclear receptor related 1
OCT4	Octamer binding protein-4
OLIG	Oligodendrocyte lineage transcription factor
OTX2	Orthodenticle homeobox 2
p75	p75 nerve growth factor receptor
PAX	Paired box
PCR	Polymerase chain reaction
PI3K	phosphatidylinositol-3-kinase
PITX3	Paired-like homeodomain 3
PKA	Protein Kinase A
PSA-NCAM	Poly-sialated neural cell adhesion molecule
PTCH	Patched
Rab23	RAB23, member RAS oncogene family
RNA	Ribonucleic acid
rpm	Revolutions per minute
RT-PCR	Reverse transcriptase polymerase chain reaction
SD	Standard deviation
SHH	Sonic hedgehog
SOX	SRY (sex determining region Y)-box
SR	Serum replacement
SUFU	Suppressor of fused
TGF	Tumour growth factor
TH	Tyrosine hydroxylase
TRA	Tumour recognition antigen
TUJ1	Beta-III Tubulin
WNT	Wingless

BIBLIOGRAPHY

- Agren, M., Kogerman, P., Kleman, M., Wessling, M. & Toftgard, R. Expression of the Ptch1 Tumor Suppressor Gene is Regulated By Alternative Promoters and a Single Functional Gli-Binding Site. *Gene* 330, 101-114 (2004).
- Allen, B., Tenzen, T. & McMahon, A. The Hedgehog-Binding Proteins Gas1 and Cdo Cooperate to Positively Regulate Shh Signaling During Mouse Development. *Genes Dev* 21(10), 1244-1257 (2007).
- Andersson, E., Tryggvason, U., Deng, Q., Friling, S., Alekseenko, Z., Robert, B., Perlmann, T. & Ericson, J. Identification of Intrinsic Determinants of Midbrain Dopamine Neurons. *Cell* 124(2), 393-405 (2006).
- Avilion, A., Nicolis, S., Pevny, L., Perez, L., Vivian, N. & Lovell-Badge, R. Multipotent Cell Lineages in Early Mouse Development Depend on Sox2 Function. *Genes Dev* 17(1), 126-140 (2003).
- Babaie, Y., Herwig, R., Greber, B., Brink, T., Wruck, W., Groth, D., Lehrach, H., Burdon, T. & Adjaye, J. Analysis of Oct4-Dependent Transcriptional Networks Regulating Self-Renewal and Pluripotency in Human Embryonic Stem Cells. *Stem Cells* 25(2), 500-510 (2007).
- Bacigaluppi, M., Pluchino, S., Martino, G., Kilic, E. & Hermann, D. Neural Stem/Precursor Cells for the Treatment of Ischemic Stroke. *J Neurol Sci* 265(1-2), 73-77 (2008).
- Baharvand, H., Mehrjardi, N., Hatami, M., Kiani, S., Rao, M. & Haghghi, M. Neural Differentiation From Human Embryonic Stem Cells in a Defined Adherent Culture Condition. *INTERNATIONAL JOURNAL OF DEVELOPMENTAL BIOLOGY* 51(5), 371 (2007).
- Bai, C. B., Auerbach, W., Lee, J. S., Stephen, D. & Joyner, A. Gli2, But Not Gli1, is Required for Initial Shh Signaling and Ectopic Activation of the Shh Pathway. *Development* 129(20), 4753-4761 (2002).
- Bai, C. B. & Joyner, A. Gli1 Can Rescue the in Vivo Function of Gli2. *Development* 128(24), 5161-5172 (2001).
- Bai, C. B., Stephen, D. & Joyner, A. All Mouse Ventral Spinal Cord Patterning By Hedgehog is Gli Dependent and Involves an Activator Function of Gli3. *Dev Cell* 6(1), 103-115 (2004).
- Baldassa, S., Gnesutta, N., Fascio, U., Sturani, E. & Zippel, R. Sclip, a Microtubule-Destabilizing Factor, Interacts With Rasgrf1 and Inhibits Its Ability to Promote Rac Activation and Neurite Outgrowth. *J Biol Chem* 282(4), 2333-2345 (2007).
- Bartel, D. P. MicroRNAs: Genomics, Biogenesis, Mechanism, and Function. *Cell* 116(2), 281-297 (2004).
- Barth, K., Kishimoto, Y., Rohr, K., Seydler, C., Schulte-Merker, S. & Wilson, S. Bmp Activity Establishes a Gradient of Positional Information Throughout the Entire Neural Plate. *Development* 126(22), 4977-4987 (1999).
- Beattie, G., Lopez, A., Bucay, N., Hinton, A., Firpo, M., King, C. & Hayek, A. Activin a Maintains Pluripotency of Human Embryonic Stem Cells in the Absence of Feeder Layers. *Stem Cells* 23(4), 489-495 (2005).
- Ben-Hur, T., Idelson, M., Khaner, H., Pera, M., Reinhartz, E., Itzik, A. & Reubinoff, B. Transplantation of Human Embryonic Stem Cell-Derived Neural Progenitors Improves Behavioral Deficit in Parkinsonian Rats. *Stem Cells* 22(7), 1246-1255 (2004).

- Ben-Nun, I. F. & Benvenisty, N. Human Embryonic Stem Cells as a Cellular Model for Human Disorders. *Molecular and Cellular Endocrinology* (2006).
- Bendall, S., Stewart, M., Menendez, P., George, D., Vijayaragavan, K., Werbowetski-Ogilvie, T., Ramos-Mejia, V., Rouleau, A., Yang, J., Bosse, M. *et al.* Igf and Fgf Cooperatively Establish the Regulatory Stem Cell Niche of Pluripotent Human Cells in Vitro. *Nature* 448(7157), 1015-1021 (2007).
- Benjamini, Y. & Hochberg, Y. Controlling the False Discovery Rate: A Practical and Powerful Approach to Multiple Testing. *Journal of the Royal Statistical Society. Series B (Methodological)* 289-300 (1995).
- Berman, D., Karhadkar, S., Hallahan, A., Pritchard, J., Eberhart, C., Watkins, D., Chen, J., Cooper, M., Taipale, J., Olson, J. *et al.* Medulloblastoma Growth Inhibition By Hedgehog Pathway Blockade. *Science* 297(5586), 1559-1561 (2002).
- Bibel, M., Richter, J., Schrenk, K., Tucker, K., Staiger, V., Korte, M., Goetz, M. & Barde, Y. Differentiation of Mouse Embryonic Stem Cells Into a Defined Neuronal Lineage. *Nat Neurosci* 7(9), 1003-1009 (2004).
- Bieche, I., Maucuer, A., Laurendeau, I., Lachkar, S., Spano, A., Frankfurter, A., Levy, P., Manceau, V., Sobel, A., Vidaud, M. *et al.* Expression of Stathmin Family Genes in Human Tissues: Non-Neural-Restricted Expression for Sclip. *Genomics* 81(4), 400-410 (2003).
- Biesecker, L. What You Can Learn From One Gene: Gli3. *J Med Genet* 43(6), 465-469 (2006).
- Bigelow, R., Chari, N., Uden, A., Spurgers, K., Lee, S., Roop, D., Toftgard, R. & McDonnell, T. Transcriptional Regulation of Bcl-2 Mediated By the Sonic Hedgehog Signaling Pathway Through Gli-1. *J Biol Chem* 279(2), 1197-1205 (2004).
- Bjorklund, L., Sanchez-Pernaute, R., Chung, S., Andersson, T., Chen, I., Mcnaught, K., Brownell, A., Jenkins, B., Wahlestedt, C., Kim, K. S. *et al.* Embryonic Stem Cells Develop Into Functional Dopaminergic Neurons After Transplantation in a Parkinson Rat Model. *Proc Natl Acad Sci U S A* 99(4), 2344-2349 (2002).
- Bongso, A., Fong, C., Ng, S. & Ratnam, S. Isolation and Culture of Inner Cell Mass Cells From Human Blastocysts. *Hum Reprod* 9(11), 2110-2117 (1994).
- Bonilla, S., Hall, A., Pinto, L., Attardo, A., Gotz, M., Huttner, W. & Arenas, E. Identification of Midbrain Floor Plate Radial Glia-Like Cells as Dopaminergic Progenitors. *Glia* 56(8), 809-820 (2008).
- Boyer, L., Lee, T. I., Cole, M., Johnstone, S., Levine, S., Zucker, J., Guenther, M., Kumar, R., Murray, H., Jenner, R. *et al.* Core Transcriptional Regulatory Circuitry in Human Embryonic Stem Cells. *Cell* 122(6), 947-956 (2005).
- Briscoe, J. Making a Grade: Sonic Hedgehog Signalling and the Control of Neural Cell Fate. *EMBO J* 28(5), 457-465 (2009).
- Briscoe, J., Chen, Y., Jessell, T. & Struhl, G. A Hedgehog-Insensitive Form of Patched Provides Evidence for Direct Long-Range Morphogen Activity of Sonic Hedgehog in the Neural Tube. *Mol Cell* 7(6), 1279-1291 (2001).
- Briscoe, J. & Ericson, J. Specification of Neuronal Fates in the Ventral Neural Tube. *Curr Opin Neurobiol* 11(1), 43-49 (2001).
- Briscoe, J., Pierani, A., Jessell, T. & Ericson, J. A Homeodomain Protein Code Specifies Progenitor Cell Identity and Neuronal Fate in the Ventral Neural Tube. *Cell* 101(4), 435-445 (2000).

- Briscoe, J., Sussel, L., Serup, P., Hartigan-O'Connor, D., Jessell, T., Rubenstein, J. & Ericson, J. Homeobox Gene Nkx2.2 and Specification of Neuronal Identity By Graded Sonic Hedgehog Signalling. *Nature* 398(6728), 622-627 (1999).
- Briscoe, J. & Ericson, J. The Specification of Neuronal Identity By Graded Sonic Hedgehog Signalling. *Seminars in Cell and Developmental Biology* (1999).
- Brons, I., Smithers, L., Trotter, M., Rugg-Gunn, P., Sun, B., Chuva De Sousa Lopes, S. M., Howlett, S. K., Clarkson, A., Ahrlund-Richter, L., Pedersen, R. *et al.* Derivation of Pluripotent Epiblast Stem Cells From Mammalian Embryos. *Nature* 448(7150), 191-195 (2007).
- Burke, R., Nellen, D., Bellotto, M., Hafen, E., Senti, K., Dickson, B. & Basler, K. Dispatched, a Novel Sterol-Sensing Domain Protein Dedicated to the Release of Cholesterol-Modified Hedgehog From Signaling Cells. *Cell* 99(7), 803-815 (1999).
- Cai, C., Thorne, J. & Grabel, L. Hedgehog Serves as a Mitogen and Survival Factor During Embryonic Stem Cell Neurogenesis. *Stem Cells* 26(5), 1097-1108 (2008).
- Cai, L., Ye, Z., Zhou, B., Mali, P., Zhou, C. & Cheng, L. Promoting Human Embryonic Stem Cell Renewal Or Differentiation By Modulating Wnt Signal and Culture Conditions. *Cell Res* 17(1), 62-72 (2007).
- Carpenter, D., Stone, D., Brush, J., Ryan, A., Armanini, M., Frantz, G., Rosenthal, A. & De Sauvage, F. J. Characterization of Two Patched Receptors for the Vertebrate Hedgehog Protein Family. *Proc Natl Acad Sci U S A* 95(23), 13630-13634 (1998).
- Carpenter, M., Inokuma, M., Denham, J., Mujtaba, T., Chiu, C. & Rao, M. S. Enrichment of Neurons and Neural Precursors From Human Embryonic Stem Cells. *Exp Neurol* 172(2), 383-397 (2001).
- Cayuso, J., Ulloa, F., Cox, B., Briscoe, J. & Marti, E. The Sonic Hedgehog Pathway Independently Controls the Patterning, Proliferation and Survival of Neuroepithelial Cells By Regulating Gli Activity. *Development* 133(3), 517-528 (2006a).
- Cayuso, J., Ulloa, F., Cox, B., Briscoe, J. & Marti, E. The Sonic Hedgehog Pathway Independently Controls the Patterning, Proliferation and Survival of Neuroepithelial Cells By Regulating Gli Activity. *Development* 133(3), 517-528 (2006b).
- Chambers, I., Colby, D., Robertson, M., Nichols, J., Lee, S., Tweedie, S. & Smith, A. Functional Expression Cloning of Nanog, a Pluripotency Sustaining Factor in Embryonic Stem Cells. *Cell* 113(5), 643-655 (2003).
- Chamoun, Z., Mann, R., Nellen, D., Von Kessler, D. P., Bellotto, M., Beachy, P. & Basler, K. Skinny Hedgehog, an Acyltransferase Required for Palmitoylation and Activity of the Hedgehog Signal. *Science* 293(5537), 2080-2084 (2001).
- Chan, K., Wu, S., Nissom, P., Oh, S. & Choo, A. Generation of High-Level Stable Transgene Expressing Human Embryonic Stem Cell Lines Using Chinese Hamster Elongation Factor-1 Alpha Promoter System. *Stem Cells Dev* 17(4), 825-836 (2008).
- Chan, K., Zhang, J., Chia, N., Chan, Y., Sim, H. S., Tan, K. S., Oh, S., Ng, H. & Choo, A. Klf4 and Pbx1 Directly Regulate Nanog Expression in Human Embryonic Stem Cells. *Stem Cells* 27(9), 2114-2125 (2009).
- Charbaut, E., Curmi, P., Ozon, S., Lachkar, S., Redeker, V. & Sobel, A. Stathmin Family Proteins Display Specific Molecular and Tubulin Binding Properties. *J Biol Chem* 276(19), 16146-16154 (2001).
- Charron, F., Stein, E., Jeong, J., McMahon, A. & Tessier-Lavigne, M. The Morphogen Sonic Hedgehog is an Axonal Chemoattractant That Collaborates With Netrin-1 in Midline Axon Guidance. *Cell* 113(1), 11-23 (2003).

- Chen, M., Wilson, C., Li, Y., Law, K. K., Lu, C., Gacayan, R., Zhang, X., Hui, C. C. & Chuang, P. Cilium-Independent Regulation of Gli Protein Function By Sufu in Hedgehog Signaling is Evolutionarily Conserved. *Genes Dev* 23(16), 1910-1928 (2009).
- Cheng, L., Jia, H., Lohr, M., Bagherzadeh, A., Holmes, D., Selwood, D. & Zachary, I. Anti-Chemorepulsive Effects of Vascular Endothelial Growth Factor and Placental Growth Factor-2 in Dorsal Root Ganglion Neurons Are Mediated Via Neuropilin-1 and Cyclooxygenase-Derived Prostanoid Production. *J Biol Chem* 279(29), 30654-30661 (2004).
- Cheng, S. & Bishop, J. Suppressor of Fused Represses Gli-Mediated Transcription By Recruiting the Sap18-Msin3 Corepressor Complex. *Proc Natl Acad Sci U S A* 99(8), 5442-5447 (2002).
- Cheung, H., Zhang, X., Ribeiro, A., Mo, R., Makino, S., Puvindran, V., Law, K. K., Briscoe, J. & Hui, C. C. The Kinesin Protein Kif7 is a Critical Regulator of Gli Transcription Factors in Mammalian Hedgehog Signaling. *Sci Signal* 2(76), ra29 (2009).
- Chiang, C., Litingtung, Y., Lee, E., Young, K., Corden, J., Westphal, H. & Beachy, P. Cyclopia and Defective Axial Patterning in Mice Lacking Sonic Hedgehog Gene Function. *Nature* 383(6599), 407-413 (1996).
- Chiba, S., Lee, Y. M., Zhou, W. & Freed, C. Noggin Enhances Dopamine Neuron Production From Human Embryonic Stem Cells and Improves Behavioral Outcome After Transplantation Into Parkinsonian Rats. *Stem Cells* 26(11), 2810-2820 (2008).
- Chin, A., Padmanabhan, J., Oh, S. & Choo, A. Defined and Serum-Free Media Support Undifferentiated Human Embryonic Stem Cell Growth. *Stem Cells Dev* (2009a).
- Chin, M., Mason, M., Xie, W., Volinia, S., Singer, M., Peterson, C., Ambartsumyan, G., Aimiwu, O., Richter, L., Zhang, J. *et al.* Induced Pluripotent Stem Cells and Embryonic Stem Cells Are Distinguished By Gene Expression Signatures. *Cell Stem Cell* 5(1), 111-123 (2009b).
- Cho, M. S., Lee, Y. E., Kim, J. Y., Chung, S., Cho, Y. H., Kim, D. S., Kang, S., Lee, H., Kim, M. H., Kim, J. H. *et al.* Highly Efficient and Large-Scale Generation of Functional Dopamine Neurons From Human Embryonic Stem Cells. *Proc Natl Acad Sci U S A* 105(9), 3392-3397 (2008).
- Choo, A., Padmanabhan, J., Chin, A., Fong, W. & Oh, S. Immortalized Feeders for the Scale-Up of Human Embryonic Stem Cells in Feeder and Feeder-Free Conditions. *J Biotechnol* 122(1), 130-141 (2006).
- Chou, Y., Khuon, S., Herrmann, H. & Goldman, R. Nestin Promotes the Phosphorylation-Dependent Disassembly of Vimentin Intermediate Filaments During Mitosis. *Mol Biol Cell* 14(4), 1468-1478 (2003).
- Chuang, P. & McMahon, A. Vertebrate Hedgehog Signalling Modulated By Induction of a Hedgehog-Binding Protein. *Nature* 397(6720), 617-621 (1999).
- Chung, S., Andersson, T., Sonntag, K., Bjorklund, L., Isacson, O. & Kim, K. S. Analysis of Different Promoter Systems for Efficient Transgene Expression in Mouse Embryonic Stem Cell Lines. *Stem Cells* 20(2), 139-145 (2002).
- Chung, S., Hedlund, E., Hwang, M., Kim, D. W., Shin, B., Hwang, D., Jung Kang, U., Isacson, O. & Kim, K. S. The Homeodomain Transcription Factor Pitx3 Facilitates Differentiation of Mouse Embryonic Stem Cells Into Ahd2-Expressing Dopaminergic Neurons. *Mol Cell Neurosci* 28(2), 241-252 (2005).
- Colas, J. & Schoenwolf, G. Towards a Cellular and Molecular Understanding of Neurulation. *Dev Dyn* 221(2), 117-145 (2001).

- Cooper, M., Porter, J., Young, K. & Beachy, P. Teratogen-Mediated Inhibition of Target Tissue Response to Shh Signaling. *Science* 280(5369), 1603-1607 (1998).
- Corbit, K., Aanstad, P., Singla, V., Norman, A., Stainier, D. & Reiter, J. Vertebrate Smoothed Functions At the Primary Cilium. *Nature* 437(7061), 1018-1021 (2005).
- Crawford, T. & Roelink, H. The Notch Response Inhibitor Dapt Enhances Neuronal Differentiation in Embryonic Stem Cell-Derived Embryoid Bodies Independently of Sonic Hedgehog Signaling. *Dev Dyn* 236(3), 886-892 (2007).
- Crossley, P., Martinez, S. & Martin, G. Midbrain Development Induced By Fgf8 in the Chick Embryo. *Nature* 380(6569), 66-68 (1996).
- Dahmane, N. & Ruiz I Altaba, A. Sonic Hedgehog Regulates the Growth and Patterning of the Cerebellum. *Development* 126(14), 3089-3100 (1999).
- Dahmane, N., Sanchez, P., Gitton, Y., Palma, V., Sun, T., Beyna, M., Weiner, H. & Ruiz I Altaba, A. The Sonic Hedgehog-Gli Pathway Regulates Dorsal Brain Growth and Tumorigenesis. *Development* 128(24), 5201-5212 (2001).
- Dai, P., Akimaru, H., Tanaka, Y., Maekawa, T., Nakafuku, M. & Ishii, S. Sonic Hedgehog-Induced Activation of the Gli1 Promoter is Mediated By Gli3. *J Biol Chem* 274(12), 8143-8152 (1999).
- Darr, H., Mayshar, Y. & Benvenisty, N. Overexpression of Nanog in Human Es Cells Enables Feeder-Free Growth While Inducing Primitive Ectoderm Features. *Development* 133(6), 1193-1201 (2006).
- De Lau, L. M. & Breteler, M. Epidemiology of Parkinson's Disease. *Lancet Neurol* 5(6), 525-535 (2006).
- Deckelbaum, R., Chan, G., Miao, D., Goltzman, D. & Karaplis, A. Ihh Enhances Differentiation of Cfk-2 Chondrocytic Cells and Antagonizes Pthrp-Mediated Activation of Pka. *J Cell Sci* 115(Pt 14), 3015-3025 (2002).
- Dietrich, J., Noble, M. & Mayer-Proschel, M. Characterization of A2B5+ Glial Precursor Cells From Cryopreserved Human Fetal Brain Progenitor Cells. *Glia* 40(1), 65-77 (2002).
- Ding, Q., Motoyama, J., Gasca, S., Mo, R., Sasaki, H., Rossant, J. & Hui, C. C. Diminished Sonic Hedgehog Signaling and Lack of Floor Plate Differentiation in Gli2 Mutant Mice. *Development* 125(14), 2533-2543 (1998).
- Doi, A., Park, I., Wen, B., Murakami, P., Aryee, M., Irizarry, R., Herb, B., Ladd-Acosta, C., Rho, J., Loewer, S. *et al.* Differential Methylation of Tissue- and Cancer-Specific CpG Island Shores Distinguishes Human Induced Pluripotent Stem Cells, Embryonic Stem Cells and Fibroblasts. *Nat Genet* 41(12), 1350-1353 (2009).
- Dravid, G., Ye, Z., Hammond, H., Chen, G., Pyle, A., Donovan, P., Yu, X. & Cheng, L. Defining the Role of Wnt/Beta-Catenin Signaling in the Survival, Proliferation, and Self-Renewal of Human Embryonic Stem Cells. *Stem Cells* 23(10), 1489-1501 (2005).
- Du, Z., Li, X., Nguyen, G. & Zhang, S. Induced Expression of Olig2 is Sufficient for Oligodendrocyte Specification But Not for Motoneuron Specification and Astrocyte Repression. *Mol Cell Neurosci* 33(4), 371-380 (2006).
- Dunaeva, M., Michelson, P., Kogerman, P. & Toftgard, R. Characterization of the Physical Interaction of Gli Proteins With Sufu Proteins. *J Biol Chem* 278(7), 5116-5122 (2003).
- Dvash, T., Ben-Yosef, D. & R., E. Human Embryonic Stem Cells as a Powerful Tool for Studying Human Embryogenesis. *Pediatric research* (2006).

- Dvorak, P., Dvorakova, D., Koskova, S., Vodinska, M., Najvirtova, M., Krekac, D. & Hampl, A. Expression and Potential Role of Fibroblast Growth Factor 2 and Its Receptors in Human Embryonic Stem Cells. *Stem Cells* 23(8), 1200-1211 (2005).
- Echelard, Y., Epstein, D., St-Jacques, B., Shen, L., Mohler, J., McMahon, J. & McMahon, A. Sonic Hedgehog, a Member of a Family of Putative Signaling Molecules, is Implicated in the Regulation of Cns Polarity. *Cell* 75(7), 1417-1430 (1993).
- Eggenchwiler, J., Bulgakov, O., Qin, J., Li, T. & Anderson, K. Mouse Rab23 Regulates Hedgehog Signaling From Smoothed to Gli Proteins. *Dev Biol* 290(1), 1-12 (2006).
- Eggenchwiler, J., Espinoza, E. & Anderson, K. Rab23 is an Essential Negative Regulator of the Mouse Sonic Hedgehog Signaling Pathway. *Nature* 412(6843), 194-198 (2001).
- Eiselleova, L., Matulka, K., Kriz, V., Kunova, M., Schmidtova, Z., Neradil, J., Tichy, B., Dvorakova, D., Pospisilova, S., Hampl, A. *et al.* A Complex Role for Fgf-2 in Self-Renewal, Survival, and Adhesion of Human Embryonic Stem Cells. *Stem Cells* 27(8), 1847-1857 (2009).
- Elkabetz, Y., Panagiotakos, G., Al Shamy, G., Socci, N., Tabar, V. & Studer, L. Human Es Cell-Derived Neural Rosettes Reveal a Functionally Distinct Early Neural Stem Cell Stage. *Genes Dev* 22(2), 152-165 (2008).
- Eminli, S., Utikal, J., Arnold, K., Jaenisch, R. & Hochedlinger, K. Reprogramming of Neural Progenitor Cells Into Induced Pluripotent Stem Cells in the Absence of Exogenous Sox2 Expression. *Stem Cells* 26(10), 2467-2474 (2008).
- Endoh-Yamagami, S., Evangelista, M., Wilson, D., Wen, X., Theunissen, J., Phamluong, K., Davis, M., Scales, S. J., Solloway, M., De Sauvage, F. J. *et al.* The Mammalian Cos2 Homolog Kif7 Plays an Essential Role in Modulating Hh Signal Transduction During Development. *Curr Biol* 19(15), 1320-1326 (2009).
- Epstein, D., McMahon, A. & Joyner, A. Regionalization of Sonic Hedgehog Transcription Along the Anteroposterior Axis of the Mouse Central Nervous System is Regulated By Hnf3-Dependent and -Independent Mechanisms. *Development* 126(2), 281-292 (1999).
- Ericson, J., Briscoe, J., Rashbass, P., Van Heyningen, V. & Jessell, T. M. Graded Sonic Hedgehog Signaling and the Specification of Cell Fate in the Ventral Neural Tube. *Cold Spring Harb Symp Quant Biol* 62, 451-466 (1997).
- Ericson, J., Morton, S., Kawakami, A., Roelink, H. & Jessell, T. Two Critical Periods of Sonic Hedgehog Signaling Required for the Specification of Motor Neuron Identity. *Cell* 87(4), 661-673 (1996).
- Evans, M. & Kaufman, M. Establishment in Culture of Pluripotential Cells From Mouse Embryos. *Nature* 292(5819), 154-156 (1981).
- Falcon, S. & Gentleman, R. Using Gostats to Test Gene Lists for Go Term Association. *Bioinformatics* 23(2), 257 (2007).
- Farkas, L., Dunker, N., Roussa, E., Unsicker, K. & Krieglstein, K. Transforming Growth Factor-Beta(S) Are Essential for the Development of Midbrain Dopaminergic Neurons in Vitro and in Vivo. *J Neurosci* 23(12), 5178-5186 (2003).
- Faulkner, J. & Keirstead, H. Human Embryonic Stem Cell-Derived Oligodendrocyte Progenitors for the Treatment of Spinal Cord Injury. *Transpl Immunol* 15(2), 131-142 (2005).
- Feng, B., Ng, J., Heng, J. & Ng, H. Molecules That Promote Or Enhance Reprogramming of Somatic Cells to Induced Pluripotent Stem Cells. *Cell Stem Cell* 4(4), 301-312 (2009).
- Ferretti, E., De Smaele, E., Miele, E., Laneve, P., Po, A., Pelloni, M., Paganelli, A., Di Marcotullio, L., Caffarelli, E., Screpanti, I. *et al.* Concerted MicroRNA Control of Hedgehog

Signalling in Cerebellar Neuronal Progenitor and Tumour Cells. *EMBO J* 27(19), 2616-2627 (2008).

Ferri, A., Lin, W., Mavromatakis, Y., Wang, J., Sasaki, H., Whitsett, J. & Ang, S. L. Foxa1 and Foxa2 Regulate Multiple Phases of Midbrain Dopaminergic Neuron Development in a Dosage-Dependent Manner. *Development* 134(15), 2761-2769 (2007).

Fong, H., Hohenstein, K. & Donovan, P. Regulation of Self-Renewal and Pluripotency By Sox2 in Human Embryonic Stem Cells. *Stem Cells* 26(8), 1931-1938 (2008).

Freed, W., Chen, J., Bäckman, C., Schwartz, C., Vazin, T., Cai, J., Spivak, C., Lupica, C., Rao, M., Zeng, X. *et al.* Gene Expression Profile of Neuronal Progenitor Cells Derived From Hescs: Activation of Chromosome 11p15.5 and Comparison to Human Dopaminergic Neurons. *PLoS ONE* 3(1), e1422 (2008).

Freitas-Andrade, M., Carmeliet, P., Stanimirovic, D. & Moreno, M. Vegfr-2-Mediated Increased Proliferation and Survival in Response to Oxygen and Glucose Deprivation in Plgf Knockout Astrocytes. *J Neurochem* 107(3), 756-767 (2008).

Fukuda, S., Kato, F., Tozuka, Y., Yamaguchi, M., Miyamoto, Y. & Hisatsune, T. Two Distinct Subpopulations of Nestin-Positive Cells in Adult Mouse Dentate Gyrus. *J Neurosci* 23(28), 9357-9366 (2003).

Gage, F. Mammalian Neural Stem Cells. *Science* 287(5457), 1433-1438 (2000).

Gaiano, N., Nye, J. S. & Fishell, G. Radial Glial Identity is Promoted By Notch1 Signaling in the Murine Forebrain. *Neuron* 26(2), 395-404 (2000).

Gan, Q., Yoshida, T., Mcdonald, O. & Owens, G. Concise Review: Epigenetic Mechanisms Contribute to Pluripotency and Cell Lineage Determination of Embryonic Stem Cells. *Stem Cells* 25(1), 2-9 (2007).

Corp., G. Geron and Fda Reach Agreement on Clinical Hold: Company and Regulatory Agency Define Path to Re-Initiate Human Trials for Spinal Cord Injur. (2009).

Gerrard, L., Rodgers, L. & Cui, W. Differentiation of Human Embryonic Stem Cells to Neural Lineages in Adherent Culture By Blocking Bone Morphogenetic Protein Signaling. *Stem Cells* 23(9), 1234-1241 (2005).

Gil, J. E., Woo, D. H., Shim, J., Kim, S. E., You, H. J., Park, S., Paek, S., Kim, S. K. & Kim, J. H. Vitronectin Promotes Oligodendrocyte Differentiation During Neurogenesis of Human Embryonic Stem Cells. *FEBS Lett* 583(3), 561-567 (2009).

Gimeno, L. & Martinez, S. Expression of Chick Fgf19 and Mouse Fgf15 Orthologs is Regulated in the Developing Brain By Fgf8 and Shh. *Dev Dyn* 236(8), 2285-2297 (2007).

Ginis, I., Luo, Y., Miura, T., Thies, S., Brandenberger, R., Gerecht-Nir, S., Amit, M., Hoke, A., Carpenter, M., Itskovitz-Eldor, J. *et al.* Differences Between Human and Mouse Embryonic Stem Cells. *Dev Biol* 269(2), 360-380 (2004).

Gjedde, A., Reith, J., Dyve, S., Léger, G., Guttman, M., Diksic, M., Evans, A. & Kuwabara, H. Dopa Decarboxylase Activity of the Living Human Brain. *Proceedings of the National Academy of Sciences* 88(7), 2721 (1991).

Goodrich, L., Johnson, R., Milenkovic, L., McMahon, J. & Scott, M. Conservation of the Hedgehog/Patched Signaling Pathway From Flies to Mice: Induction of a Mouse Patched Gene By Hedgehog. *Genes Dev* 10(3), 301-312 (1996).

Goulding, M., Chalepakis, G., Deutsch, U., Erselius, J. & Gruss, P. Pax-3, a Novel Murine DNA Binding Protein Expressed During Early Neurogenesis. *EMBO J* 10(5), 1135-1147 (1991).

- Greber, B., Lehrach, H. & Adjaye, J. Fibroblast Growth Factor 2 Modulates Transforming Growth Factor Beta Signaling in Mouse Embryonic Fibroblasts and Human Escs (Hescs) to Support Hesc Self-Renewal. *Stem Cells* 25(2), 455-464 (2007).
- Grinnemo, K., Sylven, C., Hovatta, O., Dellgren, G. & Corbascio, M. Immunogenicity of Human Embryonic Stem Cells. *Cell Tissue Res* 331(1), 67-78 (2008).
- Guerrero, I. & Chiang, C. A Conserved Mechanism of Hedgehog Gradient Formation By Lipid Modifications. *Trends Cell Biol* 17(1), 1-5 (2007).
- Guillaume, D. & Zhang, S. Human Embryonic Stem Cells: A Potential Source of Transplantable Neural Progenitor Cells. *Neurosurg Focus* 24(3-4), E3 (2008).
- Hallahan, A., Pritchard, J., Hansen, S., Benson, M., Stoeck, J., Hatton, B., Russell, T., Ellenbogen, R., Bernstein, I., Beachy, P. *et al.* The Smo1 Mouse Model Reveals That Notch Signaling is Critical for the Growth and Survival of Sonic Hedgehog-Induced Medulloblastomas. *Cancer Res* 64(21), 7794-7800 (2004).
- Hammond, R., Blaess, S. & Abeliovich, A. Sonic Hedgehog is a Chemoattractant for Midbrain Dopaminergic Axons. *PLoS One* 4(9), e7007 (2009).
- Han, Y. G., Spassky, N., Romaguera-Ros, M., Garcia-Verdugo, J. M., Aguilar, A., Schneider-Maunoury, S. & Alvarez-Buylla, A. Hedgehog Signaling and Primary Cilia Are Required for the Formation of Adult Neural Stem Cells. *Nat Neurosci* 11(3), 277-284 (2008).
- Hanna, J., Wernig, M., Markoulaki, S., Sun, C. W., Meissner, A., Cassady, J., Beard, C., Brambrink, T., Wu, L., Townes, T. *et al.* Treatment of Sickle Cell Anemia Mouse Model With Ips Cells Generated From Autologous Skin. *Science* 318(5858), 1920-1923 (2007).
- Hansis, C., Grifo, J. & Krey, L. Oct-4 Expression in Inner Cell Mass and Trophectoderm of Human Blastocysts. *Mol Hum Reprod* 6(11), 999-1004 (2000).
- Hargrave, M., Karunaratne, A., Cox, L., Wood, S., Koopman, P. & Yamada, T. The Hmg Box Transcription Factor Gene Sox14 Marks a Novel Subset of Ventral Interneurons and is Regulated By Sonic Hedgehog. *Dev Biol* 219(1), 142-153 (2000).
- Haycraft, C., Banizs, B., Aydin-Son, Y., Zhang, Q., Michaud, E. & Yoder, B. Gli2 and Gli3 Localize to Cilia and Require the Intraflagellar Transport Protein Polaris for Processing and Function. *PLoS Genet* 1(4), e53 (2005).
- Hedlund, E., Pruszek, J., Lardaro, T., Ludwig, W., Vinuela, A., Kim, K. S. & Isacson, O. Embryonic Stem Cell-Derived Pitx3-Enhanced Green Fluorescent Protein Midbrain Dopamine Neurons Survive Enrichment By Fluorescence-Activated Cell Sorting and Function in an Animal Model of Parkinson's Disease. *Stem Cells* 26(6), 1526-1536 (2008).
- Heo, J. S., Lee, M. Y. & Han, H. J. Sonic Hedgehog Stimulates Mouse Embryonic Stem Cell Proliferation By Cooperation of Ca²⁺/Protein Kinase C and Epidermal Growth Factor Receptor as Well as Gli1 Activation. *Stem Cells* 25(12), 3069-3080 (2007).
- Hicks, A., Lappalainen, R., Narkilahti, S., Suuronen, R., Corbett, D., Sivenius, J., Hovatta, O. & Jolkkonen, J. Transplantation of Human Embryonic Stem Cell-Derived Neural Precursor Cells and Enriched Environment After Cortical Stroke in Rats: Cell Survival and Functional Recovery. *Eur J Neurosci* 29(3), 562-574 (2009).
- Hollnagel, A., Oehlmann, V., Heymer, J., Ruther, U. & Nordheim, A. Id Genes Are Direct Targets of Bone Morphogenetic Protein Induction in Embryonic Stem Cells. *J Biol Chem* 274(28), 19838-19845 (1999).
- Hooper, J. & Scott, M. Communicating With Hedgehogs. *Nat Rev Mol Cell Biol* 6(4), 306-317 (2005).

- Hornstein, E., Mansfield, J., Yekta, S., Hu, J., Harfe, B., Mcmanus, M., Baskerville, S., Bartel, D. & Tabin, C. The MicroRNA Mir-196 Acts Upstream of Hoxb8 and Shh in Limb Development. *Nature* 438(7068), 671-674 (2005).
- Huangfu, D. & Anderson, K. Cilia and Hedgehog Responsiveness in the Mouse. *Proc Natl Acad Sci U S A* 102(32), 11325-11330 (2005).
- Huangfu, D. & Anderson, K. Signaling From Smo to Ci/Gli: Conservation and Divergence of Hedgehog Pathways From Drosophila to Vertebrates. *Development* 133(1), 3-14 (2006).
- Huangfu, D., Liu, A., Rakeman, A., Murcia, N., Niswander, L. & Anderson, K. Hedgehog Signalling in the Mouse Requires Intraflagellar Transport Proteins. *Nature* 426(6962), 83-87 (2003).
- Humphrey, R., Beattie, G., Lopez, A., Bucay, N., King, C., Firpo, M., Rose-John, S. & Hayek, A. Maintenance of Pluripotency in Human Embryonic Stem Cells is Stat3 Independent. *Stem Cells* 22(4), 522-530 (2004).
- Hynes, M., Ye, W., Wang, K., Stone, D., Murone, M., Sauvage, F. & Rosenthal, A. The Seven-Transmembrane Receptor Smoothed Cell-Autonomously Induces Multiple Ventral Cell Types. *Nat Neurosci* 3(1), 41-46 (2000a).
- Hynes, M., Ye, W., Wang, K., Stone, D. & Murone, M. ... Seven-Transmembrane Receptor Smoothed Cell-Autonomously Induces Multiple Ventral Cell *Nat Neurosci* (2000b).
- Hyslop, L., Stojkovic, M., Armstrong, L., Walter, T., Stojkovic, P., Przyborski, S., Herbert, M., Murdoch, A., Strachan, T. & Lako, M. Downregulation of Nanog Induces Differentiation of Human Embryonic Stem Cells to Extraembryonic Lineages. *Stem Cells* 23(8), 1035-1043 (2005a).
- Hyslop, L., Armstrong, L., Stojkovic, M. & Lako, M. Human Embryonic Stem Cells: Biology and Clinical Implications. *Expert Rev Mol Med* 7(19), 1-21 (2005b).
- Ingham, P. & McMahon, A. Hedgehog Signaling in Animal Development: Paradigms and Principles. *Genes Dev* 15(23), 3059-3087 (2001).
- Ingram, W., Mccue, K., Tran, T., Hallahan, A. & Wainwright, B. Sonic Hedgehog Regulates Hes1 Through a Novel Mechanism That is Independent of Canonical Notch Pathway Signalling. *Oncogene* 27(10), 1489-1500 (2008).
- Ingram, W., Wicking, C., Grimmond, S., Forrest, A. & Wainwright, B. Novel Genes Regulated By Sonic Hedgehog in Pluripotent Mesenchymal Cells. *Oncogene* 21(53), 8196-8205 (2002).
- Inzunza, J., Gertow, K., Stromberg, M., Matilainen, E., Blennow, E., Skottman, H., Wolbank, S., Ahrlund-Richter, L. & Hovatta, O. Derivation of Human Embryonic Stem Cell Lines in Serum Replacement Medium Using Postnatal Human Fibroblasts as Feeder Cells. *Stem Cells* 23(4), 544-549 (2005).
- Irizarry, R., Hobbs, B., Collin, F., Beazer-Barclay, Y. D., Antonellis, K., Scherf, U. & Speed, T. Exploration, Normalization, and Summaries of High Density Oligonucleotide Array Probe Level Data. *Biostatistics* 4(2), 249 (2003).
- Iso, T., Kedes, L. & Hamamori, Y. Hes and Herp Families: Multiple Effectors of the Notch Signaling Pathway. *J Cell Physiol* 194(3), 237-255 (2003).
- Itsykson, P., Ilouz, N., Turetsky, T., Goldstein, R., Pera, M., Fishbein, I., Segal, M. & Reubinoff, B. Derivation of Neural Precursors From Human Embryonic Stem Cells in the Presence of Noggin. *Mol Cell Neurosci* 30(1), 24-36 (2005).
- James, D., Levine, A., Besser, D. & Hemmati-Brivanlou, A. Tgfbeta/Activin/Nodal Signaling is Necessary for the Maintenance of Pluripotency in Human Embryonic Stem Cells. *Development* 132(6), 1273-1282 (2005).

- Jeong, S., Chu, K., Jung, K., Kim, S. U., Kim, M. & Roh, J. K. Human Neural Stem Cell Transplantation Promotes Functional Recovery in Rats With Experimental Intracerebral Hemorrhage. *Stroke* 34(9), 2258-2263 (2003).
- Jiang, X., Gwee, Y., Mckeown, S., Bronner-Fraser, M., Lutzko, C. & Lawlor, E. Isolation and Characterization of Neural Crest Stem Cells Derived From in Vitro-Differentiated Human Embryonic Stem Cells. *Stem Cells Dev* 18(7), 1059-1070 (2009).
- Jeong, J. & McMahon, A. Growth and Pattern of the Mammalian Neural Tube Are Governed By Partially Overlapping Feedback Activities of the Hedgehog Antagonists Patched 1 and Hhip1. *Development* 132(1), 143-154 (2005).
- Jeong, Y. & Epstein, D. Distinct Regulators of Shh Transcription in the Floor Plate and Notochord Indicate Separate Origins for These Tissues in the Mouse Node. *Development* 130(16), 3891 (2003).
- Jessell, T. M. Neuronal Specification in the Spinal Cord: Inductive Signals and Transcriptional Codes. *Nat Rev Genet* 1(1), 20-29 (2000).
- Jin, K., Zhu, Y., Sun, Y., Mao, X. O., Xie, L. & Greenberg, D. Vascular Endothelial Growth Factor (Vegf) Stimulates Neurogenesis in Vitro and in Vivo. *Proc Natl Acad Sci U S A* 99(18), 11946-11950 (2002).
- Jin, K. L., Mao, X. O., Nagayama, T., Goldsmith, P. & Greenberg, D. Induction of Vascular Endothelial Growth Factor and Hypoxia-Inducible Factor-1alpha By Global Ischemia in Rat Brain. *Neuroscience* 99(3), 577-585 (2000).
- Joannides, A., Fiore-Herich, C., Battersby, A., Athauda-Arachchi, P., Bouhon, I., Williams, L., Westmore, K., Kemp, P., Compston, A., Allen, N. *et al.* A Scaleable and Defined System for Generating Neural Stem Cells From Human Embryonic Stem Cells. *Stem Cells* 25(3), 731-737 (2007).
- Josephson, R., Muller, T., Pickel, J., Okabe, S., Reynolds, K., Turner, P., Zimmer, A. & McKay, R. Pou Transcription Factors Control Expression of Cns Stem Cell-Specific Genes. *Development* 125(16), 3087-3100 (1998).
- Kania, G., Corbeil, D., Fuchs, J., Tarasov, K., Blyszczuk, P., Huttner, W., Boheler, K. & Wobus, A. Somatic Stem Cell Marker Prominin-1/Cd133 is Expressed in Embryonic Stem Cell-Derived Progenitors. *Stem Cells* 23(6), 791-804 (2005).
- Kawasaki, H., Mizuseki, K., Nishikawa, S., Kaneko, S., Kuwana, Y., Nakanishi, S., Nishikawa, S. & Sasai, Y. Induction of Midbrain Dopaminergic Neurons From Es Cells By Stromal Cell-Derived Inducing Activity. *Neuron* 28(1), 31-40 (2000).
- Kenney, A., Cole, M. & Rowitch, D. Nmyc Upregulation By Sonic Hedgehog Signaling Promotes Proliferation in Developing Cerebellar Granule Neuron Precursors. *Development* 130(1), 15-28 (2003).
- Kenney, A. M. & Rowitch, D. H. Sonic Hedgehog Promotes G1 Cyclin Expression and Sustained Cell Cycle Progression in Mammalian Neuronal Precursors. *Mol. Cell. Biol.* 20(23), 9055-9067 (2000).
- Killeen, M. & Sybingco, S. Netrin, Slit and Wnt Receptors Allow Axons to Choose the Axis of Migration. *Dev Biol* 323(2), 143-151 (2008).
- Kim, J., Inoue, K., Ishii, J., Vanti, W., Voronov, S., Murchison, E., Hannon, G. & Abeliovich, A. A MicroRNA Feedback Circuit in Midbrain Dopamine Neurons. *Science* 317(5842), 1220-1224 (2007).
- Kim, J., Krichevsky, A., Grad, Y., Hayes, G., Kosik, K., Church, G. & Ruvkun, G. Identification of Many MicroRNAs That Copurify With Polyribosomes in Mammalian Neurons. *Proc Natl Acad Sci U S A* 101(1), 360-365 (2004).

- Kim, S. U. & De Vellis, J. Stem Cell-Based Cell Therapy in Neurological Diseases: A Review. *J Neurosci Res* 87(10), 2183-2200 (2009).
- Kinzler, K. & Vogelstein, B. The Gli Gene Encodes a Nuclear Protein Which Binds Specific Sequences in the Human Genome. *Mol Cell Biol* 10(2), 634-642 (1990).
- Kiprilov, E., Awan, A., Desprat, R., Velho, M., Clement, C., Byskov, A., Andersen, C., Satir, P., Bouhassira, E., Christensen, S. *et al.* Human Embryonic Stem Cells in Culture Possess Primary Cilia With Hedgehog Signaling Machinery. *J Cell Biol* 180(5), 897-904 (2008).
- Kittappa, R., Chang, W., Awatramani, R. & McKay, R. The Foxa2 Gene Controls the Birth and Spontaneous Degeneration of Dopamine Neurons in Old Age. *Plos Biol* 5(12), e325 (2007).
- Koebnick, K. & Pieler, T. Gli-Type Zinc Finger Proteins as Bipotential Transducers of Hedgehog Signaling. *Differentiation* 70(2-3), 69-76 (2002).
- Kogerman, P., Grimm, T., Kogerman, L., Krause, D., Uden, A., Sandstedt, B., Toftgard, R. & Zaphiropoulos, P. Mammalian Suppressor-of-Fused Modulates Nuclear-Cytoplasmic Shuttling of Gli-1. *Nat Cell Biol* 1(5), 312-319 (1999).
- Kosik, K. & Krichevsky, A. The Elegance of the Micrnas: A Neuronal Perspective. *Neuron* 47(6), 779-782 (2005).
- Krichevsky, A., King, K., Donahue, C., Khrapko, K. & Kosik, K. A Microna Array Reveals Extensive Regulation of Micrnas During Brain Development. *RNA* 9(10), 1274-1281 (2003).
- Krichevsky, A., Sonntag, K., Isacson, O. & Kosik, K. Specific Micrnas Modulate Embryonic Stem Cell-Derived Neurogenesis. *Stem Cells* 24(4), 857-864 (2006).
- Kuroda, T., Tada, M., Kubota, H., Kimura, H., Hatano, S., Suemori, H., Nakatsuji, N. & Tada, T. Octamer and Sox Elements Are Required for Transcriptional Cis Regulation of Nanog Gene Expression. *Mol Cell Biol* 25(6), 2475-2485 (2005).
- Lai, K., Kaspar, B., Gage, F. & Schaffer, D. Sonic Hedgehog Regulates Adult Neural Progenitor Proliferation in Vitro and in Vivo. *Nat Neurosci* 6(1), 21-27 (2003).
- Lamba, D., Karl, M., Ware, C. & Reh, T. A. Efficient Generation of Retinal Progenitor Cells From Human Embryonic Stem Cells. *Proc Natl Acad Sci U S A* 103(34), 12769-12774 (2006).
- Lazzari, G., Colleoni, S., Giannelli, S., Brunetti, D., Colombo, E., Lagutina, I., Galli, C. & Broccoli, V. Direct Derivation of Neural Rosettes From Cloned Bovine Blastocysts: A Model of Early Neurulation Events and Neural Crest Specification in Vitro. *Stem Cells* 24(11), 2514-2521 (2006).
- Lee, C. S., Buttitta, L., May, N. R., Kispert, A. & Fan, C. M. Shh-N Upregulates Sfrp2 to Mediate Its Competitive Interaction With Wnt1 and Wnt4 in the Somitic Mesoderm. *Development* 127(1), 109-118 (2000).
- Lee, D. S., Yu, K., Rho, J. Y., Lee, E., Han, J. S., Koo, D. B., Cho, Y. S., Kim, J., Lee, K. K. & Han, Y. M. Cyclopamine Treatment of Human Embryonic Stem Cells Followed By Culture in Human Astrocyte Medium Promotes Differentiation Into Nestin- and Gfap-Expressing Astrocytic Lineage. *Life Sci* 80(2), 154-159 (2006).
- Lee, G., Kim, H., Elkabetz, Y., Al Shamy, G., Panagiotakos, G., Barberi, T., Tabar, V. & Studer, L. Isolation and Directed Differentiation of Neural Crest Stem Cells Derived From Human Embryonic Stem Cells. *Nat Biotechnol* 25(12), 1468-1475 (2007a).
- Lee, H., Shamy, G., Elkabetz, Y., Schofield, C., Harrision, N., Panagiotakos, G., Socci, N., Tabar, V. & Studer, L. Directed Differentiation and Transplantation of Human Embryonic Stem Cell-Derived Motoneurons. *Stem Cells* 25(8), 1931-1939 (2007b).

- Lee, J. D. & Treisman, J. Sightless Has Homology to Transmembrane Acyltransferases and is Required to Generate Active Hedgehog Protein. *Curr Biol* 11(14), 1147-1152 (2001).
- Lee, S. H., Lumelsky, N., Studer, L., Auerbach, J. & McKay, R. Efficient Generation of Midbrain and Hindbrain Neurons From Mouse Embryonic Stem Cells. *Nat Biotechnol* 18(6), 675-679 (2000).
- Lendahl, U., Zimmerman, L. & McKay, R. Cns Stem Cells Express a New Class of Intermediate Filament Protein. *Cell* 60(4), 585-595 (1990).
- Levenstein, M., Ludwig, T., Xu, R., Llanas, R., Vandenheuvél-Kramer, K., Manning, D. & Thomson, J. Basic Fibroblast Growth Factor Support of Human Embryonic Stem Cell Self-Renewal. *Stem Cells* 24(3), 568-574 (2006).
- Li, J., Wang, G., Wang, C., Zhao, Y., Zhang, H., Tan, Z., Song, Z., Ding, M. & Deng, H. Mek/Erk Signaling Contributes to the Maintenance of Human Embryonic Stem Cell Self-Renewal. *Differentiation* 75(4), 299-307 (2007).
- Li, X., Du, Z., Zarnowska, E., Pankratz, M., Hansen, L., Pearce, R. & Zhang, S. Specification of Motoneurons From Human Embryonic Stem Cells. *Nat Biotechnol* 23(2), 215-221 (2005).
- Li, X., Hu, B., Jones, S., Zhang, Y., Lavaute, T., Du, Z. & Zhang, S. Directed Differentiation of Ventral Spinal Progenitors and Motor Neurons From Human Embryonic Stem Cells By Small Molecules. *Stem Cells* 26(4), 886-893 (2008).
- Liem, K. J., He, M., Ocbina, P. & Anderson, K. Mouse Kif7/Costal2 is a Cilia-Associated Protein That Regulates Sonic Hedgehog Signaling. *Proc Natl Acad Sci U S A* 106(32), 13377-13382 (2009).
- Liem, K. J., Jessell, T. & Briscoe, J. Regulation of the Neural Patterning Activity of Sonic Hedgehog By Secreted Bmp Inhibitors Expressed By Notochord and Somites. *Development* 127(22), 4855-4866 (2000).
- Liem, K. J., Tremml, G. & Jessell, T. A Role for the Roof Plate and Its Resident Tgfbeta-Related Proteins in Neuronal Patterning in the Dorsal Spinal Cord. *Cell* 91(1), 127-138 (1997).
- Lim, U. M., Sidhu, K. & Tuch, B. Derivation of Motor Neurons From Three Clonal Human Embryonic Stem Cell Lines. *Curr Neurovasc Res* 3(4), 281-288 (2006).
- Lindvall, O. & Hagell, P. Role of Cell Therapy in Parkinson Disease. *Neurosurg Focus* 13(5), e2 (2002).
- Lin, W., Metzakopian, E., Mavromatakis, Y., Gao, N., Balaskas, N., Sasaki, H., Briscoe, J., Whitsett, J., Goulding, M., Kaestner, K. *et al.* Foxa1 and Foxa2 Function Both Upstream of and Cooperatively With Lmx1A and Lmx1B in a Feedforward Loop Promoting Mesodiencephalic Dopaminergic Neuron Development. *Dev Biol* 333(2), 386-396 (2009).
- Liu, Y., Helms, A. & Johnson, J. Distinct Activities of Msx1 and Msx3 in Dorsal Neural Tube Development. *Development* 131(5), 1017-1028 (2004).
- Lipinski, R., Cook, C., Barnett, D., Gipp, J., Peterson, R. & Bushman, W. Sonic Hedgehog Signaling Regulates the Expression of Insulin-Like Growth Factor Binding Protein-6 During Fetal Prostate Development. *Dev Dyn* 233(3), 829-836 (2005).
- Litingtung, Y. & Chiang, C. Specification of ventral neuron types is mediated by an antagonistic interaction between Shh and Gli3. *Nat Neurosci* 3(10):979-85(2000).
- Loh, Y. H., Wu, Q., Chew, J., Vega, V., Zhang, W., Chen, X., Bourque, G., George, J., Leong, B., Liu, J. *et al.* The Oct4 and Nanog Transcription Network Regulates Pluripotency in Mouse Embryonic Stem Cells. *Nat Genet* 38(4), 431-440 (2006).

- Lothian, C. & Lendahl, U. An Evolutionarily Conserved Region in the Second Intron of the Human Nestin Gene Directs Gene Expression to Cns Progenitor Cells and to Early Neural Crest Cells. *Eur J Neurosci* 9(3), 452-462 (1997).
- Lu, Q., Cai, L., Rowitch, D., Cepko, C. & Stiles, C. Ectopic Expression of Olig1 Promotes Oligodendrocyte Formation and Reduces Neuronal Survival in Developing Mouse Cortex. *Nat Neurosci* 4(10), 973-974 (2001).
- Lu, Q., Yuk, D., Alberta, J., Zhu, Z., Pawlitzky, I., Chan, J., McMahon, A., Stiles, C. & Rowitch, D. Sonic Hedgehog--Regulated Oligodendrocyte Lineage Genes Encoding Bhlh Proteins in the Mammalian Central Nervous System. *Neuron* 25(2), 317-329 (2000).
- Lupo, G., Harris, W. & Lewis, K. Mechanisms of Ventral Patterning in the Vertebrate Nervous System. *Nat Rev Neurosci* 7(2), 103-114 (2006).
- Ma, Y., Erkner, A., Gong, R., Yao, S., Taipale, J., Basler, K. & Beachy, P. Hedgehog-Mediated Patterning of the Mammalian Embryo Requires Transporter-Like Function of Dispatched. *Cell* 111(1), 63-75 (2002).
- Machold, R., Hayashi, S., Rutlin, M., Muzumdar, M., Nery, S., Corbin, J., Gritli-Linde, A., Dellovade, T., Porter, J., Rubin, L. *et al.* Sonic Hedgehog is Required for Progenitor Cell Maintenance in Telencephalic Stem Cell Niches. *Neuron* 39(6), 937-950 (2003).
- Madison, B., Mckenna, L., Dolson, D., Epstein, D. & Kaestner, K. Foxf1 and Foxl1 Link Hedgehog Signaling and the Control of Epithelial Proliferation in the Developing Stomach and Intestine. *J Biol Chem* 284(9), 5936-5944 (2009).
- Maherali, N. & Hochedlinger, K. Guidelines and Techniques for the Generation of Induced Pluripotent Stem Cells. *Stem Cell* 3(6), 595-605 (2008).
- Mahlapu, M., Enerback, S. & Carlsson, P. Haploinsufficiency of the Forkhead Gene Foxf1, a Target for Sonic Hedgehog Signaling, Causes Lung and Foregut Malformations. *Development* 128(12), 2397-2406 (2001).
- Mansouri, A. & Gruss, P. Pax3 and Pax7 Are Expressed in Commissural Neurons and Restrict Ventral Neuronal Identity in the Spinal Cord. *Mech Dev* 78(1-2), 171-178 (1998).
- Marson, A., Foreman, R., Chevalier, B., Bilodeau, S., Kahn, M., Young, R. & Jaenisch, R. Wnt Signaling Promotes Reprogramming of Somatic Cells to Pluripotency. *Cell Stem Cell* 3(2), 132-135 (2008).
- Marti, E., Takada, R., Bumcrot, D., Sasaki, H. & McMahon, A. Distribution of Sonic Hedgehog Peptides in the Developing Chick and Mouse Embryo. *Development* 121(8), 2537-2547 (1995).
- Martin, D., Skidmore, J., Philips, S. T., Vieira, C., Gage, P., Condie, B., Raphael, Y., Martinez, S. & Camper, S. Pitx2 is Required for Normal Development of Neurons in the Mouse Subthalamic Nucleus and Midbrain. *Dev Biol* 267(1), 93-108 (2004).
- Martinelli, D. & Fan, C. M. Gas1 Extends the Range of Hedgehog Action By Facilitating Its Signaling. *Genes Dev* 21(10), 1231-1243 (2007).
- Mathur, D., Danford, T., Boyer, L., Young, R., Gifford, D. & Jaenisch, R. Analysis of the Mouse Embryonic Stem Cell Regulatory Networks Obtained By Chip-Chip and Chip-Pet. *Genome Biol* 9(8), R126 (2008).
- Maye, P., Becker, S., Siemen, H., Thorne, J., Byrd, N., Carpentino, J. & Grabel, L. Hedgehog Signaling is Required for the Differentiation of Es Cells Into Neurectoderm. *Dev Biol* 265(1), 276-290 (2004).
- Migdal, M., Huppertz, B., Tessler, S., Comforti, A., Shibuya, M., Reich, R., Baumann, H. & Neufeld, G. Neuropilin-1 is a Placenta Growth Factor-2 Receptor. *J Biol Chem* 273(35), 22272-22278 (1998).

- Ming, J., Kaupas, M., Roessler, E., Brunner, H., Golabi, M., Tekin, M., Stratton, R., Sujansky, E., Bale, S. & Muenke, M. Mutations in Patched-1, the Receptor for Sonic Hedgehog, Are Associated With Holoprosencephaly. *Hum Genet* 110(4), 297-301 (2002).
- Ming, J. & Muenke, M. Holoprosencephaly: From Homer to Hedgehog. *Clin Genet* 53(3), 155-163 (1998).
- Mitsui, K., Tokuzawa, Y., Itoh, H., Segawa, K., Murakami, M., Takahashi, K., Maruyama, M., Maeda, M. & Yamanaka, S. The Homeoprotein Nanog is Required for Maintenance of Pluripotency in Mouse Epiblast and Es Cells. *Cell* 113(5), 631-642 (2003).
- Mizuseki, K., Sakamoto, T., Watanabe, K., Muguruma, K., Ikeya, M., Nishiyama, A., Arakawa, A., Suemori, H., Nakatsuji, N., Kawasaki, H. *et al.* Generation of Neural Crest-Derived Peripheral Neurons and Floor Plate Cells From Mouse and Primate Embryonic Stem Cells. *Proc Natl Acad Sci U S A* 100(10), 5828-5833 (2003).
- Mullor, J., Sanchez, P. & Ruiz I Altaba, A. Pathways and Consequences: Hedgehog Signaling in Human Disease. *Trends Cell Biol* 12(12), 562-569 (2002).
- Munoz-Sanjuan, I. & Brivanlou, A. Neural Induction, the Default Model and Embryonic Stem Cells. *Nat Rev Neurosci* 3(4), 271-280 (2002).
- Nichols, J., Zevnik, B., Anastasiadis, K., Niwa, H., Klewe-Nebenius, D., Chambers, I., Scholer, H. & Smith, A. Formation of Pluripotent Stem Cells in the Mammalian Embryo Depends on the Pou Transcription Factor Oct4. *Cell* 95(3), 379-391 (1998).
- Niwa, H., Miyazaki, J. & Smith, A. Quantitative Expression of Oct-3/4 Defines Differentiation, Dedifferentiation Or Self-Renewal of Es Cells. *Nat Genet* 24(4), 372-376 (2000).
- Noggle, S., Weiler, D. & Condie, B. Notch Signaling is Inactive But Inducible in Human Embryonic Stem Cells. *Stem Cells* 24(7), 1646-1653 (2006).
- Northcott, P., Fernandez-L, A., Hagan, J., Ellison, D. W., Grajkowska, W., Gillespie, Y., Grundy, R., Van Meter, T., Rutka, J., Croce, C. *et al.* The Mir-17/92 Polycistron is Up-Regulated in Sonic Hedgehog-Driven Medulloblastomas and Induced By N-Myc in Sonic Hedgehog-Treated Cerebellar Neural Precursors. *Cancer Res* 69(8), 3249-3255 (2009).
- Nusslein-Volhard, C. & Wieschaus, E. Mutations Affecting Segment Number and Polarity in Drosophila. *Nature* 287(5785), 795-801 (1980).
- Obayashi, S., Tabunoki, H., Kim, S. U. & Satoh, J. Gene Expression Profiling of Human Neural Progenitor Cells Following the Serum-Induced Astrocyte Differentiation. *Cell Mol Neurobiol* 29(3), 423-438 (2009).
- Ohtsuka, T., Sakamoto, M., Guillemot, F. & Kageyama, R. Roles of the Basic Helix-Loop-Helix Genes Hes1 and Hes5 in Expansion of Neural Stem Cells of the Developing Brain. *J Biol Chem* 276(32), 30467-30474 (2001).
- Okada, Y., Shimazaki, T., Sobue, G. & Okano, H. Retinoic-Acid-Concentration-Dependent Acquisition of Neural Cell Identity During in Vitro Differentiation of Mouse Embryonic Stem Cells. *Dev Biol* 275(1), 124-142 (2004).
- Olanow, C., Kordower, J., Lang, A. & Obeso, J. Dopaminergic Transplantation for Parkinson's Disease: Current Status and Future Prospects. *Ann Neurol* 66(5), 591-596 (2009).
- Oliver, T., Grasfeder, L., Carroll, A., Kaiser, C., Gillingham, C., Lin, S. M., Wickramasinghe, R., Scott, M. & Wechsler-Reya, R. J. Transcriptional Profiling of the Sonic Hedgehog Response: A Critical Role for N-Myc in Proliferation of Neuronal Precursors. *Proc Natl Acad Sci U S A* 100(12), 7331-7336 (2003).
- Ono, Y., Nakatani, T., Sakamoto, Y., Mizuhara, E., Minaki, Y., Kumai, M., Hamaguchi, A., Nishimura, M., Inoue, Y., Hayashi, H. *et al.* Differences in Neurogenic Potential in Floor

- Plate Cells Along an Anteroposterior Location: Midbrain Dopaminergic Neurons Originate From Mesencephalic Floor Plate Cells. *Development* 134(17), 3213-3225 (2007).
- Palma, V., Lim, D. A., Dahmane, N., Sanchez, P., Brionne, T., Herzberg, C., Gitton, Y., Carleton, A., Alvarez-Buylla, A. & Ruiz I Altaba, A. Sonic Hedgehog Controls Stem Cell Behavior in the Postnatal and Adult Brain. *Development* 132(2), 335-344 (2005).
- Pan, Y., Bai, C. B., Joyner, A. & Wang, B. Sonic Hedgehog Signaling Regulates Gli2 Transcriptional Activity By Suppressing Its Processing and Degradation. *Mol Cell Biol* 26(9), 3365-3377 (2006).
- Pan, Y. & Wang, B. A Novel Protein-Processing Domain in Gli2 and Gli3 Differentially Blocks Complete Protein Degradation By the Proteasome. *J Biol Chem* 282(15), 10846-10852 (2007).
- Pankratz, M., Li, X., Lavaute, T., Lyons, E., Chen, X. & Zhang, S. Directed Neural Differentiation of HESCs Via an Obligated Primitive Anterior Stage. *Stem Cells* 25(6), 2006 (2007).
- Park, C., Minn, Y. K., Lee, J. & Choi, D. H. In Vitro and in Vivo Analyses of Human Embryonic Stem Cell-Derived Dopamine Neurons. *J Neurochem* 92(5), 1265-76 (2005).
- Park, H. L., Bai, C., Platt, K. A. & Matise, M. P. Mouse Gli1 Mutants Are Viable But Have Defects in Shh Signaling in Combination With a Gli2 mutation. *Development* 127(8):1593-605 (2000).
- Park, S., Lee, K. S., Lee, Y. J., Shin, H., Cho, H. Y., Wang, K., Kim, Y. S., Lee, H. T., Chung, K., Kim, E. Y. *et al.* Generation of Dopaminergic Neurons in Vitro From Human Embryonic Stem Cells Treated With Neurotrophic Factors. *Neurosci Lett* 359(1-2), 99-103 (2004).
- Pathi, S., Pagan-Westphal, S., Baker, D., Garber, E., Rayhorn, P., Bumcrot, D., Tabin, C., Blake Pepinsky, R. & Williams, K. Comparative Biological Responses to Human Sonic, Indian, and Desert Hedgehog. *Mech Dev* 106(1-2), 107-117 (2001).
- Pebay, A., Wong, R., Pitson, S., Wolvetang, E., Peh, G. S., Filipczyk, A., Koh, K. L., Tellis, I., Nguyen, L. & Pera, M. Essential Roles of Sphingosine-1-Phosphate and Platelet-Derived Growth Factor in the Maintenance of Human Embryonic Stem Cells. *Stem Cells* 23(10), 1541-1548 (2005).
- Peddada, S., Yasui, D. & Lasalle, J. Inhibitors of Differentiation (Id1, Id2, Id3 and Id4) Genes Are Neuronal Targets of Mecp2 That Are Elevated in Rett Syndrome. *Hum Mol Genet* 15(12), 2003-2014 (2006).
- Peh, G. S., Lang, R., Pera, M. & Hawes, S. Cd133 Expression By Neural Progenitors Derived From Human Embryonic Stem Cells and Its Use for Their Prospective Isolation. *Stem Cells Dev* 18(2), 269-282 (2009).
- Pera, M., Andrade, J., Houssami, S., Reubinoff, B., Trounson, A., Stanley, E., Ward-Van Oostwaard, D. & Mummery, C. Regulation of Human Embryonic Stem Cell Differentiation By Bmp-2 and Its Antagonist Noggin. *J Cell Sci* 117(Pt 7), 1269-1280 (2004).
- Perrier, A., Tabar, V., Barberi, T., Rubio, M., Bruses, J., Topf, N., Harrison, N. & Studer, L. Derivation of Midbrain Dopamine Neurons From Human Embryonic Stem Cells. *Proc Natl Acad Sci U S A* 101(34), 12543-12548 (2004).
- Pevny, L., Sockanathan, S., Placzek, M. & Lovell-Badge, R. A Role for Sox1 in Neural Determination. *Development* 125(10), 1967-1978 (1998).
- Placantonakis, D., Tomishima, M., Lafaille, F., Desbordes, S., Jia, F., Socci, N., Viale, A., Lee, H., Harrison, N., Tabar, V. *et al.* Bac Transgenesis in Human Embryonic Stem Cells as a Novel Tool to Define the Human Neural Lineage. *Stem Cells* 27(3), 521-532 (2009).

- Pomp, O., Brokhman, I., Ben-Dor, I., Reubinoff, B. & Goldstein, R. Generation of Peripheral Sensory and Sympathetic Neurons and Neural Crest Cells From Human Embryonic Stem Cells. *Stem Cells* 23(7), 923-930 (2005).
- Pons, S., Trejo, J., Martinez-Morales, J. R. & Marti, E. Vitronectin Regulates Sonic Hedgehog Activity During Cerebellum Development Through Creb Phosphorylation. *Development* 128(9), 1481-1492 (2001).
- Porter, J., Young, K. & Beachy, P. Cholesterol Modification of Hedgehog Signaling Proteins in Animal Development. *Science* 274(5285), 255-259 (1996).
- Poulain, F., Chauvin, S., Wehrle, R., Desclaux, M., Mallet, J., Vodjdani, G., Dusart, I. & Sobel, A. Scip is Crucial for the Formation and Development of the Purkinje Cell Dendritic Arbor. *J Neurosci* 28(29), 7387-7398 (2008).
- Pruszak, J., Sonntag, K., Aung, M., Sanchez-Pernaute, R. & Isacson, O. Markers and Methods for Cell Sorting of Human Embryonic Stem Cell-Derived Neural Cell Populations. *Stem Cells* 25(9), 2257-2268 (2007).
- Pyle, A., Lock, L. & Donovan, P. Neurotrophins Mediate Human Embryonic Stem Cell Survival. *Nat Biotechnol* 24(3), 344-350 (2006).
- Rahnama, F., Toftgard, R. & Zaphiropoulos, P. Distinct Roles of Ptch2 Splice Variants in Hedgehog Signalling. *Biochem J* 378(Pt 2), 325-334 (2004).
- Ramos, C. & Robert, B. Msh/Msx Gene Family in Neural Development. *Trends Genet* 21(11), 624-632 (2005).
- Raynal, J., Dugast, C., Le Van Thai, A. & Weber, M. Winged Helix Hepatocyte Nuclear Factor 3 and Pou-Domain Protein Brn-2/N-Oct-3 Bind Overlapping Sites on the Neuronal Promoter of Human Aromatic L-Amino Acid Decarboxylase Gene. *Brain Res Mol Brain Res* 56(1-2), 227-237 (1998).
- Reubinoff, B., Itsykson, P., Turetsky, T., Pera, M., Reinhartz, E., Itzik, A. & Ben-Hur, T. Neural Progenitors From Human Embryonic Stem Cells. *Nat Biotechnol* 19(12), 1134-1140 (2001).
- Reubinoff, B., Pera, M., Fong, C., Trounson, A. & Bongso, A. Embryonic Stem Cell Lines From Human Blastocysts: Somatic Differentiation in Vitro. *Nat Biotechnol* 18(4), 399-404 (2000).
- Rho, J. Y., Yu, K., Han, J. S., Chae, J., Koo, D. B., Yoon, H., Moon, S., Lee, K. K. & Han, Y. M. Transcriptional Profiling of the Developmentally Important Signalling Pathways in Human Embryonic Stem Cells. *Hum Reprod* 21(2), 405-412 (2006).
- Richards, M., Tan, S., Fong, C., Biswas, A., Chan, W. & Bongso, A. Comparative Evaluation of Various Human Feeders for Prolonged Undifferentiated Growth of Human Embryonic Stem Cells. *Stem Cells* 21(5), 546-556 (2003).
- Roelink, H., Augsburger, A., Heemskerk, J., Korzh, V., Norlin, S., Ruiz I Altaba, A., Tanabe, Y., Placzek, M., Edlund, T., Jessell, T. *et al.* Floor Plate and Motor Neuron Induction By Vhh-1, a Vertebrate Homolog of Hedgehog Expressed By the Notochord. *Cell* 76(4), 761-775 (1994).
- Roelink, H., Porter, J., Chiang, C., Tanabe, Y., Chang, D., Beachy, P. & Jessell, T. Floor Plate and Motor Neuron Induction By Different Concentrations of the Amino-Terminal Cleavage Product of Sonic Hedgehog Autoproteolysis. *Cell* 81(3), 445-455 (1995).
- Roessler, E., Belloni, E., Gaudenz, K., Jay, P., Berta, P., Scherer, S., Tsui, L. & Muenke, M. Mutations in the Human Sonic Hedgehog Gene Cause Holoprosencephaly. *Nat Genet* 14(3), 357-360 (1996).

- Roessler, E., Du, Y., Mullor, J., Casas, E., Allen, W., Gillessen-Kaesbach, G., Roeder, E., Ming, J., Ruiz I Altaba, A. & Muenke, M. Loss-of-Function Mutations in the Human Gli2 Gene Are Associated With Pituitary Anomalies and Holoprosencephaly-Like Features. *Proc Natl Acad Sci U S A* 100(23), 13424-13429 (2003).
- Rohatgi, R., Milenkovic, L. & Scott, M. Patched1 Regulates Hedgehog Signaling At the Primary Cilium. *Science* 317(5836), 372-376 (2007).
- Romer, J., Kimura, H., Magdaleno, S., Sasai, K., Fuller, C., Baines, H., Connelly, M., Stewart, C., Gould, S., Rubin, L. *et al.* Suppression of the Shh Pathway Using a Small Molecule Inhibitor Eliminates Medulloblastoma in Ptc1(+/-)P53(-/-) Mice. *Cancer Cell* 6(3), 229-240 (2004).
- Roussa, E., Farkas, L. & Kriegstein, K. Tgf-Beta Promotes Survival on Mesencephalic Dopaminergic Neurons in Cooperation With Shh and Fgf-8. *Neurobiol Dis* 16(2), 300-310 (2004).
- Ruiz De Almodovar, C., Lambrechts, D., Mazzone, M. & Carmeliet, P. Role and Therapeutic Potential of Vegf in the Nervous System. *Physiol Rev* 89(2), 607-648 (2009).
- Ruiz I Altaba, A. Gli Proteins Encode Context-Dependent Positive and Negative Functions: Implications for Development and Disease. *Development* 126(14), 3205-3216 (1999).
- Ryan, A., Blumberg, B., Rodriguez-Esteban, C., Yonei-Tamura, S., Tamura, K., Tsukui, T., De La Pena, J., Sabbagh, W., Greenwald, J., Choe, S. *et al.* Pitx2 Determines Left-Right Asymmetry of Internal Organs in Vertebrates. *Nature* 394(6693), 545-551 (1998).
- Sacchetti, P., Sousa, K., Hall, A., Liste, I., Steffensen, K., Theofilopoulos, S., Parish, C., Hazenberg, C., Richter, L., Hovatta, O. *et al.* Liver X Receptors and Oxysterols Promote Ventral Midbrain Neurogenesis in Vivo and in Human Embryonic Stem Cells. *Cell Stem Cell* 5(4), 409-419 (2009).
- Saito, H., Komada, M., Suzuki, M., Nakayama, R., Motoyama, J., Shiota, K. & Ishibashi, M. Expression of the Mouse Fgf15 Gene is Directly Initiated By Sonic Hedgehog Signaling in the Diencephalon and Midbrain. *Dev Dyn* 232(2), 282-292 (2005).
- Sakamoto, M., Hirata, H., Ohtsuka, T., Bessho, Y. & Kageyama, R. The Basic Helix-Loop-Helix Genes Hesr1/Hey1 and Hesr2/Hey2 Regulate Maintenance of Neural Precursor Cells in the Brain. *J Biol Chem* 278(45), 44808-44815 (2003).
- Sander, M., Paydar, S., Ericson, J., Briscoe, J., Berber, E., German, M., Jessell, T. & Rubenstein, J. Ventral Neural Patterning By Nkx Homeobox Genes: Nkx6.1 Controls Somatic Motor Neuron and Ventral Interneuron Fates. *Genes Dev* 14(17), 2134-2139 (2000).
- Santagati F, A. K., Schmidt V, Schmitt-John T, Suzuki M, Yamamura K, Imai K. Identification of Cis-Regulatory Elements in the Mouse Pax9/Nkx2-9 Genomic Region: Implication for Evolutionary Conserved Synteny. *Genetics* 165(1), 235-42
- Sasaki, H., Hui, C., Nakafuku, M. & Kondoh, H. A Binding Site for Gli Proteins is Essential for Hnf-3beta Floor Plate Enhancer Activity in Transgenics and Can Respond to Shh in Vitro. *Development* 124(7), 1313-1322 (1997).
- Sasaki, H., Nishizaki, Y., Hui, C., Nakafuku, M. & Kondoh, H. Regulation of Gli2 and Gli3 Activities By an Amino-Terminal Repression Domain: Implication of Gli2 and Gli3 as Primary Mediators of Shh Signaling. *Development* 126(17), 3915-3924 (1999).
- Sato, N., Meijer, L., Skaltsounis, L., Greengard, P. & Brivanlou, A. Maintenance of Pluripotency in Human and Mouse Embryonic Stem Cells Through Activation of Wnt Signaling By a Pharmacological Gsk-3-Specific Inhibitor. *Nat Med* 10(1), 55-63 (2004).

- Schell-Apacik, C., Rivero, M., Knepper, J., Roessler, E., Muenke, M. & Ming, J. Sonic Hedgehog Mutations Causing Human Holoprosencephaly Impair Neural Patterning Activity. *Hum Genet* 113(2), 170-177 (2003).
- Sharp, J., Frame, J., Siegenthaler, M., Nistor, G. & Keirstead, H. S. Human Embryonic Stem Cell-Derived Oligodendrocyte Progenitor Cell Transplants Improve Recovery After Cervical Spinal Cord Injury. *Stem Cells* 28(1), 152-163 (2010).
- Sheng, T., Chi, S., Zhang, X. & Xie, J. Regulation of Gli1 Localization By the Camp/Protein Kinase a Signaling Axis Through a Site Near the Nuclear Localization Signal. *J Biol Chem* 281(1), 9-12 (2006).
- Shin, S., Mitalipova, M., Noggle, S., Tibbitts, D., Venable, A., Rao, R. & Stice, S. Long-Term Proliferation of Human Embryonic Stem Cell-Derived Neuroepithelial Cells Using Defined Adherent Culture Conditions. *Stem Cells* 24(1), 125-138 (2006).
- Simpson, F., Kerr, M. & Wicking, C. Trafficking, Development and Hedgehog. *Mech Dev* 126(5-6), 279-288 (2009).
- Singh, S., Tokhunts, R., Baubet, V., Goetz, J., Huang, Z., Schilling, N., Black, K., Mackenzie, T., Dahmane, N. & Robbins, D. Sonic Hedgehog Mutations Identified in Holoprosencephaly Patients Can Act in a Dominant Negative Manner. *Hum Genet* 125(1), 95-103 (2009).
- Skidmore, J., Cramer, J., Martin, J. & Martin, D. Cre Fate Mapping Reveals Lineage Specific Defects in Neuronal Migration With Loss of Pitx2 Function in the Developing Mouse Hypothalamus and Subthalamic Nucleus. *Mol Cell Neurosci* 37(4), 696-707 (2008).
- Smidt, M. & Burbach, J. How to Make a Mesodiencephalic Dopaminergic Neuron. *Nat Rev Neurosci* 8(1), 21-32 (2007).
- Smyth, G. Limma: Linear Models for Microarray Data. *Bioinformatics and computational biology solutions using R and bioconductor. New York: Springer* 397-420 (2005).
- Sondell, M., Lundborg, G. & Kanje, M. Vascular Endothelial Growth Factor Has Neurotrophic Activity and Stimulates Axonal Outgrowth, Enhancing Cell Survival and Schwann Cell Proliferation in the Peripheral Nervous System. *J Neurosci* 19(14), 5731-5740 (1999).
- Sondell, M., Sundler, F. & Kanje, M. Vascular Endothelial Growth Factor is a Neurotrophic Factor Which Stimulates Axonal Outgrowth Through the Flk-1 Receptor. *Eur J Neurosci* 12(12), 4243-4254 (2000).
- Sonntag, K., Pruszak, J., Yoshizaki, T., Van Arensbergen, J., Sanchez-Pernaute, R. & Isacson, O. Enhanced Yield of Neuroepithelial Precursors and Midbrain-Like Dopaminergic Neurons From Human Embryonic Stem Cells Using the Bone Morphogenic Protein Antagonist Noggin. *Stem Cells* 25(2), 411-418 (2007).
- Sonntag, K., Simantov, R., Kim, K. S. & Isacson, O. Temporally Induced Nurr1 Can Induce a Non-Neuronal Dopaminergic Cell Type in Embryonic Stem Cell Differentiation. *Eur J Neurosci* 19(5), 1141-1152 (2004).
- Soundararajan, P., Lindsey, B., Leopold, C. & Rafuse, V. Easy and Rapid Differentiation of Embryonic Stem Cells Into Functional Motoneurons Using Sonic Hedgehog-Producing Cells. *Stem Cells* 25(7), 1697-1706 (2007).
- Stone, D., Murone, M., Luoh, S., Ye, W., Armanini, M., Gurney, A., Phillips, H., Brush, J., Goddard, A., De Sauvage, F. J. *et al.* Characterization of the Human Suppressor of Fused, a Negative Regulator of the Zinc-Finger Transcription Factor Gli. *J Cell Sci* 112 (Pt 23), 4437-4448 (1999).

- Suter, D., Tirefort, D., Julien, S. & Krause, K. A Sox1 to Pax6 Switch Drives Neuroectoderm to Radial Glia Progression During Differentiation of Mouse Embryonic Stem Cells. *Stem Cells* 27(1), 49-58 (2009).
- Tabar, V., Panagiotakos, G., Greenberg, E., Chan, B., Sadelain, M., Gutin, P. & Studer, L. Migration and Differentiation of Neural Precursors Derived From Human Embryonic Stem Cells in the Rat Brain. *Nat Biotechnol* 23(5), 601-606 (2005).
- Taipale, J., Chen, J., Cooper, M., Wang, B., Mann, R., Milenkovic, L., Scott, M. & Beachy, P. Effects of Oncogenic Mutations in Smoothed and Patched Can be Reversed By Cyclopamine. *Nature* 406(6799), 1005-1009 (2000).
- Takagi, Y., Takahashi, J., Saiki, H., Morizane, A., Hayashi, T., Kishi, Y., Fukuda, H., Okamoto, Y., Koyanagi, M., Ideguchi, M. *et al.* Dopaminergic Neurons Generated From Monkey Embryonic Stem Cells Function in a Parkinson Primate Model. *J Clin Invest* 115(1), 102-109 (2005).
- Takahashi, K., Tanabe, K., Ohnuki, M., Narita, M., Ichisaka, T., Tomoda, K. & Yamanaka, S. Induction of Pluripotent Stem Cells From Adult Human Fibroblasts By Defined Factors. *Cell* 131(5), 861-872 (2007).
- Takahashi, K. & Yamanaka, S. Induction of Pluripotent Stem Cells From Mouse Embryonic and Adult Fibroblast Cultures By Defined Factors. *Cell* 126(4), 663-676 (2006).
- Tan, Y., Xie, Z., Ding, M., Wang, Z., Yu, Q., Meng, L., Zhu, H., Huang, X., Yu, L., Meng, X. *et al.* Increased Levels of Foxal Transcription Factor in Pluripotent P19 Embryonal Carcinoma Cells Stimulate Neural Differentiation. *Stem Cells Dev* (2009).
- Tanaka, S., Kamachi, Y., Tanouchi, A., Hamada, H., Jing, N. & Kondoh, H. Interplay of Sox and Pou Factors in Regulation of the Nestin Gene in Neural Primordial Cells. *Mol Cell Biol* 24(20), 8834-8846 (2004).
- Tenzen, T., Allen, B., Cole, F., Kang, J., Krauss, R. & McMahon, A. The Cell Surface Membrane Proteins Cdo and Boc Are Components and Targets of the Hedgehog Signaling Pathway and Feedback Network in Mice. *Dev Cell* 10(5), 647-656 (2006).
- Tesar, P., Chenoweth, J., Brook, F., Davies, T., Evans, E., Mack, D., Gardner, R. & McKay, R. New Cell Lines From Mouse Epiblast Share Defining Features With Human Embryonic Stem Cells. *Nature* 448(7150), 196-199 (2007).
- Tessier-Lavigne, M. & Goodman, C. The Molecular Biology of Axon Guidance. *Science* 274(5290), 1123 (1996).
- Thomson, J., Itskovitz-Eldor, J., Shapiro, S. S., Waknitz, M., Swiergiel, J., Marshall, V. & Jones, J. Embryonic Stem Cell Lines Derived From Human Blastocysts. *Science* 282(5391), 1145-1147 (1998).
- Uchida, N., Buck, D., He, D., Reitsma, M., Masek, M., Phan, T., Tsukamoto, A., Gage, F. & Weissman, I. Direct Isolation of Human Central Nervous System Stem Cells. *Proc Natl Acad Sci U S A* 97(26), 14720-14725 (2000).
- Uziel, T., Karginov, F., Xie, S., Parker, J., Wang, Y., Gajjar, A., He, L., Ellison, D., Gilbertson, R., Hannon, G. *et al.* The Mir-17~92 Cluster Collaborates With the Sonic Hedgehog Pathway in Medulloblastoma. *Proc Natl Acad Sci U S A* 106(8), 2812-2817 (2009).
- Vallier, L., Alexander, M. & Pedersen, R. Activin/Nodal and Fgf Pathways Cooperate to Maintain Pluripotency of Human Embryonic Stem Cells. *J Cell Sci* 118(Pt 19), 4495-4509 (2005).

- Vallier, L., Mendjan, S., Brown, S., Chng, Z., Teo, A., Smithers, L., Trotter, M., Cho, C. H., Martinez, A., Rugg-Gunn, P. *et al.* Activin/Nodal Signalling Maintains Pluripotency By Controlling Nanog Expression. *Development* 136(8), 1339-1349 (2009).
- Vallier, L., Reynolds, D. & Pedersen, R. Nodal Inhibits Differentiation of Human Embryonic Stem Cells Along the Neuroectodermal Default Pathway. *Dev Biol* 275(2), 403-421 (2004).
- Varjosalo, M. & Taipale, J. Hedgehog: Functions and Mechanisms. *Genes Dev* 22(18), 2454-2472 (2008).
- Vazin, T., Becker, K., Chen, J., Spivak, C., Lupica, C., Zhang, Y., Worden, L. & Freed, W. A Novel Combination of Factors, Termed Spie, Which Promotes Dopaminergic Neuron Differentiation From Human Embryonic Stem Cells. *PLoS One* 4(8), e6606 (2009).
- Vazin, T., Chen, J., Lee, C. T., Amable, R. & Freed, W. Assessment of Stromal-Derived Inducing Activity in the Generation of Dopaminergic Neurons From Human Embryonic Stem Cells. *Stem Cells* 26(6), 1517-1525 (2008).
- Vokes, S., Ji, H., Mccuine, S., Tenzen, T., Giles, S., Zhong, S., Longabaugh, W., Davidson, E., Wong, W. & McMahon, A. Genomic Characterization of Gli-Activator Targets in Sonic Hedgehog-Mediated Neural Patterning. *Development* 134(10), 1977-1989 (2007).
- Wall, D., Mears, A., Mcneill, B., Mazerolle, C., Thurig, S., Wang, Y., Kageyama, R. & Wallace, V. Progenitor Cell Proliferation in the Retina is Dependent on Notch-Independent Sonic Hedgehog/Hes1 Activity. *J Cell Biol* 184(1), 101-112 (2009).
- Wang, B. & Li, Y. Evidence for the Direct Involvement of β Trcp in Gli3 Protein Processing. *Proc Natl Acad Sci U S A* 103(1), 33-38 (2006).
- Wang, B., Fallon, J. F. & Beachy, P. A. Hedgehog-Regulated Processing of Gli3 Produces an Anterior/Posterior Repressor Gradient in the Developing Vertebrate Limb. *Cell* 100(4), 423-434 (2000). Wang, Y., Zhou, Z., Walsh, C. & McMahon, A. Selective Translocation of Intracellular Smoothed to the Primary Cilium in Response to Hedgehog Pathway Modulation. *Proc Natl Acad Sci U S A* 106(8), 2623-2628 (2009).
- Watanabe, Y., Duprez, D., Monsoro-Burq, A. H., Vincent, C. & Le Douarin, N. M. Two Domains in Vertebral Development: Antagonistic Regulation By Shh and Bmp4 Proteins. *Development* 125(14), 2631-2639 (1998).
- Wechsler-Reya, R. J. & Scott, M. Control of Neuronal Precursor Proliferation in the Cerebellum By Sonic Hedgehog. *Neuron* 22(1), 103-114 (1999).
- Wei, C. L., Miura, T., Robson, P., Lim, S. K., Xu, X., Lee, M. Y., Gupta, S., Stanton, L., Luo, Y., Schmitt, J. *et al.* Transcriptome Profiling of Human and Murine ESCs Identifies Divergent Paths Required to Maintain the Stem Cell State. *Stem Cells* 23(2), 166-185 (2005).
- Wernig, M., Zhao, J., Pruszak, J., Hedlund, E., Fu, D., Soldner, F., Broccoli, V., Constantine-Paton, M., Isacson, O. & Jaenisch, R. Neurons Derived From Reprogrammed Fibroblasts Functionally Integrate Into the Fetal Brain and Improve Symptoms of Rats With Parkinson's Disease. *Proc Natl Acad Sci U S A* 105(15), 5856-5861 (2008).
- Whitfield, J. The Neuronal Primary Cilium--an Extrasynaptic Signaling Device. *Cell Signal* 16(7), 763-767 (2004).
- Wichterle, H., Lieberam, I., Porter, J. & Jessell, T. Directed Differentiation of Embryonic Stem Cells Into Motor Neurons. *Cell* 110(3), 385-397 (2002).
- Wijgerde, M., McMahon, J., Rule, M. & McMahon, A. A Direct Requirement for Hedgehog Signaling for Normal Specification of All Ventral Progenitor Domains in the Presumptive Mammalian Spinal Cord. *Genes Dev* 16(22), 2849-2864 (2002).
- Wilson, P. & Stice, S. Development and Differentiation of Neural Rosettes Derived From Human Embryonic Stem Cells. *Stem Cell Rev* 2(1), 67-77 (2006).

- Woo, S. M., Kim, J., Han, H. W., Chae, J., Son, M. Y., Cho, S., Chung, H., Han, Y. M. & Kang, Y. Notch Signaling is Required for Maintaining Stem-Cell Features of Neuroprogenitor Cells Derived From Human Embryonic Stem Cells. *BMC Neurosci* 10, 97 (2009).
- Wood, H. & Episkopou, V. Comparative Expression of the Mouse Sox1, Sox2 and Sox3 Genes From Pre-Gastrulation to Early Somite Stages. *Mech Dev* 86(1-2), 197-201 (1999).
- Wu, H., Xu, J., Pang, Z., Ge, W., Kim, K. J., Bianchi, B., Chen, C., Sudhof, T. & Sun, Y. E. Integrative Genomic and Functional Analyses Reveal Neuronal Subtype Differentiation Bias in Human Embryonic Stem Cell Lines. *Proc Natl Acad Sci U S A* 104(34), 13821-13826 (2007).
- Xiao, L., Yuan, X. & Sharkis, S. Activin a Maintains Self-Renewal and Regulates Fibroblast Growth Factor, Wnt, and Bone Morphogenic Protein Pathways in Human Embryonic Stem Cells. *Stem Cells* 24(6), 1476-1486 (2006).
- Xu, C., Rosler, E., Jiang, J., Lebkowski, J., Gold, J., O'Sullivan, C., Delavan-Boorsma, K., Mok, M., Bronstein, A. & Carpenter, M. Basic Fibroblast Growth Factor Supports Undifferentiated Human Embryonic Stem Cell Growth Without Conditioned Medium. *Stem Cells* 23(3), 315-323 (2005).
- Xu, C., Inokuma, M. S., Denham, J., Golds, K., Kundu, P., Gold, J. D. & Carpenter, M. K. Feeder-Free Growth of Undifferentiated Human Embryonic Stem Cells. *Nat Biotech* 19(10), 971-974 (2001).
- Xu, N., Papagiannakopoulos, T., Pan, G., Thomson, J. & Kosik, K. MicroRNA-145 Regulates Oct4, Sox2, and Klf4 and Represses Pluripotency in Human Embryonic Stem Cells. *Cell* 137(4), 647-658 (2009).
- Xu, R., Sampsel-Barron, T. L., Gu, F., Root, S., Peck, R., Pan, G., Yu, J., Antosiewicz-Bourget, J., Tian, S., Stewart, R. *et al.* Nanog is a Direct Target of Tgfbeta/Activin-Mediated Smad Signaling in Human Escs. *Cell Stem Cell* 3(2), 196-206 (2008).
- Yan, Y., Yang, D., Zarnowska, E., Du, Z., Werbel, B., Valliere, C., Pearce, R., Thomson, J. & Zhang, S. Directed Differentiation of Dopaminergic Neuronal Subtypes From Human Embryonic Stem Cells. *Stem Cells* 23(6), 781-790 (2005).
- Yao, S., Lum, L. & Beachy, P. The Ihog Cell-Surface Proteins Bind Hedgehog and Mediate Pathway Activation. *Cell* 125(2), 343-357 (2006).
- Ye, W., Shimamura, K., Rubenstein, J., Hynes, M. & Rosenthal, A. Fgf and Shh Signals Control Dopaminergic and Serotonergic Cell Fate in the Anterior Neural Plate. *Cell* 93(5), 755-766 (1998).
- Yoon, J., Gilbertson, R., Iannaccone, S., Iannaccone, P. & Walterhouse, D. Defining a Role for Sonic Hedgehog Pathway Activation in Desmoplastic Medulloblastoma By Identifying Gli1 Target Genes. *Int J Cancer* 124(1), 109-119 (2009).
- Yoon, J., Kita, Y., Frank, D., Majewski, R., Konicek, B., Nobrega, M., Jacob, H., Walterhouse, D. & Iannaccone, P. Gene Expression Profiling Leads to Identification of Gli1-Binding Elements in Target Genes and a Role for Multiple Downstream Pathways in Gli1-Induced Cell Transformation. *J Biol Chem* 277(7), 5548-5555 (2002).
- Young, K., Merson, T., Sothibundhu, A., Coulson, E. & Bartlett, P. P75 Neurotrophin Receptor Expression Defines a Population of Bdnf-Responsive Neurogenic Precursor Cells. *J Neurosci* 27(19), 5146-5155 (2007).
- Yu, J., Vodyanik, M., Smuga-Otto, K., Antosiewicz-Bourget, J., Frane, J., Tian, S., Nie, J., Jonsdottir, G., Ruotti, V., Stewart, R. *et al.* Induced Pluripotent Stem Cell Lines Derived From Human Somatic Cells. *Science* 318(5858), 1917-1920 (2007).

Zaehres, H., Lensch, M., Daheron, L., Stewart, S., Itskovitz-Eldor, J. & Daley, G. High-Efficiency RNA Interference in Human Embryonic Stem Cells. *Stem Cells* 23(3), 299-305 (2005).

Zhang, S., Wernig, M., Duncan, I., Brustle, O. & Thomson, J. In Vitro Differentiation of Transplantable Neural Precursors From Human Embryonic Stem Cells. *Nat Biotechnol* 19(12), 1129-1133 (2001).

Zhang, W., Kang, J., Cole, F., Yi, M. & Krauss, R. Cdo Functions At Multiple Points in the Sonic Hedgehog Pathway, and Cdo-Deficient Mice Accurately Model Human Holoprosencephaly. *Dev Cell* 10(5), 657-665 (2006).

Zhang, X., Ramalho-Santos, M. & McMahon, A. Smoothened Mutants Reveal Redundant Roles for Shh and Ihh Signaling Including Regulation of L/R Asymmetry By the Mouse Node. *Cell* 105(6), 781-792 (2001).

Zhao, Y., Tong, C. & Jiang, J. Hedgehog Regulates Smoothened Activity By Inducing a Conformational Switch. *Nature* 450(7167), 252-258 (2007).

Zhou, Q. & Anderson, D. The Bhlh Transcription Factors Olig2 and Olig1 Couple Neuronal and Glial Subtype Specification. *Cell* 109(1), 61-73 (2002).

APPENDIX A MICROARRAY DATA

Table A 1 List of significantly upregulated genes (> 1.5-fold) in SHH-NP. Genes are ranked according to their fold change values.

<i>Symbol</i>	Description	Fold change		p-value	
		SHH vs Vector	SHH vs H3	SHH vs Vector	SHH vs H3
<i>NKX2-2</i>	NK2 homeobox 2	17.496	15.376	3.89E-10	7.08E-07
<i>FOXD1</i>	forkhead box D1	8.568	7.644	1.05E-11	7.83E-08
<i>NTRK2</i>	neurotrophic tyrosine kinase, receptor, type 2	7.999	5.892	7.26E-10	9.23E-07
<i>FOXA1</i>	forkhead box A1	7.648	8.422	2.20E-12	3.68E-08
<i>HEY2</i>	hairly/enhancer-of-split related with YRPW motif 2	7.045	3.405	1.52E-09	1.63E-06
<i>DDC</i>	dopa decarboxylase (aromatic L-amino acid decarboxylase)	6.556	6.574	4.76E-10	7.88E-07
<i>SYT4</i>	synaptotagmin IV	6.507	2.800	2.16E-08	1.08E-05
<i>POSTN</i>	periostin, osteoblast specific factor	6.395	1.825	9.21E-05	4.18E-03
<i>CYP1B1</i>	cytochrome P450, family 1, subfamily B, polypeptide 1	6.131	5.502	1.33E-09	1.54E-06
<i>NTN1</i>	netrin 1	5.990	5.998	2.54E-10	4.95E-07
<i>PCDH8</i>	protocadherin 8	5.906	4.155	2.69E-05	1.68E-03
<i>C4orf18</i>	chromosome 4 open reading frame 18	4.671	2.875	2.74E-08	1.29E-05
<i>C8orf46</i>	chromosome 8 open reading frame 46	4.655	4.352	1.01E-08	6.08E-06
<i>SPARCL1</i>	SPARC-like 1 (hevin)	4.385	3.838	1.76E-11	8.75E-08
<i>ST18</i>	suppression of tumorigenicity 18 (breast carcinoma) (zinc finger protein)	4.335	4.123	4.90E-09	3.53E-06
<i>COL12A1</i>	collagen, type XII, alpha 1	4.178	1.989	3.06E-07	6.46E-05
<i>FSTL5</i>	follistatin-like 5	4.138	2.448	9.56E-06	7.78E-04
<i>PRMT8</i>	protein arginine methyltransferase 8	4.136	4.144	3.04E-08	1.31E-05
<i>BCOR</i>	BCL6 co-repressor	3.996	1.801	2.80E-07	6.14E-05
<i>NEUROD1</i>	neurogenic differentiation 1	3.991	1.845	1.57E-06	2.15E-04
<i>CRHBP</i>	corticotropin releasing hormone binding protein	3.942	3.824	2.00E-09	1.99E-06
<i>PLCL1</i>	phospholipase C-like 1	3.891	3.477	9.51E-07	1.48E-04
<i>MTTP</i>	microsomal triglyceride transfer protein	3.873	2.900	1.20E-06	1.76E-04
<i>MOXD1</i>	monooxygenase, DBH-like 1	3.847	1.657	1.12E-06	1.68E-04
<i>DCLK1</i>	doublecortin-like kinase 1	3.769	1.890	2.04E-06	2.61E-04
<i>COL3A1</i>	collagen, type III, alpha 1	3.759	3.125	4.33E-09	3.25E-06
<i>OXCT1</i>	3-oxoacid CoA transferase 1	3.526	1.672	4.60E-05	2.51E-03
<i>PROS1</i>	protein S (alpha)	3.506	2.122	1.61E-07	4.24E-05
<i>NKX6-1</i>	NK6 homeobox 1	3.465	3.635	3.25E-11	1.27E-07
<i>FOXF2</i>	forkhead box F2	3.453	3.771	2.69E-12	3.68E-08
<i>FOXA2</i>	forkhead box A2	3.443	3.449	2.34E-09	2.19E-06
<i>FOXF1</i>	forkhead box F1	3.401	2.568	1.19E-07	3.45E-05
<i>PCDH20</i>	protocadherin 20	3.380	3.246	7.31E-07	1.21E-04
<i>OLIG1</i>	oligodendrocyte transcription factor 1	3.234	3.719	1.01E-10	2.93E-07
<i>PTCH1</i>	patched homolog 1 (Drosophila)	3.162	2.832	4.03E-09	3.15E-06
<i>FLRT2</i>	fibronectin leucine rich transmembrane protein 2	3.060	2.131	5.42E-09	3.79E-06
<i>FREMI</i>	FRAS1 related extracellular matrix 1	3.038	2.719	8.50E-11	2.73E-07
<i>ARL13B</i>	ADP-ribosylation factor-like 13B	2.966	1.809	5.42E-06	5.35E-04
<i>GOLSYN</i>	Golgi-localized protein	2.943	2.310	2.79E-07	6.14E-05
<i>SLC4A4</i>	solute carrier family 4, sodium bicarbonate cotransporter, member 4	2.936	2.385	2.41E-06	2.96E-04

<i>VEPH1</i>	ventricular zone expressed PH domain homolog 1 (zebrafish)	2.884	2.134	3.57E-06	4.00E-04
<i>PITX2</i>	paired-like homeodomain 2	2.829	2.413	5.37E-09	3.79E-06
<i>TBX3</i>	T-box 3	2.807	1.681	2.91E-04	1.01E-02
<i>EBF3</i>	early B-cell factor 3	2.738	1.619	2.94E-04	1.02E-02
<i>PTCHD1</i>	patched domain containing 1	2.721	4.719	2.11E-11	9.62E-08
<i>PAPPA</i>	pregnancy-associated plasma protein A, pappalysin 1	2.645	1.688	1.34E-06	1.93E-04
<i>SPG3A</i>	spastic paraplegia 3A (autosomal dominant)	2.629	2.477	1.66E-08	8.96E-06
<i>RASD1</i>	RAS, dexamethasone-induced 1	2.628	2.019	1.49E-07	4.10E-05
<i>PCSK1</i>	proprotein convertase subtilisin/kexin type 1	2.545	2.551	1.80E-08	9.38E-06
<i>SCG3</i>	secretogranin III	2.522	1.668	6.60E-07	1.13E-04
<i>SHH</i>	sonic hedgehog homolog (Drosophila)	2.515	2.526	7.52E-06	6.57E-04
<i>FAT3</i>	FAT tumor suppressor homolog 3 (Drosophila)	2.506	2.430	2.95E-07	6.27E-05
<i>STMN3</i>	stathmin-like 3	2.459	1.604	7.86E-06	6.81E-04
<i>POU3F2</i>	POU class 3 homeobox 2	2.389	2.209	2.14E-08	1.08E-05
<i>GABRA2</i>	gamma-aminobutyric acid (GABA) A receptor, alpha 2	2.386	2.821	2.33E-07	5.51E-05
<i>EGR2</i>	early growth response 2 (Krox-20 homolog, Drosophila)	2.384	1.705	5.67E-05	2.92E-03
<i>HES6</i>	hairy and enhancer of split 6 (Drosophila)	2.343	1.501	9.93E-06	7.98E-04
<i>SHISA3</i>	shisa homolog 3 (Xenopus laevis)	2.279	2.314	6.81E-05	3.34E-03
<i>SLIT1</i>	slit homolog 1 (Drosophila)	2.264	2.557	8.41E-08	2.72E-05
<i>RHBDL3</i>	rhomoid, veinlet-like 3 (Drosophila)	2.257	1.786	2.21E-06	2.78E-04
<i>GRHL1</i>	grainyhead-like 1 (Drosophila)	2.250	1.963	3.00E-08	1.30E-05
<i>NRP1</i>	neuropilin 1	2.240	1.528	4.35E-06	4.64E-04
<i>NR2E1</i>	nuclear receptor subfamily 2, group E, member 1	2.197	4.102	1.10E-09	1.34E-06
<i>PGBD5</i>	piggyBac transposable element derived 5	2.185	1.574	2.69E-05	1.68E-03
<i>HHIP</i>	hedgehog interacting protein	2.171	2.261	1.08E-06	1.63E-04
<i>KLHDC8A</i>	kelch domain containing 8A	2.167	1.775	9.78E-08	2.99E-05
<i>BHLHB5</i>	basic helix-loop-helix domain containing, class B, 5	2.126	1.889	1.64E-04	6.49E-03
<i>ANKH</i>	ankylosis, progressive homolog (mouse)	2.118	1.725	1.27E-06	1.84E-04
<i>RPS6KA2</i>	ribosomal protein S6 kinase, 90kDa, polypeptide 2	2.111	1.525	2.38E-04	8.61E-03
<i>TTC6</i>	tetratricopeptide repeat domain 6	2.107	2.027	3.11E-06	3.60E-04
<i>MAB21L1</i>	mab-21-like 1 (C. elegans)	2.103	1.871	1.93E-05	1.31E-03
<i>JAM2</i>	junctional adhesion molecule 2	2.097	1.515	6.01E-05	3.06E-03
<i>BICC1</i>	bicaudal C homolog 1 (Drosophila)	2.091	1.596	1.75E-04	6.80E-03
<i>RGS20</i>	regulator of G-protein signaling 20	2.075	1.988	1.57E-08	8.65E-06
<i>SLIT2</i>	slit homolog 2 (Drosophila)	2.068	1.507	7.77E-06	6.75E-04
<i>SOHLH2</i>	spermatogenesis and oogenesis specific basic helix-loop-helix 2	2.064	2.358	4.15E-06	4.46E-04
<i>PDE4B</i>	phosphodiesterase 4B, cAMP-specific (phosphodiesterase E4 dunce homolog, Drosophila)	2.059	1.669	7.24E-07	1.21E-04
<i>GLRB</i>	glycine receptor, beta	2.052	1.708	1.32E-05	9.92E-04
<i>MTHFD2L</i>	methylenetetrahydrofolate dehydrogenase (NADP+ dependent) 2-like	2.047	1.624	2.05E-05	1.38E-03

<i>PTPRO</i>	protein tyrosine phosphatase, receptor type, O	2.043	1.510	3.30E-05	1.93E-03
<i>FAT4</i>	FAT tumor suppressor homolog 4 (Drosophila)	2.042	1.811	1.54E-05	1.10E-03
<i>NLRP2</i>	NLR family, pyrin domain containing 2	2.041	1.600	5.63E-05	2.92E-03
<i>VSTM2A</i>	V-set and transmembrane domain containing 2A	2.035	2.078	8.06E-05	3.78E-03
<i>RGMA</i>	RGM domain family, member A	2.030	2.826	2.73E-09	2.37E-06
<i>CCDC48</i>	coiled-coil domain containing 48	2.010	1.843	8.02E-06	6.91E-04
<i>NRXN1</i>	neurexin 1	2.006	1.653	2.13E-05	1.41E-03
<i>RASSF2</i>	Ras association (RalGDS/AF-6) domain family member 2	1.995	1.639	2.06E-05	1.38E-03
<i>EGFR</i>	epidermal growth factor receptor (erythroblastic leukemia viral (v-erb-b) oncogene homolog, avian)	1.974	1.625	1.66E-06	2.26E-04
<i>FOXD2</i>	forkhead box D2	1.955	1.691	4.82E-06	4.89E-04
<i>FZD9</i>	frizzled homolog 9 (Drosophila)	1.947	2.023	2.04E-06	2.61E-04
<i>MAGEL2</i>	MAGE-like 2	1.945	2.081	1.23E-07	3.53E-05
<i>FGF19</i>	fibroblast growth factor 19	1.940	1.895	1.05E-07	3.13E-05
<i>RCAN1</i>	regulator of calcineurin 1	1.937	1.524	1.80E-05	1.24E-03
<i>KCNJ8</i>	potassium inwardly-rectifying channel, subfamily J, member 8	1.923	1.987	6.56E-08	2.31E-05
<i>ARX</i>	aristaless related homeobox	1.920	2.143	2.20E-08	1.08E-05
<i>SLC40A1</i>	solute carrier family 40 (iron-regulated transporter), member 1	1.916	1.743	5.81E-06	5.64E-04
<i>PGF</i>	placental growth factor	1.914	2.097	1.66E-05	1.16E-03
<i>ARL4A</i>	ADP-ribosylation factor-like 4A	1.908	1.520	8.92E-07	1.41E-04
<i>ZFH3</i>	zinc finger homeobox 3	1.901	1.534	5.55E-04	1.61E-02
<i>C8orf4</i>	chromosome 8 open reading frame 4	1.901	1.919	9.63E-08	2.96E-05
<i>SPP1</i>	secreted phosphoprotein 1	1.899	1.983	1.82E-05	1.25E-03
<i>CSPG5</i>	chondroitin sulfate proteoglycan 5 (neuroglycan C)	1.894	1.964	2.27E-07	5.42E-05
<i>LRRTM2</i>	leucine rich repeat transmembrane neuronal 2	1.888	1.549	7.61E-06	6.63E-04
<i>ITGB8</i>	integrin, beta 8	1.878	1.758	1.34E-05	9.98E-04
<i>RASSF4</i>	Ras association (RalGDS/AF-6) domain family member 4	1.870	1.868	3.47E-08	1.44E-05
<i>ELMO1</i>	engulfment and cell motility 1	1.864	1.543	2.68E-05	1.68E-03
<i>OLFML3</i>	olfactomedin-like 3	1.861	1.745	1.12E-05	8.74E-04
<i>MCTP1</i>	multiple C2 domains, transmembrane 1	1.860	1.627	4.57E-05	2.50E-03
<i>NLGN1</i>	neuroligin 1	1.857	1.666	2.14E-05	1.42E-03
<i>KCND3</i>	potassium voltage-gated channel, Shal-related subfamily, member 3	1.853	1.668	3.01E-05	1.80E-03
<i>RAB33A</i>	RAB33A, member RAS oncogene family	1.846	1.517	1.92E-06	2.51E-04
<i>OLFM4</i>	olfactomedin 4	1.831	1.891	1.43E-04	5.92E-03
<i>PLEKHH2</i>	pleckstrin homology domain containing, family H (with MyTH4 domain) member 2	1.828	2.014	4.87E-05	2.63E-03
<i>PHOX2B</i>	paired-like homeobox 2b	1.827	1.574	1.40E-03	3.16E-02
<i>SOX1</i>	SRY (sex determining region Y)-box 1	1.827	1.899	2.04E-06	2.61E-04
<i>OTP</i>	orthopedia homeobox	1.805	1.790	2.67E-05	1.67E-03
<i>ZC3HAV1</i>	zinc finger CCCH-type, antiviral 1	1.796	1.502	1.17E-05	9.02E-04
<i>NTNG1</i>	netrin G1	1.791	1.855	5.76E-07	1.04E-04
<i>FLT4</i>	fms-related tyrosine kinase 4	1.790	1.597	9.33E-04	2.36E-02
<i>ANGPT1</i>	angiopoietin 1	1.788	1.773	3.31E-06	3.77E-04
<i>PIK3R3</i>	phosphoinositide-3-kinase, regulatory subunit 3 (gamma)	1.784	1.521	5.77E-06	5.63E-04

<i>HES5</i>	hairy and enhancer of split 5 (Drosophila)	1.779	2.390	1.09E-07	3.23E-05
<i>DYNCH1</i>	dynein, cytoplasmic 1, intermediate chain 1	1.777	1.557	2.53E-04	9.01E-03
<i>FAM181A</i>	family with sequence similarity 181, member A	1.767	1.620	6.54E-06	6.11E-04
<i>VSY1</i>	visual system homeobox 1	1.766	1.904	5.65E-05	2.92E-03
<i>LOC100132832</i>	similar to postmeiotic segregation increased 2-like 5	1.765	1.718	1.44E-04	5.93E-03
<i>CXCR7</i>	chemokine (C-X-C motif) receptor 7	1.757	2.160	2.91E-09	2.48E-06
<i>SNCAIP</i>	synuclein, alpha interacting protein	1.736	1.850	2.52E-08	1.20E-05
<i>TOX2</i>	TOX high mobility group box family member 2	1.736	2.430	7.60E-09	4.95E-06
<i>NRCAM</i>	neuronal cell adhesion molecule	1.735	2.468	5.13E-10	8.02E-07
<i>RGMB</i>	RGM domain family, member B	1.730	1.857	4.21E-08	1.66E-05
<i>FHOD3</i>	formin homology 2 domain containing 3	1.716	1.554	2.53E-05	1.62E-03
<i>FABP7</i>	fatty acid binding protein 7, brain	1.697	1.771	1.69E-08	9.05E-06
<i>HS3ST3B1</i>	heparan sulfate (glucosamine) 3-O-sulfotransferase 3B1	1.695	1.957	2.82E-06	3.36E-04
<i>LONRF2</i>	LON peptidase N-terminal domain and ring finger 2	1.693	1.741	3.96E-05	2.22E-03
<i>HIVEP2</i>	human immunodeficiency virus type I enhancer binding protein 2	1.690	1.572	1.99E-05	1.34E-03
<i>TMTC2</i>	transmembrane and tetratricopeptide repeat containing 2	1.688	1.715	1.01E-05	8.08E-04
<i>GNG2</i>	guanine nucleotide binding protein (G protein), gamma 2	1.678	1.719	3.20E-07	6.66E-05
<i>FLJ20160</i>	FLJ20160 protein	1.668	1.925	7.40E-06	6.49E-04
<i>GRIK3</i>	glutamate receptor, ionotropic, kainate 3	1.667	1.644	5.87E-04	1.67E-02
<i>QKI</i>	quaking homolog, KH domain RNA binding (mouse)	1.666	1.685	3.00E-07	6.36E-05
<i>FOXB1</i>	forkhead box B1	1.662	1.607	1.32E-04	5.57E-03
<i>GLI1</i>	glioma-associated oncogene homolog 1 (zinc finger protein)	1.661	1.819	6.74E-06	6.22E-04
<i>PDPN</i>	podoplanin	1.655	1.838	1.54E-07	4.16E-05
<i>KIAA0182</i>	KIAA0182	1.651	1.660	2.43E-07	5.70E-05
<i>ADAMTS12</i>	ADAM metallopeptidase with thrombospondin type 1 motif, 12	1.650	1.657	1.05E-06	1.60E-04
<i>NEDD4</i>	neural precursor cell expressed, developmentally down-regulated 4	1.640	1.689	1.85E-06	2.44E-04
<i>SLC44A5</i>	solute carrier family 44, member 5	1.637	2.018	1.03E-06	1.58E-04
<i>PNMA2</i>	paraneoplastic antigen MA2	1.633	1.661	1.83E-07	4.70E-05
<i>SPON1</i>	spondin 1, extracellular matrix protein	1.630	2.009	5.57E-08	2.06E-05
<i>FAM107A</i>	family with sequence similarity 107, member A	1.627	2.744	5.81E-10	8.40E-07
<i>FGD3</i>	FYVE, RhoGEF and PH domain containing 3	1.625	1.596	2.23E-04	8.19E-03
<i>SPOCK1</i>	sparc/osteonectin, cwcv and kazal-like domains proteoglycan (testican) 1	1.624	1.630	4.69E-06	4.81E-04
<i>C20orf103</i>	chromosome 20 open reading frame 103	1.619	1.696	1.73E-06	2.31E-04
<i>CXCL12</i>	chemokine (C-X-C motif) ligand 12 (stromal cell-derived factor 1)	1.619	2.315	2.78E-07	6.14E-05
<i>KCNK1</i>	potassium voltage-gated channel, Shaw-related subfamily, member 1	1.618	1.511	1.53E-04	6.17E-03
<i>DCX</i>	doublecortin	1.618	1.996	9.42E-08	2.92E-05
<i>C12orf39</i>	chromosome 12 open reading frame 39	1.613	1.536	6.72E-05	3.32E-03

<i>NES</i>	nestin	1.610	1.513	6.53E-06	6.11E-04
<i>LMCD1</i>	LIM and cysteine-rich domains 1	1.602	1.535	1.77E-05	1.22E-03
<i>FLJ14213</i>	protor-2	1.594	1.549	1.20E-05	9.20E-04
<i>COTL1</i>	coactosin-like 1 (Dictyostelium)	1.582	1.619	2.84E-05	1.74E-03
<i>SULF1</i>	sulfatase 1	1.582	1.724	1.92E-06	2.51E-04
<i>BTBD11</i>	BTB (POZ) domain containing 11	1.576	1.535	8.79E-04	2.25E-02
<i>LRIG1</i>	leucine-rich repeats and immunoglobulin-like domains 1	1.567	1.598	2.66E-05	1.67E-03
<i>SYT6</i>	synaptotagmin VI	1.564	1.508	4.68E-05	2.55E-03
<i>PAPLN</i>	papilin, proteoglycan-like sulfated glycoprotein	1.564	1.611	2.60E-03	4.94E-02
<i>CRB1</i>	crumbs homolog 1 (Drosophila)	1.564	1.857	5.95E-08	2.14E-05
<i>LL22NC03-75B3.6</i>	KIAA1644 protein	1.563	1.588	1.92E-06	2.51E-04
<i>PLXNC1</i>	plexin C1	1.555	1.917	8.95E-08	2.81E-05
<i>CAPN6</i>	calpain 6	1.546	4.214	1.20E-10	3.13E-07
<i>CHN2</i>	chimerin (chimaerin) 2	1.538	1.536	3.30E-06	3.77E-04
<i>DTX4</i>	deltex 4 homolog (Drosophila)	1.536	1.676	1.53E-05	1.10E-03
<i>INSM2</i>	insulinoma-associated 2	1.529	1.790	7.59E-05	3.61E-03
<i>MGST1</i>	microsomal glutathione S-transferase 1	1.528	1.557	1.71E-05	1.19E-03
<i>INHBB</i>	inhibin, beta B	1.521	1.634	2.47E-04	8.83E-03
<i>SPOCK3</i>	sparc/osteonectin, cwcv and kazal-like domains proteoglycan (testican) 3	1.520	1.962	3.84E-06	4.24E-04
<i>MLC1</i>	megalencephalic leukoencephalopathy with subcortical cysts 1	1.516	1.593	1.50E-05	1.08E-03
<i>OSBPL6</i>	oxysterol binding protein-like 6	1.515	1.775	3.06E-05	1.83E-03
<i>ELL2</i>	elongation factor, RNA polymerase II, 2	1.512	2.325	4.50E-08	1.75E-05
<i>COL21A1</i>	collagen, type XXI, alpha 1	1.505	1.704	2.97E-06	3.48E-04
<i>ATP2C2</i>	ATPase, Ca ⁺⁺ transporting, type 2C, member 2	1.504	1.930	8.33E-06	7.07E-04

Table A 2 List of significantly downregulated genes (>1.5-fold) in SHH-NP. Genes are ranked according to their fold change values.

<i>Symbol</i>	Description	Fold change		p-value	
		SHH vs Vector	SHH vs H3	SHH vs Vector	SHH vs H3
<i>ID1</i>	inhibitor of DNA binding 1, dominant negative helix-loop-helix protein	0.167	0.193	3.22E-11	1.27E-07
<i>KBTBD10</i>	kelch repeat and BTB (POZ) domain containing 10	0.216	0.428	6.96E-04	1.90E-02
<i>GLT8D4</i>	glycosyltransferase 8 domain containing 4	0.236	0.247	1.42E-09	1.61E-06
<i>LPL</i>	lipoprotein lipase	0.238	0.150	1.29E-11	7.83E-08
<i>LGALS1</i>	lectin, galactoside-binding, soluble, 1	0.254	0.367	1.40E-07	3.92E-05
<i>COL1A2</i>	collagen, type I, alpha 2	0.268	0.410	1.54E-05	1.10E-03
<i>TFPI</i>	tissue factor pathway inhibitor (lipoprotein-associated coagulation inhibitor)	0.286	0.290	7.49E-08	2.53E-05
<i>PAX3</i>	paired box 3	0.292	0.267	1.19E-11	7.83E-08
<i>MSX2</i>	msh homeobox 2	0.301	0.222	7.38E-12	6.73E-08
<i>LGALS3</i>	lectin, galactoside-binding, soluble, 3	0.302	0.320	4.30E-09	3.25E-06
<i>CTTN</i>	cortactin	0.305	0.578	4.09E-04	1.28E-02
<i>SNAI2</i>	snail homolog 2 (Drosophila)	0.323	0.404	3.83E-09	3.03E-06
<i>ACTN3</i>	actinin, alpha 3	0.323	0.608	4.89E-04	1.47E-02
<i>CDH6</i>	cadherin 6, type 2, K-cadherin (fetal kidney)	0.329	0.390	4.04E-08	1.61E-05
<i>PDGFRA</i>	platelet-derived growth factor receptor, alpha polypeptide	0.339	0.527	6.58E-05	3.26E-03
<i>RRAS</i>	related RAS viral (r-ras) oncogene homolog	0.342	0.506	3.39E-06	3.83E-04
<i>PLAU</i>	plasminogen activator, urokinase	0.355	0.422	6.27E-07	1.09E-04
<i>SMEK2</i>	SMEK homolog 2, suppressor of mek1 (Dictyostelium)	0.358	0.653	1.03E-03	2.54E-02
<i>MSX1</i>	msh homeobox 1	0.359	0.177	1.02E-10	2.93E-07
<i>APOE</i>	apolipoprotein E	0.364	0.429	1.99E-06	2.57E-04
<i>UNC5C</i>	unc-5 homolog C (C. elegans)	0.366	0.364	1.90E-09	1.93E-06
<i>CLDN11</i>	claudin 11	0.376	0.600	1.46E-06	2.04E-04
<i>CPNE8</i>	copine VIII	0.384	0.508	6.88E-07	1.17E-04
<i>GADD45B</i>	growth arrest and DNA-damage-inducible, beta	0.385	0.561	2.93E-04	1.01E-02
<i>WRNIP1</i>	Werner helicase interacting protein 1	0.385	0.626	1.89E-03	3.91E-02
<i>CLDN3</i>	claudin 3	0.385	0.593	7.01E-05	3.39E-03
<i>MAF</i>	v-maf musculoaponeurotic fibrosarcoma oncogene homolog (avian)	0.394	0.657	1.77E-05	1.22E-03
<i>RIPK4</i>	receptor-interacting serine-threonine kinase 4	0.397	0.571	4.06E-06	4.39E-04
<i>CAT</i>	catalase	0.400	0.660	8.47E-05	3.93E-03
<i>BST2</i>	bone marrow stromal cell antigen 2	0.407	0.546	1.36E-05	1.01E-03
<i>CEBPD</i>	CCAAT/enhancer binding protein (C/EBP), delta	0.410	0.594	1.19E-03	2.81E-02
<i>BOC</i>	Boc homolog (mouse)	0.410	0.452	9.72E-06	7.86E-04
<i>ICAM1</i>	intercellular adhesion molecule 1	0.415	0.540	1.85E-06	2.44E-04
<i>BICD1</i>	bicaudal D homolog 1 (Drosophila)	0.420	0.652	8.43E-04	2.19E-02
<i>PTGS1</i>	prostaglandin-endoperoxide synthase 1 (prostaglandin G/H synthase and cyclooxygenase)	0.428	0.531	8.81E-06	7.28E-04
<i>MAB21L2</i>	mab-21-like 2 (C. elegans)	0.428	0.480	1.60E-07	4.24E-05

<i>GREM1</i>	gremlin 1, cysteine knot superfamily, homolog (<i>Xenopus laevis</i>)	0.432	0.226	6.09E-09	4.16E-06
<i>ROR1</i>	receptor tyrosine kinase-like orphan receptor 1	0.435	0.599	5.44E-05	2.85E-03
<i>S100A4</i>	S100 calcium binding protein A4	0.437	0.513	4.86E-06	4.90E-04
<i>PRRX1</i>	paired related homeobox 1	0.440	0.419	2.12E-07	5.16E-05
<i>COL1A1</i>	collagen, type I, alpha 1	0.440	0.527	1.33E-05	9.95E-04
<i>TNNT1</i>	troponin T type 1 (skeletal, slow)	0.444	0.535	8.25E-06	7.03E-04
<i>KRT19</i>	keratin 19	0.447	0.497	8.22E-07	1.33E-04
<i>PCDHGC3</i>	protocadherin gamma subfamily C, 3	0.450	0.621	2.69E-07	6.02E-05
<i>AHNAK</i>	AHNAK nucleoprotein	0.453	0.502	1.24E-06	1.80E-04
<i>FIGF</i>	c-fos induced growth factor (vascular endothelial growth factor D)	0.459	0.281	1.52E-11	8.30E-08
<i>GPR160</i>	G protein-coupled receptor 160	0.460	0.625	3.71E-05	2.12E-03
<i>COL9A3</i>	collagen, type IX, alpha 3	0.461	0.433	1.82E-07	4.70E-05
<i>TFAP2C</i>	transcription factor AP-2 gamma (activating enhancer binding protein 2 gamma)	0.465	0.447	2.87E-08	1.29E-05
<i>FXRD5</i>	FXRD domain containing ion transport regulator 5	0.471	0.603	7.41E-06	6.49E-04
<i>ZNF385B</i>	zinc finger protein 385B	0.476	0.560	8.10E-04	2.13E-02
<i>STX3</i>	syntaxin 3	0.476	0.573	5.90E-04	1.68E-02
<i>CUL4B</i>	cullin 4B	0.480	0.644	7.27E-05	3.49E-03
<i>RSPO3</i>	R-spondin 3 homolog (<i>Xenopus laevis</i>)	0.481	0.243	1.94E-10	4.02E-07
<i>CDON</i>	Cdon homolog (mouse)	0.482	0.349	1.39E-10	3.32E-07
<i>CDH11</i>	cadherin 11, type 2, OB-cadherin (osteoblast)	0.487	0.652	1.59E-04	6.37E-03
<i>CDC42EP5</i>	CDC42 effector protein (Rho GTPase binding) 5	0.490	0.610	2.00E-06	2.58E-04
<i>FOS</i>	v-fos FBJ murine osteosarcoma viral oncogene homolog	0.498	0.475	6.28E-07	1.09E-04
<i>BMP5</i>	bone morphogenetic protein 5	0.505	0.527	8.24E-07	1.33E-04
<i>MAGEA3</i>	melanoma antigen family A, 3	0.505	0.635	3.92E-06	4.28E-04
<i>ID2</i>	inhibitor of DNA binding 2, dominant negative helix-loop-helix protein	0.505	0.496	8.93E-08	2.81E-05
<i>HIST1H2A C</i>	histone cluster 1, H2ac	0.506	0.660	2.54E-03	4.85E-02
<i>BAIAP2L1</i>	BAI1-associated protein 2-like 1	0.507	0.557	2.61E-07	5.88E-05
<i>MYL9</i>	myosin, light chain 9, regulatory	0.516	0.343	2.44E-09	2.19E-06
<i>FBXO2</i>	F-box protein 2	0.516	0.573	2.90E-05	1.77E-03
<i>C7orf58</i>	chromosome 7 open reading frame 58	0.517	0.581	2.40E-05	1.56E-03
<i>CNTNAP2</i>	contactin associated protein-like 2	0.517	0.382	2.78E-08	1.29E-05
<i>FAM123A</i>	family with sequence similarity 123A	0.518	0.594	4.36E-06	4.64E-04
<i>SPINT1</i>	serine peptidase inhibitor, Kunitz type 1	0.518	0.602	3.68E-04	1.19E-02
<i>SERPINB9</i>	serpin peptidase inhibitor, clade B (ovalbumin), member 9	0.519	0.647	6.99E-07	1.19E-04
<i>PPP1R1A</i>	protein phosphatase 1, regulatory (inhibitor) subunit 1A	0.520	0.607	1.21E-06	1.77E-04
<i>PLCD4</i>	phospholipase C, delta 4	0.523	0.606	3.55E-05	2.04E-03
<i>TPD52L1</i>	tumor protein D52-like 1	0.524	0.557	1.66E-05	1.16E-03
<i>WIP1I</i>	WD repeat domain, phosphoinositide interacting 1	0.527	0.539	8.38E-07	1.35E-04
<i>CDH1</i>	cadherin 1, type 1, E-cadherin (epithelial)	0.529	0.515	2.47E-04	8.83E-03
<i>VAMP8</i>	vesicle-associated membrane protein 8 (endobrevin)	0.531	0.361	1.69E-06	2.28E-04
<i>ZIC5</i>	Zic family member 5 (odd-paired homolog, <i>Drosophila</i>)	0.531	0.442	6.12E-07	1.08E-04

<i>SCML4</i>	sex comb on midleg-like 4 (Drosophila)	0.531	0.164	6.02E-12	6.58E-08
<i>MMP23B</i>	matrix metallopeptidase 23B	0.532	0.665	5.72E-04	1.64E-02
<i>MAFF</i>	v-maf musculoaponeurotic fibrosarcoma oncogene homolog F (avian)	0.535	0.661	1.10E-04	4.80E-03
<i>DACT1</i>	dapper, antagonist of beta-catenin, homolog 1 (Xenopus laevis)	0.536	0.556	7.45E-07	1.23E-04
<i>IFIT3</i>	interferon-induced protein with tetratricopeptide repeats 3	0.536	0.614	6.44E-05	3.22E-03
<i>ZIC2</i>	Zic family member 2 (odd-paired homolog, Drosophila)	0.537	0.450	2.47E-08	1.18E-05
<i>KRT18</i>	keratin 18	0.537	0.542	2.17E-06	2.75E-04
<i>HIST1H2B G</i>	histone cluster 1, H2bg	0.539	0.636	1.04E-03	2.56E-02
<i>PCDH7</i>	protocadherin 7	0.540	0.580	8.99E-05	4.11E-03
<i>EMP3</i>	epithelial membrane protein 3	0.540	0.611	5.12E-06	5.14E-04
<i>IFITM1</i>	interferon induced transmembrane protein 1 (9-27)	0.545	0.643	2.43E-05	1.58E-03
<i>C13orf15</i>	chromosome 13 open reading frame 15	0.547	0.374	3.82E-10	7.08E-07
<i>BNC1</i>	basonuclin 1	0.551	0.564	1.79E-04	6.92E-03
<i>RCAN3</i>	RCAN family member 3	0.552	0.497	3.65E-06	4.09E-04
<i>WWC2</i>	WW and C2 domain containing 2	0.554	0.643	4.67E-04	1.41E-02
<i>RAB11FIP1</i>	RAB11 family interacting protein 1 (class I)	0.555	0.591	1.43E-05	1.05E-03
<i>HOXC6</i>	homeobox C6	0.555	0.368	2.16E-08	1.08E-05
<i>ATF3</i>	activating transcription factor 3	0.556	0.552	1.57E-07	4.19E-05
<i>GUCA1A</i>	guanylate cyclase activator 1A (retina)	0.558	0.579	3.31E-06	3.77E-04
<i>UNC5B</i>	unc-5 homolog B (C. elegans)	0.559	0.592	1.21E-05	9.22E-04
<i>GDF15</i>	growth differentiation factor 15	0.559	0.414	1.95E-06	2.53E-04
<i>TNFRSF11 B</i>	tumor necrosis factor receptor superfamily, member 11b	0.560	0.269	2.92E-08	1.30E-05
<i>ANXA2</i>	annexin A2	0.562	0.499	4.48E-07	8.50E-05
<i>EVII</i>	ecotropic viral integration site 1	0.563	0.599	3.39E-06	3.83E-04
<i>RSPO1</i>	R-spondin homolog (Xenopus laevis)	0.563	0.462	3.41E-09	2.78E-06
<i>PTGS2</i>	prostaglandin-endoperoxide synthase 2 (prostaglandin G/H synthase and cyclooxygenase)	0.564	0.337	3.89E-08	1.59E-05
<i>ELTD1</i>	EGF, latrophilin and seven transmembrane domain containing 1	0.566	0.375	8.33E-08	2.71E-05
<i>ZFP36</i>	zinc finger protein 36, C3H type, homolog (mouse)	0.566	0.609	8.83E-05	4.05E-03
<i>TGFBI</i>	transforming growth factor, beta-induced, 68kDa	0.567	0.462	6.45E-07	1.11E-04
<i>PCDH10</i>	protocadherin 10	0.568	0.535	8.57E-06	7.18E-04
<i>MAP3K8</i>	mitogen-activated protein kinase kinase kinase 8	0.574	0.458	9.32E-07	1.46E-04
<i>GADI</i>	glutamate decarboxylase 1 (brain, 67kDa)	0.575	0.579	1.65E-06	2.24E-04
<i>FAM150B</i>	family with sequence similarity 150, member B	0.575	0.396	2.90E-07	6.25E-05
<i>CYR61</i>	cysteine-rich, angiogenic inducer, 61	0.576	0.643	5.61E-06	5.51E-04
<i>TFAP2A</i>	transcription factor AP-2 alpha (activating enhancer binding protein 2 alpha)	0.578	0.534	3.99E-08	1.60E-05
<i>TWIST1</i>	twist homolog 1 (Drosophila)	0.581	0.504	3.82E-07	7.49E-05
<i>SLC7A8</i>	solute carrier family 7 (cationic amino acid transporter, y+ system), member 8	0.581	0.423	1.43E-08	7.98E-06
<i>MEF2C</i>	myocyte enhancer factor 2C	0.583	0.563	9.30E-06	7.62E-04
<i>KRT8</i>	keratin 8	0.585	0.661	2.81E-05	1.73E-03

<i>BAMBI</i>	BMP and activin membrane-bound inhibitor homolog (<i>Xenopus laevis</i>)	0.586	0.449	5.65E-08	2.07E-05
<i>F2RL2</i>	coagulation factor II (thrombin) receptor-like 2	0.591	0.602	5.60E-05	2.91E-03
<i>RASGEF1A</i>	RasGEF domain family, member 1A	0.593	0.592	1.24E-04	5.26E-03
<i>MAGEA2B</i>	melanoma antigen family A, 2B	0.600	0.657	8.60E-06	7.19E-04
<i>MPP1</i>	membrane protein, palmitoylated 1, 55kDa	0.602	0.543	1.86E-07	4.74E-05
<i>TACSTD1</i>	tumor-associated calcium signal transducer 1	0.607	0.558	1.61E-04	6.43E-03
<i>MGMT</i>	O-6-methylguanine-DNA methyltransferase	0.607	0.657	1.40E-03	3.16E-02
<i>FBLN2</i>	fibulin 2	0.608	0.620	3.40E-05	1.98E-03
<i>RAB3B</i>	RAB3B, member RAS oncogene family	0.609	0.545	2.12E-07	5.16E-05
<i>RNF135</i>	ring finger protein 135	0.610	0.661	3.86E-05	2.18E-03
<i>TAGLN</i>	transgelin	0.611	0.296	4.29E-11	1.57E-07
<i>C9orf150</i>	chromosome 9 open reading frame 150	0.611	0.630	4.09E-06	4.41E-04
<i>ID3</i>	inhibitor of DNA binding 3, dominant negative helix-loop-helix protein	0.612	0.512	4.71E-08	1.81E-05
<i>GLI3</i>	GLI-Kruppel family member GLI3	0.613	0.603	4.47E-06	4.68E-04
<i>BMP2</i>	bone morphogenetic protein 2	0.613	0.479	1.98E-07	4.95E-05
<i>PPFIBP2</i>	PTPRF interacting protein, binding protein 2 (liprin beta 2)	0.615	0.615	1.39E-05	1.03E-03
<i>ALG10B</i>	asparagine-linked glycosylation 10 homolog B (yeast, alpha-1,2-glucosyltransferase)	0.617	0.611	8.33E-05	3.89E-03
<i>GAL</i>	galanin prepropeptide	0.618	0.391	7.18E-05	3.46E-03
<i>FOXA3</i>	forkhead box A3	0.618	0.587	1.70E-04	6.66E-03
<i>SAMD4A</i>	sterile alpha motif domain containing 4A	0.619	0.665	3.25E-06	3.73E-04
<i>FAP</i>	fibroblast activation protein, alpha	0.623	0.439	8.22E-07	1.33E-04
<i>MAGEA2</i>	melanoma antigen family A, 2	0.627	0.661	7.67E-05	3.63E-03
<i>PTPRM</i>	protein tyrosine phosphatase, receptor type, M	0.628	0.601	1.02E-06	1.56E-04
<i>JAG1</i>	jagged 1 (Alagille syndrome)	0.630	0.632	1.64E-05	1.15E-03
<i>CDS1</i>	CDP-diacylglycerol synthase (phosphatidate cytidyltransferase) 1	0.631	0.518	1.23E-07	3.53E-05
<i>PMP22</i>	peripheral myelin protein 22	0.633	0.531	1.36E-06	1.94E-04
<i>DMRT3</i>	doublesex and mab-3 related transcription factor 3	0.634	0.550	1.14E-05	8.87E-04
<i>SLC26A6</i>	solute carrier family 26, member 6	0.637	0.656	6.19E-05	3.13E-03
<i>TLE1</i>	transducin-like enhancer of split 1 (E(sp1) homolog, <i>Drosophila</i>)	0.639	0.647	5.96E-06	5.72E-04
<i>TMEM204</i>	transmembrane protein 204	0.640	0.528	4.38E-06	4.65E-04
<i>HSPB1</i>	heat shock 27kDa protein 1	0.641	0.657	2.38E-05	1.55E-03
<i>TFAP2B</i>	transcription factor AP-2 beta (activating enhancer binding protein 2 beta)	0.642	0.574	7.86E-07	1.29E-04
<i>MRCL3</i>	myosin regulatory light chain MRCL3	0.642	0.597	1.06E-06	1.60E-04
<i>COL8A2</i>	collagen, type VIII, alpha 2	0.643	0.608	8.69E-06	7.24E-04
<i>PHLDA2</i>	pleckstrin homology-like domain, family A, member 2	0.647	0.457	2.93E-07	6.27E-05
<i>EYA4</i>	eyes absent homolog 4 (<i>Drosophila</i>)	0.650	0.458	1.12E-06	1.68E-04
<i>OLFM3</i>	olfactomedin 3	0.657	0.385	2.44E-09	2.19E-06
<i>VAMP5</i>	vesicle-associated membrane protein 5 (myobrevin)	0.666	0.528	1.60E-07	4.24E-05
<i>ZNF185</i>	zinc finger protein 185 (LIM domain)	0.667	0.596	1.54E-04	6.18E-03

APPENDIX B GLI BINDING SITES ANALYSIS

Table B 1 List of SHH upregulated genes that have putative GLI binding sites within 5 kb of the 5' upstream region from the transcriptional start site.

Gene Name	Chr	Strand	No. of binding sites	NCBI36 (March 2006) genome coordinates
FZD9	7	1	8	;72481606;72481853;72481875;72482104;72482320;72483067;72484598;72485502
RAB33A	X	1	8	;129129153;129129588;129130120;129130516;129130618;129131992;129132854;129132880
VSX1	20	-1	8	;25011505;25012240;25012526;25012646;25013160;25013277;25015330;25015527
LL22NC03-75B3.6	22	-1	7	;43029839;43029989;43030996;43031831;43031863;43031997;43032026
NKX2-2	20	-1	7	;21443440;21444126;21445002;21445631;21446000;21446079;21446266
STMN3	20	-1	7	;61756113;61756586;61757610;61758173;61758187;61758959;61759752
ATBF1	16	-1	6	;71551550;71552606;71553830;71554216;71555143;71555698
DSCR1	21	-1	6	;34909918;34910454;34910621;34911242;34913941;34914009
FGF19	11	-1	6	;69228284;69228297;69228830;69229223;69230020;69231791
FOXA2	20	-1	6	;22512908;22513270;22513312;22513957;22514033;22517225
GLI1	12	1	6	;56138973;56140064;56141787;56142041;56142299;56142451
HES5	1	-1	6	;2451751;2453850;2453901;2454104;2454904;2455611
MFSD6	2	1	6	;191004024;191004217;191004305;191004326;191005626;191007076
PGF	14	-1	6	;74491925;74493288;74494277;74494969;74495100;74495713
PTCHD1	X	1	6	;23259788;23259840;23260188;23260346;23261869;23262487
CCDC48	3	1	5	;130231796;130232141;130233496;130234185;130234597
CSPG5	3	-1	5	;47595763;47597782;47598556;47599213;47599436
CYP1B1	2	-1	5	;38156808;38157766;38159555;38159613;38160929
FOXF2	6	1	5	;1330402;1332821;1333599;1333836;1334917
GRIK3	1	-1	5	;37273227;37273290;37274905;37275515;37277119
MLC1	22	-1	5	;48865548;48865615;48867677;48867693;48868854
RASSF2	20	-1	5	;4730054;4730455;4731106;4732534;4734522
RPS6KA2	6	-1	5	;167197269;167197843;167197920;167198219;167198770
SOHLH2	13	-1	5	;35688075;35688364;35688896;35689796;35691050

AC079061.8	8	-1	4	;110726460;110726917;110730589;110730724
ANKH	5	-1	4	;14925285;14925961;14926129;14929322
BHLHE22	8	1	4	;65652242;65653282;65655024;65655041
COTL1	16	-1	4	;83209763;83210848;83210995;83212427
EGR2	10	-1	4	;64245902;64247566;64248012;64249585
FOXA1	14	-1	4	;37134954;37134958;37135660;37137384
FOXF1	16	1	4	;85096876;85099150;85101068;85101355
GABRA2	4	-1	4	;46086388;46087546;46089110;46089872
MAB21L1	13	-1	4	;34950716;34951077;34951504;34951979
NR2E1	6	1	4	;108590803;108592768;108593565;108594629
NRP1	10	-1	4	;33665708;33666300;33666589;33667007
OTP	5	-1	4	;76970181;76970428;76970531;76972821
PTCH1	9	-1	4	;97311302;97311437;97314067;97314385
SHH	7	-1	4	;155300111;155300211;155300369;155302360
AC009656.11	11	1	3	;36375441;36376159;36376172
C12orf39	12	1	3	;21568383;21568656;21569793
C8orf46	8	1	3	;67563655;67563809;67564748
CAPN6	X	-1	3	;110393870;110394824;110398095
COL3A1	2	1	3	;189545278;189545664;189546826
EBF3	10	-1	3	;131652106;131652904;131655389
ELL2	5	-1	3	;95326026;95326108;95327644
FAM107A	3	-1	3	;58531888;58532052;58532765
FLT4	5	-1	3	;180009778;180010059;180011267
FOXD2	1	1	3	;47673562;47676053;47676094
GNG2	14	1	3	;51485345;51485511;51485658
HES6	2	-1	3	;238813366;238813379;238815601
HEY2	6	1	3	;126108554;126109501;126111963
KLHDC8A	1	-1	3	;203580189;203580474;203581099
LRIG1	3	-1	3	;66634504;66635413;66638035
MTHFD2L	4	1	3	;75255621;75256139;75258771
NTN1	17	1	3	;8862429;8864096;8864474
OLFM4	13	1	3	;52498738;52499748;52499915
OLIG1	21	1	3	;33361359;33361545;33363804
PGBD5	1	-1	3	;228581001;228581627;228581797
PLXNC1	12	1	3	;93062670;93063011;93066864
POU3F2	6	1	3	;99385491;99387104;99389053
QKI	6	1	3	;163752067;163752884;163754525
RASD1	17	-1	3	;17340450;17343633;17344940
RGS20	8	1	3	;54952321;54954099;54955431
RHBDL3	17	1	3	;27614231;27616075;27616521
SNCAIP	5	1	3	;121750997;121752028;121753944
SPOCK1	5	-1	3	;136863461;136864219;136865564
SYT4	18	-1	3	;39111618;39113416;39113927
TMTC2	12	1	3	;81601591;81601702;81604746
ANGPT1	8	-1	2	;108580847;108582437

BTBD11	12	1	2	;106495361;106498430
C20orf103	20	1	2	;9440625;9443173
DCAMKL1	13	-1	2	;35598574;35602873
DCX	X	-1	2	;110543426;110544671
ELMO1	7	-1	2	;36902210;36905884
FAM181A	14	1	2	;93459325;93461207
FGD3	9	1	2	;94775996;94777226
FOXB1	15	1	2	;58082783;58082799
HIVEP2	6	-1	2	;143138521;143140512
HS3ST3B1	17	1	2	;14143984;14145083
JAM2	21	1	2	;25929963;25931330
KCNJ8	12	-1	2	;21821600;21821780
LONRF2	2	-1	2	;100306470;100307043
MGST1	12	1	2	;16397485;16398212
NES	1	-1	2	;154914597;154915381
NKX6-1	4	-1	2	;85638908;85640392
NLGN1	3	1	2	;174801364;174802856
NTRK2	9	1	2	;86471814;86475065
PAPLN	14	1	2	;72773046;72773862
PNMA2	8	-1	2	;26423287;26424403
PRMT8	12	1	2	;3466055;3468781
PROS1	3	-1	2	;95175589;95178980
SHISA3	4	1	2	;42090073;42091052
SLC40A1	2	-1	2	;190156432;190157618
SLC4A4	4	1	2	;72317244;72320677
SPOCK3	4	-1	2	;168395136;168395185
SPP1	4	1	2	;89113107;89115867
ST18	8	-1	2	;53289592;53289966
SYT6	1	-1	2	;114484420;114484969
TBX3	12	-1	2	;113605897;113606559
ZC3HAV1	7	-1	2	;138445448;138447240
ADAMTS12	5	-1	1	;33929360
ARL13B	3	1	1	;95179967
ARL4A	7	1	1	;12691862
ARX	X	-1	1	;24948229
ATP2C2	16	1	1	;82958047
BICC1	10	1	1	;59941684
C20orf100	20	1	1	;42034002
C4orf18	4	-1	1	;159315230
C8orf4	8	1	1	;40127562
CRHBP	5	1	1	;76280725
EGFR	7	1	1	;55052083
FAT4	4	1	1	;126453009
FLRT2	14	1	1	;85154682
HHIP	4	1	1	;145785912

INHBB	2	1	1	;120818017
INSM2	14	1	1	;35068959
ITGB8	7	1	1	;20333860
KCND3	1	-1	1	;112327076
MOXD1	6	-1	1	;132764358
MTTP	4	1	1	;100711136
OXCT1	5	-1	1	;41908808
PAPPA	9	1	1	;117955474
PCDH8	13	-1	1	;52323404
PITX2	4	-1	1	;111766765
PLEKHH2	2	1	1	;43721687
RASSF4	10	1	1	;44782105
SLIT1	10	-1	1	;98936553
TTC6	14	1	1	;37330662
VEPH1	3	-1	1	;158699514
LMCD1	3	1	0	
PHOX2B	4	-1	0	
SCG3	15	1	0	
OSBPL6	2	1	0	
GLRB	4	1	0	
FHOD3	18	1	0	
SLIT2	4	1	0	
OLFML3	1	1	0	
PCSK1	5	-1	0	
NEUROD1	2	-1	0	
PDE4B	1	1	0	
POSTN	13	-1	0	
DYNC111	7	1	0	
DDC	7	-1	0	
PTPRO	12	1	0	
FABP7	6	1	0	
SOX1	13	1	0	
COL12A1	6	-1	0	
CRB1	1	1	0	
VSTM2A	7	1	0	

Table B 2 List of SHH upregulated genes that have putative GLI binding sites within 5 kb of the 3' downstream region from the transcriptional start site.

Gene Name	Chr	Strand	No. of binding sites	NCBI36 (March 2006) genome coordinates
STMN3	20	-1	10	;61738659;61739139;61739997;61740022;61740381;61741203;61742099;61742424;61742438;61743022
NKX2-2	20	-1	8	;21435749;21435912;21436720;21436951;21436955;21437332;21437362;21440495
PGF	14	-1	7	;74475458;74475984;74476709;74477157;74477183;74477619;74477671
RASD1	17	-1	7	;17334611;17335648;17335794;17336270;17336351;17336501;17339086
NTN1	17	1	7	;9084482;9084698;9084856;9084914;9085197;9087102;9088076
HES6	2	-1	7	;238807423;238807492;238808274;238809654;238810489;238810734;238811159
FGD3	9	1	7	;94837741;94838378;94840147;94840156;94841107;94841942;94842654
DDC	7	-1	7	;50493623;50496104;50496411;50496677;50496987;50497308;50497329
C20orf100	20	1	7	;42130891;42131962;42132720;42132967;42133493;42133670;42134593
LMCD1	3	1	6	;8584290;8584452;8586437;8587144;8587365;8588169
FGF19	11	-1	6	;69218951;69218960;69219624;69221328;69223029;69223042
PLEKHH2	2	1	6	;43847492;43849284;43849516;43849649;43850535;43851004
FAM181A	14	1	6	;93465733;93465904;93467123;93467518;93468439;93469682
MLC1	22	-1	6	;48838431;48839817;48839886;48840090;48841198;48841581
CSPG5	3	-1	5	;47574123;47575145;47575565;47576735;47578730
MTTP	4	1	5	;100764473;100764735;100766112;100766603;100766903
FOXF1	16	1	5	;85106186;85108099;85108134;85108433;85108890
PNMA2	8	-1	5	;26416559;26417997;26419262;26419329;26419703
RPS6KA2	6	-1	5	;166742258;166742291;166743111;166744528;166745003
FLT4	5	-1	5	;179963764;179963868;179967096;179967689;179967726
RASSF2	20	-1	5	;47101113;47111103;4711458;4712261;4712811
OLIG1	21	1	5	;33366791;33367351;33368463;33369690;33369984
PCDH8	13	-1	5	;52313626;52313699;52314389;52316110;52316376
ZC3HAV1	7	-1	4	;138378035;138378380;138381650;138382574
SLIT1	10	-1	4	;98745985;98746489;98746993;98748130
C8orf46	8	1	4	;67591096;67591164;67593911;67595601
SHH	7	-1	4	;155284761;155285326;155285582;155285877
CRHBP	5	1	4	;76301778;76303836;76304151;76304479
OTP	5	-1	4	;76957648;76957791;76958991;76959563
ANKH	5	-1	4	;14761346;14762296;14762834;14762850
PGBD5	1	-1	4	;228523183;228524095;228524653;228524868
HES5	1	-1	4	;2446376;2447319;2449054;2449560
LL22NC03-75B3.6	22	-1	4	;42973083;42973326;42973509;42976688
PAPLN	14	1	4	;72809256;72810002;72811279;72813576
FABP7	6	1	4	;123147422;123148974;123149090;123150538
NES	1	-1	4	;154904027;154904378;154904887;154905650

MTHFD2 L	4	1	4	;75389394;75390798;75391306;75391319
FOXD2	1	1	4	;47681468;47681560;47681983;47682106
ARX	X	-1	4	;24928975;24930107;24930128;24931650
FZD9	7	1	4	;72488481;72489992;72492108;72492630
PAPPA	9	1	4	;118201348;118202504;118202560;118203048
RAB33A	X	1	3	;129149392;129149778;129150523
OLFM4	13	1	3	;52523677;52526715;52527089
COTL1	16	-1	3	;83154710;83156949;83156962
INHBB	2	1	3	;120827711;120828316;120828332
OLFML3	1	1	3	;114327885;114328718;114330095
TTC6	14	1	3	;37382286;37383512;37385455
LRIG1	3	-1	3	;66509847;66510899;66511284
KLHDC8 A	1	-1	3	;203568631;203569747;203571319
SYT6	1	-1	3	;114433690;114433931;114436454
ADAMTS 12	5	-1	3	;33559408;33559412;33561745
NRP1	10	-1	3	;33522712;33524401;33525276
FAM107 A	3	-1	3	;58523989;58526544;58526717
DCX	X	-1	3	;110428330;110428686;110429830
PROS1	3	-1	3	;95072050;95073370;95075670
SOX1	13	1	3	;111771896;111771900;111774614
BTBD11	12	1	3	;106575879;106577803;106579469
VEPH1	3	-1	3	;158457544;158457705;158459571
PRMT8	12	1	3	;3573432;3573883;3575364
GLI1	12	1	2	;56154612;56156476
SPP1	4	1	2	;89123510;89126655
FOXF2	6	1	2	;1341335;1342384
ATP2C2	16	1	2	;83055878;83059492
ANGPT1	8	-1	2	;108331629;108332521
ARL13B	3	1	2	;95258135;95258270
PDE4B	1	1	2	;66613312;66614739
ELMO1	7	-1	2	;36857561;36860560
SOHLH2	13	-1	2	;35636259;35636624
GNG2	14	1	2	;51505264;51507253
MFSD6	2	1	2	;191073251;191074392
PTPRO	12	1	2	;15639399;15642953
FLRT2	14	1	2	;85161083;85164488
SPOCK1	5	-1	2	;136338821;136340312
BICC1	10	1	2	;60261453;60262767
MOXD1	6	-1	2	;132657045;132659696
GRIK3	1	-1	2	;37038694;37039085
NTRK2	9	1	2	;86618907;86619978
RASSF4	10	1	2	;44808964;44809621
C20orf103	20	1	1	;9462028
KCNJ8	12	-1	1	;21807797
OSBPL6	2	1	1	;178973407
C12orf39	12	1	1	;21578467
ITGB8	7	1	1	;20417554
SYT4	18	-1	1	;39101553
SLC4A4	4	1	1	;72655101
SLC40A1	2	-1	1	;190133019

SNCAIP	5	1	1	;121828904
CCDC48	3	1	1	;130245842
FHOD3	18	1	1	;32615370
TMTC2	12	1	1	;82054481
INSM2	14	1	1	;35076760
SLIT2	4	1	1	;20231285
BHLHE22	8	1	1	;65659611
NKX6-1	4	-1	1	;85628694
RHBDL3	17	1	1	;27676085
FOXA2	20	-1	1	;22510098
C8orf4	8	1	1	;40134657
ST18	8	-1	1	;53186724
RGS20	8	1	1	;55035363
EGFR	7	1	1	;55244190
HHIP	4	1	1	;145882235
PITX2	4	-1	1	;111755837
KCND3	1	-1	1	;112115278
SHISA3	4	1	1	;42101864
AC07906 1.8	8	-1	1	;110652391
TBX3	12	-1	1	;113591704
FOXB1	15	1	1	;58089590
POSTN	13	-1	1	;37033695
LONRF2	2	-1	1	;100265947
C4orf18	4	-1	1	;159266980
DYNC111	7	1	1	;95568154
ARL4A	7	1	1	;12699922
NLGN1	3	1	1	;175486095
NR2E1	6	1	1	;108618210
VSX1	20	-1	1	;25003691
SPOCK3	4	-1	1	;167889370
AC00965 6.11	11	1	1	;36445296
MGST1	12	1	1	;16409194
CRB1	1	1	1	;195718042
CAPN6	X	-1	1	;110371973
JAM2	21	1	1	;26012787
HS3ST3B 1	17	1	1	;14191131
FAT4	4	1	1	;126635617
VSTM2A	7	1	0	
GABRA2	4	-1	0	
MAB21L 1	13	-1	0	
PTCHD1	X	1	0	
PTCH1	9	-1	0	
EBF3	10	-1	0	
HEY2	6	1	0	
HIVEP2	6	-1	0	
QKI	6	1	0	
POU3F2	6	1	0	
COL12A1	6	-1	0	
DSCR1	21	-1	0	
PCSK1	5	-1	0	

COL3A1	2	1	0	
NEUROD1	2	-1	0	
ATBF1	16	-1	0	
GLRB	4	1	0	
CYP1B1	2	-1	0	
PLXNC1	12	1	0	
DCAMKL1	13	-1	0	
FOXA1	14	-1	0	
EGR2	10	-1	0	
ELL2	5	-1	0	
PHOX2B	4	-1	0	
SCG3	15	1	0	
OXCT1	5	-1	0	

Table B 3 List of SHH downregulated genes with putative GLI binding sites within 5 kb of the 5' upstream region from the transcriptional start site

Gene Name	Chr	Strand	Transcript Start Site	No. of binding sites	Binding Site Start
GDF15	19	1	18357968	11	;42;210;1372;2849;2998;3108;3396;3935;4038;4158;4171
EMP3	19	1	53520454	9	;1404;1886;2313;3054;3132;3294;3395;3435;4897
MYL9	20	1	34603311	9	;1203;1207;1286;2265;2618;3040;4840;4945;4979
AHNAK	11	-1	62039950	9	;523;604;895;2867;2981;3155;3715;3877;4951
RCAN3	1	1	24701974	9	;132;1649;1697;2026;2056;2086;2109;2161;2733
LGALS1	22	1	36401559	8	;268;298;427;635;769;1485;1870;4189
CDH1	16	1	67328696	8	;450;953;2268;3319;3485;3682;4253;4735
ICAM1	19	1	10242765	8	;295;1280;1596;2074;2226;2636;3269;4475
KRT8	12	-1	51577238	8	;1210;1559;3168;3177;3406;3449;4614;4753
KBTBD10	2	1	170074458	8	;146;533;838;1024;1512;2023;2184;3545
MMP23B	1	1	1557423	8	;6;2218;2353;2605;2626;2788;3039;3802
COL1A1	17	-1	45616456	7	;886;1081;1143;3824;3934;4069;4513
HSPB1	7	1	75769859	7	;38;674;1169;1330;1456;2956;4393
BAIAP2L1	7	-1	97760007	7	;197;1167;1476;2021;2034;3228;4748
JAG1	20	-1	10566334	7	;266;593;872;876;1176;2628;3819
VAMP8	2	1	85658228	7	;497;2478;2974;3020;4176;4558;4810
GAL	11	1	68208559	7	;448;492;1767;3386;3427;4106;4252
FBXO2	1	-1	11631037	7	;187;1822;1835;2616;2930;4419;4572
COL9A3	20	1	60918859	7	;83;841;1804;1961;3427;4394;4928
PPFIBP2	11	1	7491627	7	;55;68;709;1926;2196;3818;4468
VAMP5	2	1	85665042	7	;669;813;960;1430;1745;2500;3713

BST2	19	-1	17374750	6	;557;863;1183;1498;2341;3986
ZFP36	19	1	44589293	6	;118;2129;2814;2857;3811;3832
CAT	11	1	34417054	6	;1181;1194;1747;3062;4553;4596
MAFF	22	1	36927944	6	;6;1226;1328;2623;2861;3231
PTGS1	9	1	124173050	6	;470;834;1932;2217;2237;3958
PHLDA2	11	-1	2906079	6	;14;1120;1285;2458;3330;4387
COL8A2	1	-1	36333424	6	;669;985;1283;1708;3950;4938
TAGLN	11	1	116575296	6	;60;637;2005;2484;3053;4775
ID2	2	1	8739564	6	;698;1192;2346;3046;3250;4169
APOE	19	1	50100879	5	;218;823;1647;3712;3990
GADD45B	19	1	2427135	5	;378;1414;3875;4005;4090
TACSTD1	2	1	47449954	5	;1282;1799;2990;4126;4544
PDGFRA	4	1	54790204	5	;168;1634;2370;2721;3000
COL1A2	7	1	93861809	5	;635;648;2147;3545;3664
ATF3	1	1	210805320	5	;833;2182;2874;3250;4914
CDC42EP5	19	-1	59668022	5	;771;1256;1730;2756;4339
CYR61	1	1	85819041	5	;462;710;1267;4317;4325
BNC1	15	-1	81715659	5	;850;2375;3848;3988;4330
RASGEF1A	10	-1	43009990	5	;1425;2112;3729;4524;4817
BAMBI	10	1	29006430	5	;2633;2769;3537;3849;4271
S100A4	1	-1	151782722	5	;1021;1145;3754;4168;4725
GUCA1A	6	1	42231162	5	;1099;1817;2517;3288;4312
SERPINB9	6	-1	2832507	5	;395;2149;2568;2832;3104
ID1	20	1	29656753	5	;167;1919;1963;3113;4264
RRAS	19	-1	54830364	4	;234;600;3520;3988
HOXC6	12	1	52708461	4	;764;1140;2420;3426
PRRX1	1	1	168899937	4	;401;2297;2505;4071
HIST1H2BG	6	-1	26324470	4	;2527;3203;3751;4205
GAD1	2	1	171381446	4	;143;147;1610;3559
KRT19	17	-1	36933396	4	;99;4094;4279;4603
RNF135	17	1	26322082	4	;683;1843;4148;4428
IFITM1	11	1	304041	4	;2326;2391;3376;4445
CUL4B	X	-1	119542476	4	;176;189;1570;3550
PCDH7	4	1	30331135	4	;2686;3313;4423;4814
RIPK4	21	-1	42032614	4	;2389;2610;2888;3699
MGMT	10	1	131155510	4	;810;1036;1145;2911
UNC5B	10	1	72642298	4	;2310;2436;3725;4157
TLE1	9	-1	83388423	4	;2442;2802;2811;3578
FXYD5	19	1	40337467	4	;623;1511;2761;3479
KRT18	12	1	51628922	4	;1045;1548;3629;4568
IFIT3	10	1	91082246	4	;2167;3802;3993;4366
TFAP2A	6	-1	10504902	4	;2186;2900;3536;4879
HIST1H2AC	6	1	26232432	4	;986;2576;3366;4233
PMP22	17	-1	15073822	4	;1088;2306;2931;4679
RAB3B	1	-1	52157425	4	;828;1923;2308;3381
CLDN11	3	1	171619359	3	;2486;4081;4382
TMEM204	16	1	1523659	3	;45;736;3712
LGALS3	14	1	54665574	3	;1085;2703;3443
DMRT3	9	1	966964	3	;2993;4148;4791
CDH11	16	-1	63538186	3	;2627;3126;3698
ZIC5	13	-1	99413276	3	;197;726;3665
CPNE8	12	-1	37332259	3	;184;3445;4669
TFPI	2	-1	188051553	3	;1440;2915;2994

RSPO3	6	1	127481749	3	;2907;3165;4045
SLC7A8	14	-1	22664346	3	;874;1305;2049
PCDHGA12	5	1	140835753	3	;173;186;2239
ANXA2	15	-1	58426625	3	;1426;1984;3120
MPP1	X	-1	153660162	3	;1481;4656;4827
MAF	16	-1	78185729	3	;3005;3853;4918
MAGEA2	X	-1	151669044	3	;2662;4425;4767
ROR1	1	1	64012281	3	;594;2153;2579
AP005329.1	18	1	3237528	2	;736;1418
TWIST1	7	-1	19121633	2	;4118;4499
TFAP2C	20	1	54637765	2	;745;4565
CDH6	5	1	31229553	2	;1048;3554
F2RL2	5	-1	75947064	2	;1866;4210
SAMD4A	14	1	54104387	2	;3974;4513
CTTN	11	1	69922292	2	;2461;3340
GREM1	15	1	30797497	2	;3588;4581
TNFRSF11B	8	-1	120004978	2	;781;4564
CNTNAP2	7	1	145444902	2	;1796;1808
UNC5C	4	-1	96308712	2	;3576;4451
GPR160	3	1	171239397	2	;1980;3708
MAGEA3	X	-1	151685309	2	;2468;2705
SCML4	6	-1	108130060	2	;956;2821
WRNIP1	6	1	2710665	2	;2438;3070
TPD52L1	6	1	125517119	2	;419;4341
ID3	1	-1	23757012	2	;889;4063
PLAU	10	1	75340896	2	;2059;2375
DACT1	14	1	58174527	2	;2645;4952
CLDN3	7	-1	72821263	2	;1252;2181
ELTD1	1	-1	79128037	2	;1701;1714
MSX2	5	1	174084181	1	;1171
CDON	11	-1	125331927	1	;2942
MAP3K8	10	1	30762872	1	;1857
WIPI1	17	-1	63929018	1	;4656
STX3	11	1	59279108	1	;57
FOXA3	19	1	51059358	1	;755
MAB21L2	4	1	151722753	1	;2468
ALG10B	12	1	36996824	1	;1282
C9orf150	9	1	12765012	1	;4452
FOS	14	1	74815284	1	;4613
BOC	3	1	114414065	1	;4075
FIGF	X	-1	15273640	1	;1588
BMP2	20	1	6696745	1	;3775
SNAI2	8	-1	49992880	1	;723
TFAP2B	6	1	50894398	1	;532
C13orf15	13	1	40929542	1	;3700
ZIC2	13	1	99432320	1	;2975
GLI3	7	-1	41967072	1	;2631
FAP	2	-1	162735448	0	
CDS1	4	1	85723081	0	
LPL	8	1	19840870	0	
EYA4	6	1	133604188	0	
BMP5	6	-1	55728199	0	
MSX1	4	1	4912293	0	

PTGS2	1	-1	184907592	0	
OLFM3	1	-1	102040721	0	
RSPO1	1	-1	37850071	0	

Table B 4 List of SHH downregulated genes with putative GLI binding sites within 5 kb of the 3' downstream region from the transcriptional start site.tart

Gene Name	Chr	Strand	Transcript Start Site	No. of binding sites	Binding Site Start
BST2	19	-1	17374750	11	;260;1460;2180;2312;2999;3303;3382;3478;4359;4589;4969
KRT8	12	-1	51577238	10	;1111;1495;1775;2702;2834;3002;3292;3946;4557;4933
LGALS1	22	1	36401559	9	;1687;1953;2343;2356;2480;3988;4001;4867;4880
MMP23B	1	1	1557423	9	;46;379;390;435;2914;3587;3850;4217;4699
RNF135	17	1	26322082	9	;161;1575;3358;3371;3549;3633;3974;4794;4867
GDF15	19	1	18357968	8	;1350;1820;3024;3190;3325;3810;3958;4746
CDH1	16	1	67328696	8	;542;706;969;3202;3861;4156;4169;4278
GAL	11	1	68208559	8	;231;572;800;1102;1158;1335;1724;1866
SLC7A8	14	-1	22664346	8	;132;390;1882;2421;2457;3050;3138;4778
PPFIBP2	11	1	7491627	8	;856;1354;2048;3227;3276;3846;4242;4737
PHLDA2	11	-1	2906079	8	;1163;2295;3296;3519;3896;4047;4816;4834
AHNAK	11	-1	62039950	8	;50;405;1459;2887;2903;3160;4074;4635
KRT18	12	1	51628922	8	;1250;1553;1695;2225;2238;3021;3807;4122
APOE	19	1	50100879	7	;505;940;2111;2762;3399;3610;3622
COL1A1	17	-1	45616456	7	;943;2156;3666;3823;4280;4626;4630
RRAS	19	-1	54830364	7	;349;581;1379;1971;2834;2991;2998
HSPB1	7	1	75769859	7	;1216;2321;3336;3394;4082;4383;4871
MYL9	20	1	34603311	7	;465;1663;2451;2570;3123;3291;4330
FBXO2	1	-1	11631037	7	;625;2021;3183;3538;3551;4046;4461
IFITM1	11	1	304041	7	;532;650;1913;1920;2582;3111;3176
ID3	1	-1	23757012	7	;394;1468;3120;3530;4178;4184;4188
TFAP2C	20	1	54637765	6	;1677;1963;2123;2526;3580;3698
BAIAP2L1	7	-1	97760007	6	;1441;2558;3064;4166;4301;4314
HIST1H2B G	6	-1	26324470	6	;129;417;825;1900;3421;4770
COL9A3	20	1	60918859	6	;1785;1798;1953;2702;4102;4115
BNC1	15	-1	81715659	6	;1679;1859;2966;3219;4585;4589
RASGEF1A	10	-1	43009990	6	;533;1320;2397;2812;4328;4636
WRNIP1	6	1	2710665	6	;1700;1855;2268;2732;3384;4528
RCAN3	1	1	24701974	6	;621;821;1706;2376;2389;3387
GUCA1A	6	1	42231162	6	;53;1567;1889;3371;3740;4939
CLDN11	3	1	171619359	5	;636;2272;2776;3581;4650
DMRT3	9	1	966964	5	;11;1833;2372;2586;2937
CTTN	11	1	69922292	5	;67;364;1061;1917;4389

GAD1	2	1	171381446	5	;486;626;2339;3817;4592
FOXA3	19	1	51059358	5	;103;194;1320;1928;2481
TNFRSF11 B	8	-1	120004978	5	;3051;3273;3812;4052;4218
MAFF	22	1	36927944	5	;660;3147;3898;4347;4968
GPR160	3	1	171239397	5	;1966;2158;3216;4068;4100
UNC5B	10	1	72642298	5	;1006;1667;2020;2682;2857
MPP1	X	-1	153660162	5	;957;2108;2608;3463;3605
ZIC2	13	1	99432320	5	;695;2076;2303;4907;4969
CLDN3	7	-1	72821263	5	;33;1931;2628;3091;3997
ID1	20	1	29656753	5	;778;2274;3378;3644;4425
TMEM204	16	1	1523659	4	;68;1128;1279;2032
GADD45B	19	1	2427135	4	;1549;3211;3545;4418
TACSTD1	2	1	47449954	4	;683;1217;2015;4670
EMP3	19	1	53520454	4	;973;1210;3770;4875
ICAM1	19	1	10242765	4	;835;2342;2916;3939
KRT19	17	-1	36933396	4	;1049;2464;3067;3364
PCDHGA1 2	5	1	140835753	4	;3433;4092;4355;4376
TLE1	9	-1	83388423	4	;290;3393;3557;4402
FXVD5	19	1	40337467	4	;860;1036;2338;3722
S100A4	1	-1	151782722	4	;17;1351;1462;4010
MSX1	4	1	4912293	4	;944;3085;4241;4335
ID2	2	1	8739564	4	;179;2111;3502;4471
PLAU	10	1	75340896	4	;125;819;3311;4197
HOXC6	12	1	52708461	3	;1039;1259;1900
ZFP36	19	1	44589293	3	;544;1844;3320
VAMP8	2	1	85658228	3	;274;1487;4616
CDS1	4	1	85723081	3	;1198;4269;4737
F2RL2	5	-1	75947064	3	;2455;3627;3792
MAP3K8	10	1	30762872	3	;2510;3174;4584
WIPI1	17	-1	63929018	3	;2446;3781;4291
STX3	11	1	59279108	3	;1399;1775;3730
LPL	8	1	19840870	3	;2543;2710;3136
C9orf150	9	1	12765012	3	;2649;2734;3679
FOS	14	1	74815284	3	;1402;3665;3678
BOC	3	1	114414065	3	;1295;1695;3337
PTGS1	9	1	124173050	3	;2078;3935;4326
PCDH7	4	1	30331135	3	;3697;4105;4237
BAMBI	10	1	29006430	3	;767;1347;2066
TPD52L1	6	1	125517119	3	;3126;3453;3466
MSX2	5	1	174084181	2	;899;4862
TWIST1	7	-1	19121633	2	;422;4089
CAT	11	1	34417054	2	;1607;2313
JAG1	20	-1	10566334	2	;2430;3083
CDH6	5	1	31229553	2	;3637;4010
CDH11	16	-1	63538186	2	;3700;3704
KBTBD10	2	1	170074458	2	;23;4719
ZIC5	13	-1	99413276	2	;3971;4228
COL1A2	7	1	93861809	2	;2581;4949
ALG10B	12	1	36996824	2	;2189;2967
CNTNAP2	7	1	145444902	2	;2225;4035
CDC42EP5	19	-1	59668022	2	;3623;4168
VAMP5	2	1	85665042	2	;2957;4721

MAGEA3	X	-1	151685309	2	;608;862
EYA4	6	1	133604188	2	;4478;4849
TAGLN	11	1	116575296	2	;1767;4242
C13orf15	13	1	40929542	2	;2115;3352
IFIT3	10	1	91082246	2	;186;4795
DACT1	14	1	58174527	2	;2012;3177
MAGEA2	X	-1	151669044	2	;1387;3353
HIST1H2A C	6	1	26232432	2	;723;1014
PMP22	17	-1	15073822	2	;1002;3455
RAB3B	1	-1	52157425	2	;682;3973
RSPO1	1	-1	37850071	2	;3853;3941
AP005329.1	18	1	3237528	1	;4989
LGALS3	14	1	54665574	1	;817
PDGFRA	4	1	54790204	1	;3329
SAMD4A	14	1	54104387	1	;848
GREM1	15	1	30797497	1	;4007
ATF3	1	1	210805320	1	;928
CYR61	1	1	85819041	1	;4695
RIPK4	21	-1	42032614	1	;3612
MGMT	10	1	131155510	1	;856
FIGF	X	-1	15273640	1	;4442
BMP5	6	-1	55728199	1	;3107
BMP2	20	1	6696745	1	;3575
SNAI2	8	-1	49992880	1	;4078
COL8A2	1	-1	36333424	1	;3238
TFAP2B	6	1	50894398	1	;4070
GLI3	7	-1	41967072	1	;4053
MAF	16	-1	78185729	1	;1197
SERPINB9	6	-1	2832507	1	;701
ELTD1	1	-1	79128037	1	;4559
ROR1	1	1	64012281	1	;3573
FAP	2	-1	162735448	0	
PRRX1	1	1	168899937	0	
CDON	11	-1	125331927	0	
CPNE8	12	-1	37332259	0	
TFPI	2	-1	188051553	0	
RSPO3	6	1	127481749	0	
MAB21L2	4	1	151722753	0	
UNC5C	4	-1	96308712	0	
CUL4B	X	-1	119542476	0	
SCML4	6	-1	108130060	0	
ANXA2	15	-1	58426625	0	
PTGS2	1	-1	184907592	0	
TFAP2A	6	-1	10504902	0	
OLFM3	1	-1	102040721	0	

APPENDIX C PUBLICATIONS

Publication reported in this thesis

Wu SM, Choo AB, Yap MG, Chan KK. Role of Sonic hedgehog signaling and the expression of its components in human embryonic stem cells. *Stem Cell Research* 2010 4:38-49

Other publications not reported in this thesis

Generation of high-level stable transgene expressing human embryonic stem cell lines using Chinese hamster elongation factor-1 alpha promoter system. Chan KK, Wu SM, Nissom PM, Oh SK, Choo AB. *Stem Cells Dev.* 2008 17(4):825-36.

Identification of Sonic hedgehog target genes in human embryonic stem cell derived neuroprogenitors. Wu SM, Beh TT, Chan HS, Choo AB, Yap MG, Chan KK. [Manuscript in preparation]